



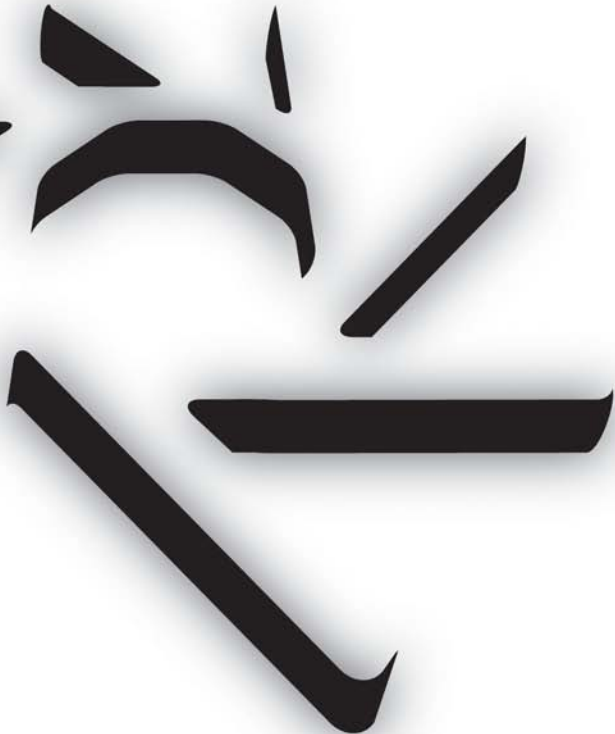
20^a RAU

**REUNIÃO ANUAL DE
USUÁRIOS DO LNLS**

22 E 23 FEVEREIRO 2010



**RESUMO DE
TRABALHOS CIENTÍFICOS**



20^a RAU

**REUNIÃO ANUAL DE
USUÁRIOS DO LNLS**

22 E 23 FEVEREIRO 2010



**RESUMO DE
TRABALHOS CIENTÍFICOS**

COORDENAÇÃO
Chairmen

Carlos Alberto Pérez (LNLS)
Waldemar Augusto de Almeida Macedo (CDTN)

COMITÊ CIENTÍFICO
Scientific Committee

Flávio Garcia (LNLS)
Gerardo Gerson Bezerra de Souza (UFRJ)
Íris Concepción Linares de Torriani (Unicamp e LNLS)
Jayr de Amorin Filho (CTBE)
Mario Ernesto Giroldo Valério (UFS)
Paulo Fernando Papaleo Fichtner (UFRGS)
Pedro Augusto de Paula Nascente (UFSCar)
Ricardo Tadeu Lopes (UFRJ)
Robson Augusto Souza dos Santos (UFMG)
Rogério Paniago (UFMG)

COMITÊ LOCAL
Local Organizing Committee

Milena Francelin Camargo
Dennis Massarotto Campos
Guilherme Tavares de Oliveira

SECRETÁRIA
Secretary

Ana Lucia Ferreira



20^a RAU
REUNIÃO ANUAL DE
USUÁRIOS DO LNSL
22 E 23 FEVEREIRO 2010

20ª REUNIÃO ANUAL DE USUÁRIOS

Laboratório Nacional de Luz Síncrotron
22 e 23 de fevereiro de 2010 – Campinas-SP, Brasil

20th ANNUAL USERS' MEETING

Brazilian Synchrotron Light Laboratory
February 22 - 23, 2010 – Campinas-SP, Brazil

PREFÁCIO

Prezados Pesquisadores,

Chegamos à 20ª edição da Reunião Anual de Usuários do Laboratório Nacional de Luz Síncrotron (RAU/LNLS), evento que congrega os pesquisadores que utilizam a infraestrutura ímpar disponível no LNLS e este é o momento oportuno para avaliarmos resultados científicos e debatermos questões relevantes para o desenvolvimento contínuo da Instituição.

Aberto a pesquisadores-usuários de diferentes áreas científicas e procedentes de instituições de todo o País e do exterior, o Laboratório busca obter na RAU subsídios importantes para o adequado planejamento de sua operação, manutenção e expansão. É importante, portanto, a participação efetiva de todos tanto nos debates científicos quanto nas discussões relacionadas aos projetos de melhoria e ampliação da instrumentação disponível para a pesquisa.

É oportuno lembrar que o *campus* abriga atualmente um complexo de Laboratórios Nacionais denominado Centro Nacional de Pesquisa em Energia e Materiais (CNPEM). Além do LNLS, aqui estão o Laboratório Nacional de Biociências (LNBio), anteriormente designado Centro de Biologia Molecular Estrutural (CeBiME), cuja operação começou em 2001, e o recém-inaugurado Laboratório Nacional de Ciência e Tecnologia do Bioetanol (CTBE). Abriga ainda o Centro de Nanociência e Nanotecnologia Cesar Lattes (C2Nano), hoje vinculado ao LNLS e que futuramente também deverá ganhar o status de Laboratório Nacional. As características singulares das instalações existentes no *campus* abrem continuamente perspectivas de desenvolvimento de projetos científicos multidisciplinares e exploração de novas vertentes científicas, contribuindo para impulsionar nosso desenvolvimento econômico e social.

Em relação à programação da 20ª RAU, o Comitê Organizador selecionou 36 trabalhos científicos para apresentação no formato de Comunicação Oral. Para Palestras Plenárias foram convidados especialistas de diversas áreas, que apresentarão novas tendências em microscopia de raios-x, espectro-microscopia com luz síncrotron, sobre progressos recentes na caracterização espectroscópica de materiais avançados e sistemas complexos. Além deles, há nas Plenárias uma palestra sobre as novas ferramentas para a caracterização estrutural de macromoléculas, e uma palestra sobre a história do LNLS e os 20 anos de RAU.

As já tradicionais Sessões Temáticas ocorrerão em paralelo, com inclusão de uma nova Sessão, dedicada inteiramente aos temas diretamente relacionados com as atividades do CTBE, uma vez que as atividades relacionadas ao LNBio já estão contempladas. Ressaltamos que esta RAU inclui ainda dois Workshops Satélites que são dedicados aos avanços na aplicação de radiação síncrotron na caracterização de materiais.

Os participantes terão ainda a oportunidade de conhecer o atual estágio da expansão do LNLS, representativo do constante esforço institucional e governamental para dotar o Brasil de novas e melhores condições na ciência experimental. Será visto, por exemplo, que 2009 caracterizou-se como um ano marcado por importantes melhorias na infraestrutura à disposição dos usuários. Foi iniciado o comissionamento do primeiro ondulador instalado no anel de armazenamento de elétrons. Foi igualmente comissionado o wiggler supercondutor de 4 Tesla, dispositivo que melhora o desempenho da Fonte de Luz Síncrotron na faixa de raios-x duros.

O projeto da segunda fonte brasileira de luz síncrotron, esboçado em 2008 e que recebeu o aval inicial do Ministério de Ciência e Tecnologia (MCT), também será tema de Palestras Plenárias.

Esperamos que a programação e a dinâmica da 20ª RAU sejam aproveitadas integralmente por todos os pesquisadores-usuários que participarão desta edição marcante no contexto da história institucional e do próprio evento.

Agradecemos aos membros do Comitê Científico pelo empenho na análise dos trabalhos submetidos e efetiva participação na elaboração do formato final do programa da RAU. Agradecemos também aos organizadores dos Workshops Satélites, Eduardo Granado e Daniela Zanchet. Agradecemos ainda aos funcionários e colaboradores da Secretaria Geral, Secretaria de Apoio aos Usuários, áreas de Comunicação, Convênios e Projetos e Tecnologia da Informação que, com profissionalismo e dedicação, trabalharam nos meses precedentes e trabalharão durante a RAU para que o evento transcorra de maneira adequada e correspondente às expectativas de todos os participantes. Agradecemos finalmente ao MCT (contrato de gestão), CNPq, CAPES, FAPESP, CLAF e PETROBRAS pelo apoio financeiro outorgado.

Carlos Alberto Pérez e Waldemar Augusto de Almeida Macedo
Coordenadores da 20ª RAU

ORIENTAÇÕES AOS PARTICIPANTES *Guidelines to Participants*

Prezado Participante, / *Dear Participant,*

Seja bem-vindo ao Centro Nacional de Pesquisa em Energia e Materiais (CNPEM), que congrega o Laboratório Nacional de Luz Síncrotron (LNLS). A equipe envolvida na organização da 20ª Reunião Anual de Usuários fez o melhor possível para recebê-lo. Para sua orientação, pedimos atenção para as informações abaixo.

Welcome to the CNPEM, Brazilian Synchrotron Light Laboratory (LNLS). The organizing of the 20th Annual User's Meeting has done its best to make sure everything will run smoothly. Please, read carefully the following instructions.

1. TRASLADOS / Transfer

Traslados entre HOTEL / CNPEM / HOTEL serão feitos em ônibus especial:
A shuttle will be provided for the transportation from HOTEL / CNPEM / HOTEL:

Dia 22/02, segunda-feira / Monday 22nd

Saída do Hotel às 07h15	Saída do CNPEM às 21h00
-------------------------	-------------------------

<i>Departure from hotel at 07:15 am</i>	<i>Departure from CNPEM at 09:00 pm</i>
---	---

Dia 23/02, terça-feira / Tuesday 23th
--

Saída do Hotel às 07h15	Saída do CNPEM às 14h00 e 17h00
-------------------------	---------------------------------

<i>Departure from hotel at 07:15 am</i>	<i>Departure from CNPEM at 2:00 and 5:00 pm</i>
---	---

2. SESSÕES / Sessions

As Comunicações Orais e Sessões Temáticas ocorrerão em diferentes locais no CNPEM:
Oral presentations and technical sessions will be held at four different locations at CNPEM campus:

- (A) Prédio do Anel – Auditório
- (B) Prédio Amarelo – Sala de Leitura (Biblioteca)
- (C) Prédio LNBio – Sala 69
- (D) Prédio Amarelo – Sala 50
- (E) Prédio C2Nano – Sala de Seminários
- (F) Prédio CTBE – Auditório e Salas de Seminários

3. LOCALIZAÇÃO DOS PAINÉIS / Posters Location

Os painéis deverão ser afixados no primeiro dia da reunião (22/02), logo após a recepção do crachá. A localização dos painéis estará sinalizada por etiquetas com numeração correspondente à indicada no Sumário deste Livro de Resumos.

The posters must be in its designated place in the first day of the meeting (Feb 22nd), just after registration. The poster location will be indicated by tags corresponding to the same numbers present in the Abstract Book.

4. CRACHÁ DE IDENTIFICAÇÃO / *Identification Badge*

O crachá de identificação deve ser usado durante a sua permanência no CNPEM.
The identification badge must be used at all times during your stay at CNPEM.

5. GUARDA-VOLUME / *Lockers*

Para sua comodidade, guarda-volumes estão disponíveis na entrada do Prédio do Anel.
For your convenience, lockers are available at the entrance of the Storage Ring Building.

6. ALMOÇO / *Lunch*

Os almoços serão servidos no refeitório do CNPEM, a partir do horário indicado no programa.
Lunch will be served at the CNPEM canteen, following the schedule in the program.

7. CÓPIAS XEROX / *Photocopies*

Cópias xerográficas devem ser solicitadas à Biblioteca do CNPEM e custam R\$ 0,10 (dez centavos) cada. Dependendo da quantidade de cópias, elas serão enviadas posteriormente pelo correio, mediante pagamento antecipado.
Photocopies must be requested at CNPEM Library, at a cost of R\$ 0,10 (ten cents) each. Depending on quantity, they may be sent after the meeting by mail, after pre-payment.

8. TELEFONE / *Pay-phones*

Há um telefone público disponível no campus do CNPEM, na entrada do Prédio Amarelo. Cartões magnéticos podem ser adquiridos no refeitório.
One pay-phone is available at CNPEM, at the entrance of administration building. Phone cards can be purchased at CNPEM canteen.

9. E-MAIL

Computadores de uso coletivo estarão disponíveis. Informe-se na secretaria do evento. Siga as instruções afixadas no local para acesso aos e-mails.
Computers will be available. In order to access your e-mail, please follow instructions posted at the room.

AGENDA

22 de Fevereiro, segunda-feira

- 08h00 Recepção / Inscrição
- 08h30 Abertura
Diretores dos Laboratórios Nacionais que integram o CNPEM
- 09h10 RAU 20 anos
Aldo Felix Craievich (USP / SP)
- 09h40 Status e Perspectivas da LNLS-1
Ruy Hanazaki do Amaral Farias (LNLS)
- 10h00 Foto Oficial
- 10h10 Café
- 10h30 Plenária I - "Synchrotron Based X-ray Microprobes: Towards a Multimodal Approach"
Jean Susini (ESRF / France)
- 11h20 Plenária II - "The Macromolecular Crystallography Village at the Diamond Light Source: High-throughput and automation from microfocus to MAD"
Gwyndaf Evans (Diamond Light Source / UK)
- 12h10 Almoço
- 13h30 Comunicações Orais
- 15h00 Sessões Temáticas
- 18h00 Painéis
- 19h00 Confraternização
- 21h00 Saída do ônibus para o hotel

23 de Fevereiro, terça-feira

- 08h30 Comunicações Orais
- 10h10 Café
- 10h30 Plenária III - "Hard X-ray Photoemission Spectroscopy on Complex Systems: from Surface to Bulk Sensitivity"
Giancarlo Panaccione (TASC-INFN / Italy)
- 11h20 Plenária IV - "LNLS-2 - Scientific Cases and Machine Design"
Yves Petroff (LNLS) / Antonio Ricardo Droher Rodrigues (LNLS)
- 12h10 Encerramento
- 13h00 Almoço

22 de Fevereiro, segunda-feira

COMUNICAÇÕES ORAIS

PROGRAMAÇÃO - COMUNICAÇÕES ORAIS

Sessão 1 - Prédio do Anel, Auditório

Chairperson: Eduardo Granado

13h30 Acoplamento Magnético entre os Íons de Gd e Pr e Efeito Magnetocalórico no Composto $Gd_{0.5}Pr_{0.5}Al_2$

Alexandre Magnus G. Carvalho (Pág. 185)

13h50 In-plane Strain Anisotropy Due to Induced Re-Crystallization Process (IBIEC) by Means of X-ray Multiple Diffraction

Adenilson Oliveira dos Santos (Pág. 193)

14h10 Probing Vacancies in CeO_2 Thin Films Through Ce Valence States: a XANES and XPS Investigation

Ismael Leandro Graff (Pág. 169)

14h30 Small-angle X-ray Scattering (SAXS) of Ordered Magnetic Systems

Fanny Béron (Pág. 194)

Sessão 2 - Prédio Amarelo, Sala 50

Chairperson: Ana Lúcia Ferreira de Barros

13h30 Ionic Fragmentation of Selenium Oxychloride Under VUV Irradiation

Carlos Della Védova Omar (Pág. 71)

13h50 Positive and Negative Ionic Desorption from Condensed Formic Acid Photoexcited Around the O 1s-edge: Relevance to Cometary and Planetary Surfaces

Maria Luiza Miranda Rocco (Pág. 68)

14h10 Study of the Oxidation State by Comparative Analysis of Resonant Inelastic X-Ray Scattering Emission

Juan Jose Leani (Pág. 67)

14h30 Ionic Fragmentation of SO_2 After S 1s Excitation

Arnaldo Naves de Brito (Pág. 74)

Sessão 3 - Prédio Amarelo, Sala de Leitura da Biblioteca

Chairperson: Danilo de Paiva Almeida

13h30 Fabricação de Strain Gauges para Aplicações em Altas Temperaturas

Mariana Amorim Fraga (Pág. 126)

13h50 X-ray Study of Carbide Evolution of Cr-Mo Steels During Aging

Luis Fernando Lemus Torres (Pág. 123)

14h10 Proton Conducting Membrane Based on SPEEK and Modified Silica for Direct Ethanol Fuel Cell

Florêncio Gomes Ramos Filho (Pág. 121)

14h30 Development of Catalytic Materials for Glycerol Hydrogenolysis

Cristiane Barbieri Rodella (Pág. 129)

Sessão 4 - Prédio LNBio, Sala 69

Chairperson: André Ambrósio

13h30 Functional and Structural Insights Into the Role of Fez Family Proteins in Axonal Outgrowth

Marcos Rodrigo Alborghetti (Pág. 23)

13h50 Characterization of the Periplasmic-Binding Protein Pbp from *Xanthomonas Axonopodis* pv. Citri

Andrea Balan Fernandes (Pág. 43)

14h10 The *Xanthomonas Citri* Effector Protein PthA Transactivates Citrus Genes Associated with Citrus Canker Development

Andre Luiz Araújo Pereira (Pág. 53)

14h30 Proteomic Analysis of Extracellular Matrix of Dental Plaque Formed in the Presence of Sucrose or Glucose and Fructose

Gisele Pedroso Moi (Pág. 56)

23 de Fevereiro, terça-feira

COMUNICAÇÕES ORAIS

Sessão 1 - Prédio do Anel, Auditório

Chairperson: Fábio Henrique Barros de Lima

08h30 Structural Properties of Pd/Ce-Zr Mixed Oxide Nanotubes

Leandro Marcelo Acuña (Pág. 161)

08h50 EXAFS Characterization of the Local Disorder in Y2O3 Nanoparticles Produced Via a Coconut Water-Assisted Sol-Gel Method

Zélia Soaes Macedo (Pág. 163)

09h10 Study of the Morphology Evolution of Vanadium Pentoxide Nanostructures by TEM and SAXS

Waldir Júnior Avansi (Pág. 182)

09h30 Nitrate Hydrogenation on Pt,In/Al₂O₃. EXAFS and XANES Characterization of Fresh and Used Catalysts

José Ramallo-Lopez (Pág. 205)

09h50 Transition Metal Cations Doping in Ammonium Dihydrogen Phosphate As Examined by Synchrotron Radiation Renninger Scanning

Claudio Marcio Rocha Remédios (Pág. 183)

Sessão 2 - Prédio Amarelo, Sala de Leitura da Biblioteca

Chairperson: Pedro Augusto de Paula Nascente

08h30 In-situ XANES Study of Pt_xPd_{1-x} (x = 1, 0.7 or 0.5) Nanoparticles Subjected to H₂ Reduction

Fabiano Bernardi (Pág. 206)

- 08h50 Observation of Pd Magnetism in Carbon Nanotube Catalyst Nanoparticles by X-ray Circular Dichroism
Daniel Bretas Roa (Pág. 208)
- 09h10 Structure of PbTe(SiO₂)/SiO₂ Multilayers Deposited on Si (111)
Gunter Kellerman (Pág. 213)
- 09h30 Characterization of Magnetic Nanourchins and Nanoflowers
Leandro Martin Socolovsky (Pág. 232)
- 09h50 Mechanical Deformation of Gold Atomic-size Nanowires
Maureen Joel Lagos (Pág. 220)

Sessão 3 - Prédio Amarelo, Sala 50

Chairperson: Silvana Moreira

- 08h30 Development and In Vitro Evaluation of Surfactant Systems for Controlled Release of Zidovudine
Victor Hugo Vitorino Sarmiento (Pág. 109)
- 08h50 Study of the Bioaccumulation Kinetic of Lead and Copper by Living Aquatic Macrophytes Eicchornia Crassipes
Fernando Rodolfo Espinoza (Pág. 79)
- 09h10 Investigation of Low-cost Bio-adsorbents for Heavy Metals
Wladimir Hernandez Flores (Pág. 95)
- 09h30 Evaluation of Long-term Effects of Tibolone in Femoral Bone by Synchrotron X-Ray Microfluorescence Microscopy
Inayá Correa Barbosa Lima (Pág. 73)
- 09h50 Identification of Metabolites in the Roots of Coffee Plants by ¹H NMR Analyses
Denilson Ferreira de Oliveira (Pág. 99)

Sessão 4 - Prédio LNBio, Sala 69

Chairperson: Ricardo Aparício

- 08h30 SAXS Studies of Flexible Multidomain Proteins
Júlio César da Silva (Pág. 28)
- 08h50 The Crystal Structures of Human Transthyretin (TTR) Binding Flavonoids
Daniela Barreto Barbosa Trivella (Pág. 13)
- 09h10 Structural Studies with a Phospholipase A2 Homologue Complexed to Mn²⁺ Ions Possible Role for Myotoxicity Inhibition
Rafael Junqueira Borges (Pág. 19)
- 09h30 SAXS Studies of DNA Self-assembled Structures
Cristiano Luis Pinto de Oliveira (Pág. 25)
- 09h50 Crystal Structure of a Cyclophilin from Citrus Sinensis in Complex with Cyclosporin A at 1.87 Maximum Resolution
Bruna Medéia de Campos (Pág. 21)

22 de Fevereiro, segunda-feira

SESSÕES TEMÁTICAS

PROGRAMAÇÃO - SESSÕES TEMÁTICAS

Prédio do Anel, Auditório

Chairperson: Mario Ernesto Giroldo Valério

14h30 - 17h00 Status e Perspectivas das Linhas XAS / XAFS I e XAFS II / DXAS

Gustavo Azevedo e Flávio Garcia

Prédio Amarelo, Sala de Leitura da Biblioteca

Chairperson: Rogerio Paniago

14h30 - 17h00 Status e Perspectivas das Linhas XRD I e XRD II / XPD

Daniela Zanchet, Ângelo Malachias de Souza e Eduardo Granado

Prédio Amarelo, Sala 50

Chairperson: Geraldo Gerson Bezerra de Souza

14h30 - 17h00 Status e Perspectivas das Linhas Soft X-Rays / SGM / TGM / PGM / SXS

Arnaldo Naves de Brito, Richard Landers e Abner de Siervo

Prédio LNBio, Sala 69

Chairperson: Iris Concepción Linares de Torriani

14h30 - 17h00 Status e Perspectivas das Linhas MX I e MX II / MAS / RMN / VUVF

Mário Murakami, Ana Carolina Zeri e Adriana Franco Paes Leme

Prédio CTBE, Sala 01

Chairperson: Celso Santilli

14h30 - 17h00 Status e Perspectivas das Linhas SAXS I e SAXS II

Harry Westfahl Jr.

Prédio CTBE, Sala 02

Chairperson: Ricardo Tadeu Lopes

14h30 - 17h00 Status e Perspectivas das Linhas XRF

Carlos A. Pérez

Prédio C2Nano, Sala 01

Chairperson: Paulo Fernando Papaleo Fichtner

14h30 - 17h00 Status e Perspectivas da Microscopia Eletrônica

Antonio J. Ramirez

Prédio C2Nano, Sala 02

Chairperson: Emanuel Carrilho

14h30 - 17h00 Status e Perspectivas das Linhas STM / AFM e Microfabricação

Gilberto Medeiros e Ângelo Gobbi

Prédio CTBE, Auditório do CTBE

Chairperson: Jayr de Amorim Filho

14h30 - 17h00 Status e Perspectivas do CTBE

Sumário

Parte I Plenárias

Hard X-ray Photoemission Spectroscopy on complex systems: from surface to bulk sensitivity <i>G. Panaccione</i>	3
The Macromolecular Crystallography Village at the Diamond Light Source: High-throughput and automation from microfocus to MAD <i>G. Evans</i>	4
Synchrotron based X-ray microprobes: Towards a multimodal approach <i>J. Susini</i>	5
Pretreatment technologies for production of 2G bioethanol from Agricultural waste and crops <i>Bjerre AB</i>	7

Parte II Biologia Estrutural

Análises estruturais do estado oligomérico do receptor ativador da proliferação de peroxissomo isotipo α através de SAXS <i>Bernardes, A., Oliveira Neto M., Polikarpov, I.</i>	11
Structural Studies of Selenocysteine Synthase (SELA) from <i>Escherichia coli</i> <i>Cassago, A., Manzine, LR, Pereira, H.M, Horjales,E., Thiemann, O. H.</i>	12
THE CRYSTAL STRUCTURES OF HUMAN TRANSTYRETIN (TTR) BINDING FLAVONOIDS <i>Trivella, D.B.B., REIS, C.V., Polikarpov, I.</i>	13
Detección de la presencia de drogas del tipo P-C-P en tejido óseo humano, de pacientes con osteoporosis <i>Fernández de Rapp, M. E., Fábregas, I. O.</i>	14

Determination of the molecular weight of proteins in solution from a single SAXS measurement on a relative scale <i>Oliveira Neto M., Fischer, H., Napolitano, H. B., Polikarpov, I., Craievich AF</i>	15
Structural analysis of the carbohydrate recognition domain from lectin of <i>Canavalia brasiliensis</i> and their relation with nitric oxide-release <i>Delatorre, P., Bezerra, E.H.S., Rocha, B.A.M., Naganao, C.S., Moura TR, Bezerra, M. J. B., Cavada, B.S.</i>	16
Crystal structure of Lys-49-phospholipase A2 myotoxin from <i>Bothrops neuwiedi</i> complexed to myristic acid <i>Rocha, B.A.M., Delatorre, P., Toyama MH, Cavada, B.S.</i>	17
Estruturas de baixa resolução de Celobiohidrolase I de <i>Trichoderma harzianum</i> 3844. <i>Rosseto, Flávio R., Serpa, V.I., Colussi, F., Oliveira Neto M., Polikarpov, I.</i>	18
Structural Studies with a Phospholipase A₂ Homologue Complexed to Mn²⁺ Ions Possible Role for Myotoxicity Inhibition <i>Borges, R. J., (dos) Santos, J. I., Soares, A. M., Fontes, M. R. M.</i>	19
Estudos estruturais do PPARγ complexado com ligantes naturais <i>Puhl, A. C., Campos, J. L. O., Polikarpov, I.</i>	20
Crystal Structure of a Cyclophilin from <i>Citrus sinensis</i> in complex with Cyclosporin A at 1.87 maximum resolution <i>Campos, B.M., Souza, T.A.C.B., Barbosa, J.A.R.G., Benedetti C.E.</i>	21
Identification of hNek6 interaction partners in the context of complex networks <i>Meirelles, G. V., Lanza, D.C.F, Silva, J.C., Santana JB, Paes Leme, A.F., Torriani, I., Kobarg, J.</i>	22
FUNCTIONAL AND STRUCTURAL INSIGHTS INTO THE ROLE of FEZ FAMILY PROTEINS IN AXONAL OUTGROWTH <i>Alborghetti, MR, Silva, J.C., Furlan AS, Torriani, I., Kobarg, J.</i>	23
The FEZ1 protein homo-dimerizes via a disulfide Bond <i>Furlan AS, Alborghetti, MR, Silva, J.C., Paes Leme, A.F., Sforça, ML, Torriani, I., Zeri, A.C.; Zeri, A; Zeri, A.C.M., Kobarg, J.</i>	24
SAXS studies of DNA self-assembled structures <i>Oliveira, C. L. P, Pedersen, J.S., Andersen, F. F., Knudsen, B. R., Irish, E., Labean, T., Andersen, E. S., Kjems, J.</i>	25
A <i>in situ</i> SAXS Study of Glucagon Fibrillation <i>Oliveira, C. L. P, Behrens, M. A., Pedersen, J. S., Erlacher, K, Otzen, D. E., Pedersen, J.S.</i>	26
Structural studies of Intrinsically Unstructured Proteins by Small-Angle X-ray Scattering <i>Silva, J.C., Lanza, D.C.F, Bressan, G.C., Kobarg, J., Torriani, I.L.</i>	27

SAXS studies of flexible multidomain proteins <i>Silva, J.C., Borges, J.C., Quaresma, A. J. C., Bressan, G.C., Kobarg, J., Ramos, C.H.I., Torriani, I.L.</i>	28
OLIGOMERIZATION STATES OF LEUCYL AMINOPEPTIDASE FROM <i>Leptospira interrogans</i> <i>Álvares, A.C.M., Silva, A. J., Barbosa, J.A.R.G., Santana, J. M., Freitas, S. M.</i>	29
Self-association of the chymotrypsin inhibitor from <i>Schizolobium parahyba</i> seeds and its binary complex with alpha-chymotrypsin <i>Silva, A. J., Álvares, A.C.M., Barbosa, J.A.R.G., Freitas, S. M.</i>	30
Low resolution structural studies of human RACK-1 <i>Gonçalves, K.A., Borges, J.C., Silva, J.C., Papa, PF, Torriani, I., Kobarg, J.</i>	31
Physicochemical characterization of the protease inhibitor BTC1 in complex with 20S Proteasome <i>Souza, L. C., Joanitti, G. A., Silva, A. J., Lottermann, M. T., Camargo, R., Martins de Sá, C, Freitas, S. M.</i>	32
Implementation of new NMR Methods for Protein Studies <i>Neves, J.L., Sforça, ML, Zeri, A.C.</i>	33
Crystallographic studies of <i>Schizolobium parahyba</i> chymotrypsin inhibitor in complex with chymotrypsin <i>Silva, A. J., Santos, C. R., Barbosa, J.A.R.G., Freitas, S. M.</i>	34
ADAM-9, 10, 12, 17 and 19 expression in normal and cancer cells <i>Câmara, P.R.S, Yokoo, S, Belloni, M, Paes Leme, A.F.</i>	35
Crystal structure of TK1436, a branching enzyme from the hyperthermophilic archaeon <i>Thermococcus kodakaraensis</i> <i>Santos, C. R., Tonoli, C. C. C., Arni, R.K., Murakami, M. T.</i>	36
Expressão, Purificação e Estudos Biofísicos e Estruturais da endo-1,4-β- Glicanase de <i>Bacillus subtilis</i> <i>Akao, P.K., Ruller,R., Murakami, M. T.</i>	37
Crystal Structure of the Nucleoside diphosphate kinase b from <i>Leishmania major</i> <i>Trindade, D.M., Tonoli, C. C. C., Arni, R.K., de Oliveira, A.H.C., Murakami, M. T.</i>	38
<hr/>	
Parte III Biologia Molecular e Química de Proteínas	
<hr/>	
Study of interaction between nona-peptide BPP9a and β-cyclodextrin: NMR Structural Elucidation <i>Lula, I., Sinisterra R. D., Santos, R.A.S., Denadai, A M L</i>	41

Análise de lesões causadas no DNA pela fotoquimioterapia PUVA (psoralenos mais luz ultravioleta A) <i>de Paula-Pereira Jr., M. V., Soares, M., C. Lage, Leitão, A.C.</i>	42
Characterization of the periplasmic-binding protein Pbp from <i>Xanthomonas axonopodis</i> pv. <i>citri</i> <i>Balan, A., Barbosa, J.A.R.G.</i>	43
The <i>Xanthomonas</i> Type III Effector Protein PthA Interacts with Citrus Proteins Involved in Nuclear Transport, Protein Folding and inhibits K63-linked Ubiquitination Associated with DNA Repair <i>Domingues, M. N., Souza, T. A., Cernadas, R. A., Oliveira, M. L. P., Docena, C., Farah, C.S., Benedetti C.E.</i>	44
The splicing-associated SR protein SFRS9 undergoes arginino methylation and localizes to nucleoli upon inhibition of cellular methylation <i>Bressan, G.C., Moraes, E.C., Manfiolli A, Kuniyoshi, T.M., Passos, D. O., GOMES MD, Kobarg, J.</i>	45
Thermal- and chemical-unfolding studies of yeast Hsp40 <i>SIS1</i> and mutants <i>Borges, J.C., Cyr, D.M., Ramos, C.H.I.</i>	46
Protein-Protein interactions and structural analysis of citrus proteins involved in transcriptional control during citrus canker disease. <i>Souza, T. A., Quaresma, A. J. C., Sforça, ML, Cernadas, R. A., Domingues, M. N., Zeri, A. C., Benedetti C.E.</i>	47
Iron and zinc mapping by SR-XRF in protein spots of liver tissue samples of Nile tilapia (<i>Oreochromis niloticus</i>) <i>Neves, R.C.F., da Silva, M. A. O., Santos, F.A., Lima, P. M., Arruda, M. A. Z., Pérez, C. A., Padilha, P. M.</i>	48
Studies on the phosphorylation and subcellular distribution of the $\alpha 4$ protein <i>Smetana, J. H. C., Bressan, G.C., Kobarg, J., Zanchin, N. I. T</i>	49
Identificação de IL-7Rα IC interacting proteins using the yeast three-hybrid system <i>Zenati PP, Yunes, J. A., Kobarg, J.</i>	50
Characterization of Interactions Between PthA Protein from <i>Xanthomonas citri</i> and Citrus Proteins Involved in Transcription Control, RNA Stability and Cell Proliferation <i>Soprano, A. S, Souza, T. A., Benedetti C.E.</i>	51
Overexpression of MAP kinase and WRKY genes in Troyer citrange increased resistance to it <i>Xanthomonas axonopodis</i> pv. <i>citri</i> <i>Oliveira, M. L. P., Benedetti C.E.</i>	52

The Xanthomonas citri effector protein PthA transactivates citrus genes associated with citrus canker development <i>Pereira, A. L. A., Cernadas, R. A., Oliveira, M. L. P., Benedetti C.E.</i>	53
Caracterização da função da proteína ISG95 no metabolismo de RNA <i>Simabuco, F. M., Vaz, T. H., Paes Leme, A.F., Zanchin, N. I. T.</i>	54
Development of a Library for Biomass-Conversion Enzymes <i>Ribeiro, D. A., Murakami, M. T., Ruller, R., Squina, F. M.</i>	55
Proteomic analysis of extracellular matrix of dental plaque formed in the presence of sucrose or glucose and fructose. <i>Moi, G.P., Paes Leme, A.F., Cury, J. A.</i>	56
SAXS IN STRUCTURAL STUDIES ON SECRETION CHAPERONES FROM <i>Xanthomonas axonopodis</i> pv. <i>citri</i> <i>Fattori, J., Aparicio, R., Tasic, L.</i>	57
Mass Spectrometry Analysis of Secretion Chaperones from <i>Xanthomonas axonopodis</i> pv. <i>citri</i> <i>Martins, A. M., Arruda, M. A. Z., Tasic, L.</i>	58
Expression and Purification of cTPxIII and TrxI^{C33S} and Mutation of cTPxIII of <i>Saccharomyces cerevisiae</i> for Formation of Mixed Disulfide Protein Complexes. <i>Santos, V.F., Netto, L.E.S., Oliveira, M.A.</i>	59
<hr/>	
Parte IV Ciência Atômica e Molecular	
<hr/>	
Electronic excitation and ionic dissociation of volatile organics compounds of sulfur related with the ocean-atmosphere cycle: DMS and DMDS <i>Grangeiro, L.B., Bernini, R.B., Rodrigues, F. N., Coutinho, L. H., de Souza, G.G.B.</i>	63
Fragmentation Dynamic of Chlorobenzene and Toluene Induced by Synchrotron Radiation <i>Fernandes, D.H.L., G. Ferreira, Turci, C. C., Guerra, A. C. O., A.L.F. de Barros.</i>	64
NEXAFS study of the radiation damage in biomolecules: methionine, cysteine, cystine and insulin. <i>Simões, G., Grangeiro, L.B., de Souza, G.G.B.</i>	65
ELECTRONIC PROPERTIES OF THE COORDINATION COMPOUNDS OF THE LIGANDS DMIT, DMIO AND DMT IN THE C 1s, N1s and O1s REGIONS. <i>Ferreira, G. B., Lopes, L. J. S., Turci, C. C., A.L.F. de Barros, Almeida, G.C., Guerra, A. C. O.</i>	66

STUDY OF THE OXIDATION STATE BY COMPARATIVE ANALYSIS OF RESONANT INELASTIC X-RAY SCATTERING EMISSION <i>H. J. Sánchez, Valentinuzzi, M. C., Leani, J.J., Pérez, C. A.</i>	67
Positive and negative ionic desorption from condensed formic acid photoexcited around the O 1s-edge: relevance to cometary and planetary surfaces <i>Andrade, D. P. P., Boechat-Roberty, H.M., Pilling, S., E. F. da Silveira, Rocco, M.L.M.</i>	68
Multiple photoionization of Ne in the K-shell region and its comparison to electron impact data. The roles of direct outer-shell electron ejection and inner-shell ionization <i>ACF Santos, Almeida, D. P., Homem, M. G. P.</i>	69
Dissociative Photoionization of FC(O)SCH₂CH₃ following the shallow and innershell core electronic properties <i>Rodriguez Pirani, Lucas, Erben, Mauricio F., Geronés, Mariana, Romano, Rosana M., Cavasso Filho, R. L., Della Védova, Carlos O.</i>	70
Ionic fragmentation of selenium oxychloride under VUV irradiation <i>Erben, Mauricio F., Geronés, Mariana, Rodriguez Pirani, Lucas, Cavasso Filho, R. L., Romano, Rosana M., Della Védova, Carlos O.</i>	71
STUDY OF THE OXIDATION STATE BY COMPARATIVE ANALYSIS OF RESONANT INELASTIC X-RAY SCATTERING EMISSION <i>H. J. Sánchez, Valentinuzzi, M. C.</i>	72
Evaluation of long-term effects of tibolone in femoral bone by Synchrotron X-Ray Microfluorescence Microscopy <i>LIMA, I., Sales, E., Granjeiro, J. M., GUZMAN-SILVA, M.A., CARVALHO, A.C.B., Lopes, R.T.</i>	73
Ionic fragmentation of SO₂ after S 1s excitation <i>Naves de Brito, A., Mocellin, A., Cavasso Filho, R. L., Lago, A. F., Mundim, M. S. P.</i>	74
Photodissociation of Glycine by UV H₂ Lamp Radiation <i>Ferreira-Rodrigues, A. M., Homem, M. G. P., Naves de Brito, A., C.R. Ponciano, E. F. da Silveira</i>	75
<hr/>	
Parte V Geociência, Meio-ambiente e Aplicações em Materiais Biológicos	
<hr/>	
Study of the bioaccumulation kinetic of lead and copper by living aquatic macrophytes <i>Eicchornia crassipes</i> <i>Espinoza Quiñones, F.R., Palacio, S.M., Szymanski, N., Manenti, D. R., Módenes, A.N., Borba, F.H.</i>	79

Study of Cr(VI) reduction by activated carbon using high resolution X-ray emission spectroscopy <i>Módenes, A.N., Espinoza Quiñones, F.R., Palacio, S.M., Stutz, G., Tirao G., Camera, A.S.</i>	80
Inorganic and organic pollutant removal from tannery effluent by an integrated photo-Fenton and Electro-coagulation process <i>Palacio, S.M., Espinoza Quiñones, F.R., Módenes, A.N., Borba, F.H, Manenti, D. R., Szymanski, N.</i>	81
Estudo da reprogramação de células-tronco murinas a nível atômico <i>Cardoso, S.C., Stelling, M.P., B Paulsen, Rehen, S</i>	82
Determinación de la distribución de As y otros elementos en embriones de sapo común argentino (<i>Chaunus arenarum</i>) desarmados en agua contaminada con arsénico o clorpirifos por SR-TXRF <i>Pérez, C. A., Venturino,A., R.D. Pérez, Rubio, M., Bongiovanni, G.A.</i>	83
X-Ray Fluorescence with Synchrotron Radiation to Elemental Analysis of Lead and Calcium Content of Primary Teeth <i>de Souza Guerra, C, Gerlach, R.F., Pinto, N.G.V, Cardoso, S.C., Moreira, S., Almeida,A.P., Silva, C. L., Oliveira, L. F., Braz, D., Barroso, R.C.</i>	84
Study of Bone Implant Interface by Synchrotron Radiation X-Ray Microfluorescence <i>LIMA, I., Calasans-Maia, Granjeiro, J. M., Sales,E., Rossi A. M., Lopes, R.T., Gasperini, F. M.</i>	85
Bidimensional Mapping of the bone matrix of young and old rats by X ray Microfluorescence with Synchrotron Radiation <i>LIMA, I., Sales,E., Pérez, C. A., Lopes, R.T.</i>	86
Administration of Strontium Ranelate in Wistar rats by X-ray Microfluorescence with Synchrotron Radiation <i>LIMA, I., Taam, P. ; Taam, Pedro, Sales,E., Alves, D.L.H., Lopes, R.T.</i> ...	87
Substratos meteoríticos contribuem para a sobrevivência de <i>Deinococcus radiodurans</i> em condições simuladas de migração interplanetária <i>Dalmaso, G. Z. L., Galante, D., LIMA, I. G. P., Naves de Brito, A., Barbosa, J.A.R.G., Leitão, A.C., C. Lage</i>	88
DETERMINATION OF MULTIELEMENTS IN SERUM SAMPLES FROM PATIENTS WITH SICKLE CELL ANEMIA (SCA) BY SRTXRF <i>Canellas,C.G.L, Leitão,R.G., Carvalho, S.M.F, de Jesus, E.F.O., Anjos, M. J., Lopes, R.T.</i>	89

DETERMINATION OF MULTIELEMENTS IN SERUM SAMPLES FROM PATIENTS WITH SICKLE CELL ANEMIA (SCA) BY SRTXRF	90
TXRF ANALYSIS OF LOW Z ELEMENTS IN SERUM OF PATIENTES WITH IDIOPATHIC THROMBOCYTOPENIC PURPURA BY SYNCHROTRON RADIATION <i>Pereira, M.O., Canellas,C.G.L, Leitão,R.G., de Jesus, E.F.O., Carvalho, S.M.F, Anjos, M. J., Lopes, R.T.</i>	91
ELEMENTAL CONCENTRATION ANALYSIS IN PCa, BPH AND NORMAL PROSTATE TISSUES USING SRTXRF <i>Anjos, M. J., Leitão,R.G., Canellas,C.G.L, Palumbo, A.J, Souza, P.A.V.R, Nasciutti, L.E, Lopes, R.T.</i>	92
DETERMINATION OF LOW Z ELEMENTS IN SERUM OF PATIENTS WITH LEUKEMIAS BY SYNCHROTRON RADIATION <i>Soares, Júlio César de A.C.R., Canellas,C.G.L, Leitão,R.G., Carvalho, S.M.F, de Jesus, E.F.O., Anjos, M. J., Lopes, R.T.</i>	93
Efeito da aplicação de extratos fitoterápicos para tratamento de úlcera péptica na composição multielementar da mucosa gástrica de roedores <i>Vieira, L. D., J. Mesa, Silva, K. T., Hiruma-Lima, C. A., Kushima, H.</i>	94
Investigation of low-cost bio-adsorbents for heavy metals <i>W.H. Flores, Marques, J. F., Gündel, A., Jacques, R.A</i>	95
Utilização de fluorescência de raios-X com radiação síncrotron e ferramentas quimiométricas em análises químicas de amostras de solos da Antártica Marítima <i>GUERRA, M.B.B., Pereira Filho, E. R.</i>	96
TERMINALIA CATAPPA AS BIOINDICATOR OF ENVIRONMENTAL POLLUTION IN CUBATÃO CITY BY SR-TXRF <i>Moreira, S., Barroso, R.C., Vives, A. E. S., Geraldo, S. M., Cardoso, S.C. .</i>	97
EVALUATION OF HEAVY METALS IN ATMOSPHERIC EMISSIONS FROM AUTOMOTIVE INDUSTRY BY SR-TXRF <i>Moreira, S., Weber Neto, J.</i>	98
Identification of metabolites in the roots of coffee plants by ¹H NMR analyses <i>Oliveira, D. F., Machado, A.R.T., Campos, V.A.C., Silva, W. J. R., Zeri, A.C.</i>	99
MONITORING AND EVALUATION OF DUCT EMISSION AND STATIONARY SOURCES OF CERAMIC INDUSTRIES BY SR-TXRF <i>Moreira, S., Fonseca, Roney J.</i>	100

Quantificação de metais pesados presentes no material particulado na cidade de Limeira (SP) por SR-TXRF <i>CANTERAS, F. B., Rodrigues, L.V., Moreira, S.</i>	101
ANALYSIS OF SYNCHROTRON X-RAY DIFFRACTION PATTERNS FROM FLUOROTIC ENAMEL SAMPLES <i>Barroso, R.C., Porto, IM, Gonçalves, M.V.C, Gerlach, R.F., Droppa Jr., R., Braz, D.</i>	102
<hr/>	
Parte VI Matéria Mole e Fluídos Complexos	
<hr/>	
SMALL-ANGLE X-RAY SCATTERING STUDIES IN STERIC STABILIZED pH RESPONSIVE POLYSTYRENE COLLOIDAL PARTICLES <i>Peruzzo, P. J., Anbinder, P. S., Plivelic, T.S., Amalvy, J. I.</i>	105
The influence of polyelectrolyte layers on phosphatidylcholine liposomes <i>Lionzo, M. I. Z., Lorenzini, G. C., Silveira, N. P.</i>	106
SAXS characterization of thermoresponsive soft matter-based systems <i>Azzaroni, O., Picco, A., Bruvera, I.J., Ceolin M.</i>	107
Evidences of hydrotropic organization in aqueous solution by SAXS <i>MACHADO, D. S., Schmitt, C.C. ou Cavalheiro, C.C.S, Neumann, M. G., Oliveira Neto M., Craievich AF, Polikarpov, I.</i>	108
DEVELOPMENT AND IN VITRO EVALUATION OF SURFACTANT SYSTEMS FOR CONTROLLED RELEASE OF ZIDOVUDINE <i>Carvalho, F. C., Sarmiento, V.H.V, Chiavacci, L.A., Barbi, M. S., Gremião, M. P. D.</i>	109
SURFACTANT SYSTEMS FOR NASAL AZT DELIVERY: STRUCTURAL, RHEOLOGICAL AND MUCOADHESIVE PROPERTIES <i>Carvalho, F. C., Barbi, M. S., Sarmiento, V.H.V, Chiavacci, L.A., Netto, F.M., Gremião, M. P. D.</i>	110
SAXS measurement and modeling of <i>in situ</i> formation of mesoporous silica <i>Oliveira, C. L. P., Sundblom, A., Palmqvist, A., Pedersen, J.S.</i>	111
Determinação de propriedades estruturais de coacervados de xantana e poli(etilenoimina) por espalhamento de raios-x a baixos ângulos <i>Guerra, J. P. T. A., Bellettini, I. C., Minatti, E.</i>	112

Parte VII Materiais Estruturais e Aplicações na Indústria

Optical proprieties of calcogenic alloys under VUV irradiation <i>Almeida, D. P., Moura, P. R., C.R. Ponciano, Campos, C. E. M., De Lima, J.C.</i>	115
MORPHOLOGICAL STUDY OF PP/EPDM/ORGANOCLAY NANOCOMPOSITE DEFORMED BY UNIAXIAL COMPRESSION <i>Machado, G, Thompson, A., Dal Acqua, N, Teixeira, S.R., Bianchi, O., Crespo, S.J.</i>	116
Desenvolvimento de um Protótipo de Micro-Sensor de Pressão Piezoresistivo de SiC <i>Fraga, M. A., Massi, M., Oliveira, I.C., Maciel, H. S.</i>	117
SAXS evaluation of Renex-based self-assembly for mullite preparation <i>Garcia, R. B. R., QUEIROZ, HIURE A. A. S, Pascoli, A.S., Kawachi, E. Y.</i>	118
Estudo do Processo de Redução dos Íons Eu Durante a Síntese via Sol-Gel Protéico de Aluminatos de Sr e Ca <i>Montes, PJR, Valerio, M.E.G.</i>	119
INVESTIGATION OF NANOSTRUCTURE AND PROPERTIES OF SOL-GEL DERIVED ZIRCONIUM OXIDE-SPEEK MEMBRANES FOR DIRECT ETHANOL FUEL CELLS <i>Kawaguti C.A., DAHMOUCHE, K, Gomes, A.S.</i>	120
Proton conducting membrane based on SPEEK and modified silica for direct ethanol fuel cell <i>de Ramos Filho, F. G., DAHMOUCHE, K, Gomes, A.S.</i>	121
Expansão térmica negativa e transição de fase do $\text{In}_2\text{Mo}_3\text{O}_{12}$ <i>Ari M., Marinkovic, B. A., Jardim, P. M., de Avillez, R. R., Rizzo, F., Ferreira, F. F.</i>	122
X-ray Study of Carbide Evolution of Cr-Mo Steels during Aging <i>Lemus, L.F., J. H. Rodrigues, dos Santos, D. S., L. H. Almeida</i>	123
Effect of addition of acrylic acid and thioglycolic acid on nanostructure and thermal stability of PMMA/ montmorillonite nanocomposites <i>Soares, B.G., DAHMOUCHE, K, Silva, A.A.</i>	124
Estudo dos catalisadores compósitos à base de Pd e nanoóxidos à base de Nb e de Zr <i>Lagrega, E. R., dos Santos, D. S., Conceição, M. O. T.</i>	125

Fabricação de Strain Gauges para Aplicações em Altas Temperaturas <i>Fraga, M. A., Massi, M., Oliveira, I.C., Furlan, H., Wakavaiachi, S. M., Maciel, H. S.</i>	126
Non-destructive Analyses of Internal Stresses, Texture and Damage in Engineering Materials Using High-Energy Synchrotron X-Ray Diffraction <i>H. (C.) Pinto, Ch. Genzel, A. Pyzalla, T. Wroblewski</i>	127
Characterization of the activation process of LTS industrial catalysts by <i>in situ</i> X ray diffraction <i>Rodella, C. B., Zanchet, D.</i>	128
Development of catalytic materials for glycerol hydrogenolysis <i>R.J.Chimentão, Rodella, C. B., Ferreira, R. A. A., Queiroz, C. M. S., VICENTINI, Valéria Perfeito, Zanchet, D.</i>	129
Estudo dos efeitos do bombardeamento atômico com gás nobre sobre a microestrutura de aços <i>Droppa Jr., R., Ochoa, E.A., H. (C.) Pinto, F. Alvarez, Garcia, J.</i>	130
XRD STUDIES OF ENGINEERING MATERIALS USING THERMOMECHANICAL SIMULATOR <i>Wu, L., Isaac, A., Ramirez, A.J.</i>	131
Friction Stir Welding of ISO 3183 X80M Steel <i>Santos, T. F. A., Ramirez, A.J., Hermenegildo.T,F, Benati, D. M., Afonso, C R M</i>	132
Numerical Modelling and Experimental Analysis during Solidification of Arc Weld in Ni-Cr-Fe Alloys with Hf Additions <i>Unfried S., J., Fonseca, E. B., Afonso, C R M, Ramirez, A.J.</i>	133
<hr/> Parte VIII Métodos e Instrumentação <hr/>	
Pressure cell for XPD, XAS and SAXS experiments using Synchrotron Light <i>Orlando, M. T. D., J.L.Passamai Jr, Martinez, L. G., Rossi, J. L., Corrêa, H. P. S., Garcia, F., Ferreira, F. F., Melo, F. C. L., Souza Jr, F. G.</i>	137
Current Status of the High Energy Resolution System of the XRF Beamline <i>Pérez, C. A., H. J. Sánchez</i>	138
Synchrotron and Neutron Diffraction of Standard Reference Samples for Powder Diffraction Developed at IPEN-CNEN/SP <i>Martinez, L. G., Galvão, A. S. A., Mazzocchi, V. L., Parente, C.B.R., Corrêa, H. P. S., Orlando, M. T. D.</i>	139

THE ZINC DISTRIBUTION IN PROSTATE TISSUES BY μSRXRF <i>Leitão, R.G., Anjos, M. J., Canellas, C.G.L, Pereira, M.O., Pereira, G.R., Correia, R. C., Palumbo, A.J, Souza, P.A.V.R, Ferreira, L. C., Nasciutti, L.E, Lopes, R.T.</i>	140
Scanning of citrus leaves to evaluate stages of citrus greening disease using micro synchrotron radiation X-ray fluorescence in association with chemometric tools <i>Pereira, F. M. V., Milori, D. M. B. P.</i>	141
Microchips de PDMS/SiO₂/Vidro contendo Detecção Condutométrica Sem Contato: Estudo de Configurações e Geometrias dos Eletrodos <i>Lima, R. S., Piazzetta, O.M.H, Gobbi, A. L., Carrilho, E., Coltro, W. K. T., Rodrigues Filho, U.P., Nascente, P. A. P.</i>	142
Detecção direta de raios x com APD de 10 mm x 10 mm <i>Kakuno, E. M., Scorzato. C. R., Giacomolli, B.A.</i>	143
The new XAFS beamline at LNLS <i>Azevedo, G. de M., Fabbris, G. F. L., Sotero, A.P.S., Oliveira, J.J., Gasperini, A. A., Rodrigues, F, Neuschwander, R.</i>	144
Metal mesh resonant filters for terahertz frequencies <i>Melo A. M., Kornberg, M. A., Kaufmann, P., Piazzetta, O.M.H, Gobbi, A. L., Bortolucci, E. C., Zakia, M.B.P., Bauer, O. H., Poglitsch, A., da Silva, A. M. P. A.</i>	145
Design, fabrication and tests of metal microstructures applied to studies of DNA damage <i>Melo A. M., Krawczyk, P., Bortolucci, E. C., Gobbi, A. L., Piazzetta, O.M.H</i>	146
Fabricação de plataformas microfluídicas a partir do uso de toner <i>Coltro, W. K. T.</i>	147
In situ SEM High Temperature Deformation Experiments to Quantification of Susceptibility and Grain Boundary Sliding in Ductility Dip Cracking of Ni-Base Alloys <i>Torres, E. A., Ramirez, A.J.</i>	148
Paper based microfluidic devices for low-cost diagnostics. Bioassays and fundamental issues <i>Carrilho, E.</i>	149
<hr/>	
Parte IX Propriedades Estruturais, Eletrônicas e Magnéticas de Sólidos	
<hr/>	
Fabrication and Testing of RF-MEMS Switches Using PCB Techniques <i>Silva, M. W. B., Kretly, L. C.</i>	153

EXAFS and XANES of Ca₂MnReO₆ under pressure up to 1.2 GPa	
<i>Orlando, M. T. D., J.L.Passamai Jr, Depianti, J. B., Souza, D. O., Rodrigues, V. A., Corrêa, H. P. S., Rossi, J. L., Martinez, L. G., Melo, F. C. L.</i>	154
Properties of nanostructured Pd/gadolinia-doped ceria nanotubes: XPD, XANES and HRTEM investigation	
<i>Muñoz, F.F., Acuña, L. M., Cabezas, M.D., Baker, R.T., Fuentes, R. O.</i>	155
Pressure Effect on Structure of Cardanol/Furfural/PAni Blends A Synchrotron XRD Study	
<i>Souza Jr, F. G., Orlando, M. T. D., Michel, R. C., Pinto, J.C., Cosme, T. A., Oliveira, G. E.</i>	156
The local structure of TM-doped (TM= Fe, Co and Mn) magnetic semiconductor studied by XAS	
<i>Meneses, C. T., Lima, R. J. S., Duque J.G.S.</i>	157
Morphology of PAni / γ-Fe₂O₃ hybrids - A SAXS study	
<i>Marins, J. A., Souza Jr, F. G., Pinto, J.C., Oliveira, G. E., Manzini R., C. H., Lima, L. M. T. R.</i>	158
High Pressure Local Probe of Structural Phase Transitions in RNiO₃ (R= Nd, Pr)	
<i>Nestor E. Massa, Garcia, F., Alonso, J.A.</i>	159
Lattice distortions produced in the X-ray Multiple Diffraction peak under electric field.	
<i>Almeida, J. M. A., dos Santos, A. O., de Menezes, A. S., Cardoso, L.P., Sasaki, J.M.</i>	160
Structural Properties of Pd/Ce-Zr Mixed Oxide Nanotubes	
<i>Acuña, L. M., Muñoz, F.F., Cabezas, M.D., Fantini, M. C. A., Lamas, D. G., Baker, R.T., Fuentes, R. O.</i>	161
EXAFS and XRD study of Pb_{1-x}R_xZr_{0.40}Ti_{0.60}O₃ (R = La, Ba) ferroelectric ceramic materials	
<i>Mesquita, A., Michalowicz, A., Mastelaro, V.R.</i>	162
EXAFS characterization of the local disorder in Y₂O₃ nanoparticles produced via a coconut water-assisted sol-gel method	
<i>Macedo, Z.S., Valerio, M.E.G., Gomes, M.A.</i>	163
Pressure study of Ca₂CrReO₆ by EXAFS and XANES up to 1.2 GPa	
<i>Souza, D. O., Orlando, M. T. D.</i>	164
Structural study of Ca₂CrReO₆	
<i>Corrêa, H. P. S., Cavalcante, I. P., Bozano, D. F., Orlando, M. T. D., Souza, D.O., Martinez, L. G., Rossi, J. L.</i>	165

Development of Conducting Polyaniline/Poly(lactic acid) Nanofibers by Electrospinning <i>Picciani, P.H.S, Soares, B.G., Souza Jr, F. G., MEDEIROS, E. S., MATTOSO, Luiz Henrique Capparelli</i>	166
Structural and dielectric characterization of $Ba_{0,9}Sr_{0,1}Zr_xTi_{1-x}O_3$ system <i>Favarim, H.R., Mastelaro, V.R., Michalowicz, A., Doriguetto, A.C., Neves P.P</i>	167
X-ray absorption spectroscopy characterization of nanocrystalline $SrTi_{1-x}Fe_xO_3$ <i>da Silva, L. F., M.I.B.Bernardi, Mastelaro, V.R.</i>	168
Probing vacancies in CeO_2 thin films through Ce valence states: a XANES and XPS investigation <i>I. L. Graff, V. Fernandes, J. Varalda, P. F. P. Fichtner, AMARAL L., Mosca, D. H.</i>	169
Transições martensíticas em ligas de Heusler do Tipo $Ni_2Mn_{1,44}Sn_{0,56}$ <i>Alves, A.L, Nascimento, V. P., Passamani, E. C., Proveti, J. R., A. Y. Takeuchi</i>	170
X-ray powder diffraction study of fine-grained ZrO_2-Sc_2O_3 dense ceramics <i>Abdala, P. M., Craievich AF, Fantini, M. C. A., Lamas, D. G.</i>	171
EXAFS AND XEOL SIMULTANEOUS MEASUREMENTS OF $CdWO_4$ <i>Novais, S. M. V., Valerio, M.E.G., Macedo, Z.S.</i>	172
XEOL and EXAFS investigations of the long-lasting phosphor $CdSiO_3$ <i>Abreu, C. M., Novais, S. M. V., Silva, R.S., Valerio, M.E.G., Macedo, Z.S.</i> .	173
In-situ structural characterization of nano-sized scandia-doped zirconia. <i>Fernández Werner, L., Suescun, L., Abdala, P. M., Lamas, D. G., Chen, H., Craievich AF</i>	174
Caracterização estrutural da hidroxiapatita usando radiação síncrotron <i>Lima, T.A.R.M., Valerio, M.E.G., Sarmento, V.H.V</i>	175
ESTUDO DO EFEITO DA DOPAGEM NAS PROPRIEDADES MAGNÉTICAS E ESTRUTURAIS DO SISTEMA $Cu_{1-x}TM_xO$ (TM=Fe,Ni,Mn e La) e Al <i>SANTOS, C.L, Duque J.G.S., Meneses, C. T.</i>	176

NANOSTRUCTURAL CHARACTERIZATION OF POLYBUTADIENE-MODIFIED EPOXY RESIN: EFFECT OF THE CURING AGENT <i>Lima, V.D., Soares, B.G., DAHMOUCHE, K</i>	177
IRON-STABILIZED NANOCRYSTALLINE ZrO_2 SOLID SOLUTIONS: A PRELIMINARY STUDY BY X-RAY DIFFRACTION AND VIBRATIONAL SPECTROSCOPIES <i>Alconchel, S. A., Pierini, B. T., Abdala, P. M., Lamas, D. G.</i>	178
ELETRONIC PROPERTIES OF COORDINATION COMPOUNDS OF INDIUM, BISMUTH AND ANTIMONY WITH MALEONITRILEDITHIOLATE (MNT) LIGAND IN THE C1s AND N1s REGIONS <i>Almeida, G.C., Lopes, L. J. S., A.L.F. de Barros, Guerra, A. C. O., Ferreira, G. B., Turci, C. C.</i>	179
ELECTRONIC PROPERTIES OF THE NEUTRAL COORDINATION COMPOUNDS OF THE DMIT LIGAND IN THE S 1s REGION. <i>Turci, C. C., Ferreira, G. B., Guerra, A. C. O., Lopes, L. J. S., Comerlato, N.M.</i>	180
Estructura atómica, dinámica local, anarmonicidad y expansión térmica en nanoaleaciones Fe_xAu_{100-x}: Determinación del potencial interatómico mediante EXAFS empleando teoría de perturbaciones estadístico-cuántica. <i>Lede, E. J., Socolovsky, L. M.</i>	181
Study of the Morphology Evolution of Vanadium Pentoxide Nanostructures by TEM and SAXS <i>Avansi, W., Oliveira, C. L. P., Leite, E.R., Ribeiro, C., Mastelaro, V.R.</i>	182
Transition Metal Cations Doping in Ammonium Dihydrogen Phosphate As Examined by Synchrotron Radiation Renninger Scanning <i>C. M. R. Remedios, Lai, X, Roberts, K. J., GOMES, E.J.L., de Menezes, A. S., Cardoso, L.P.</i>	183
Influence of microstructure on the corrosion behavior of nitrocarburized AISI H13 Influence of microstructure on the corrosion behavior of nitrocarburized AISI H13 tool steel obtained by pulsed DC plasma <i>Basso, R. L. O., Candal, R.J., C. A. Figueroa, Wisnivesky, D., F. Alvarez</i> ..	184
Acoplamento magnético entre os íons de Gd e Pr e efeito magnetocalórico no composto $Gd_{0,5}Pr_{0,5}Al_2$ <i>A. Magnus G. Carvalho, Garcia, F., de Sousa, V. S. R., von Ranke, P. J., Rocco, D. L., Loula, G. D., E. J. Carvalho, Coelho, A. A., da Silva, L. M., Gandra F. G</i>	185

Structural and optical properties of CaTiO₃ perovskite-based materials obtained by microwave-assisted hydrothermal synthesis: An experimental and theoretical insight <i>Moreira M. L., Mastelaro, V.R., Longo, V. M., E. C. Paris, Longo, E., Varela, J.A., Andrés, J.</i>	186
Study Of Copper Hardened Composites With Nanoparticles Of Alumina <i>Bagnato, O. R., Francisco, F. R., Barros, R. M.</i>	187
Gênese e propriedades estruturais e fotocatalíticas de partículas micro e nanoestruturadas de ZnO. <i>Feltrin, C.W, Rodrigues, A, Bernardi, F., Moraes, J., Alves, M.C.M.</i>	188
Propriedades Estruturais de Vidros Aluminato de Cálcio Dopados com Praseodímio <i>Sampaio, J. A., Peixoto, S. M. B., Filadelpho, M. C., dos Santos, D. R., Baesso, M.L.</i>	189
Caracterização do ambiente químico do neodímio em vidro aluminato de cálcio com baixa concentração de sílica <i>Peixoto, S. M. B., Filadelpho, M. C., dos Santos, D. R., Sampaio, J. A.</i>	190
Controle morfológico de nanopartículas de óxido de gadolínio dopados com íon európio(III) <i>Gaspar, R. D. L., Sigoli, F.A., MAZALI, I. O.</i>	191
CARACTERIZAÇÃO DE ROCHAS CARBONÁTICAS <i>Bagnato, O. R., Francisco, F. R., Brandão, E.M.</i>	192
In-plane strain anisotropy due to induced re-crystallization process (IBIEC) by means of X-ray multiple diffraction <i>dos Santos, A. O., Lang R, de Menezes, A. S., Menezes, E. A., AMARAL L., Cardoso, L.P.</i>	193
Small-angle X-ray scattering (SAXS) of ordered magnetic systems <i>Beron, F., Vargas, J. M., Sharma, S.K., Pirota, K. R., Knobel, M.</i>	194
Microfluídica em PDMS e papel com detecção eletroquímica <i>Carvalho, R. F., Kubota, L.T., Martins, L. F.</i>	195
Construção de Dispositivos Microfluídicos Contendo Multi-Canais e Eletrodos Integrados para Detecção Amperométrica Simultânea <i>Silva, J. A. F.</i>	196
<hr/>	
Parte X Superfícies, Interfaces e Nanossistemas	
<hr/>	
Characterization of ultra-thin films of Au deposited on Pd(111) <i>Pancotti A., Carazzolle M.F., Tallarico, D.A., de Siervo A., Nascente, P. A. P., Landers R, Kleiman, G.G.</i>	199

Estudo da morfologia de híbridos de maghemita e polianilina usando AFM <i>Lopes, M. C., Souza Jr, F. G., Marins, J. A., Pinto, J.C., Oliveira, G. E., Manzini R., C. H., Lima, L. M. T. R.</i>	200
Estudio de superficies de películas de O-DMS utilizando TXRF-XANES <i>A.M. Mudarra Navarro, F. Golmar, Rodríguez Torres, C. E.</i>	201
SMALL-ANGLE X-RAY SCATTERING STUDIES IN COLLOIDAL SILICA/PMMA NANOCOMPOSITES <i>Peruzzo, P. J., Anbinder, P. S., Plivelic, T.S., Amalvy, J. I.</i>	202
Fotofragmentação do politiofeno induzida por luz síncrotron na borda 1s do enxofre <i>Rita, J.R.S., Rocco, M.L.M., Roman, L. S., Arantes, C.</i>	203
EFFECTS OF ULTRAVIOLET LIGHT ON ALQ₃ THIN FILMS STUDIED BY PHOTOABSORPTION AND PHOTOEMISSION <i>Ricardo, W., Rocco, M.L.M., M. Cremona, Araujo, G.S, Quirino, W.</i>	204
Nitrate hydrogenation on Pt_xIn/Al₂O₃. EXAFS and XANES characterization of fresh and used catalysts <i>Ramallo-López, J. M., Requejo, F. G., E.E.Miro, Marchesini, F. A.</i>	205
In-situ XANES study of Pt_xPd_{1-x} (x = 1, 0.7 or 0.5) nanoparticles subjected to H₂ reduction <i>Bernardi, F., Alves, M.C.M., KILIAN, A. S., BOITA, Jocenir., Rodrigues, A, Morais, J.</i>	206
Characterization of titanium dioxide films obtained with a vacuum arc <i>A. Kleiman, Lamas, D. G., A. Márquez</i>	207
Observation of Pd magnetism in carbon nanotube catalyst nanoparticles by X-ray circular dichroism <i>Roa, D. B, Lacerda, R. G., Magalhaes-Paniago, R., de Siervo A.</i>	208
Structural analyses of Laponite RD particles by SAXS <i>Batista, T., MACHADO, D. S., Oliveira Neto M., Schmitt, C.C. ou Cavalheiro, C.C.S, Polikarpov, I., A.F. Craievich, Neumann, M. G.</i>	209
PROPRIEDADES ESTRUTURAIS E MAGNÉTICAS EM NANOPARTÍCULAS DE $\alpha - Fe_2O_3$ <i>Lima, R. J. S., Jesus, J. R., Cunha, T. R., Moura, K. O., Duque J.G.S., Meneses, C. T.</i>	210
Electronics, local structure and morphology of heterogeneous nanoparticles investigated by SAXS and XAFS techniques <i>Giovanetti, L. J., Ramallo-López, J. M., Requejo, F. G., E. V. Shevchenko, Craievich AF</i>	211

Aplicação de AFM/EFM na caracterização de eletrodos carbono cerâmicos	
<i>Arguello, J., ARENAS, Leliz Ticona, Pimentel, V. L., Gushikem, Y.</i>	212
Structure of PbTe(SiO₂)/SiO₂ multilayers deposited on Si (111)	
<i>Kellermann, G., Rodriguez, E., Cesar, C. L., E. Jimenez, Barbosa, L. C., Craievich AF</i>	213
Caracterização de Processos de Silanização em Superfície de SiO₂ por MEV, XPS e AFM para Construção de Biossensores	
<i>Lima, R. S., Rodrigues Filho, U.P., Nascente, P. A. P., Piazzetta, O.M.H, Gobbi, A. L., Pimentel, V. L., Coltro, W. K. T., Carrilho, E.</i>	214
Efficient Microwave-Assisted Hydrothermal Synthesis of CuO Sea Urchin-Like Architectures via a Mesoscale Self-Assembly	
<i>Volanti, D.P., Orlandi, M.O., Longo, E., Andrés, J.....</i>	215
Alterações composicionais induzidas por luz ultravioleta de vácuo em filmes finos calcogênicos	
<i>Moura, P. R., Almeida, D. P.</i>	216
Caracterização estrutural e química da superfície de Cu₈₄Al₁₆(100) e Cu₉₀Au₁₀(100) usando XPD	
<i>Martins, M. D., Cotta, A. C., Soares, E.A., W. A. A. Macedo</i>	217
Síntese e caracterização de nanopartículas de Pt suportadas em γ-alumina.	
<i>Meira, D. M., Ribeiro, R.U., Zanchet, D., Bueno, J.M.C.</i>	218
Characterization of TiO₂ films made by anodic oxidation on Ti-6Al-4V	
<i>Vera, M. L., Ares, A.E., Rosenberger, M. R., Lamas, D. G., Schvezov, C. E.</i>	219
Mechanical Deformation of Gold Atomic-size Nanowires	
<i>Lagos, M.J., Sato F., D. S. Galvao, Ugarte, D.</i>	220
Study under pressure of XANES spectra in K-edge of zirconium in ZrO₂-CeO₂ nanopowders at different concentrations of ceria	
<i>Caravaca, M.A., Casali, R.A., Ponce, C.A., Garcia, F., Lamas, D. G., Fuentes, R. O.....</i>	221
Estudo de catalisadores industriais LTS por absorção de raios X <i>in situ</i> no processo de ativação e na reação de deslocamento água - gás	
<i>Oliveira, D. C., Oliveira, M. P., Zanchet, D.</i>	222
Estudo da ativação de catalisadores comerciais LTS por XPS	
<i>Oliveira, D. C., Zambello, F. R., Zanchet, D.....</i>	223
Monitoring the formation of Cu-based nanoparticles by in-situ DXAS	
<i>BOITA, Jocenir., Bernardi, F., KILIAN, A. S., Rodrigues, A, Alves, M.C.M., Morais, J.</i>	224

Structural Properties Control of InP Semiconductor NWs <i>Th. Chiaramonte, Tizei, L. H. G., Ugarte, D., Cotta, M.A.</i>	225
Obtenção e crescimento de nanopartículas de prata em N,N-dimetilformamida <i>LUIZ P. DA COSTA, Silva, JMDE, Souza, E. R., Sigoli, F.A., MAZALI, I. O.</i>	226
Characterization by High Resolution Transmission Electron Microscopy of Nanometric TiO₂/MoO₃ Synthesized in Porous Vycor Glass. <i>Santos, E. B., MAZALI, I. O.</i>	227
Utilização da espectroscopia de alta resolução da borda de absorção (XANES) na investigação das propriedades oxi-redutoras de catalisadores a base de cério <i>Mortola, V. B., Duarte, R. B., Bueno, J.M.C.</i>	228
Análise de difração de raios-x em nanoestruturas cristalinas via método de elementos finitos <i>Calseverino, C., Malachias, A.</i>	229
Síntese e estudo da remoção de ligante de um nanocatalisador de Ni para aplicações em reações de reforma <i>Braga, A. H., Parizotto, N. V., Borin, A., Zanchet, D.</i>	230
Determination of the thickness and crystalline structure of TiO₂ coatings made by sol-gel dip coating <i>Alterach, M.A., Rosenberger, M. R., Ares, A.E., Lamas, D. G., Schvezov, C. E.</i>	231
Characterization of magnetic nanourchins and nanoflowers <i>Socolovsky, L. M., Lloret, P.E., Ybarra, G., Moína, C</i>	232
A novel approach for high resolution strain mapping and elastic properties assessments of alloyed strained nanostructures <i>Montoro, L. A., Medeiros-Ribeiro, G., Ramirez, A.J.</i>	233
Analysis of Sb dopant influence on SnO₂ nanoparticles morphology and growth mechanism <i>Stroppa, D. G., Montoro, L. A., Leite, E.R., Ramirez, A.J.</i>	234

Parte I

Plenárias

Hard X-ray Photoemission Spectroscopy on complex systems: from surface to bulk sensitivity

G. Panaccione¹

Consiglio Nazionale delle Ricerche - Milano Italy

High resolution Hard X-Ray (> 5 keV of kinetic energy) PhotoEmission (HAXPES) has proven to be an excellent tool not only to reach high bulk sensitivity but also to directly access the electronic states near the Fermi level, i.e., to the energy scale of the electronic correlation. In this talk, a review of the recent results obtained within the VOLPE (VOLume PhotoEmission from solids) project, operational at beamline ID16 of ESRF, will be presented, together with a review of selected results from other HAXPES experimental setups. In particular, we will report results obtained on strongly correlated systems (cuprates, vanadates, manganites), where the comparison between truly bulk sensitive core level and valence band spectra i) allows a reliable estimate of the correlation term and ii) reveals new screening mechanism in transition metal oxides. Furthermore, HAXPES data from buried interfaces will be presented, where exploiting a depth sensitivity as high as 150 Angstrom, a reliable spectroscopic access to real devices or capped samples is obtained.

Acknowledgements:

The Macromolecular Crystallography Village at the Diamond Light Source: High-throughput and automation from microfocus to MAD

G. Evans¹

Diamond Light Source - Didcot Oxfor United Kingdom

Diamond Light Source is a 3rd generation synchrotron offering significant facilities for structural life science research. One component of the life sciences is a suite of six beamlines for macromolecular crystallography (MX), five of which are now in either full operation or being commissioned and one that is at the design stage. The three fully operational beamlines are high throughput MAD beamlines satisfying the majority of scientific demand. The fourth line, now in early operation, is a dedicated tuneable microfocus MX work. The fifth line is a fixed wavelength high throughput beamline. The presentation outlines these beamline facilities paying particular attention to the design and use of the I24 microfocus beamline and how it integrates with the nearby Wellcome Membrane Protein Laboratory to create a unique facility for producing diffraction quality crystals and diffraction data from very challenging structural biology projects. Results from the first year of the I24 beamline will be presented along with future plans and requirements.

Acknowledgements:

Synchrotron based X-ray microprobes: Towards a multimodal approach

J. Susini¹

European Synchrotron Radiation Facility - Grenoble Cedex France

The dramatic growth of nanoscience and nanotechnologies is currently fostering the development of high spatial resolution analytical techniques [1]. In this context, synchrotron based techniques have the potential to become mainstream tools for analysis, imaging and spectroscopy in a number of applications, as exemplified by the current evolution of hard X-ray microscopy. Hence, considering the concomitant developments of laboratory instruments and dedicated synchrotron beamlines worldwide [2], a very competitive context can be anticipated for the coming years. Within this perspective, synchrotron based analytical techniques (diffraction, imaging and micro-spectroscopies) will play an important role by offering unique capabilities in the study of complex systems. Ultimately, this complexity can be envisioned in three dimensions: composition, time and space. The main fields of applications are driven by the unique attributes of X-ray microscopy in this spectral range [3]: i) access to K-absorption edges and fluorescence emission lines of medium-light elements and L,M-edges of heavy materials for microspectroscopy, chemical or trace element mapping; ii) higher penetration depths compared to soft X-rays allowing imaging of thicker samples; iii) favorable wavelengths for diffraction studies and iv) generally large focal lengths and depths of focus which are advantageous for the use of specific sample environments (in-situ, high pressure, controlled temperatures.). Typical experiments can be broadly divided into two categories: i) morphological studies which require high spatial resolution and are therefore well adapted to 2D or 3D transmission full-field microscopy. ii) studies dealing with co-localization and/or speciation of trace elements in heterogeneous matrices at the sub-micron scale. Scanning X-ray microscopy, in transmission and/or X-ray fluorescence modes, tends to be better suited for the latter cases, which often require both low detection limits and spectroscopic analysis capabilities. Compared to other techniques, synchrotron X-ray fluorescence microprobes display a unique combination of features. Associated with high detection efficiency, the radiation damage is minimized and accurate quantification is possible [4]. The possibility of in-situ experiments remains a unique attribute of synchrotron based analytical methods. Photon penetration depth of hard X-rays enables specific sample environments to be developed to study realistic systems in their near-native environment rather than model systems. The ability to perform in-situ analysis with environmental chambers offering high or low temperature conditions, high pressure, or preserving sample hydration explains the increasing interest from communities such as Planetary and Earth sciences [5], environmental science [6], biology [7] and cultural heritage [8]. A natural evolution of the elemental (X-ray fluorescence) or structural (X-ray diffraction) mappings are the extension towards in-depth third dimension. The knowledge of the elemental variation along this third dimension intrinsically improves the data

quality and therefore its interpretation. Compared to the standard absorption X-ray Computed Tomography, Fluoro-tomography is more challenging since it is limited by self-absorption and matrix effect. A multimodal strategy has been developed to overcome these physical limitations and is based on an algorithm solution which relies on the combination of several signals (transmission, fluorescence and scattering) to derive the volumetric distribution of elements [9-10]. Similar approach has been used for X-ray diffraction computed tomography as local structural probe for heterogeneous diluted materials [11]. This lecture aims at giving a short overview of the main development trends of synchrotron based X-ray microscopy and spectro-microscopy. Following a brief description of their characteristics, the strengths and weaknesses of spectro-microscopy techniques will be discussed and illustrated by examples of applications in materials sciences, biology and environmental science.

Acknowledgements: The Author wishes to thank M. Salomé, R. Tucoulou, G. Criado-Martinez, P. Bleuet, M. Cotte, J. Cauzid, S. Bohic, P. Cloetens and A. Solé for their contributions.

Referências

- [1] Adams, Van Vaek, R. Barret, *Spectrochim Acta B60* (2005) [2] M. Howells, C. Jacobsen and T. Warwick in *Science of Microscopy*, Vol. II, ed. P.W. Hawkes and J. C.H. Spence, (Springer) (2007). [3] J. Susini, M. Salomé, B. Fayard, R. Ortega and B. Kaulich, *Surf. Rev. Lett.*, 9 (2002). [4] B. Fayard, M. Salomé, K. Takemoto, H. Kihara, J. Susini, *Journal of Electron Spectroscopy and Related Phenomena*, 170, 19-24 (2009). [5] P. Bleuet, A. Simionivichi, L. Lemelle, T. Ferroir, P. Cloetens, R. Tucoulou and J. Susini, *Applied Physics Letters*, 92 (2008). [6] E. Lombi and J. Susini, *Plant Soil*, MARSCHNER REVIEW, 17 January (2009). [7] S. Bohic, K. Murphy, W. Paulus, P. Cloetens, M. Salomé, J. Susini and K. Double, *Analytica Chemistry*, 80 (24) (2008). [8] M. Cotte, J. Susini, J. Dik, K. Janssens, *Accounts of Chemical Research*, in press. [9] B. Golosio, A. Somogyi, A. Simionivichi, P. Bleuet, J. Susini, *Applied Physics Letters* 84(12) (2002). [10] P. Bleuet, P. Cloetens, P. Gergaud, D. Mariolle, N. Chevallier, R. Tucoulou, J. Susini and A. Chabli, *Review of Scientific Instruments*, 80 (2009). [11] P. Bleuet, E. Welcomme, E. Dooryhee, J. Susini, J-L Hodeau and Ph. Walter, *Nature Materials* 7(6) (2008).

Pretreatment technologies for production of 2G bioethanol from Agricultural waste and crops

A.B. Thomsen

Risø National Laboratory

2nd generation (2G) bioethanol is on the verge of industrialisation and companies around the world are starting up demonstration plants. One of the heaviest economical posts of the processes involved in 2G bioethanol production is the pretreatment of biomass, which is needed to open the rigid structure of lignocellulose facilitating further enzymatic hydrolysis to fermentable sugars. In Denmark, Ris DTU has studied and developed different pretreatment technologies for more than 20 years with special emphasis on conversion of agriculture waste and crops to ethanol. Among the most significant results from this research is development of two promising pretreatment systems, the wet oxidation process, which is now close to commercialization by the company BioGasol and the IBUS (hydrothermal) pretreatment, which is now ready for demonstration (4000 kg/hour capacity) in Kalundborg in Denmark. The IBUS facility is a milestone in Danish bio-ethanol research and was presented at the climate conference COP15 as a main event. New pretreatment technologies are still under development. One of the more promising is plasma pretreatment being a pure chemical treatment at ambient temperature and pressure using ozone as reagent for oxidizing lignin and improving the following enzymatic hydrolysis and fermentation. Ensiling (or silage treatment) is another promising pretreatment technology being an anaerobic biological process that conserves biomass and at the same time degrades lignin and opens for enzymatic hydrolysis of polysaccharides to simple sugars. The advantage in both methods is the high dry matter loading being more than 50%.

The different pretreatment technologies will be presented and discussed for their future utilisation in bioethanol production and biorefinery concepts.

Parte II

Biologia Estrutural

Análises estruturais do estado oligomérico do receptor ativador da proliferação de peroxissomo isotipo α através de SAXS

Bernardes, A.¹, Oliveira Neto M.¹, and Polikarpov, I.¹

Universidade de São Paulo - São Carlos - São Carlos SP Brazil

Os receptores ativadores da proliferação de peroxissomos (PPARs) possuem um importante papel no controle de diversos processos biológicos relacionados, principalmente ao metabolismo lipídico e ao processo inflamatório, desempenhando papéis-chave em várias doenças cardiovasculares. Na expressão gênica, os PPARs se ligam a elementos responsivos específicos após a heterodimerização com receptores X retinóides e ativam a transcrição em resposta a uma variedade de ligantes endógenos e exógenos, incluindo certos ácidos graxos e fibratos. A caracterização desse receptor pode levar ao melhor entendimento de sua função e o desenvolvimento de moléculas alvos para o tratamento de muitas doenças metabólicas. Como o modo de dimerização afeta diretamente as interfaces disponíveis para interação com corretores e, portanto, diretamente o processo de regulação transcricional realizada pelos receptores nucleares, estudos mais detalhados de oligomerização dos receptores nucleares estão sendo necessários, pois homo- e heterodimerizações são alternativas que podem representar um nível adicional (e pouco estudado até agora) de regulação de funcionamento de receptores nucleares. Para melhorar nossa compreensão do funcionamento do PPAR α , assim como as interações entre receptor:ligante e receptor:receptor, estudos oligoméricos foram realizados com a proteína em solução através do uso de espalhamento de raios-X a baixo ângulo (SAXS). Como resultado, nós apresentamos análises estruturais do estado oligomérico do PPAR α LBD em solução, para diferentes concentrações de proteína e a formação de heterodímeros na presença de seu parceiro obrigatório de heterodimerização, RXR. Esses resultados mostraram claramente que a proteína apresenta-se monomérica em solução, diferente dos outros membros desta superfamília de receptores nucleares, podendo ser este um estado inativo da proteína no processo de regulação transcricional.

Acknowledgements: Este trabalho foi suportado pela FAPESP

Structural Studies of Selenocysteine Synthase (SELA) from *Escherichia coli*

Cassago, A.¹, Manzine, LR¹, Pereira, H.M¹, Horjales, E.¹, and Thiemann, O. H.¹

Universidade de São Paulo - São Carlos - São Carlos SP Brazil

The biosynthesis of the 21th amino acid, selenocysteine (Sec or U) requires a complex enzymatic machinery composed of Selenocysteine Synthase (SELA), Selenocysteine Elongation Factor (SELB or EFSec), Selenophosphate Synthetase (SELD) and a specific tRNA^{sec} (SELC). The selenocysteine residue is incorporated into a nascent protein at a UGA stop codon that is marked as a Sec incorporation site by the presence of a Selenocysteine Insertion Sequence (SECIS). SELA plays a central role in this pathway by modifying the serine residue in the tRNA^{sec} and converting it into selenocysteine. This enzyme forms a homodecameric complex that specifically recognizes and binds to tRNA^{sec}. The specific interaction of SELA and its cognate tRNA remains unclear. Our aim is to elucidate the SELA-tRNA^{sec} molecular recognition mechanism. For this purpose, we have initiated a crystallization screening program to identify the conditions of obtaining SELA and SELA-tRNA^{sec} crystals. As preliminary results we have crystals of SELA protein and SELA-tRNA^{sec} complex diffracting at a resolution ranging from 7 to 20. This data was collected at the Laboratório Nacional de Luz Síncrotron (LNLS) located in Campinas, SP. Since these results, we are trying new conditions to increase the quality of the crystals to a better resolution. Our first analysis suggest a trigonal or hexagonal symmetry from the data so far collected.

Acknowledgements: This work was supported by IFSC, LNLS and FAPESP.

THE CRYSTAL STRUCTURES OF HUMAN TRANSTHYRETIN (TTR) BINDING FLAVONOIDS

Trivella, D.B.B.¹, REIS, C.V.¹, and Polikarpov, I.¹

Universidade de São Paulo - São Carlos - São Carlos SP Brazil

Human transthyretin (TTR) is a tetrameric beta-sheet rich carrier protein involved in amyloid diseases. TTR carries two identical funnel shaped hormone binding sites placed at its tetramer interface. These channels naturally bind the thyroid hormone thyroxine (T4) in human plasma. However, less than 10% of TTR is bound to T4 in normal conditions. The free tetramers are more propensely to dissociate and the resulting monomeric subunits can undergo conformational changes, leading to re-assembly into amyloid fibrils. TTR point mutations can accelerate tetramer dissociation and/ or monomer unfolding, resulting in early onset of TTR amyloidosis. Different classes of small molecules can bind into the free TTR T4 sites, strongly delaying TTR fibril formation. However, the majority of TTR fibril formation inhibitors display side effects under prolonged use. Therefore, we are testing a set of food flavonoids as TTR inhibitors using a well known TTR acid mediated aggregation assay. The flavonoids pointed as moderated and good TTR inhibitors from initial acid aggregation screenings were select. TTR acid aggregation curves were then carried out with different concentrations of the selected flavonoids to obtain the EC50 values. Concomitantly, these compounds were submitted to co-crystallization experiments with the wild type and the V30M mutant human TTR. Good crystals were obtained after 3 days in a PEG based crystallization screening. X-ray diffraction experiments were conducted at the MX-2 beam line (LNLS Campinas, Brasil) resulting in excellent data sets collect with approximately 1.7 resolution. After data processing and phasing, a well electron density was verified for the majority of the flavonoids tested. Protein and ligand atoms were refined returning good atomic models for TTR interaction with flavonoids. Data revealed that the number and position of the hydroxyl groups attached to the bioflavonoids play important role in their molecular recognition to TTR. Furthermore, the number, type and distance of ligand:protein contacts observed in the crystallographic data correlate well with the EC50 values extracted from the acid aggregation experiments. These data are important to guide further small molecule development to treat TTR amyloid diseases.

Acknowledgements: This work was supported by grants from Fundação de Amparo a Pesquisa do Estado de São Paulo (FAPESP) and Conselho Nacional de Desenvolvimento Científico e Tecnológico (CNPq). We are grateful for the Brazilian National Synchrotron Light Laboratory (LNLS, Campinas, Brazil) for the use of beam line MX-2.

Deteción de la presencia de drogas del tipo P-C-P en tejido óseo humano, de pacientes con osteoporosis

Fernández de Rapp, M. E.¹ and Fábregas, I. O.¹

Consejo Nacional de Investigaciones Científicas y Técnicas - Buenos Aires Argentina

Pequeñas cantidades de tejido óseo de pacientes de osteoporosis, que habiendo sufrido alguna fractura fueron sometidos a intervenciones quirúrgicas con pérdidas de porciones mínimas de hueso, se trataron con dos drogas del tipo P-C-P (alendronato y risedronato de sodio). Los fragmentos óseos, de menos de 2g, fueron lavados y molidos en mortero, y se colocaron en un molino planetario durante dos períodos de tres horas cada uno. Las muestras fueron rotadas a una velocidad de 100 rpm, para estimular el contacto entre los polvos. De las 18 muestras, a nueve se les agregó 1g de alendronato monosódico trihidratado (A) y a otras nueve 1g de risedronato de sodio hemipentahidrato (R), en una suspensión de alcohol etílico. Se extrajo el alcohol y se lo reemplazó por agua destilada. Las muestras se colocaron en una estufa de cultivo a 35 x C durante un mes y finalmente fueron lavadas hasta la extracción total de la parte soluble. Las muestras fueron analizadas por XRD en el LNLS y en CITEFA, por FTIR en CITEFA, se calcularon las relaciones Ca/P y se hicieron micrografías. En todos los análisis se detectó la presencia de un recubrimiento en las partículas del polvo de huesos. La disminución de la relación Ca/P estadísticamente significativa confirma el aporte de fósforo de los P-C-P. Las fases formadas sobre los huesos no corresponden a polimorfos conocidos de las drogas utilizadas. Las fases presentes no han sido encontradas en la bibliografía ni entre las patentes de todos los polimorfos del A o del R. Aparentemente, la Ha no ha sufrido ninguna alteración importante, conservando su estructura cristalina. Sus parámetros de red están en los valores correspondientes a la Ha hexagonal P63/m. Las drogas utilizadas son de segunda y tercera generación. La presencia del N en formas más complejas determina el aumento de su poder para disminuir o detener la resorción del tejido óseo. Las pruebas clínicas de la utilización del R han demostrado que es 100 veces más activo que el A en la disminución de los porcentajes de fracturas, relación que no está muy de acuerdo con el pequeño aumento en la densidad ósea (BMD) del paciente bajo tratamiento con R. Según se ve en las micrografías el material depositado en la superficie del hueso es del tipo rod-like con estructura ortogonal (cúbica o tetragonal). El A forma en la superficie del hueso una capa de partículas muy pequeñas de forma esférica aplanada aparentemente en una capa continua.

Acknowledgements: R. Droppa, D12A-XRD1 del LNLS, A. Fernandez, R. Tarulla de CITEFA y Personal de microscopía del CMA, de CITEFA y de la CNEA.

Determination of the molecular weight of proteins in solution from a single SAXS measurement on a relative scale

Oliveira Neto M.¹, Fischer, H.², Napolitano, H. B.³, Polikarpov, I.¹, and Craievich AF²

¹ Universidade de São Paulo - São Carlos - São Carlos SP Brazil

² Universidade de São Paulo - São Paulo - São Paulo SP Brazil

³ Universidade Estadual de Goiás - Anápolis GO Brazil

An important step in the characterization of proteins is the determination of their molecular weights and their multimeric state in solution. Accuracies of classical methodologies for the determination of the molecular weight of proteins in dilute solution were recently evaluated by Mylonas and Svergun [1]. These authors demonstrate that the molecular weight of a protein can be obtained by comparing the experimental SAXS curve produced by the protein in dilute solution (*i*) to another experimental SAXS curve corresponding to a standard protein with known molecular weight, or (*ii*) to a SAXS curve corresponding to pure water leading in this case to the determination of SAXS intensity of the studied protein in an absolute scale. Both of these procedures require the determination of at least two SAXS curves. In addition, the first procedure requires the precise knowledge of the protein concentration, which is frequently not known with high accuracy, and the second method needs the determination of the SAXS intensity by water with a considerable precision, which implies in rather long counting times. Both methodologies yield the molecular weight of proteins with an error of about 10 % provided the solute concentration is measured with an accuracy of 5–10 %, which might not always be straightforward. A novel procedure for the determination of the molecular weight of proteins in diluted solution from a single SAXS curve measured on a relative scale is available, by using experimental data of a single small angle X-ray scattering (SAXS) curve measured on a relative scale. This procedure does not require the measurement of SAXS intensity on an absolute scale and does not involve a comparison with another SAXS curve determined from a known standard protein. The proposed procedure can be applied to monodisperse systems of proteins in dilute solution, either in monomeric or multimeric state, and it was successfully tested by applying it to SAXS data measured for 21 proteins with known molecular weights. The molecular weights determined by using this novel method of all the measured set deviate from their known values by less than 10 % and the average discrepancy was 5.3 %.

[1] E. Mylonas and D. I. Svergun. 2007 *J. Appl. Cryst.* **40**, 245249.

Acknowledgements: This work was supported by Fapesp.

Structural analysis of the carbohydrate recognition domain from lectin of *Canavalia brasiliensis* and their relation with nitric oxide-release

Delatorre, P.¹, Bezerra, E.H.S.², Rocha, B.A.M.², Naganao, C.S.², Moura TR², Bezerra, M. J. B.², and Cavada, B.S.²

¹ Universidade Federal da Paraíba - João Pessoa PB Brazil

² Universidade Federal do Ceará - Fortaleza CE Brazil

Diocleinae lectins are a group with high homology in their primary structure that complains Carbohydrate Recognition Domain (CRD) and metal bind site. Legume lectins shows discrepancies in biological activities, which are wildly investigate through haemagglutination inhibition assay, isothermal titration microcalorimetry and co-crystallization with mono and oligosaccharides. Here we report the crystallization of *Canavalia brasiliensis* seed lectin, identifying the α -aminobutyric acid (Abu) binding pocket. Based on the hypothesis that carbohydrate affinity performed by lectins is related to CRD design, the relationship between tridimensional structural and NO release was used to elucidate changes that justify such differences. Our study establishes a correlation between CRD amino acid side chains position and this biological stimulation.

Acknowledgements: This work was partly financed by Fundação Cearense de Apoio ao Desenvolvimento Científico e Tecnológico (FUNCAP), Conselho Nacional de Desenvolvimento Científico e Tecnológico (CNPq), Coordenação de Aperfeiçoamento de Pessoal de Nível Superior (CAPES), Laboratório Nacional de Luz Síncrotron (LNLS), Campinas Brazil.

Crystal structure of Lys-49-phospholipase A2 myotoxin from *Bothrops neuwiedi* complexed to myristic acid

Rocha, B.A.M.¹, Delatorre, P.², Toyama MH³, and Cavada, B.S.¹

¹ Universidade Federal do Ceará - Fortaleza CE Brazil

² Universidade Federal da Paraíba - João Pessoa PB Brazil

³ Universidade Estadual de Campinas - Campinas SP Brazil

The enzyme phospholipase A2 (PLA₂) catalyzes the hydrolysis of the sn-2 acyl chain of phospholipids, forming fatty acids and lysophospholipids. Many basic snake phospholipases with molecular mass between 13KDa and 16 KDa were purified from *Bothrops* genus. These proteins present an amino acid substitution at position 49 (Aspartic to Lysine). Due to this modification they display a weaker catalytic activity, which occurs by the reduction of Ca²⁺ binding properties. Although, PLA₂ (Lys-49) is still capable to disrupt biologic membranes by charge interactions with sulfate glycans associated to cell membrane. This work objective obtaining phospholipase (K49) tridimensional structure from *Bothrops neuwiedi*, and intend to understand the mechanism calcium-independent through physicochemical characteristics of the enzyme and the interaction of fatty acid placed at non-catalytic enzyme site. The purified protein was crystallized with 0.1 M Tris-HCl pH 8,5, 0.2 M lithium sulfate, and 30 % (w/v) PEG 4000 as a precipitating agent using the sitting-drop vapour-diffusion method. The crystals belonged to the monoclinic space group P21, with unit-cell parameters a = 38.8 , b = 70.4 , c = 44.0 , α = 90.0, β = 109.3 and γ = 90.0. The structure was refined at 2.2 of resolution to a final R factor of 0.211 and R free of 0.229, using 11,130 unique reflections. This is a dimeric PLA₂ structure in which the catalytic site is comprised by HIS48, LYS49 and TYR49. The inactive enzymatic sites of all molecules are located on the surface and are fully exposed to the solvent, in this site can be observed a myristic acid bound. The final protein model consists of 121 amino-acid residues and 71 water molecules.

Acknowledgements: This work was partly financed by FUNCAP, CNPq, CAPES. We also thanks to Laboratório Nacional de Luz Síncrotron (LNLS), Campinas Brazil.

Estruturas de baixa resolução de Celobiohidrolase I de *Trichoderma harzianum* 3844.

Rosseto, Flávio R.¹, Serpa, V.I.¹, Colussi, F.¹, Oliveira Neto M.¹, and Polikarpov, I.¹

Universidade de São Paulo - São Carlos - São Carlos SP Brazil

Atualmente fontes de energia alternativas e sustentáveis têm ganhado cada vez mais importância. Desta forma, estudos vêm auxiliando na busca de novas soluções e melhorias destas fontes.

O bagaço de cana, uma fonte ainda pouco utilizada, é uma das mais abundantes biomassas existentes no Brasil e a transformação deste em escala industrial em bioetanol através de hidrólise enzimática da celulose mostra-se uma fonte energética bastante promissora. Complexos celulolíticos necessários para a hidrólise são produzidos principalmente por fungos filamentosos e algumas fontes bacterianas.

As celobiohidrolases (exoglicanases), constituem a classe de enzimas expressa em maior quantidade no complexo celulolítico de *Trichoderma reesei*. Para a hidrólise de moléculas de celulose são necessárias, ainda, outras celulasas em conjunto com estas enzimas: as beta-glicosidases e as endoglucanases. A CBHI atua na catálise da hidrólise de ligações glicosídicas β (1-4) nas moléculas de celulose, liberando celobiose das extremidades não redutoras das cadeias.

O conhecimento estrutural das enzimas destes complexos celulolíticos é uma ferramenta fundamental para o progresso da produção de bioetanol de segunda geração. Visando tais estudos, análises estruturais por Espalhamento de raios-x a baixo ângulo (SAXS) foram utilizadas para determinar estruturas de baixa resolução de celobiohidrolase I (CBHI) de *Trichoderma harzianum*.

Os envelopes obtidos por SAXS de CBHI e do domínio CORE mostraram que a proteína encontra-se na forma monomérica em solução. O modelo obtido apresentou bom ajuste à estrutura cristalográfica de CBHI de *T. reesei*, que possui grande similaridade com CBHI de *T. harzianum*.

Acknowledgements: Conselho Nacional de Desenvolvimento Científico e Tecnológico (CNPq), Fundação de Amparo à Pesquisa do Estado de São Paulo (FAPESP) e Laboratório Nacional de Luz Síncrotron (LNLS).

Structural Studies with a Phospholipase A₂ Homologue Complexed to Mn²⁺ Ions Possible Role for Myotoxicity Inhibition

Borges, R. J.¹, (dos) Santos, J. I.¹, Soares, A. M.², and Fontes, M. R. M.¹

¹ Universidade Estadual Paulista - Botucatu - Botucatu SP Brazil

² Universidade de São Paulo - Ribeirão Preto - Ribeirão Preto SP Brazil

Snakes from *Bothrops* genus are responsible for the great majority of the ophidian accidents that happen in Brazil. Their venom contains many toxins, being of relevance the phospholipases A₂ (PLA₂s). PLA₂s are small, stable and calcium-dependent enzymes that hydrolyze the ester sn-2 bond of phospholipids, liberating lysophospholipids and fatty acids. Otherwise, PLA₂s homologues are non-catalytic but present a wide range of pharmacological activities, such as hypotension, cardiotoxicity, neurotoxicity and myotoxicity. Myotoxic activity has been the focus of many studies, since the serum therapy is not efficient against the muscular injury induced by these PLA₂s. Recent studies show a reduction in myotoxic activity of bothropstoxin-I (BthTX-I, a PLA₂ homologue) in the presence of divalent ions when injected in rats. In order to understand the reason of this reduction and trying to get insights into the mechanisms of phospholipases A₂ homologues action, the co-crystallization of the basic PLA₂ homologue piratoxin-I (PrTX-I) from *Bothrops pirajai* with manganese ions were performed. The crystallographic structure of this complex was determined at 1.9 Å and present 92.3% of completeness and $R_{merge}=10.1\%$. Preliminary results indicate electronic densities that may correspond to the manganese ions, deserving to be highlighted the presence of one ion in the hydrophobic channel. This region is known to be the local of interaction of many inhibitors of PLA₂s homologues. Comparative studies are being realized to comprehend the reduction of the myotoxic activity when the manganese ions interact with the toxin.

Acknowledgements: This work was supported by FAPESP, LNILS and CNPQ.

Estudos estruturais do PPAR γ complexado com ligantes naturais

Puhl, A. C.¹, Campos, J. L. O.¹, and Polikarpov, I.¹

Universidade de São Paulo - São Carlos - São Carlos SP Brazil

Os receptores nucleares são uma das classes mais importantes de sinalização intracelular e estão envolvidos em praticamente todas as funções fisiológicas do organismo, pois são potentes reguladores do desenvolvimento, divisão, diferenciação celular, metabolismo e estão relacionados com diversas doenças metabólicas e vários tipos de câncer, sendo considerados alvos para novas alternativas de tratamento. A subfamília dos receptores ativadores de proliferação de peroxissomos é constituída por três isotipos (PPAR- α , PPAR β e PPAR- γ) e está envolvido em doenças como diabetes, obesidade, dislipidemias e aterosclerose. Ele está envolvido principalmente na diferenciação de adipócitos e homeostase metabólica. O PPAR γ tem se tornado um receptor de grande interesse biomédico porque foi demonstrado que uma nova classe de fármacos antidiabéticos chamados tiazolidinedionas (TZDs), que atuam como sensibilizadores da insulina in vivo, se ligam ao PPAR γ com alta afinidade in vitro, e dessa forma os ácidos graxos foram propostos como sendo ligantes naturais. Objetivo: co-cristalizar o domínio de ligação ao ligante (LBD) do PPAR γ com ligantes naturais e resolver a estruturas cristalográficas. Metodologia: o PPAR γ LBD foi co-cristalizado com ligantes naturais utilizando a técnica da gota pendurada e coletados no LNLS. Resultados: os cristais complexados com luteolina foram obtidos na solução contendo citrato de sódio 0.85M, HEPES 100 mM pH 7.5. Grupo espacial C2 (a=92, b=62, c=118) e resolução 2.6 Å. A estrutura foi resolvida por substituição molecular utilizando a estrutura 1PRG (PDB).

Acknowledgements: CAPES, FAPESP

Crystal Structure of a Cyclophilin from *Citrus sinensis* in complex with Cyclosporin A at 1.87 maximum resolution

Campos, B.M.¹, Souza, T.A.C.B.², Barbosa, J.A.R.G.², and Benedetti C.E.¹

¹ Centro de Biologia Molecular Estrutural - Campinas SP Brazil

² Laboratório Nacional de Luz Síncrotron - Campinas SP Brazil

Cyclophilins are a family of proteins that exhibit peptidyl-prolyl cis-trans isomerase activity. Our laboratory isolated a cyclophilin (CYP) from *Citrus sinensis* that interacts with the effector protein PthA from *Xanthomonas citri*, the bacterial pathogen responsible for the citrus canker disease. The crystal structure of the recombinant citrus CYP complexed with its inhibitor cyclosporin A (CsA) has been determined by molecular replacement, from a trigonal crystal that contains a dimer per asymmetric unit. The structure has been refined to an R-factor of 0.1483 and R-free of 0.1968 against data of 1.87 maximum resolution. The structure belongs to space group P3₂21 with a = b = 83.84 and c = 85.44 , $\alpha = \beta = 90^\circ$ and $\gamma = 120^\circ$. The crystal structure of CYP shows the typical cyclophilin fold - a β -barrel composed of eight antiparallel β -strands closed off by two helices.

Acknowledgements:

Identification of hNek6 interaction partners in the context of complex networks

Meirelles, G. V.¹, Lanza, D.C.F², Silva, J.C.², Santana JB³, Paes Leme, A.F.¹, Torriani, I.¹, and Kobarg, J.¹

¹ Laboratório Nacional de Luz Síncrotron - Campinas SP Brazil

² Universidade Estadual de Campinas - Campinas SP Brazil

³ Centro de Biologia Molecular Estrutural - Campinas SP Brazil

Physical protein-protein interactions are fundamental to all biological processes, which are integrated by large complex networks, like the human kinome and its associated proteins. To explain the heterogeneous nature of complex networks, a scale-free model was recently proposed in which the degree distribution in many large networks follows a power-law, characterized by the presence of few highly connected nodes, called hubs. One branch of the kinome network are the NIMA-related kinases (Neks) are widespread among eukaryotes and the mammalian Neks represent an evolutionarily conserved family of 11 serine/threonine kinases related to the *Aspergillus nidulans* mitotic regulator NIMA. Those that have been studied are associated to cell cycle-related functions, and diverse human pathologies, which highlight Neks as potential chemotherapeutic targets. Human Nek6 was recently found to be linked to carcinogenesis, but as for the majority of Neks, the molecular structure, interacting partners and signaling pathways are still unknown. In this work we present a preliminary Small Angle X-ray Scattering (SAXS) model of hNek6 structure, showing that it is a mostly globular protein. We also present here the identification of hNek6 interacting partners by two-hybrid system screens and their analysis within the context of complex networks in an attempt to uncover the pathways that hNek6 operates in cell, offering an insights concerning its importance during cell life and its role in cancer.

Acknowledgements: Agradecemos o Fapesp, CNPq e LNLS pelo apoio financeiro.

FUNCTIONAL AND STRUCTURAL INSIGHTS INTO THE ROLE of FEZ FAMILY PROTEINS IN AXONAL OUTGROWTH

Alborghetti, MR¹, Silva, J.C.², Furlan AS³, Torriani, I.³, and Kobarg, J.³

¹ Centro de Biologia Molecular Estrutural - Campinas SP Brazil

² Universidade Estadual de Campinas - Campinas SP Brazil

³ Laboratório Nacional de Luz Síncrotron - Campinas SP Brazil

The FEZ (fasciculation and elongation protein zeta) family designation was first proposed by Bloom and Horvitz in 1997 by their genetic analysis of the *C. elegans* gene *unc-76*. The *unc-76* function is necessary for normal fascicle structure and is required specifically for axon-axon interactions in *C. elegans*. Until today, little is known about FEZ2 protein function. The mRNA of FEZ2 is ubiquitously expressed in all tested rat tissues in contrast to FEZ1, which is almost exclusively expressed in the rat brain. Previous studies have implicated the conserved C-terminal region in protein-protein interaction (PPI) mediated by coiled-coil regions. Here we show both conserved and non-conserved evolutionary features of the members of the FEZ family. We set out to use FEZ2 itself as bait in a yeast two-hybrid assay and screened human fetal brain and bone marrow cDNA libraries for potential FEZ2-interacting proteins. Subsequently, we tested the identified proteins also against FEZ1 and UNC-76 (C-terminal regions). Furthermore, we confirmed the interaction among FEZ1 and SCOCO (short coiled-coil protein), a interaction that had been previously reported between their orthologs UNC-76 and UNC-69, that cooperate in axonal outgrowth. We performed low resolution structural studies of the complex between 6xHis-FEZ1(1-392) and GST-SCOCO (42-122) by SAXS (Small Angle X-ray Scattering). SAXS data were collected at the D02A-SAXS2 beamline of the Brazilian Synchrotron Light Laboratory (LNLS). The predicted hetero-tetrameric state was indeed observed, which consists of two GST-SCOCO molecules attached to the previously observed dimer formed by two FEZ1 molecules. In vivo this dimeric state could be important for kinesin mediated protein transport along the microtubuli. The protein FEZ1 may interact with kinesin KIF3a or directly with tubulin and at the same time may interact with its cargo molecules (e.g. SCOCO). Thereby, FEZ1 may be classified as a dimeric and bivalent transport adaptor, essential to axon outgrowth and normal pre-synaptic organization, transporting cargoes such as mitochondria, vesicles and proteins required for differentiation at the axon tip.

Acknowledgements: Supported by Fapesp, CNPq and the LNLS.

The FEZ1 protein homo-dimerizes via a disulfide Bond

Furlan AS¹, Alborghetti, MR², Silva, J.C.³, Paes Leme, A.F.¹, Sforça, ML¹, Torriani, I.¹, Zeri, A.C.; Zeri, A; Zeri, A.C.M.¹, and Kobarg, J.¹

¹ Laboratório Nacional de Luz Síncrotron - Campinas SP Brazil

² Centro de Biologia Molecular Estrutural - Campinas SP Brazil

³ Universidade Estadual de Campinas - Campinas SP Brazil

The human proteins FEZ1 (fasciculation and elongation protein zeta 1) and FEZ2 are orthologs of the protein UNC-76 from *C. elegans*, involved in the growth and fasciculation of the axon. Pull down assays showed that the protein FEZ1 interacts with other proteins (e.g. SCOCO), mitochondria and vesicles, via its C-terminal region. These components may therefore represent cargoes to be transported along the microtubule, and the transport may be mediated by FEZ1 association to kinases (KIF3A). We previously showed that FEZ1 dimerizes in its N-terminal region and interacts through its C-terminus with other proteins. Here we study the fragment FEZ1(92-194) to verify the prediction for a coiled-coil region in this region and the formation of a probable disulfide bond through Cys-133, both of which are possibly important to mediate the proteins homo-dimerization. We obtained purified samples of FEZ1(92-194) and performed native acryl amide gel electrophoresis under reducing or non-reducing conditions. Furthermore, we performed Small Angle X-ray Scattering (SAXS) measurements, where we confirmed that the molecular mass of the non-reduced sample (dimer) was exactly twice the mass of the TCEP-reduced one. (monomer). We are starting to perform Nuclear Magnetic Resonance analyses, which so far suggest the a structured region of about 15 amino acids in the N-terminal region of FEZ1(92-194). Finally, a comparative mass spectrometry analysis of reduced and non-reduced protein samples showed that the cysteine could be oxidized in the full-length FEZ1 protein. In summary, our results suggest that FEZ1 dimerizes via its N-terminal through a disulfide bond and coiled-coil interactions. The disulfide bond may be important for FEZ1 role as a bivalent adaptor molecule, since it establishes a strong link between the monomers. Our model suggests that the FEZ1 C-terminal can be divided in two regions: one may interact with microtubule associated proteins (tubulin, KIF3A, CLASP2 are FEZ1 interactors) while the other one may interact with candidate cargo proteins (SCOCO), vesicles and mitochondria.

Acknowledgements: Supported by FAPESP, CNPQ and the LNLS.

SAXS studies of DNA self-assembled structures

Oliveira, C. L. P¹, Pedersen, J.S.¹, Andersen, F. F.¹, Knudsen, B. R.¹, Irish, E.², Labean, T.², Andersen, E. S.¹, and Kjems, J.¹

¹ Aarhus University - Aarhus Denmark

² Duke University Medical Center - Durham CN United States of America

For over 20 years, DNA has been recognized as a useful construction material for nanotechnology because of its readily programmable molecular recognition and predictable local geometry. Many artificial, self-assembled DNA nanostructures have been reported using various geometric structures and functionalities, including one- and two-dimensional periodically patterned structures, three-dimensional polyhedra, DNA computers, and mechanical devices. The visualization and analysis of these structures is a very important issue, in order to confirm and judge the conformation of the formed structures. Electron microscopy techniques are one of the major tools in this respect permitting the direct visualization of the structures in real space. However, one of the intrinsic limitations of this technique is the requirement for fixation and staining of the samples, which both might lead to artefacts. On other hand, the small angle X-ray scattering (SAXS) technique permits the study of the structure in solution giving information on a large ensemble of the structures simultaneously. We performed SAXS experiments on self-assembly 2D ('tiles' and 'tracks') and 3D DNA structures (cages and boxes). For the data analysis new modelling methods had to be developed in order to take into account the expected overall geometry of the structures, the DNA strand base pairing, and the known structural elements. Employing several modelling approaches [1,2] we have obtained the three-dimensional structures, structural dimensions and polydispersity levels for the studied DNA self-assembled systems in solution.

References

- [1] F. F. Andersen et al. 2008 Nucleic Acids Research., 36, 1113.
- [2] E. S. Andersen et al. 2009 Nature 459(7243), 73-76.

Acknowledgements:

A *in situ* SAXS Study of Glucagon Fibrillation

Oliveira, C. L. P.¹, Behrens, M. A.¹, Pedersen, J. S.¹, Erlacher, K.², Otzen, D. E.¹, and Pedersen, J.S.¹

¹ Aarhus University - Aarhus Denmark

² Bruker BioSpin GmBH - Rheinstetten Germany

Protein amyloid formation proceeds through a number of different stages. Oligomeric species observed at early stages have aroused particular interest because of evidence for their involvement in cytotoxic processes such as membrane permeabilization. It is unclear whether these oligomers are obligate precursors to fibrils or represent dead-end species which impede fibrillation. Because of the many interconverting species present during amyloid formation, it is important to study the process as non-invasively as possible. Small angle X-ray scattering (SAXS) measurements allow us to monitor structural changes in solution *in situ* for a population of different species over time. Here [1] SAXS was used to provide a detailed time-resolved structural description of the *in situ* fibrillation of the 29-residue peptide hormone glucagon at pH 2.5 from monomer and early oligomers to mature fibers. Investigation of the pseudo-equilibrium behavior in the lag phase prior to fibrillation at several concentrations showed that glucagon can be found as monomers, dimers, trimers or hexamers in the concentration range from 1–10 mg/ml. After the lag phase, a short rod-like protofibril is formed and subsequently grows in length and assembles into long triple bundled mature fibers. Applying several newly developed modeling tools to the experimental data the full process, from early oligomerization stages up to the mature fiber formation could be described as associations between glucagon molecules. The modeled fibrillation process is described in Figure 1. We propose that on-pathway fibrillar intermediates, which accumulate substantially during fibrillation at high protein concentrations, share this elongated shape which easily allow them to be incorporated into mature fibrils. This contrasts with the annular shape that is suggested to be involved in cytotoxic membrane permeabilization and which may represent a dead-end species off the fibrillar pathway.

Reference

[1] C. L. P. Oliveira et al. 2009 J. Mol. Biol., 387, 147.

Acknowledgements:

Structural studies of Intrinsically Unstructured Proteins by Small-Angle X-ray Scattering

Silva, J.C.¹, Lanza, D.C.F¹, Bressan, G.C.², Kobarg, J.², and Torriani, I.L.¹

¹ Universidade Estadual de Campinas - Campinas SP Brazil

² Laboratório Nacional de Luz Síncrotron - Campinas SP Brazil

The tenet that a three-dimensional protein structure dictates its biological role has been defied by the increasing evidence of natively unstructured proteins which display functions that require conformational disorder. For example, membrane transport, molecular recognition, post-translational modifications, cellular signaling and regulatory mechanisms are important functions often accomplished by *intrinsically unfolded proteins*. For these reasons, there is a clear need for the development of approaches that lead to qualitative and quantitative characterization of flexible and intrinsically unstructured proteins in solution. Dealing with protein structure determination of intrinsically unstructured proteins (IUP), or natively unfolded proteins is a new challenge to be faced. A significant effort has already been directed toward developing empirical sequence based bioinformatic tools for disorder prediction in the IUP structures. Nonetheless, much of the progress on protein structure characterization has been achieved mainly with macromolecules with well-defined and rather rigid tertiary structures. Structural analyses of flexible macromolecules almost exclude high-resolution techniques. In such cases, the *Small-Angle X-ray Scattering (SAXS)* technique can efficiently reveal the spatial conformation, the organization of protein domains, including disordered and unknown parts of the molecule, and allows the study of conformational changes. SAXS provides important dimensional parameters of the protein conformation and a quantitative analysis on the degree of compactness (degree of folding) of an IUP. A new approach, employing ensemble optimization, has been specially developed to analyze flexible structures. In this work we have explored all sorts of strategies to single out the range of possibilities of IUP structural characterization provided by the SAXS technique. Some of our studies on two human IUPs are presented. We have studied the *Fasciculation and Elongation Zeta-1 protein (FEZ1)* which is related to axon growth and may be related to schizophrenia, and the human protein called *Ki-1/57* whose functional available data suggests its complex role in gene expression regulation.

Acknowledgements: FAPESP, CNPq, LNLS, CeBiME

SAXS studies of flexible multidomain proteins

Silva, J.C.¹, Borges, J.C.², Quaresma, A. J. C.³, Bressan, G.C.³, Kobarg, J.³, Ramos, C.H.I.¹, and Torriani, I.L.¹

¹ Universidade Estadual de Campinas - Campinas SP Brazil

² Instituto de Quimica de Sao Carlos - São Carlos SP Brazil

³ Laboratório Nacional de Luz Síncrotron - Campinas SP Brazil

Proteins with well structured domains linked by flexible regions are generally involved in important biological functions. These structural features are often observed in proteins that interact with DNA or RNA and in some chaperones. From the point of view of high resolution structure solving, these proteins pose a real challenge when NMR or crystallographic methods are employed. The existence of flexible regions in the molecules is sometimes a real obstacle. The *Small Angle X-ray Scattering (SAXS)* provides low resolution data that in many instances allows the investigation of important details in biological structure-function key problems. SAXS can efficiently reveal the spatial conformation, the organization of protein domains, including disordered and unknown parts of the molecule, and allows the study of conformational changes. Moreover, the most potentially useful outcome of this technique is the possibility of performing a low-resolution modeling of the protein. These modeling methods allow us to restore the conformational space as well as the possible conformations adopted by flexible multidomain proteins in solution. *Ab initio* methods, using the well known *dummy atoms (DA)* and *dummy residues (DR)* routines, lead to the calculation of the low-resolution models of proteins in solution. The DR-based method has the advantage of being chain-like compatible and considers the number of residues known a priori from the amino acids sequence. For flexible multidomain proteins, there is still the *rigid body modeling method*, which combines high resolution of the domains and simulated flexible loops of unknown structures linking them. In this work we describe the results of the structural analysis of two types of multidomain proteins: the deleted-domain mutants of the protein HSP40 Sis1, whose functional activity is under study, and one heterogeneous nuclear protein from family Q1 (hnRNP Q), which is related to a wide array of RNA important functions.

Acknowledgements: FAPESP, CNPq, LNLS, CeBiME

OLIGOMERIZATION STATES OF LEUCYL AMINOPEPTIDASE FROM *Leptospira interrogans*

Álvares, A.C.M.¹, Silva, A. J.¹, Barbosa, J.A.R.G.², Santana, J. M.¹, and Freitas, S. M.¹

¹ Universidade de Brasília - Brasília DF Brazil

² Laboratório Nacional de Luz Síncrotron - Campinas SP Brazil

The leucyl aminopeptidase of the *L. interrogans* (LAPLi) adopts well-packed self-assembled hexameric form (320 kDa) and cleaves the N-terminal region of proteins in leucine residues. The gram-negative spirochete *L. interrogans* is responsible for the leptospirosis disease and LAP is associated to the pathogenicity of this bacteria. In this work we present the LAPLi activity studies and its oligomerization as a function of concentration and temperature. The hydrodynamic measurements were recorded by DynaPro LSR Light Scattering Detector (DLS) of the Brazilian Synchrotron Light Laboratory (LNLS). The assays were done with monomer LAPLi (14 M) in Tris-HCl 25 mM NaCl 200 mM pH 8.5 at 25°C. DLS data showed that LAPLi oligomerization process is temperature-dependent. The hexameric form (330 kDa, R_h 6.8 nm) occurs only at 50°C, in all studied concentrations. Enzymatic activity assays varying temperature and pH also indicate that LAP is more active at 50°C. In addition, no structural change of the enzyme was detected from the fluorescence spectra at 25 to 55°C. The data obtained from DLS, uorescence and enzymatic activity assays suggest a high activity of the LAP at neutral pH and its high stability until 55°.

Acknowledgements: CNPq, ABTLuS (LNLS) e FINEP

Self-association of the chymotrypsin inhibitor from *Schizolobium parahyba* seeds and its binary complex with alpha-chymotrypsin

Silva, A. J.¹, Álvares, A.C.M.¹, Barbosa, J.A.R.G.², and Freitas, S. M.¹

¹ Universidade de Brasília - Brasília DF Brazil

² Laboratório Nacional de Luz Síncrotron - Campinas SP Brazil

Schizolobium parahyba chymotrypsin inhibitor (SPCI) is a Kunitz type chymotrypsin inhibitor isolated from *Schizolobium parahyba* seeds. In this work we study self-association of the SPCI and its binary complex with α -chymotrypsin by Dynamic Light Scattering (DLS) and Fluorescence Spectroscopy methods. Hydrodynamic parameter showed a dynamic equilibrium of molecular forms (monomer, dimer and trimer) of the SPCI in solution ($Pd = 0.36$) with prevalence of the dimeric form ($D_h = 6.10$ nm and $M_W = 43.40$ kDa) at pH 7.6 and 25°C in contrast with monomeric form ($D_h = 3.8$ nm, $M_W = 21.00$ kDa and $Pd = 0.12$) in other pHs. The chymotrypsin appears as a monomer ($D_h = 5.4$ nm and $M_W = 24.00$ kDa) at pH 7.6 and its interaction with calcium ions causes hydration layer loss (~ 1.4 nm), which facilitated the formation of some dimmers (less than 2 % of the solution). Hydration layer loss is due to conformation changes of chymotrypsin as indicated by the bathochromic displacement of maximum emission spectra of tryptophan from 333 to 356 nm upon the addition of calcium. Binary complex formed a ternary ($D_h = 7.00$ nm and $M_W = 71.00$ kDa) with chymotrypsin at pH 7.6 and 0.5 ionic strength, indicating the preservation of the dimerization region of inhibitor in this condition. These results showed that SPCI tends to self-associate mainly as dimer, chymotrypsin and binary complex as monomer, in natural biological conditions.

Key-words: Kunitz-type chymotrypsin inhibitor, self-association, dynamic light scattering, fluorescence spectroscopy.

Acknowledgements: Supported by CAPES, FINATEC, LNLS, FINEP and FAPDF.

Low resolution structural studies of human RACK-1

Gonçalves, K.A.¹, Borges, J.C.², Silva, J.C.³, Papa, PF⁴, Torriani, I.¹, and Kobarg, J.¹

¹ Laboratório Nacional de Luz Síncrotron - Campinas SP Brazil

² Instituto de Química de São Carlos - São Carlos SP Brazil

³ Universidade Estadual de Campinas - Campinas SP Brazil

⁴ Centro de Biologia Molecular Estrutural - Campinas SP Brazil

The adaptor protein RACK1 (receptor of activated kinase 1) was originally identified as an anchoring protein for protein kinase C. RACK1 is a 36-kDa protein and contains seven WD40 repeats that mediate its protein-protein interactions. RACK1 is ubiquitously expressed and has been implicated in diverse cellular processes, including: protein translation and stress signaling. Here, we performed a biophysical analysis of human RACK-1 with the aim of obtaining low resolution structural information about human RACK-1. We expressed RACK-1 in *E.coli* with a C-terminal 6xHis fusion tag and we obtained reasonable amounts of soluble protein. Circular dichroism analysis showed RACK-1 as a well structured protein. Small angle X-ray scattering (SAXS) experiments demonstrated that the maximum dimension obtained for the particle was 60 Å and the molecule radius of gyration was 20.6 Å, which indicated a quite compact protein. Using a BSA (Bovine Serum Albumin) solution as standard, the molecular mass for RACK-1 was estimated from the SAXS data as being 40 kDa. The scattering curve calculated from the atomic coordinates of the molecular dynamics model showed a good agreement with the experimental data. Ab initio calculations were used to restore the low resolution molecular envelope of RACK1 and this envelope can be brought to a satisfactory alignment with the MD RACK1 structure. The hydrodynamic properties of the RACK-1 protein were established by both sedimentation velocity and sedimentation equilibrium ultracentrifugation experiments. The main species observed on RACK-1 sedimentation velocity experiments presented a $s^{0}_{20,w}$ of 3.00 +/- 0.01 S, suggesting a molecular mass of 36.4 +/- 0.8 kDa. All hydrodynamic data, together with the frictional ratio supplied by SedFit software, suggest that RACK-1 is a particle with a frictional ratio of around 1.3, thus being, slightly asymmetric.

Acknowledgements: Financial support by: FAPESP, CNPq and ABTLuS.

Physicochemical characterization of the protease inhibitor BTCl in complex with 20S Proteasome

Souza, L. C.¹, Joanitti, G. A.¹, Silva, A. J.¹, Lottermann, M. T.¹, Camargo, R.¹, Martins de Sá, C.¹, and Freitas, S. M.¹

Universidade de Brasília - Brasília DF Brazil

The black-eyed pea trypsin/chymotrypsin inhibitor (BTCl) is a Bowman-Birk protease inhibitor isolated from *Vigna unguiculata* seeds that inhibits trypsin and chymotrypsin simultaneously. This inhibitor was found recently to alter significantly the proliferation and viability of breast cancer, but the mechanism underlying the anti-carcinogenic function of BTCl remains far to be elucidated. Our recent studies show that BTCl can strongly inhibit the 20S proteasome activity and it might be related with its anti-carcinogenic function. The interaction of BTCl with proteasome was analyzed using the Dynamic Light Scattering DynaPro DLS detector with an 800 nm wavelength laser and Dynamics V6 software. BTCl forms a trimer at 15.0 μM and proteasome forms a monomer at 21.4 nM. BTCl associates with proteasome in 45 min of incubation and alters the structure of this molecule, as indicated by the increase in hydrodynamic diameter of the complex from 21.9 nm to 22.7 nm. BTCl and proteasome form a thermostable (until 55°C) and a stable complex at pH ranging from 6 to 12 and this complex tends to dissociate in 2 mM NaCl. At pH 2 and 4, both BTCl and proteasome form aggregate. In conclusion, BTCl interacts with 20S proteasome by forming a stable complex until 55°C at a broad range of pH.

Acknowledgements: Supported by CNPq e ABTLuS.

Implementation of new NMR Methods for Protein Studies

Neves, J.L.¹, Sforça, ML¹, and Zeri, A.C.¹

Laboratório Nacional de Luz Síncrotron - Campinas SP Brazil

Motivated by the great relevance of NMR to study structure, dynamics and kinetics of proteins [1], we show here the implementation of new NMR methodologies, capable to speed up the experiments and extend the range of applications of the CeBiME (Centro de Biologia Molecular Estrutural) NMR facility to nucleic acids and large proteins.

More specifically we show the implementation of Projection Reconstruction (PR) experiments [2] (to speed up the experiments), two dimensional ³¹P based experiments [3] (to study nucleic acids) and CRINEPT experiments [4] (to study large proteins).

Additionally we developed a virtualized linux system, running as guest machine for diverse operational systems, that includes a set of necessary pre-installed free softwares for NMR data processing and structure calculation. It is just necessary that the users register by e-mailing the software developers.

Referências

1. J. Cavanagh, *Protein NMR spectroscopy*. Elsevier Academic Press, California, 2nd Edition, 2007.
2. E. Kupce and R. Freeman, *Journal of American Chemical Society*, 125, 13958-13959, 2003.
3. A. Ono, T. Makita, et.al. *Magnetic Resonance In Chemistry*, 34, S40-S46, 1996.
4. R. Riek, K. Pervushin, K. Wuthrich, *Trends in Biochemical Sciences*, 25, 462-468, 2000.

Acknowledgements: This work was supported by FAPESP

Crystallographic studies of *Schizolobium parahyba* chymotrypsin inhibitor in complex with chymotrypsin

Silva, A. J.¹, Santos, C. R.², Barbosa, J.A.R.G.², and Freitas, S. M.¹

¹ Universidade de Brasília - Brasília DF Brazil

² Laboratório Nacional de Luz Síncrotron - Campinas SP Brazil

Schizolobium parahyba chymotrypsin inhibitor (SPCI) is a Kunitz type inhibitor able to inhibit chymotrypsin by forming a stable binary complex. Serineproteinase inhibitors are of great interest in medicine and agriculture areas due their potential to suppress ovarian cancer cell invasion and peritoneal disseminated metastasis in vivo and an adverse effect on insect development. Knowledge of the three-dimensional structure of this complex will provide details of the mechanism of inhibition and insight for prospective in protein engineering. The crystallization of SPCI-chymotrypsin complex was refined and x-ray diffraction data resolution improved progressively from 4.0 to 2.8 . New refinements using the seeding procedure were carried out improving the resolution to 2.6 . This latter crystal belongs to space group P_{21} with unit-cell parameters $a = 44.7$, $b = 64.18$, $c = 168.40$, and the *Rmerge* is 0.54 for 25016 unique reflections. SPCI-chymotrypsin complex reached the maximum degree of crystal quality for three-dimensional resolution of its structure at 2.6 .

Keywords: SPCI-chymotrypsin complex, crystallization, X-ray diffraction.

Acknowledgements: Supported by CAPES, CNPq, FAPESP and ABTLuS.

ADAM-9, 10, 12, 17 and 19 expression in normal and cancer cells

Câmara, P.R.S¹, Yokoo, S¹, Belloni, M¹, and Paes Leme, A.F.¹

Laboratório Nacional de Luz Síncrotron - Campinas SP Brazil

Head and neck squamous cell carcinoma (HNSCC) is the fifth most common malignancy worldwide, representing a major international health problem. The up-regulation of proteolytic ADAMs (a disintegrin and metalloproteinase) has been documented for a number of cancers, including HNSCC, with some correlation to parameters of disease progression. Over the last few years the ADAM family have been associated with the process of proteolytic shedding of membrane-associated proteins and hence the rapid modulation of key cell signalling pathways in the tumour microenvironment. Furthermore, numerous members of the ADAM family have been associated with tumorigenesis and tumour progression. Members of the ADAM family of membrane-anchored peptidases are key regulators of epidermal growth factor receptor (EGFR) signaling by converting membrane-anchored precursors of EGFR-ligands into soluble growth factors. Indeed, communication between G protein-coupled receptor (GPCR) and EGFR signalling systems involves cell surface proteolysis of EGF-like precursors. Thus, triple membrane-passing signaling pathways are observed among GPCR, ADAMs and EGFR. The aim of this study was to compare the expression of ADAMs 9, 10, 12, 17 and 19 in normal queratinocytes (HaCat) and oral squamous cell carcinoma (SCC-9) by Real Time PCR to correlate to cancer disease. The results revealed that all ADAMs showed higher mRNA expression in SCC-9 cells comparing to normal queratinocytes cells. These data suggest that all these proteases could play a role in the oral cancer development. However, it is not known whether they share the same partners, mainly intracellularly, to be determined by mass spectrometry analysis, which can reveal the ligand specificity of several ADAMs that could be critical for either EGFR signal transactivation or other pathways that they can be involved.

Acknowledgements: This work is supported by CNPq, ABTLUS and FAPESP

Crystal structure of TK1436, a branching enzyme from the hyperthermophilic archaeon *Thermococcus kodakaraensis*

Santos, C. R.¹, Tonoli, C. C. C.¹, Arni, R.K.², and Murakami, M. T.¹

¹ Laboratório Nacional de Luz Síncrotron - Campinas SP Brazil

² Universidade Estadual Paulista - São José do Rio Preto - São José do Rio Preto SP Brazil

Branching enzymes (BEs) (EC 2.4.1.18) cleave α -1,4 glucosidic bonds and transfer to new α -1,6 glucosidic bonds, forming branch points in starch and glycogen. These branches greatly increase the solubility and degradation rates of these polymers which is desirable for a number of biotechnological processes, such as the ethanol industry. BEs identified to date belong to glycoside hydrolase family 13 (GH13) and only one BE structure has been solved (it *E. coli* BE). In this work, we report the crystal structure of a BE from the hyperthermophilic archaeon *T. kodakaraensis* belonging to the glycoside hydrolase family 57 (GH57), named as TK1436. The protein was crystallized in the orthorhombic space group $P2_12_12_1$ with unit cell parameters $a = 70.67$, $b = 79.02$, $c = 134.09$ and one molecule per asymmetric unit. The structure was solved by molecular replacement methods and refined to an R_{factor} of 0.16 and R_{free} of 0.20 against data to 1.87 resolution. TK1436 represents the first member of the GH57 family with proven branching activity and its structural characterization should provide important insights onto the molecular determinants for specificity and thermostability of GH57 members.

Acknowledgements: We thank Fapesp and CNPq for financial support, and CeBiME and LNLS for providing facilities such as the automated crystallization robot and the X-ray diffraction beamline.

Expressão, Purificação e Estudos Biofísicos e Estruturais da endo-1,4- β - Glicanase de *Bacillus subtilis*

Akao, P.K.¹, Ruller, R.¹, and Murakami, M. T.¹

Laboratório Nacional de Luz Síncrotron - Campinas SP Brazil

Celulose é um dos polímeros naturais mais abundantes da terra e são basicamente constituídos de monômeros de glicose mantidos por ligações β -1,4. Nos últimos anos a biomassa celulósica tem recebido grande atenção do meio acadêmico e industrial devido ao seu potencial na produção de açúcares solúveis, produtos químicos industriais e biocombustíveis. Porém para o aproveitamento da biomassa celulósica é necessário sua redução à açúcares fermentáveis que envolve a ação sinérgica do coquetel enzimático formado por endo-1,4- β -glicanases (EC 3.2.1.4), celobiose-hidrolases ou exo- β -1, 4-glicanases (EC 3.2.1.91) e β -glicosidases (EC3.2.1.21). Assim, neste trabalho temos como objetivo a expressão, purificação, análises espectroscópicas e estudos estruturais da endo-1,4- β -glicanase de *Bacillus subtilis*. O gene *full-length* constituído pelo domínio catalítico e o módulo de ligação a carboidrato foi clonado em vetor pET28a e expresso em BL21(DE3) a 37°C induzido com 1 mM de IPTG pelo período de quatro horas. A proteína foi purificada por três passos cromatográficos utilizando uma cromatografia por afinidade (Hitrap-Chelating HP), seguida de uma troca catiônica (Hitrap SP HP) e por fim uma filtração em gel (superdex 16/60). A pureza foi confirmada por gel de poliacrilamida sob condições desnaturantes e demonstrou monodispersa através de análises por espalhamento dinâmico de luz, que indica uma amostra adequada para os estudos biofísicos e cristalográficos. A proteína foi submetida a experimentos de desnovelamento térmico monitorado por dicróismo circular, fluorescência e microcalorimetria que indicaram uma T_m de 63,5°C. Os ensaios de cristalização foram realizados e resultaram no aparecimento de microcristais e esferolitas que estão sob refinamento. A obtenção da estrutura cristalográfica combinada com estudos de desnaturação irão fornecer informações preciosas sobre o funcionamento, termoestabilidade e especificidade dessa classe de celulasas.

Acknowledgements: Este trabalho teve o apoio do Conselho Nacional de Desenvolvimento Científico e Tecnológico e da Fundação de Amparo à Pesquisa do Estado de São Paulo.

Crystal Structure of the Nucleoside diphosphate kinase b from *Leishmania major*

Trindade, D.M.¹, Tonoli, C. C. C.¹, Arni, R.K.², de Oliveira, A.H.C.³, and Murakami, M. T.¹

¹ Laboratório Nacional de Luz Síncrotron - Campinas SP Brazil

² Universidade Estadual Paulista - São José do Rio Preto - São José do Rio Preto SP Brazil

³ Universidade de São Paulo - Ribeirão Preto - Ribeirão Preto SP Brazil

Nucleoside diphosphate kinases (NDKs; EC 2.7.4.6) have been ascribed to many functions in different organisms, including regulation of gene expression in mammalian cells and participation in the purine-salvage pathways of trypanosomatids, protozoa and bacterial pathogenesis. The nucleotide salvage is a pathway present in all parasitic trypanosomatids in which nucleotides (purine and pyrimidine) are synthesized from intermediates in the degradative pathway for nucleotides. NDKs catalyze the transfer of the γ -phosphoryl group from an nucleoside triphosphate to a nucleoside diphosphate by a ping-pong mechanism involving a phosphohistidine intermediate. Despite the importance of NDK in the life cycle of trypanosomatids, no crystal structure of NDK has yet been reported to date from *Leishmania* or any other protozoan parasite. The full-length NDKb gene from *L. major* was overexpressed and purified to obtain a crystal-grade sample with high chemical purity and low structural polydispersity. Best quality crystals grew after 5-7 days in a 1:1 mixture of protein solution and 1850 mM ammonium sulfate (100mM citrate-HCl buffer pH 5.6). Diffraction data were collected to 2.18 resolution under cryogenic conditions (100 K) at the Brazilian Synchrotron Light Laboratory (Beamline W01B-MX2). The structure of NDKb was solved by molecular replacement (MR) method using the atomic coordinates of nm23-H2, a human nucleoside diphosphate kinase b (PDB code: 1NSK), as a search model. The crystal was indexed to the trigonal space group $P3_221$ and three molecules were found in the asymmetric unit. Restrained isotropic refinement was carried out using the program REFMAC5 interspersed with rounds of manual model building using the program COOT. The final model converged to a crystallographic residual of 0.1645 ($R_{free} = 0.1985$) and displays good overall stereochemistry with RMSD of 0.0304 and 2.3404° for bond lengths and bond angles, respectively. In parallel to crystallographic studies, SAXS experiments showed that its oligomeric state in solution is hexameric.

Acknowledgements: CeBiME, LNLS, FAPESP and CNPq.

Biologia Molecular e Química de Proteínas

Study of interaction between nona-peptide BPP9a and β -cyclodextrin: NMR Structural Elucidation

Lula, I.¹, Sinisterra R. D.², Santos, R.A.S.³, and Denadai, A M L³

¹ UNIVERSIDADE FEDERAL DE MINAS GERAIS - Belo Horizonte MG Brazil

² Universidade Federal de Minas Gerais - Belo Horizonte MG Brazil

³ UNIVERSIDADE FEDERAL DE MINAS GERAIS - MG Brazil

Lula, I. ^{*1}, Sinisterra R. D. ¹, Santos, R.A.S. ¹ and Denadai, A. L. ^{1,2}

¹ Universidade Federal de Minas Gerais - Belo Horizonte, MG ²CEFET-MG, Campus VII, Timoteo * ivanalula@ufmg.br

The nona-peptide BPP9a (Pyr-Trp-Pro-Arg-Pro-Gln-Ile-Pro-Pro-OH) forms an inclusion complex with β -cyclodextrin with the inclusion of the Tryptophan residue in the cavity of β -cyclodextrin molecule. NMR experiment at 500 MHz and 600 MHz with BPP9a and its β -cyclodextrin complex allowed assigning all hydrogen resonance signals of the peptide chains amino acid residues. The NOESY contour maps obtained for the free BPP9a molecule shows only intraresidual and some sequential NOE cross-peaks, suggesting that peptide backbone present a nonrigid conformation. Additionally, nuclear Overhauser effect measurement is one of the most important tools in proving the formation of the hostguest complex. NOESY technique is very useful for getting insights into the supramolecular geometry of the complex. The NOESY contour map of the BPP9a/ β -cyclodextrin complex showed the intermolecular NOE correlation between hydrogens of inner side of the β -cyclodextrin and the aromatic hydrogens of the Trp residue. These results indicate interactions between the Trp residue of the BPP9a with the internal face of β -cyclodextrin molecule, suggesting that the Trp residue is situated in the torus cavity of cyclodextrin molecule. The NOEs intermolecular observed between the BPP9a and cyclodextrin hydrogens, in solution and as detected in the BPP9a/ β -cyclodextrin 2D-NOESY experiments, could only arise if BPP9a/ β -cyclodextrin inclusion complex had been formed with 1:1 molar ratio.

Acknowledgements: **Acknowledgements:** This work was supported by FAPEMIG (Universal 2008). NMR facilities at 600 MHz and 500 MHz were supported by LNLS - Brazilian Synchrotron Light Laboratory/MCT.

Análise de lesões causadas no DNA pela fotoquimioterapia PUVA (psoralenos mais luz ultravioleta A)

de Paula-Pereira Jr., M. V.¹, Soares, M.¹, C. Lage¹, and Leitão, A.C.¹

Universidade Federal do Rio de Janeiro - Rio de Janeiro RJ Brazil

A terapia PUVA consiste na ação de psoralenos (furocumarinas) e a radiação ultravioleta A (UV-A 320 a 400nm). É utilizada no tratamento de diferentes desordens, como psoríase e vitiligo, e em patologias mais graves como o linfoma cutâneo de células T. Os psoralenos são compostos tricíclicos com estrutura planar básica e duas importantes ligações duplas em suas extremidades, uma no anel furano e a outra no anel pirona da molécula. Estas ligações, quando ativadas fotoquimicamente, interagem com os ácidos nucleicos (bases pirimidínicas) do DNA. O efeito da terapia consiste da fotoativação dos psoralenos, resultando na formação de adutos com as bases do DNA das células. Estas ligações, do tipo anel ciclobutano, são estruturalmente estáveis, sendo formadas com uma das fitas de DNA (monoadutos) ou, havendo uma base pirimidínica na fita oposta, formar uma segunda ligação (crosslink). O objetivo é estudar os efeitos da terapia PUVA na formação de lesões em DNA a partir de ensaios que correlacionem a eficiência do reparo de DNA na remoção dos adutos e a utilização de uma ferramenta de análise destas lesões. Experimentos de sobrevivência bacteriana foram realizados, com cepas de *Escherichia coli*, selvagem e mutantes para os genes de reparo por excisão de nucleotídeos (NER) *uvrABC*. Amostras de DNA bacteriano tratadas com PUVA foram extraídas e analisadas via Espectrometria de Massas (Q-Tof). Diferentes psoralenos foram utilizados nos experimentos, dentre eles: 8MOP, seu análogo monofuncional H28MOP, PSO, ANG, DMC e TMP. Os resultados indicam que o reparo NER é importante na remoção dos adutos PUVA. As análises de Espectrometria de Massas sugerem a formação de uma grande variedade de lesões (dímeros, monoadutos e crosslinks) quando da interação dos psoralenos e o DNA. Tais resultados levantam a questão do potencial genotóxico do tratamento. Os adutos formados, não sendo corretamente processados pelas células, acumulam no DNA podendo causar mutagenicidade. Desta forma busca-se a utilização de psoralenos que gerem lesões citotóxicas de menor efeito mutagênico e que sejam eficientes no controle das doenças de pele.

Acknowledgements: Agradecemos à técnica Margareth Sugano Navarro e ao Dr. Nilson Zanchin, pelo suporte técnico na utilização o Espectrômetro de Massas do Laboratório de Espectrometria de Massas (MAS), do Centro de Biologia Molecular e Estrutural (Ce-BiME) do LNLS, como parte da proposta MAS6348, submetida para utilização das instalações do laboratório.

Characterization of the periplasmic-binding protein Pbp from *xanthomonas axonopodis* pv. *citri*

Balan, A.¹ and Barbosa, J.A.R.G.¹

Laboratório Nacional de Luz Síncrotron - Campinas SP Brazil

Bacterial pathogens regulate virulence factor gene expression coordinately in response to environmental stimuli, including nutrient starvation. Many compounds are essential for the bacterial growth and their entrance must be tightly controlled by the cells. Phosphate is an important ion, which is involved in many physiological processes into the cell and virulence process. The important family of transporters called ABC are one of the ways that phosphates can get into the cell. In *Xanthomonas axonopodis* pv. *citri* genome, the causative agent of the cancrus citric disease, at least three genes encoding the putative phosphate-binding proteins from ABC transporters were identified: *pstS*, *pbp*, and *phoX*. In this work we have expressed, purified and made the preliminary characterization of the Pbp protein. The bioinformatic studies revealed the protein conserves residues involved in phosphate/phosphanate interactions. The protein was expressed in *Escherichia coli* BL21(DE3) cells after induction of the T7 promoter and purified from soluble extracts using immobilized metal affinity chromatography (IMAC). Circular Dichroism and Fluorescence revealed the protein showed an alfa/beta conformation and structural changes in presence of phosphate and phosphanate compounds. Thermal shift experiments also revealed an increased stability of Pbp in presence of different compounds such as arginine, spermidine and others, used for crystallization trials. The purified protein was able to generate spherulites and small crystals in different conditions that are being refined.

Acknowledgements: This work was supported by CNPq.

The *Xanthomonas* Type III Effector Protein PthA Interacts with Citrus Proteins Involved in Nuclear Transport, Protein Folding and inhibits K63-linked Ubiquitination Associated with DNA Repair

Domingues, M. N.¹, Souza, T. A.¹, Cernadas, R. A.¹, Oliveira, M. L. P.¹, Docena, C.², Farah, C.S.³, and Benedetti C.E.⁴

¹ Centro de Biologia Molecular e Estrutural - Campinas SP Brazil

² Universidade de São Paulo - São Paulo - Sao Paulo SP Brazil

³ Universidade de São Paulo - São Paulo - São Paulo SP Brazil

⁴ Laboratório Nacional de Luz Síncrotron - Campinas SP Brazil

The effector protein PthA from *Xanthomonas axonopodis* pv. *citri* (Xac) is sufficient to induce plant cell hypertrophy and hyperplasia. Similarly to its homolog AvrBs3, PthA is thought to directly manipulate transcription of host genes. However, although the ultimate targets of such TAL (transcription activator-like) effectors appear to be the host DNA, we hypothesized that PthA might interact with host proteins. Thus, yeast two-hybrid was employed to identify sweet orange proteins that interact with the four PthA variants from Xac strain 306. Here, in addition to the identification of alpha-importin, shown to interact with AvrBs3, we present evidence for the differential interaction between each of the PthA variants with the citrus TDX (Tetratricopeptide domain-containing thioredoxin), Cyclophilin (Cyp), Uev (Ubiquitin conjugating enzyme E2 variant) and Ubc13 proteins involved in protein folding and K63-linked ubiquitination, respectively. Interestingly, the specificity of the interactions appears to depend on the internal repetitive domain of the PthAs. In addition, the citrus Ubc13 and Uev functionally complemented the yeast *ubc13*- and *mms2*-/*uev1a*- mutants and PthA2 preferentially inhibits K63-linked ubiquitination required for DNA repair, strongly suggesting that these proteins could be involved in DNA repair pathways. Most significantly, we found that TDX, Cyp, Uev and Ubc13 interact with each other, given support to the existence of a protein complex required for PthA action.

Acknowledgements: FAPESP, CNPq and LNLS.

The splicing-associated SR protein SFRS9 undergoes arginine methylation and localizes to nucleoli upon inhibition of cellular methylation

Bressan, G.C.¹, Moraes, E.C.¹, Manfiolli A², Kuniyoshi, T.M.¹, Passos, D. O.¹, GOMES MD², and Kobarg, J.¹

¹ Laboratório Nacional de Luz Síncrotron - Campinas SP Brazil

² Universidade de São Paulo - Ribeirão Preto - Ribeirão Preto SP Brazil

The functionally and highly conserved serine- and arginine-rich proteins (SR proteins) are non-snRNPs splicing factors that may affect both constitutive and alternative splicing. The phosphorylation status of these proteins is well known regulators of their pre-mRNA splicing activity and subcellular localization. Despite evidences, any members of this protein family have been shown to be targeted by arginine methylation, a post-translational modification implicated in many aspects of RNA metabolism. In this study, we experimentally addressed the arginine methylation of the SR protein SFRS9. This protein was found as target for PRMT1-mediated arginine methylation in vitro and was immunoprecipitated from HEK-293 lysates by antibodies that recognizes both mono- and dimethyl arginines. In further fluorescence microscopy assays, the recombinant form EGFP-SFRS9 was found in some dot-like structures in the cell nuclei that resembled the nucleolar region. This particular localization was increased upon treatment with the inhibitor of cellular methylation Adox, suggesting the importance of this post-translational modification for the subnuclear localization of SFRS9. In subsequent confocal microscopy analyses, the localization of EGFP-SFRS9 in nucleoli of Adox-treated cells nuclei was confirmed by colocalization assays with marker proteins antibodies. Moreover, the localization of EGFP-SFRS9 at nuclear splicing speckles was observed unchanged as well the overall morphology of this nuclear substructure. Overall, we described a novel post-translational modification that the SR proteins may be subjected, raising new insights on the regulation of these splicing proteins and their activities in pre-mRNA splicing.

Acknowledgements: Financially supported by FAPESP, CNPq and LNLS.

Thermal- and chemical-unfolding studies of yeast Hsp40 *SIS1* and mutants

Borges, J.C.¹, Cyr, D.M.², and Ramos, C.H.I.³

¹ Instituto de Quimica de Sao Carlos - São Carlos SP Brazil

² University of North Carolina - Chapel Hill NC United States of America

³ Universidade Estadual de Campinas - Campinas SP Brazil

SIS1 is the yeast type II Hsp40, an Hsp70 co-chaperone that could also work as a chaperone itself. Although functional studies have been extensively done, little is known about the Hsp40 structure-function relation mainly considering their high diversity. Here, we study the stability of *SIS1*, two deleting mutants of its central region (*SIS1-ΔGM50* and *SIS1-ΔGM130*) and a chimera (*SYS*) of the central region of *YDJ1* (Hsp40 of type I) and N- and C-terminal regions of *SIS1* by equilibrium unfolding. Based on chemical- and thermal-induced unfolding followed by circular dichroism and differential scanning calorimetry, the unfolding profiles of these proteins were classified in two categories. *SIS1-ΔGM130* and *SYS* presented two distinct transitions while *SIS1* and *SIS1-ΔGM50* did not. Analytical ultracentrifugation showed that dimer dissociation of *SIS1-ΔGM130* and *SYS* occurred at a lower urea concentration than *SIS1* and *SIS1-ΔGM50*. The results showed that *SIS1-ΔGM130* and *SYS* were more unstable than *SIS1* and *SIS1-ΔGM50* probably by the absence of contacts between the subdomains which form the *SIS1* C-terminal domain. All together our results lead to the hypothesis that specific contacts in the C-terminus stabilize the domains and are responsible for dimerization.

Acknowledgements: Supported by: LNLS-CNPq-MCT, FAPESP and FIRCA-NIH.

Protein-Protein interactions and structural analysis of citrus proteins involved in transcriptional control during citrus canker disease.

Souza, T. A.¹, Quaresma, A. J. C.², Sforça, ML², Cernadas, R. A.¹, Domingues, M. N.¹, Zeri, A. C.³, and Benedetti C.E.¹

¹ Centro de Biologia Molecular Estrutural - Campinas SP Brazil

² Laboratório Nacional de Luz Síncrotron - Campinas SP Brazil

³ University of California at Berkeley - Berkeley CA United States of America

Citrus canker caused by *Xanthomonas axonopodis* pv. *citri* (Xac) affects almost all citrus varieties causing tissue hypertrophy and hyperplasia. Xac uses type III secretion system to inject PthA effector proteins of the AvrBs3/PthA family into the host cell. These proteins act as eukaryotic transcriptional factors activating directly promoters of host genes. To elucidate how PthA activates transcription and gain insights into its molecular mode of action, a two-hybrid approach was used to identify host proteins that interact with PthAs. Here we show that PthAs interact with a Citrus sinensis Auxin Response Factor (CsARF) and a High Mobility Group protein (CsHMG). ARF proteins play an essential role in auxin signaling as transcriptional factors that bind to promoters of auxin-regulated genes, controlling their transcription. This finding is highly relevant since many citrus genes regulated by Xac and PthAs are also regulated by auxin, and that auxin is required for canker development. Thus, the study of PthA-CsARF interaction may provide a molecular basis for the role of auxin during canker development. We also characterized a citrus HMG (CsHMG) protein implicated in the transcriptional control of genes associated with plant growth. This protein has a central structured HMG box domain flanked by an acidic DE-rich C-terminal and a basic K-rich N-terminal, both predicted to be unfolded. The purified protein was used to perform biophysical and NMR studies. Circular dichroism spectroscopy and NMR studies confirmed the initial secondary structure prediction. Functional analysis using EMSA assays with recombinant forms of CsHMG revealed a non-specific binding to DNA. Most surprisingly, CsHMG shows an as yet unreported ability to bind to synthetic RNA forms with an apparent specificity to poly-U probes. The role of both CsARF and CsHMG proteins on the transcriptional control of citrus genes up-regulated by PthA is under investigation.

Acknowledgements: This work was supported by FAPESP, CNPq and ABTLus

Iron and zinc mapping by SR-XRF in protein spots of liver tissue samples of Nile tilapia (*Oreochromis niloticus*)

Neves, R.C.F.¹, da Silva, M. A. O.², Santos, F.A.¹, Lima, P. M.¹, Arruda, M. A. Z.², Pérez, C. A.³, and Padilha, P. M.¹

¹ Universidade Estadual Paulista - Botucatu - Botucatu SP Brazil

² Universidade Estadual de Campinas - Campinas SP Brazil

³ Laboratório Nacional de Luz Síncrotron - Campinas SP Brazil

Metalloproteins and metal ions bound to proteins represent a large portion of the total number of proteins. It has been estimated that approximately 40

1. GARCIA, J.S.; MAGALHÃES, C.S.; ARRUDA, M.A.Z. Trends in metal-binding and metalloprotein analysis. *Talanta*, v.69, p.1-15, 2006. 2. GATLIN, D.M. AND WILSON, R.P. Studies on the manganese requirement of fingerling channel catfish. *Aquaculture*, v. 41, p. 85-92, 1984.

Acknowledgements: This work was supported by LNLS, INCT, FAPESP

Studies on the phosphorylation and subcellular distribution of the $\alpha 4$ protein

Smetana, J. H. C.¹, Bressan, G.C.¹, Kobarg, J.¹, and Zanchin, N. I. T¹

Laboratório Nacional de Luz Síncrotron - Campinas SP Brazil

$\alpha 4$, the mammalian orthologue of yeast Tap42, is a regulatory protein which associates with type 2A phosphatase catalytic subunits (PP2Ac, PP4c and PP6c) and regulates their activity and specificity. One of the cellular targets of the PP2Ac- $\alpha 4$ complex is the RBCC protein Mid1, a microtubule associated ubiquitin ligase whose malfunction is implicated in the pathology of the Opitz syndrome. Mid1, $\alpha 4$ and PP2Ac are part of a large microtubule associated ribonucleoproteic complex which functions in the transport of specific mRNAs. The PKC anchoring protein RACK1 has also been found as a part of this complex, suggesting that its function might be regulated by PKC mediated phosphorylation. In this study, we investigated the possibility of RACK1/PKC mediated regulation of $\alpha 4$. In vitro pull-down assays showed that $\alpha 4$ interacts specifically with RACK1. Recombinant $\alpha 4$ is phosphorylated in vitro by PKC Pan (a mixture of α , β and γ isoforms), possibly at its C-terminal unstructured region. A FLAG- $\alpha 4$ construction was expressed in HEK293 cells and its subcellular distribution was analyzed by nuclear/cytoplasmic fractionation and by immunofluorescence microscopy, showing a cytoplasmic localization. PKC activation by PMA in HEK293 cells leads to redistribution of FLAG- $\alpha 4$, with a visible concentration of the protein in a juxtannuclear structure. These findings implicate $\alpha 4$ in PKC signaling and provide novel insights into its cellular function.

Acknowledgements: This work was supported by FAPESP and CNPq.

Identificação of IL-7Ralpha IC interacting proteins using the yeast three-hybrid system

Zenati PP¹, Yunes, J. A.², and Kobarg, J.³

¹ Centro de Biologia Molecular Estrutural - Campinas SP Brazil

² Universidade Estadual de Campinas - Campinas SP Brazil

³ Laboratório Nacional de Luz Síncrotron - Campinas SP Brazil

IL-7 is a cytokine that plays an important role in development, survival and proliferation of human T lymphocytes. A number of studies demonstrated that Y449 on the IL-7R alpha chain is the main phosphorylation target for the associated Jak tyrosine kinase upon binding of IL-7 and, once phosphorylated, this Y449XXM motif may act as a docking site for both STAT 5 and PI3-K. Studies have shown that loss of this phosphorylation confers protection against IL-7-induced lymphomas and that some yet uncharacterized proteins interact with phosphorylated Tyr449 IL-7Ralpha. In this work, we used the yeast three-hybrid system to screen a lymphocyte cDNA library for IL-7RalphaIC interacting proteins. We used the pBRIDGE vector (Clontech) to express the human IL-7RalphaIC sequence (bait), fused to the Gal4 binding domain, and the kinase domain (JH-1) of Jak3, fused to the nuclear localization sequence (NLS) under the control of the MET25 promoter, which is inhibited in response to extracellular added methionine. We retrieved 14 different putative protein partners (preys) for IL-7RalphaIC. However, only two were biologically relevant in the IL-7R context. Both proteins are involved in cell cycle, apoptosis and intracellular transport control. However, we do not understand yet how these proteins integrate in the IL-7R pathway. We confirmed the interactions between bait and preys in the yeast strain Y190, and the confirmation of the interactions by in vitro pull-down assays is ongoing. For that, we sub-cloned the preys into bacterial expression vector and expressed them as GST fusion proteins in *E. coli*. The IL-7RalphaIC was expressed in fusion with a His tag. The expression conditions for these proteins are currently being optimized in order to obtain them in the soluble fraction. These novel interactions may be valuable links to the comprehension of IL-7R signaling dependent of its phosphorylation status, and the role of IL-7R in cancer.

Acknowledgements: Supported financially by: Fapesp, CNPq and the LNLS.

Characterization of Interactions Between PthA Protein from *Xanthomonas citri* and Citrus Proteins Involved in Transcription Control, RNA Stability and Cell Proliferation

Soprano, A. S¹, Souza, T. A.¹, and Benedetti C.E.¹

Centro de Biologia Molecular Estrutural - Campinas SP Brazil

Xanthomonas axonopodis pv. *citri* (Xac), the causal agent of citrus canker, is a bacterial pathogen responsible for citrus canker, a disease that seriously affects commercial citrus varieties worldwide. This disease is characterized by hyperplastic lesions on the host surface. The molecular mechanism by which Xac induce lesions and rupture of the host epidermis is not entirely clear; nevertheless, it has been shown that members of the PthA/AvrBs3 family of effector proteins are required to elicit cankers on citrus. Data from our laboratory show that transient expression of PthAs in citrus cells significantly alters the transcription of host genes associated with cell division and expansion, indicating that PthAs, like AvrBs3, also act as transcription factors. Indeed, we found that PthA proteins interact with citrus α -importin and localize to nucleus of plant cells, thus supporting the notion that they act as transcription factors. However, although the ultimate targets of PthAs appear to be the host DNA, we hypothesized that these effectors might interact with other host proteins besides α -importin. Therefore, elucidating how PthA activates transcription is important to understanding canker development. To gain insights into the molecular mode of action of PthA, a two-hybrid approach was performed to identify citrus proteins that interact with PthA4, the main effector variant. Several proteins were isolated and most of them revealed functional DNA and/or RNA binding domains. Interestingly, a number of citrus proteins previously identified as interactors of PthA3, including TRAX and WSP also display nucleic acid-binding motifs. These proteins are suggested to be involved in gene regulation in the host.

Acknowledgements: This work was supported by FAPESP, CNPq and LNLS

Overexpression of MAP kinase and WRKY genes in Troyer citrange increased resistance to it *Xanthomonas axonopodis* pv. *citri*

Oliveira, M. L. P.¹ and Benedetti C.E.¹

Centro de Biologia Molecular Estrutural - Campinas SP Brazil

The production of citrus fruits has been constantly threatened by the bacterium *Xanthomonas axonopodis* pv. *citri* (Xac), the causal agent of citrus canker. The disease is characterized by pustule-like lesions on leaves, fruits and branches. Nowadays, principals measures applied for controlling citrus canker are the immediate destruction of infected trees followed by quarantine restrictions that are enforced to prevent the spread of the pathogen. These measures have generated significant losses to the citrus growers. The present work proposes to develop citrus plants resistant to Xac. The aim was to overexpress two citrus genes previously identified in our microarray study as induced during a resistance reaction against *Xanthomonas axonopodis* pv. *aurantifolii* (Xaa) in sweet orange. The genes are related to a Mitogen-Activated Protein Kinase (MAPK) and to a WRKY factor that have been shown in other plants to mediate basal defense against pathogens. Transgenic plants of Troyer citrange overexpressing the *mapk* or the *wrky* gene were obtained by *Agrobacterium tumefaciens*-mediated transformation. The gene constructs consisted of the *mapk* or *wrky* gene cloned downstream of a Xac-inducible promoter, and the selection genes *nptII* with the Nos terminator. Initial challenging of the kanamycin-resistant plants with the pathogen showed that both MAPK and WRKY-transformed plants exhibited normal vegetative development and displayed increased tolerance to the pathogen, as revealed by the significant reduction on the severity of lesions. To our knowledge, this is the first report of a genetic transformation of citrus plants using a pathogen-inducible promoter and the *mapk* and *wrky* genes. Moreover, the data presented show that overexpression of the *mapk* and *wrky* reduces the susceptibility of citrus plants to the canker bacteria.

Acknowledgements: This work was supported by Fundação de Amparo à pesquisa do Estado de São Paulo (FAPESP) and the Conselho Nacional de Desenvolvimento Científico e Tecnológico (CNPq).

The *Xanthomonas citri* effector protein PthA transactivates citrus genes associated with citrus canker development

Pereira, A. L. A.¹, Cernadas, R. A.², Oliveira, M. L. P.², and Benedetti C.E.²

¹ Laboratório Nacional de Luz Síncrotron - Campinas SP Brazil

² Centro de Biologia Molecular Estrutural - Campinas SP Brazil

Citrus crops are seriously affected by *Xanthomonas axonopodis* pv. *citri* (Xac), the bacterium pathogen responsible for citrus canker. The bacterium enters the plant through stomata leading to intense cell enlargement (hypertrophy) and division (hyperplasia), the principal canker symptoms. It has been shown that PthA, a member of the PthA/ArvBs3 family of transcription factors, is required to elicit canker on citrus. Previous microarray experiments employing the eukaryote protein synthesis inhibitor cycloheximide (CHX) allowed us to identify major sweet orange genes that were up-regulated by Xac, early during infection. Through transient *Agrobacterium*-mediated transfection, we expressed different variants of PthA genes in citrus hypocotyls to identify PthA-dependent gene transcription. We found that most of the genes associated with canker development that are up-regulated by Xac infection were similarly up-regulated by the PthAs. For instance, transcription of genes involved in cell division and elongation, cell-wall synthesis and remodeling were significantly altered. The promoter regions of some of these genes contain TATA box-like sequences remarkably similar to the so called upa-boxes bound by AvrBs3, an effector protein from *Xanthomonas campestris* pv. *vesicatoria* that is

Acknowledgements: Supported by FAPESP, CNPq and CeBiME - LNLS.

Caracterização da função da proteína ISG95 no metabolismo de RNA

Simabuco, F. M.¹, Vaz, T. H.¹, Paes Leme, A.F.¹, and Zanchin, N. I. T¹

Laboratório Nacional de Luz Síncrotron - Campinas SP Brazil

A resposta imune por interferon (IFN) do tipo I apresenta papel fundamental no combate às infecções virais, sendo um dos principais mecanismos de imunidade inata ativada na célula logo no começo da infecção. Ao reconhecer o vírus a célula entra em um estado antiviral, ativando genes efetores chamados ISGs (*interferon stimulated genes*), responsáveis por combater a infecção viral de diferentes formas. A proteína ISG95 faz parte do grupo de ISGs cuja expressão é fortemente estimulada por IFN. O estudo da função desta proteína foi iniciado recentemente, tendo sido delimitados quatro domínios funcionais da ISG95 relacionados com metabolismo de RNA, além de ter sido demonstrado sua interação com RNA e com o domínio C-terminal da RNA polimerase II e com a homóloga humana de MUT-7, que em *C. elegans* participa do processo de RNAi. Apesar destes dados iniciais, ainda são necessários muitos estudos para se determinar a função bioquímica da ISG95, bem como para se saber como a sua indução está relacionada com a resposta celular a infecção viral. O presente trabalho visa aprofundar a análise das interações protéicas da ISG95, além de determinar se ela está envolvida no processo de splicing. Descrevemos aqui a expressão em células humanas da proteína ISG95 fusionada ao tag peptídico FLAG. A proteína de fusão foi localizada no núcleo da célula por imunofluorescência e por fracionamento celular e a interação com a RNA polimerase II foi confirmada por *Western blot*. Além disso, foram identificadas três novas proteínas candidatas a interagir com ISG95 utilizando as técnicas de imunoprecipitação da ISG95 fusionada ao FLAG, digestão proteolítica em solução e identificação por espectrometria de massas. As proteínas BTF (*Bcl-2-associated transcription factor*) e TRAP150 (*thyroid hormone receptor associated protein 150 kDa*) estão envolvidas no processo de splicing de pre-mRNA, dado que está de acordo com a interação da ISG95 com o domínio C-terminal da RNA polimerase II, o qual serve de base para formação dos complexos de splicing que ocorre concomitantemente à transcrição. A terceira proteína co-imunoprecipitada é o fator de tradução eIF4B (*eukaryotic translation initiation factor 4B*), o qual estimula a atividade de RNA helicase do fator eIF4A, sendo que a isoforma III do eIF4A (eIF4AIII) atua no processo de splicing. Estudos estão em andamento para o melhor entendimento dessas interações.

Acknowledgements: Este trabalho foi financiado pela FAPESP e pelo CNPq

Development of a Library for Biomass-Conversion Enzymes

Ribeiro, D. A.¹, Murakami, M. T.², Ruller, R.¹, and Squina, F. M.²

¹ Centro de Ciência e Tecnologia do Bioetanol - Campinas SP Brazil

² Laboratório Nacional de Luz Síncrotron - Campinas SP Brazil

Agricultural and forestry residues are an abundant and low-cost source of stored energy in the biosphere. Nowadays, biomass conversion into feedstock sugars has moved towards the forefront of the biofuel industry. However, the saccharification of plant biomass is a complicated and lengthy process, mainly due to the inherent recalcitrance and the complex heterogeneity of the polymers comprising plant cell walls. Lignocellulosic biomass must go through a pretreatment step, after a consortium of enzymes is used to break down the polysaccharides into simple sugar suitable for fermentation and ethanol production. Herein we report the approach being conducted in the Centro de Ciência e Tecnologia do Bioetanol (CTBE) aiming at the generation of a library for biomass-conversion enzymes. This effort may contribute to the field of bioenergy not only by improving techniques for detection of polysaccharide hydrolysis through capillary electrophoresis and evaluation of enzymatic deconstruction plant biomass through microscopy analyses, but also by developing studies on structural characterization of biomass-conversion enzymes.

Acknowledgements: This work was supported by FAPESP and ABTLuS

Proteomic analysis of extracellular matrix of dental plaque formed in the presence of sucrose or glucose and fructose.

Moi, G.P.¹, Paes Leme, A.F.¹, and Cury, J. A.²

¹ Laboratório Nacional de Luz Síncrotron - Campinas SP Brazil

² Universidade Estadual de Campinas - Piracicaba SP Brazil

Recent study showing that sucrose promotes changes in the extracellular matrix protein composition (ECM) of plaque-like biofilm (PLB) in vivo provide further insight into the unique cariogenic properties of this dietary carbohydrate. However, additional studies should be done using other dietary carbohydrates to evaluate whether this effect is unique to this most cariogenic dietary carbohydrate. Therefore, the protein composition of ECM of PLB formed in the presence of sucrose or glucose and fructose were analyzed by two-dimensional gel electrophoresis (2-DE) and mass spectrometry (MS). For this purpose, a crossover and split mouth study was conducted during three phases of 14 days each, during which a volunteer wore a palatal appliance containing sixteen enamel blocks. In each phase, a 20% sucrose solution or distilled and deionized water (control) and 10% glucose + 10% fructose solution or control solution were extraorally dripped onto eight blocks 8 times/day. On the 14th day, the PLB were collected, the ECM proteins were extracted, separated by 2-DE and differential protein spots ($\alpha=0.05$) were submitted to in-gel and in-solution trypsin digestion and analyzed by ESI Q-TOF MS. Of the proteins identified, 33 were exclusively found in ECM in the sucrose group, 11 were present only in glucose + fructose group, 10 appeared only in control group, and 9 in the presence of sucrose and the control solution, but upregulated in the presence of sucrose. The results showed that the proteins identified in the PLB formed in the presence and absence of different carbohydrates were mainly calcium-binding proteins and proteins related to binding properties. A number of isoforms were identified in both conditions and these data indicate that the presence of isoforms, in terms of both the number and their abundance, was altered under the three different conditions. The findings showed that the ECM protein composition of PLB formed in vivo showed distinct patterns when it was formed in the absence or presence of the different carbohydrates.

Acknowledgements: This work was supported by CAPES.

SAXS IN STRUCTURAL STUDIES ON SECRETION CHAPERONES FROM *Xanthomonas axonopodis* pv. *citri*

Fattori, J.¹, Aparicio, R.¹, and Tasic, L.¹

Universidade Estadual de Campinas - Campinas SP Brazil

The citrus canker agent, *Xanthomonas axonopodis* pv. *citri* (*Xac*), like many Gram-negative bacteria, uses secretion systems to invade its host-cells, and secretion chaperones seems to have a crucial role in selecting, unfolding and translocating the virulence factors. The structural characterization of some *Xac* chaperones was the scope of our investigations with the aim of lightening their function in virulence processes. The five hypothetical type III and IV secretion chaperones, earlier cloned in pET23a vector and with sequences confirmed by DNA sequencing, were expressed from BL21(DE3)plysS *E. coli* strains and purified in one or two steps applying the ion exchange and size exclusion chromatography. In the sequence we have concentrated protein solutions in 5 mM Tris buffer, and have quantified the purified proteins samples by absorbance at 280 nm or by Bradford method. Proteins in concentrations 1-5 mg/mL were taken to the Small Angle X-Ray Scattering (SAXS) beam line (D11A LNLS) and then SAXS experiments were performed. We used as standard solutions BSA (66.4 kDa) and lysozyme (14.3 kDa) (5 mg/mL in 5mM buffer) to fit the results. Only one of the analyzed proteins presented promissory results while others showed tendency to aggregate in higher concentrations. In parallel we are executing the crystallographic studies with two of the target proteins and the refinement tests were initialized.

Acknowledgements: This work was supported by FAPESP

Mass Spectrometry Analysis of Secretion Chaperones from *Xanthomonas axonopodis* pv. *citri*

Martins, A. M.¹, Arruda, M. A. Z.¹, and Tasic, L.¹

Universidade Estadual de Campinas - Campinas SP Brazil

Xanthomonas axonopodis pv. *citri* (*Xac*) is a Gram-negative bacterium that causes the citric canker, one of the most severe diseases of worldwide citriculture. Although the *Xac* infection mechanisms are not totally understood, the secretion chaperones¹, mainly belonging to Type III and IV Secretion Systems², are proteins that probably initiate the infection process by recognizing and delivering the virulence factors into the target-cells. In this study, *Xac* strain 306 was cultivated in LB medium enriched with orange leaves and barks extracts. It was possible to observe the greater cellular growth at these nutrient rich media in comparison with LB. Applying GC-MS analyses the preferential *Xac* consumption of specific terpenes was observed, and generation of compounds derived from phenol, ketones and furan were identified as metabolites. After few preparatory steps, *i.e.*, harvesting, lysis, and dialysis, the *Xac*'s proteins were separated by bidimensional electrophoreses. The protein containing spots were cleaved with trypsin (EC 3.4.21.4) and analyzed by MALDI-Tof (MS/MS). We already have identified 10 proteins: some of them chaperonins, proteases, a membrane protein involved in the infection process (Q8PHV8_XANAC) and a hypothetical (XAC1492; Q8MD7_XANAC) protein. We intent to execute the Shotgun analysis, design primers and clone the identified hypothetical protein, as well as, investigate the metal importance by ICP-MS.

¹ Young, J. C. et al., Nature 2004, (5), 781-791. ² Khater, L. et al., Genet. Mol. Biol. 2005, 28 (2), 321-327.

Acknowledgements: Instituto de Química - UNICAMP; Laboratório de Química Biológica; CAPES for the financial support MAS - LNLS.

Expression and Purification of cTPxIII and TrxI^{C33S} and Mutation of cTPxIII of *Saccharomyces cerevisiae* for Formation of Mixed Disulfide Protein Complexes.

Santos, V.F.¹, Netto, L.E.S.², and Oliveira, M.A.¹

¹ Universidade Estadual Paulista Julio de Mesquita Filho - Assis SP Brazil

² Universidade de São Paulo - São Paulo - São Paulo SP Brazil

Expression and Purification of cTPxIII and TrxI^{C33S} and Mutation of cTPxIII of *Saccharomyces cerevisiae* for Formation of Mixed Disulfide Protein Complexes.

Vanessa Fernandes dos Santos¹, Luis Eduardo Soares Netto² and Marcos Antonio de Oliveira¹ ¹Departamento de Biologia, Universidade Estadual Paulista, Campus do Litoral Paulista, Sao Vicente-SP, Brazil. ² Departamento de Genetica e Biologia Evolutiva, Universidade de Sao Paulo, Sao Paulo-SP, Brazil.

Thioredoxin Peroxidases (TPx) are a family of thiol-specific antioxidants proteins widely distributed and conserved among organisms. These enzymes are able to decompose hydrogen peroxidase, organic peroxides and peroxyxynitrite through highly reactive cysteines. In eukaryotes, TPx activity has been associated to different cellular processes such proliferation, differentiation, hydroxide peroxide signaling, apoptosis, tumor suppression, organism longevity and genome stability. *Saccharomyces cerevisiae* has five TPxs isoforms that are located in nucleus (nTPx), mitochondria (mTPx) and cytoplasm (cTPx, I, II, III). The cytosolic isoforms possess high activity concerning the hydrogen peroxidase. However, cTPxIII presents higher specificity towards organic peroxides substrates and null-mutants are hypersensitive to hydroperoxides. In spite of biochemical differences concerning the substrate, *Saccharomyces cerevisiae* cytosolic TPx uses reduced thioredoxin as an electron donor for the catalytic reduction. As electrons are transferred by cysteine pairs presents in active sites of both proteins, substitution of specific cysteines by serines can promote the formation of a stable protein complex, binding by mixed disulfides. Aiming the investigation of the structural aspects of the cTPxIII-TrxI interaction, we have expressed cTPxIII and the mutant TrxI^{C33S}. The cTPxIII protein was purified by immobilized metal ion affinity chromatography (IMAC) and TrxI^{C33S} by the boiling method. After purification, proteins were treated with 50 equivalents of diamide (cTPxIII) or DTT (TrxI^{C33S}). Subsequently, sample were desalted and concentrated in equimolar concentration they were incubated to promote complex formation and detected by non reducing SDS PAGE. Financial Support: FAPESP and CNPQ.

Acknowledgements:

Ciência Atômica e Molecular

Electronic excitation and ionic dissociation of volatile organics compounds of sulfur related with the ocean-atmosphere cycle: DMS and DMDS

Grangeiro, L.B.¹, Bernini, R.B.¹, Rodrigues, F. N.², Coutinho, L. H.¹, and de Souza, G.G.B.¹

¹ Universidade Federal do Rio de Janeiro - Rio de Janeiro RJ Brazil

² Instituto Federal de Educação, Ciência e Tecnologia do Rio de Janeiro - Rio de Janeiro RJ Brazil

The natural flux of sulfur to the atmosphere occurs mainly through volatile sulfur compounds (known as reduced sulfur compounds) produced in oceans. In surface waters, the responsible for the uptake of sulfate and conversion into dimethylsulfoniopropionate (DMSP) are the phytoplankton¹. The enzymatic decomposition of DMSP yields reduced sulfur compounds, like: dimethylsulfide (DMS), dimethyl disulfide (DMDS), methyl mercaptan or methanethiol (CH₃SH) and carbon disulfide (CS₂). It is believed that the earth's climate can be influenced by these reduced sulfur compounds through modification of the radiation budget. With the intention of studying electronic excitation and relaxation process of these molecules when submitted to high energy radiation, photoabsorption and ionic fragmentation spectra were obtained for dimethyl sulfide (DMS) and dimethyl disulfide (DMDS) molecules around the S 2p shell. Mass spectra, using synchrotron radiation (beamline TGM at LNS) and a time of flight spectrometer, were recorded at different energies, around the resonances observed in the photoabsorption spectrum. The experimental technique has been described previously². In DMS, the valence-shell mass spectrum (measured at 19 eV), resembles the electron-impact standard mass spectrum (measured at 70 eV electron energy NIST base). The dominant fragments correspond to m/z 62 (molecular ion), m/z 47 (S-CH₃⁺), m/z 35 (SH₃⁺) and m/z 27 (C₂H₅⁺). Extensive fragmentation occurs at the core level. For example, at 185 eV photon energy, the dominant fragments are H⁺ (m/z 1) and CH₃⁺ (m/z 15). Double ionization of the molecule is clearly demonstrated with the observation of the S⁺² fragment ion (m/z 16). Referências 1) CHARLSON, R.J.; LOVELOCK, J.E.; ANDRAE, M.O.; WARREN, S.G. Nature, 326, 655-661, 1987 2) LAGO, A.F.; SANTOS, A.C.F.; de SOUZA, G.G.B Journal of Chemical Physics, 9547-9554, 12, 2004

Acknowledgements: The authors would like to acknowledge CNPQ and LNS for financial assistance, Mr. Paulo de Tarso for the technique support during the data acquisition and Prof. Luiz Carlos Dias, from Chemistry Institute of UNICAMP, for the DMS sample donation.

Fragmentation Dynamic of Clorobenzene and Toluene Induced by Synchrotron Radiation

Fernandes, D.H.L.¹, G. Ferreira², Turci, C. C.³, Guerra, A. C. O.¹, and A.L.F. de Barros¹

¹ Centro Federal de Educação Tecnológica - Rio de Janeiro RJ Brazil

² Universidade Federal do Rio de Janeiro - Macae RJ Brazil

³ Universidade Federal do Rio de Janeiro - Rio de Janeiro RJ Brazil

Inner-shell excitation, and associated spectroscopy of the ionic fragmentation of inner shell states, are site specific probes of electronic and geometrical structure and photoionization dynamics [1]. Here we present recent results of coincidence studies in the K-edge of gaseous clorobenzene and toluene. The ionic fragmentation has been measured with tuned synchrotron light and time-of-flight mass spectrometry apparatus [2]. In the toluene the $-CH_3$ is a very poor activating group while in the clorobenzene the $-Cl$ is a very poor deactivating group. Our goal in this work is to investigate the fragmentation dynamic of those aromatic molecules following core excitation in K-edge region. How the both donor $-CH_3$ and acceptor $-Cl$ groups influencing the charge transfer into the aromatic ring? [3]. Those molecules are part of the studying of the fragmentation dynamics of some aromatic system (e.g. benzene, aniline, nitrobenzene and nitroanilines) The experiments have been performed using the Spherical Grating Monochromator (SGM) beamline at the National Laboratory of Synchrotron Light (LNLS) in Campinas-SP (research proposal D08A-SGM-8730). High purity samples were obtained commercially and used without any further purification. They were introduced into the apparatus from the vapours of the room temperature liquids after removing air and volatile impurities by a series of freeze-pump-thaw cycles. The work pressure was maintained at 1.0×10^{-6} mbar during data acquisition. The base pressure was 1×10^{-8} mbar.

[1] A.P. Hitchcock and J.J. Neville, in *Chemical Applications of Synchrotron Radiation*, T.K. Sham, ed. World Scientific (2002) 154. [2] F. Burmeister, et al., *J. Electron Spectrosc. Relat. Phenom.* (2007) in press; Lago, A.F., et al., *J. Chem. Phys.* 120 (2005) 9547. [3] A.C.O. Guerra, et al., *Inter. J. Quant. Chem.* 108 (2008) 2340.

Acknowledgements: LNLS, FAPERJ, CNPq

NEXAFS study of the radiation damage in biomolecules: methionine, cysteine, cystine and insulin.

Simões, G.¹, Grangeiro, L.B.¹, and de Souza, G.G.B.¹

Universidade Federal do Rio de Janeiro - Rio de Janeiro RJ Brazil

Amino acids are building blocks of polypeptides and proteins, the most important class of biological macromolecules. NEXAFS spectroscopy, an element-selective technique, has been applied to amino acids and proteins in recent studies [1,2]. Amino acids and their derivatives are highly susceptible to soft X-ray irradiation and undergo deep chemical transformations under prolonged or intense beam exposure [1]. When subjected to ionizing radiation, amino acids and proteins decompose, through a number of pathways such as dehydrogenation (deprotonation), dehydration, decarboxylation, decarbonilation, deamination, and desulfurization. These pathways are usually accompanied by the release of gaseous species such as H₂, H₂O, CO₂, CO, NH₃, and H₂S, as well as by the formation of CC and CN multiple bonds [1]. We hereby report on the experimental determination of N and O K-edge NEXAFS spectra of methionine, cysteine, cystine and insulin. The samples (powders) were deposited on a carbon sticky tape. Special care was taken to prepare sufficiently thin and uniform layers in order to avoid strong charging during the NEXAFS measurements. NEXAFS spectra were obtained at the Spherical Grating Monochromator beamline (SGM), LNLS-Campinas, for irradiated (3 minutes, zero order beam) and non-irradiated samples. Significant spectral changes within the measurement time were detected in high-quality NEXAFS spectra for all samples, along the N 1s border. More subtle changes were observed in the spectra obtained around the O 1s edge.

References:

[1]. Y. Zubavichus, A. Shaporenko, M. Grunze, M. Zharnikov, *Journal of Electron Spectroscopy and Related Phenomena* 134 (2004) 2533.

[2]. Weik, Martin et al, *PNAS*, 97, 623-628. 2000.

Acknowledgements: This work has been supported by LNLS under proposal D08A - SGM 8759, CAPES and CNPq. We are also indebted to Mr. Paulo de Tarso for technical assistance during data acquisition at the LNLS.

ELECTRONIC PROPERTIES OF THE COORDINATION COMPOUNDS OF THE LIGANDS DMIT, DMIO AND DMT IN THE C 1s, N1s and O1s REGIONS.

Ferreira, G. B.¹, Lopes, L. J. S.¹, Turci, C. C.¹, A.L.F. de Barros², Almeida, G.C.¹, and Guerra, A. C. O.²

¹ Universidade Federal do Rio de Janeiro - Rio de Janeiro RJ Brazil

² Centro Federal de Educação Tecnológica - Rio de Janeiro RJ Brazil

The sulphur heterocyclic systems are important coordination ligands because their electrical conduction, ferromagnetism and non-linear optic (NLO) [1] properties. The variety of the redox and polarizability of the sulphur atoms in the compounds are the main factors that contribute to those properties. However, the effect of this delocalization was not yet evaluated on the C 1s edge. Photoabsorption and Photoelectron spectra in the C 1s, O 1s and N 1s regions of DMIT, DMIO and DMT ligands have been acquired for [Ni(dmit)][NEt₄]₂, [Ni(dmio)][NEt₄]₂ and [Ni(dmt)][NEt₄]₂ compounds. All compounds were synthesized following the literature [1-3].

TEY spectra have been acquired at Spherical Grating Monochromator (SGM) beamline, LNLS-Campinas. The compounds were introduced into the main chamber as a solid samples using a carbon sticky tape. The work pressure was kept at 2×10^{-7} mBar.

The spectra analysis of these compounds allowed to identify the different chemical environment in the C 1s region. Ab initio calculations associated with improved virtual orbital (IVO) method, carried out with the GSCF3 program, were used to help us to establish the assignments. The geometric parameters were optimized using the GAMESS program.

Referências

1. Svenstrup, N.; Becher, J. *Synthesis*. 1995, 215.
2. Cassoux, P., et al., *Coord. Chemistry Reviews*, 185, 213, 1999.
3. Steimecke, G., et al., *E. Phosphorus and Sulfur*, 12, 237, 1982.

D08A-SGM-8775

Acknowledgements: LNLS, FAPERJ, CNPq, FUNEMAC

STUDY OF THE OXIDATION STATE BY COMPARATIVE ANALYSIS OF RESONANT INELASTIC X-RAY SCATTERING EMISSION

H. J. Sánchez¹, Valentinuzzi, M. C.¹, Leani, J.J.¹, and Pérez, C. A.²

¹ Universidad Nacional de Cordoba - Córdoba Cba Argentina

² Laboratório Nacional de Luz Síncrotron - Campinas SP Brazil

When atoms are irradiated with incident energy lower and close to an absorption edge, scattering peaks appear due to an inelastic process known as resonant Raman scattering (RRS). In this process, the emitted photons have a continuous energy distribution with a high energy cut-off limit. In the last few years experiments of RRS have become a very powerful technique to investigate excitations of electrons in solids. This work presents results regarding the possibility of determining the oxidation state by resonant Raman scattering using an energy dispersive system. Several measurements of samples of Mn, Fe, Cu and their oxides were carried out, using monochromatic synchrotron radiation at the XRF beamline of the LNLS (Campinas, Brazil), below and close to their absorption edges to inspect the RRS emissions. The spectra were analyzed with specific programs for fitting the experimental data to theoretical expressions. After that, residuals were determined in the low energy side of the RRS peaks and a FFT smoothing procedure was applied, taking into account the instrument functions of the detecting system. The results show an oscillation pattern that depends on the sample, i.e. on the oxidation state, being a possibility of chemical speciation determination using RRS spectroscopy. The changes in the RRS structure between the pure elements and their oxides are discriminated and suggest the possibility of structural characterization by means of resonant Raman scattering using an energy-dispersive system combined with synchrotron radiation. More measurements in different samples will be carried out to verify the present results and to establish a repetitive and reliable method of structural determination.

Acknowledgements: This work was partially supported by the LNLS (Campinas, Brazil).

Positive and negative ionic desorption from condensed formic acid photoexcited around the O 1s-edge: relevance to cometary and planetary surfaces

Andrade, D. P. P.¹, Boechat-Roberty, H.M.², Pilling, S.¹, E. F. da Silveira¹, and Rocco, M.L.M.²

¹ PUC - Rio de Janeiro - Rio de Janeiro RJ Brazil

² Universidade Federal do Rio de Janeiro - Rio de Janeiro RJ Brazil

Photon stimulated ion desorption (PSID) studies have been performed in condensed formic acid using oxygen 1s-edge synchrotron radiation from the Brazilian Synchrotron Light Source (LNLS), operating in a single-bunch mode and using time-of-flight mass spectrometry (TOF-MS) for ion analysis [1]. While the positive PSID spectrum is rich, presenting many features, the negative spectrum shows only H⁻ and O⁻ species. Ion formation was discussed in terms of the Auger Stimulated Ion Desorption (ASID) and X-ray induced electron stimulated desorption (XESD) mechanisms. The photon energy dependent studies revealed that C⁺, CH⁺, O⁺, O⁻ and H⁻ desorptions occur mainly via ASID mechanism, while for m/q = 14, m/q = 28 and the weak OH⁺/H₃⁺/C₂⁺ desorptions, the contribution due to XESD process has to be invoked. The hydroxyl anion has not been observed while the hydroxyl cation showed low intensity or was absent. Some anion formation routes from dissociative reactions are suggested taking into account the positive ion yields.

[1] Rocco, M.L.M. et al, Surface Science (in revision).

Acknowledgements: The authors acknowledge LNLS, CNPq, CAPES, FAPESP and FAPERJ for financial support.

Multiple photoionization of Ne in the K-shell region and its comparison to electron impact data. The roles of direct outer-shell electron ejection and inner-shell ionization

ACF Santos¹, Almeida, D. P.², and Homem, M. G. P.³

¹ Universidade Federal do Rio de Janeiro - Rio de Janeiro RJ Brazil

² Universidade Federal de Santa Catarina - Florianópolis SC Brazil

³ Universidade Federal de São Carlos - São Carlos SP Brazil

In this work we have measured the Ne photoion charge state distributions as a function of photon energy after a K-shell vacancy. The present results show a higher production of singly ionized ions in comparison with other experimental results. This is a surprising result since the present experimental set-up exhibits a high bias towards the detection of the multiply charged ions. Whether this difference is due to a high discrimination toward low charge states in the previously published data or to an overcompensation of the present detection efficiencies is uncertain. It is generally accepted that the atomic ionization by fast electrons is dominated by the direct ejection of a single target electron. Manson, DuBois and Toburen [S. T. Manson, R. D. DuBois and L. H. Toburen, Phys. Rev. Lett. 51, 1542 (1983)] have demonstrated that the dominant mechanism leading to double ionization of Ne by fast proton impact is direct outer-shell ionization and not the Auger channel. By combining various experimental data, we determine the multiple-ionization mechanisms in fast electron-neon collisions.

Acknowledgements: The authors would like to express their gratitude to the staff of the Brazilian Synchrotron National Facility (LNLS) for their valuable help during the course of the experiments. This work was supported by LNLS, CNPq, and FAPERJ.

Dissociative Photoionization of FC(O)SCH₂CH₃ following the shallow and innershell core electronic properties

Rodríguez Pirani, Lucas¹, Erben, Mauricio F.¹, Geronés, Mariana¹, Romano, Rosana M.¹, Cavasso Filho, R. L.², and Della Védova, Carlos O.¹

¹ Universidad Nacional de La Plata - La PLata B.A. Argentina

² Universidade Federal do ABC - Santo André SP Brazil

In recent years, a number of investigations have been performed in the LNLS concerning the chemistry family of sulfenylcarbonyl compounds. These studies have included the elucidation of photo-dissociation channels upon VUV and soft X-ray irradiation. Thus, FC(O)SCl,^[1–3] ClC(O)SCl,^[3,4] CH₃C(O)SH,^[5] CH₃OC(O)SCl^[6], CH₃C(O)SCH₃^[7], ClC(O)SCH₃, FC(O)SCH₃ and ClC(O)SCH₂CH₃ has been studied in this context. Following with this general project, we present here for the first time the study concerning to the photon impact excitation and dissociation dynamics of FC(O)SCH₂CH₃ excited at the S 2p level. Total Ion Yield (TIY) spectra and multicoincidence techniques, namely as PhotoElectronPhotoIon Coincidence (PEPICO) and PhotoElectronPhotoIonPhotoIon Coincidence (PEPIPICO) time of flight (TOF) mass spectrometry were applied. Below the S 2p threshold, located at approximately 171.5 eV, the TIY spectrum is dominated by an intense resonance centered at 165.7 eV and two shoulders around 164.0 and 166.7 eV. Similar resonance features were observed for other member of the carbonylsulfenyl family of compounds already measured FCOSCH₃. PEPICO and PEPIPICO spectra were measured at several photon energies around the S 2p edge. Possible mechanisms involved in the fragmentation of FC(O)SCH₂CH₃²⁺ ion was deduced from the shape of the PEPIPICO double coincidence peaks. Total ion yield spectrum together with the PEPICO spectra at selected photon energies using synchrotron radiation in the valence region have been measured, thereby allowing the study of the dissociation dynamics of excited FC(O)SCH₂CH₃ molecules.

Acknowledgements: This work was supported by LNLS under proposal D05A-TGM-8737, Departamento de Química, Facultad de Ciencias Exactas, UNLP, CONICET, CIC. [1] Erben, M. F.; Romano, R. M.; Della Védova, C. O. J. Phys. Chem. A 2004, 108, 3938. [2] Geronés, M.; Erben, M. F.; Romano, R. M.; Della Védova, C. O. J. Electron Spectrosc. Relat. Phenom. 2007, 155, 64. [3] Geronés, M.; Erben, M. F.; Romano, R. M.; Della Védova, C. O.; Yao, L.; Ge, M. J. Phys. Chem. A 2008, 112, 2228. [4] Erben, M. F.; Romano, R. M.; Della Védova, C. O. J. Phys. Chem. A 2005, 109, 304. [5] Erben, M. F.; Geronés, M.; Romano, R. M.; Della Védova, C. O. J. Phys. Chem. A 2006, 110, 875. [6] Erben, M. F.; Geronés, M.; Romano, R. M.; Della Védova, C. O. J. Phys. Chem. A 2007, 111, 8062. [7] Geronés, M.; Downs, A. J.; Erben, M. F.; Ge, M.; Romano, R. M.; Yao, L.; Della, Védova, Carlos O. J. Phys. Chem. A 2008, 112, 5947.

Ionic fragmentation of selenium oxychloride under VUV irradiation

Erben, Mauricio F.¹, Geronés, Mariana¹, Rodriguez Pirani, Lucas¹, Cavasso Filho, R. L.², Romano, Rosana M.¹, and Della Védova, Carlos O.¹

¹ Universidad Nacional de La Plata - La Plata B.A. Argentina

² Universidade Federal do ABC - Santo André SP Brazil

Our research group has quite recently started studying the properties of shallow- and inner-core level electrons in sulfur-containing compounds. Thus, sulfenylcarbonyl species^[1–5] and thiocyanates species^[6,7], have been studied by using synchrotron radiation and multicoincidence techniques. The recent development of a neon gas filter in the TGM line at the Brazilian Synchrotron National Laboratory, has allowed us to expand the study on the electronic properties and photoionization dynamics into the valence region. Thus, sulfenylcarbonyl compounds like FC(O)SCl^[8], ClC(O)SCl^[8] and CH₃C(O)SCH₃^[9] have been recently analyzed in this energy range. Following these studies, we became interested in selenium-containing compounds. Thus, the selenium oxychloride was the first molecule chosen to be studied. In the present work, we report preliminary results concerning the photodissociation of this molecule in the 12-300 eV range. This energy range allows us to record the Se 3d, Se 3p, Se 3s and Cl 2p edges together with the valence region. Special interest should be paid in the selenium 3d and 3p region, as comparing with the S 2p edge. Total Ion Yield (TIY) and PhotoElectronPhotoIon Coincidence (PEPICO) spectra have been measured under VUV irradiation. The isotopic distribution of the selenium and chlorine is clearly observed in the TOF spectra due to the suitable mass resolution attained in the experiments.

Acknowledgements: This work was supported by LNLS under proposal D05A-TGM-8737, Departamento de Química, Facultad de Ciencias Exactas, UNLP, CONICET, CIC, ANPCyT. [1] M. F. Erben, R. M. Romano, C. O. Della Védova, J. Phys. Chem. A. 2004, 108, 3938-3946. [2] M. Geronés, M. F. Erben, R. M. Romano, C. O. Della Védova, J. Electron Spectrosc. Relat. Phenom. 2007, 155, 64-69. [3] M. F. Erben, R. M. Romano, C. O. Della Védova, J. Phys. Chem. A. 2005, 109, 304-313. [4] M. F. Erben, M. Geronés, R. M. Romano, C. O. Della Védova, J. Phys. Chem. A. 2006, 110, 875-883. [5] M. F. Erben, M. Geronés, R. M. Romano, C. O. Della Védova, J. Phys. Chem. A. 2007, 111, 8062-8071. [6] E. Cortés, M. F. Erben, M. Geronés, R. M. Romano, C. O. Della Védova, J. Phys. Chem. A. 2009, 113, 564-572. [7] E. Cortés, M. F. Erben, M. Geronés, R. M. Romano, C. O. Della Védova, J. Phys. Chem. A. 2009, 113, 9624-9632. [8] M. Geronés, M. F. Erben, R. M. Romano, C. O. Della Védova, L. Yao, M. Ge, J. Phys. Chem. A. 2008, 112, 2228-2234. [9] M. Geronés, A. J. Downs, M. F. Erben, M. Ge, R. M. Romano, L. Yao, C. O. Della Védova, J. Phys. Chem. A. 2008, 112, 5947-5953.

STUDY OF THE OXIDATION STATE BY COMPARATIVE ANALYSIS OF RESONANT INELASTIC X-RAY SCATTERING EMISSION

H. J. Sánchez¹ and Valentinuzzi, M. C.¹

Universidad Nacional de Cordoba - Córdoba Cba Argentina

When atoms are irradiated with incident energy lower and close to an absorption edge, scattering peaks appear due to an inelastic process known as resonant Raman scattering (RRS). In this process, the emitted photons have a continuous energy distribution with a high energy cut-off limit. In the last few years experiments of RRS has become a very powerful technique to investigate excitations of electrons in solids. This work presents results regarding the possibility of determining the oxidation state by resonant Raman scattering using an energy dispersive system. Several measurements of samples of Mn, Fe, Cu and their oxides were carried out, using monochromatic synchrotron radiation at the XRF beamline of the LNLS (Campinas, Brazil), below and close to their absorption edges to inspect the RRS emissions. The spectra were analyzed with specific programs for fitting the experimental data to theoretical expressions. After that, residuals were determined in the low energy side of the RRS peaks and a FFT smoothing procedure was applied, taking into account the instrument functions of the detecting system. The results show an oscillation pattern that depends on the sample, i.e. on the oxidation state, being a possibility of chemical speciation determination using RRS spectroscopy. The changes in the RRS structure between the pure elements and their oxides are discriminated and suggest the possibility of structural characterization by means of resonant Raman scattering using an energy-dispersive system combined with synchrotron radiation. More measurements in different samples will be carried out to verify the present results and to establish a repetitive and reliable method of structural determination.

Acknowledgements: This work was partially supported by the LNLS (Campinas, Brazil).

Evaluation of long-term effects of tibolone in femoral bone by Synchrotron X-Ray Microfluorescence Microscopy

LIMA, I.¹, Sales, E.², Granjeiro, J. M.³, GUZMAN-SILVA, M.A.³, CARVALHO, A.C.B.³, and Lopes, R.T.²

¹ Universidade do Estado do Rio de Janeiro - Rio de Janeiro RJ Brazil

² Universidade Federal do Rio de Janeiro - Rio de Janeiro RJ Brazil

³ Universidade Federal Fluminense - Niterói RJ Brazil

The most common treatment, in order to combat the symptoms of menopause, is the hormone replacement therapy which gives artificial supply of estrogen and progesterone allowing the body to function with fewer menopausal symptoms. However, this long-term therapeutic administration has demonstrated disadvantages such as an increase of cancer incidence on the breast and endometrium and heart diseases. Nevertheless, other alternative appears, such as tibolone treatment. It has been used primarily for the prevention of postmenopausal osteoporosis and treatment of climacteric symptoms. The great advantage against classical replacement therapy is its specific tissue action which performs differently in each part of the organism. In this way, tibolone has almost no action on breast and endometrium locations where estrogens have action. In this work, in order to evaluate the effects of a long-term administration of tibolone, the X-ray microfluorescence with synchrotron radiation imaging technique was used. In this context, it was possible to investigate qualitatively and quantitatively bone mineral content such as calcium and strontium in bone samples, specially its distribution on bone microarchitecture. The X-ray microfluorescence with synchrotron radiation becomes a very important tool to elucidate the interaction of the major mineral components in bone, demonstrating that it can be an effective alternative technique for characterizing bone structures by 2D chemical element maps. It was possible to observe that the present study confirms the estrogenic effect of tibolone at the femoral head by the higher concentrations of some chemical elements like Ca and Sr in the trabecular regions, when compared to ovariectomized and control groups.

Acknowledgements: This work was partially supported by Conselho Nacional de Desenvolvimento Científico e Tecnológico (CNPq), FAPERJ (Fundação de Amparo à Pesquisa do Rio de Janeiro) and LNLS (Projects XRF 8051, 8774). The authors are grateful to the donation of tibolone by OFFICILAB and to the surgeons Dr. José Augusto Soares Pantaleão and Dr. Carlos Eduardo Pollastri, which performed the ovariectomy.

Ionic fragmentation of SO₂ after S 1s excitation

Naves de Brito, A.¹, Mocellin, A.¹, Cavasso Filho, R. L.², Lago, A. F.², and Mundim, M. S. P.¹

¹ Universidade de Brasília - Brasília DF Brazil

² Universidade Federal do ABC - Santo André SP Brazil

We present the measured electron-multi-ion coincidence spectra after photo-excitation of the SO₂ molecule around the S1s edge. A procedure for complete determination of all set of ions formed is described. The new measurements reported here rely on a new system capable to detect ions connected to the same ionization event arriving down to 1 nanosecond apart. The dissociation channels and its behavior with the photon energy of this molecule is presented in comparison with the Total Ion Yield (TIY). We observed a higher charge multiplicity in the sulfur atom, which is the excitation atom for SO₂ molecule. Auger cascade after the 1s core hole creation leading to 2p double hole states needs to be taken in to account to explain these observations. The time scale of the nuclear motion and decay is discussed in order to explain the intra-atomic cascade Auger leading to the observed selective charge distribution. Recombination forming an O₂ ion was found.

Acknowledgements: We thank LNLS staff for an excellent support. The data was taken at SXS beamline during multibunch and single bunch period.

Photodissociation of Glycine by UV H₂ Lamp Radiation

Ferreira-Rodrigues, A. M.¹, Homem, M. G. P.², Naves de Brito, A.³, C.R. Ponciano¹, and E. F. da Silveira¹

¹ PUC - Rio de Janeiro - Rio de Janeiro RJ Brazil

² Universidade Federal de São Carlos - São Carlos SP Brazil

³ Universidade de Brasília - Brasília DF Brazil

The amino acids found in Interstellar Medium and in Solar System bodies are of particular importance for the chemistry related to the origin of life, because they are constituents of all living organisms. Several amino acids have been identified in meteorites carbonaceous with significant concentration and evidence has been found of glycine in regions of star formation. To interpret the viability of amino acids in prebiotic chemistry is important to investigate the stability of these compounds in extraterrestrial surroundings. This study investigates, in the laboratory, the stability of glycine to the action of ultraviolet radiation, in the wavelength of the Lyman α line (~ 1216) produced by a H₂ lamp. ²⁵²Cf-PDMS mass spectrometry of positive and negative desorbed ions was performed for glycine, before and during the irradiation, and the dependence of their desorption yields on the irradiation time is determined. As a result, the relative photostability curves of the molecular and dimer ions are observed to be a single exponential decay with a time constant mean of ~ 430 min for positive and negative desorbed ions. The photodissociation cross section was obtained. However, it is observed that positive charge species decay faster than negative ones; this is attributed to effects due to polymerization on the irradiated sample surface.

Acknowledgements: This work was supported by CNPq, FAPERJ and LNLS.

**Geociência, Meio-ambiente e Aplicações em
Materiais Biológicos**

Study of the bioaccumulation kinetic of lead and copper by living aquatic macrophytes *Eichhornia crassipes*

Espinoza Quiñones, F.R.¹, Palacio, S.M.¹, Szymanski, N.¹, Manenti, D. R.¹, Módenes, A.N.¹, and Borba, F.H.¹

Universidade Estadual do Oeste do Paraná - Toledo PR Brazil

In the present work, the phytoaccumulation of lead and copper by living floating aquatic macrophytes *Eichhornia crassipes* was investigated in a greenhouse. These plants were grown in metal-doped hydroponic solutions forming, as a function of time, six collections of nutrient media, roots and leaves of plants from a batch system. The Synchrotron X-ray radiation fluorescence technique was used in order to determine the element concentrations in the nutrient media, dry roots and aerial parts of plant. The aquatic plant-based heavy metal uptake data were described by using a nonstructural kinetic model. According to the experimental data, both adsorption and bioaccumulation mechanism are present. The nonstructural kinetic models have shown good agreement with the uptake experimental data of lead and copper in all the studied cases. The results of living macrophytes *Eichhornia crassipes*-based metal bioaccumulation kinetic parameters can be used in artificial wetlands to predict the heavy metal removal dynamics from waste waters.

Acknowledgements: We gratefully acknowledge the Brazilian Light Synchrotron Laboratory (LNLS) for the partial financing of this study (project XRF-8064)

Study of Cr(VI) reduction by activated carbon using high resolution X-ray emission spectroscopy

Módenes, A.N.¹, Espinoza Quiñones, F.R.¹, Palacio, S.M.¹, Stutz, G.², Tirao G.², and Camera, A.S.¹

¹ Universidade Estadual do Oeste do Paraná - Toledo PR Brazil

² Universidad Nacional de Cordoba - Cordoba Argentina

In this work granular activated carbon has been chosen as an absorbent in order to investigate the Cr(VI) reduced by adsorption experiments. Several batch chromium-sorption experiments were carried out using 0.25 g of granular activated carbon into 50 mL metal solution containing approximately 70 and 140 mg L⁻¹ of Cr(VI) and Cr(III), respectively. Batch experiments at 3.5 pH were carried out to determine the chromium ions sorption capacity and to verify the Cr(VI) reduction. A set of 100 mg Cr treated sample pellets was prepared. Measurements of the whole Cr-K X-ray emission spectra were performed using a combination of a high-resolution Johann-type spectrometer and a high flux, 6.1-keV X-ray monochromatic beam at the D12A-XRD1 beamline at the Brazilian Synchrotron Light Laboratory. Sample, spherically focusing nearly backdiffracting Si(111) crystal analyzer and silicon pin-diode detector were positioned on the Rowland circle to fulfill the focusing condition in a vacuum chamber. Cr-K satellite lines have been characterized for all K spectra of Cr ions treated material. Based on the energy position and intensity of Cr-K satellite lines, activated carbon and non-living aquatic macrophytes roots were found to act mainly as good adsorbents, reducing first Cr(VI) to Cr(III), followed by the Cr(III) adsorption. Thus, HR-XRF technique has allowed verifying that the adsorption process is responsible by the Cr(VI) reduction and removal from metal solutions.

Acknowledgements: We gratefully acknowledge the Brazilian research supporting council (CNPq) for financial support under the project 476724-2007-4. We also thank the Brazilian Light Synchrotron Laboratory (LNLS) for the partial financing of this study (project XRD1-8113).

Inorganic and organic pollutant removal from tannery effluent by an integrated photo-Fenton and Electro-coagulation process

Palacio, S.M.¹, Espinoza Quiñones, F.R.¹, Módenes, A.N.¹, Borba, F.H.¹, Manenti, D. R.¹, and Szymanski, N.¹

Universidade Estadual do Oeste do Paraná - Toledo PR Brazil

In this work, the photo-Fenton and electrocoagulation (EC) processes were integrated in their optimum operating values in order to remove the inorganic and organic pollutants from a tannery effluent. Both photo-Fenton and electrocoagulation-based treatments were performed using 1 L lab scale reactors, where a couple of Al plates was used in the EC reactor. In order to obtain the optimal values of the photo-Fenton system state variables, a complete 3³ experimental design was applied. The response of both systems was evaluated on the basis of chemical organic demand (COD), turbidity, total suspended solid (TSS), total fixed solid (TFS), total volatile solid (TVS), and elements concentration values. All physicochemical parameter measurements were made applying the Standard Methods for each non- and treated sample. The elemental concentrations were measured using the synchrotron radiation total X-ray fluorescence technique, installed at the D09-XRF beam line at Brazilian Light Synchrotron Laboratory. The highest efficiency on the pollutant removal was achieved with a reduction of 95.6, 95.9, 96.8, 64.5, 28.3 and 88.9 % for COD, color, turbidity, TSS, TSF, and TSV values, respectively, at the photo-Fenton working conditions of 120 min reaction time, 0.5 g Fe²⁺ L⁻¹, 30 g H₂O₂ L⁻¹, and 3 initial pH. When photo-Fenton process is integrated to electrocoagulation one a minimum concentration value of 0.24 mg Cr L⁻¹ was also achieved at the EC working condition of 15 min electrolysis time. Based on the strongly organic and inorganic reduction, the integrated photo-Fenton and electrocoagulation method could be recommended instead of the individual one. In future, we will focus on how to use a photo-Fenton treatment coupled to an electrocoagulation one in a continuous waste water treatment system.

Acknowledgements: We gratefully acknowledge the Brazilian Light Synchrotron Laboratory (LNLS) for the partial financing of this study (project XRF-8133)

Estudo da reprogramação de células-tronco murinas a nível atômico

Cardoso, S.C.¹, Stelling, M.P.¹, B Paulsen¹, and Rehen, S¹

Universidade Federal do Rio de Janeiro - Rio de Janeiro RJ Brazil

Apesar de sua incontestável relevância, transplantes de órgãos são procedimentos de alto custo, realizados em circunstâncias especiais. Requerem a utilização de medicamentos que evitem rejeição e em muitos casos, o período de espera até a obtenção do órgão é superior à capacidade de sobrevivência do paciente. Além disso, a oferta atual de órgãos para transplante não supre a demanda crescente de uma sociedade em franco envelhecimento. Diante de um cenário de possibilidades restritas, a produção de células em laboratório visando o reparo de órgãos lesados foi sugerida como principal alternativa. Dava-se início a uma revolução nas ciências biomédicas, hoje conhecida como engenharia tecidual. Dentre os diferentes tipos de células-tronco, aquelas com maior potencial como biomaterial para a reposição tecidual são as células-tronco embrionárias (ES). A técnica de reprogramação celular consiste em introduzir em cada célula uma série de fatores para fazer com que ela seja capaz de se diferenciar em todos os tipos de tecidos. Células-tronco de pluripotência induzida (iPS) são obtidas após reprogramação de células somáticas por meio da indução de expressão de genes de pluripotência. O objetivo deste trabalho foi avaliar a reprogramação de células murinas adultas através de análise elementar utilizando-se a técnica de microfluorescência de Raios-X. Nossos resultados mostram que, a nível atômico, as células reprogramadas a partir de fibroblastos murinos apresentam o mesmo comportamento das células tronco embrionárias murinas.

Acknowledgements: FAPERJ e CNPq.

Determinación de la distribución de As y otros elementos en embriones de sapo común argentino (*Chaunus arenarum*) desarrollados en agua contaminada con arsénico o clorpirifos por SR-TXRF

Pérez, C. A.¹, Venturino, A.², R.D. Pérez³, Rubio, M.⁴, and Bongiovanni, G.A.⁵

¹ Laboratório Nacional de Luz Síncrotron - Campinas SP Brazil

² Laboratorio de Investigaciones Bioquímicas, Químicas y de Me - Neuquén Neuqu Argentina

³ Universidad Nacional de Cordoba - Córdoba Cba Argentina

⁴ Centro de Excelencia de Productos y Procesos de Córdoba - Cordoba Argentina

⁵ Unidad Ejecutora Neuquén-CONICET - Neuquén Neuqu Argentina

En la Patagonia Norte se produce la mayor proporción de peras y manzanas de exportación de la República Argentina y esto está asociado aun alto riesgo de contaminación hídrica con pesticidas organofosforados (OP). A esto se suma la creciente explotación minera de recursos naturales y la presencia de plantas de fabricación de cemento Portland que contaminarían ríos y arroyos del territorio neuquino con As y otros metales. Debido al fuerte impacto ambiental y sobre la salud humana de estos contaminantes se están determinando marcadoras de exposición y daño en la especie autóctona de sapo (*Chaunus arenarum*). Esta especie ocupa una posición clave en la cadena trófica y es un interesante bioindicador del impacto ambiental de contaminantes. Como parte de ese proyecto, se determinó la concentración de As y otros elementos por SR-TXRF en los diferentes estadios embrionarios de sapos expuestos a 1 y 2 ppm As o 2 ppm clorpirifos. El último estadio embrionario E25 (opérculo completo) fue alcanzado tras 9 días de incubación. No se encontró bioacumulación de As durante la etapa embrionaria. Sin embargo se observaron alteraciones en la concentración de otros elementos a partir del estadio E21 (boca abierta) y estas alteraciones podrían estar relacionadas con la ingesta de As y clorpirifos. A diferencia de otros biomarcadores estudiados en nuestro laboratorio, la técnica SR-TXRF requiere mínimas cantidades de muestra por lo que sería apropiada para realizar monitoreo ambiental. // Bibliografía: Pérez RD, Rubio M, Pérez CA., Eynard AR. and GA. Bongiovanni. (2006). *X Ray Spectrom* 35(6): 352-358. // Rubatto Birri N., Pérez RD., Cremonuzzi D, Pérez CA., Rubio M and Bongiovanni GA. (2009). *Environmental Research* (in press) // Venturino A. and Pechen de D'Angelo A.M. (2005): *Appl. Herpetol.* 2: 335-353.

Acknowledgements: The authors would like to thank LNLS - Brazilian Synchrotron Light Source, Campinas, Brazil, under proposal D09B-XRF-8606 /2009. This work was supported by the CONICET and the FONCyT, Argentina.

X-Ray Fluorescence with Synchrotron Radiation to Elemental Analysis of Lead and Calcium Content of Primary Teeth

de Souza Guerra, C¹, Gerlach, R.F.², Pinto, N.G.V³, Cardoso, S.C.⁴, Moreira, S.⁵, Almeida, A.P.⁴, Silva, C. L.⁴, Oliveira, L. F.³, Braz, D.⁴, and Barroso, R.C.³

¹ Faculdade de Odontologia de Piracicaba - UNICAMP - Piracicaba SP Brazil

² Universidade de São Paulo - Ribeirão Preto - Ribeirão Preto SP Brazil

³ Universidade do Estado do Rio de Janeiro - Rio de Janeiro RJ Brazil

⁴ Universidade Federal do Rio de Janeiro - Rio de Janeiro RJ Brazil

⁵ Universidade Estadual de Campinas - Campinas SP Brazil

Some studies have shown that superficial enamel lead concentration is related to the individual's environmental exposure to lead, and enamel has been proposed as a biomarker of lead exposure. The intention of this work is to perform in vitro L-shell XRF measurements of Pb in deciduous teeth using X-ray synchrotron radiation as excitation source. X-ray fluorescence was performed utilizing a synchrotron source due to the superior brightness, tunability of X-rays, increased signal-to-noise ratio, and smaller spot sizes achievable compared to conventional XRF analysis. So, the outstanding features of synchrotron radiation was exploited to investigate the Pb and Ca distribution in enamel on a microscopic scale. The study proposal was submitted to the Committee of Ethics in Research, according to the Resolution 196/96 of the National Commission of Ethics in Research. Parents or a guardian had to sign an informed consent prior to engagement of the child in the study. Exfoliated primary teeth were donated by children living in Santo Amaro da Purificação, Bahia State, Brazil, area of this city was contaminated as result of a lead ore smelter which operated in this city from 1960 to 1993. Five primary incisors donated by children living in contaminated neighborhood were analyzed in this study. The home-made software used to reconstruct the maps was developed at the Physics Institute of the Rio de Janeiro University State. In summary, investigated by SRXRF microprobe in the lead contamination of enamel and dentine of primary incisor of children, significant high Pb level was observed in the surface enamel.

Acknowledgements: We would like to acknowledge Dr. Carlos Alberto Perez for helping during the analysis at the XRF beamline and Anibal Araújo Alves Peixoto, for helping during collect of teeth. This research was partially supported by the LNLS/CNPq, Brazil. This study was also supported by FAPESP and CNPq.

Study of Bone Implant Interface by Synchrotron Radiation X-Ray Microfluorescence

LIMA, I.¹, Calasans-Maia², Granjeiro, J. M.², Sales, E.³, Rossi A. M.⁴, Lopes, R.T.³, and Gasperini, F. M.²

¹ Universidade do Estado do Rio de Janeiro - Rio de Janeiro RJ Brazil

² Universidade Federal Fluminense - Niterói RJ Brazil

³ Universidade Federal do Rio de Janeiro - Rio de Janeiro RJ Brazil

⁴ Centro Brasileiro de Pesquisas Físicas - Rio de Janeiro RJ Brazil

Zinc is known to play a relevant role in growth and development; it has stimulatory effects on in vitro and in vivo bone formation and an inhibitory effect on in vitro osteoclastic bone resorption. Changes in the composition of hydroxyapatite (HA) are subject of studies in order to improve the tissue response after implantation and to become more similar to the inorganic component of the bone tissue, a nonstoichiometric apatite. The objective of this study was to investigate the effect of 0.5

Acknowledgements: This work was partially supported by Conselho Nacional de Desenvolvimento Científico e Tecnológico (CNPq), FAPERJ (Fundação de Amparo à Pesquisa do Rio de Janeiro) and LCLS (Project XRF 8066).

Bidimensional Mapping of the bone matrix of young and old rats by X ray Microfluorescence with Synchrotron Radiation

LIMA, I.¹, Sales, E.², Pérez, C. A.³, and Lopes, R.T.²

¹ Universidade do Estado do Rio de Janeiro - Rio de Janeiro RJ Brazil

² Universidade Federal do Rio de Janeiro - Rio de Janeiro RJ Brazil

³ Laboratório Nacional de Luz Síncrotron - Campinas SP Brazil

The risk of fractures associated with osteoporosis has attracted a great clinical concern because of the skeletal changes observed in women after menopause, and in both sexes as a result of aging. The loss of bone mass in these conditions manifest early in vertebral cancellous bone is continuously subjected to the effects of body weight. The changes in vertebral architecture are of particular interest in the lumbar region, given the high mechanical stress applied in this segment. Studies in this regard acquire an epidemiologic nature, as early indicators that seek to characterize the risk groups. The great development of methods of bone densitometry, in the last two decades, shows that the efforts were concentrated on determining the density of trabecular bone. However, in the case of bone quality, the density of bone architecture alone does not predict the risk of fracture. The composition of the bone matrix also contributes to bone strength, because each chemical element has a specific role in osteoformation and bone quality. In addition to calcium (Ca), zinc (Zn) and strontium (Sr) also have important roles in the maturation and bone formation, and evaluation of their distribution in bone matrix is of paramount importance. The X ray microfluorescence by Synchrotron radiation has been stand out over other elemental analysis techniques due to its high brightness and non-destructive characteristic. Using this technique it is possible make a bidimensional map on the bone matrix and quantifies the concentrations of each chemical element without need destruction of the sample. The aim of this study was to evaluate the distribution of Ca, Zn and Sr in the region of the lumbar vertebrae in relation to the age of animals. For this, 10 Wistar rats with three and twelve months old were used. The bidimensional mapping was done in the L3 lumbar vertebra and the elemental distributions were calculated.

Acknowledgements: This work was partially supported by Conselho Nacional de Desenvolvimento Científico e Tecnológico (CNPq), FAPERJ (Fundação de Amparo à Pesquisa do Rio de Janeiro) and LNLS (Projects XRF 7079, 7715, 8056).

Administration of Strontium Ranelate in Wistar rats by X-ray Microfluorescence with Synchrotron Radiation

LIMA, I.¹, Taam, P. ; Taam, Pedro², Sales,E.², Alves, D.L.H.¹, and Lopes, R.T.²

¹ Universidade do Estado do Rio de Janeiro - Rio de Janeiro RJ Brazil

² Universidade Federal do Rio de Janeiro - Rio de Janeiro RJ Brazil

Several drugs have been tested in recent decades for the treatment of osteoporosis. Although tested on animals since 1993, strontium ranelate has only recently been introduced in the therapy of osteoporosis. It has the peculiarity of being the only drug to inhibit the process of bone reabsorption and stimulate bone formation simultaneously, facilitating the reconstruction of cancellous bone. However, it is not known how this drug is distributed in the bone matrix. Even as calcium, strontium has a high affinity for bone, where it is adsorbed to the bone surface and incorporated in the matrix. But, destructive tests show that even in animals treated with large doses of ranelate for long periods of time, the total amount of strontium in bone is very low compared to that of calcium. At first, no more than one in ten calcium atoms can be replaced by strontium, ensuring adequate mineralization of the matrix and preventing the induction of osteomalacia. Studies have shown that the concentration of plasma levels of strontium, depending on the mode of drug administration, is different. The properties related to absorption, distribution and elimination of a drug are critically influenced by the mode of administration. The drug administration by gastric tube is called gavage, and it is made through of the plastic tube placed into the animals mouth. The drug is mixed with water reaches a gelatinous form, without the risk of loss of drug; it goes directly into the stomach of the animal through the tube. Already in the intraperitoneal administration, the drug is solubilized and injected weekly into the peritoneal cavity in the animals. The aim of this work was to evaluate the two mode of administration of strontium ranelate: intraperitoneal and gavage. For this, the bidimensional mapping of distribution of strontium in femurs samples of rats was made.

Acknowledgements: This work was partially supported by Conselho Nacional de Desenvolvimento Científico e Tecnológico (CNPq), FAPERJ (Fundação de Amparo à Pesquisa do Rio de Janeiro) and LNLS (Project XRF 7523)

Substratos meteoríticos contribuem para a sobrevivência de *Deinococcus radiodurans* em condições simuladas de migração interplanetária

Dalmaso, G. Z. L.¹, Galante, D.², LIMA, I. G. P.¹, Naves de Brito, A.³, Barbosa, J.A.R.G.⁴, Leitão, A.C.¹, and C. Lage¹

¹ Universidade Federal do Rio de Janeiro - Rio de Janeiro RJ Brazil

² Universidade de São Paulo - São Paulo - Sao Paulo SP Brazil

³ Universidade de Brasília - Brasília DF Brazil

⁴ Laboratório Nacional de Luz Síncrotron - Campinas SP Brazil

O objetivo principal do presente estudo foi determinar a viabilidade da bactéria poli-extremófila *Deinococcus radiodurans* em ambientes extraterrestres simulados em laboratório, como modelo para vida extraterrestre. As irradiações foram feitas na linha TGM do Laboratório Nacional de Luz Síncrotron (LNLS), em configuração de feixe branco (10 a 21eV) para simular fontes naturais de radiação UV, como o Sol e *flashes* de UV de outras fontes astrofísicas. Os microorganismos foram expostos liofilizados, nos seus meios de cultura ou em tampão, às condições de temperatura, pressão e radiação análogas às encontradas na órbita da Terra. Em conjunto, foi simulado um efeito de sombreamento contra a radiação, utilizando, de forma inédita, amostras meteoríticas reais como substrato. Esses substratos foram caracterizados quanto a sua rugosidade, inoculados com os microorganismos e expostos à radiação em diversas doses, de maneira a testar a proteção fornecida pelo material. Com exposições de diferentes tempos foram construídas curvas de sobrevivência bacteriana, demonstrando a capacidade intrínseca desse microrganismo de resistir aos fatores estressantes do experimento, como vácuo, radiação ultravioleta e baixas temperaturas. Foi demonstrada também a capacidade protetora do substrato meteorítico, bem como de partículas de solos do Deserto do Atacama (Chile) e de solo simulado JSC Mars-1. Os resultados obtidos com este estudo possibilitam um melhor entendimento da sobrevivência de *D. Radiodurans* em ambientes extremos de temperatura, vácuo e radiação, e também enriquecem o conjunto de dados disponíveis na literatura sobre a potencial de contaminação interplanetária, no processo conhecido como panspermia.

Acknowledgements: Agradecemos a MSc. Andréia Meza pelo suporte na utilização dos laboratórios do Centro de Biologia Molecular e Estrutural (CeBiME), à Prof. Dra. Elizabeth Zucolloto, pelas amostras de meteoritos e ao Dr. Armando Azúa, pelas amostras de solo do Deserto do Atacama, bem como ao apoio financeiro da Fapesp, CNPq, CAPES e ABTLus.

DETERMINATION OF MULTIELEMENTS IN SERUM SAMPLES FROM PATIENTS WITH SICKLE CELL ANEMIA (SCA) BY SRTXRF

Canellas, C.G.L.¹, Leitão, R.G.¹, Carvalho, S.M.F.², de Jesus, E.F.O.¹, Anjos, M. J.³, and Lopes, R.T.¹

¹ Universidade Federal do Rio de Janeiro - Rio de Janeiro RJ Brazil

² Inst. Estadual de hematologia Arthur de Siqueira Cavalcanti - Rio de Janeiro RJ Brazil

³ Universidade do Estado do Rio de Janeiro - Rio de Janeiro RJ Brazil

The determination of trace elements levels in physiological fluids is of considerable interest in clinical chemistry. Since it has been established these levels in human serum can be utilized as indicators for several pathological conditions, the simultaneous detection of certain elements in the serum offers a very interesting approach in the diagnosis and treatment of various diseases. In this work, trace elements were analyzed in serum of patients with sickle cell anemia (SCA) by Total Reflection X-Ray Fluorescence using Synchrotron Radiation (SRTXRF). Sickle cell Anemia is a blood disorder that affects hemoglobin, the protein found in red blood cells that help carry oxygen throughout the body. SCA occurs when a person inherits two abnormal genes (one from each parent) that cause their red blood cells to change shape. Instead of being flexible and disc-shaped, these cells are more stiff and curved in the shape of the old farm tool known as a sickle (that's where the disease gets its name). There's no cure for most patients. We studied forty-three patients (15 males and 28 females) aged 18 to 50 years, suffering SCA and Sixty healthy volunteers (41 males and 19 females) aged 18 to 60 years. All the serum samples had been collected of people who live in the urban area of Rio de Janeiro City/Brazil. The measurements were performed at the X-Ray Fluorescence beam line at Brazilian National Synchrotron Light Laboratory (LNLS), in Campinas, São Paulo using a polychromatic beam. It was possible to determine the concentrations of the following elements: P, S, Cl, K, Ca, Cu, Zn, Br and Rb. The t-test ($\alpha=0.05$) was used to verify the variations in the elemental concentrations between patient group (SCA) and control group (CG). The concentrations of P, Cl, K, Fe, Cu, Zn and Br presented significant differences between group of patients with SCA and group of healthy subjects. No significant differences for the concentrations of S, Ca and Rb.

Acknowledgements: This work was developed partially at Brazilian National Synchrotron Light Laboratory (LNLS - Project XRF 6753/07) with financial support of FAPERJ.

DETERMINATION OF MULTIELEMENTS IN SERUM SAMPLES FROM PATIENTS WITH SICKLE CELL ANEMIA (SCA) BY SRTXRF

The determination of trace elements levels in physiological fluids is of considerable interest in clinical chemistry. Since it has been established these levels in human serum can be utilized as indicators for several pathological conditions, the simultaneous detection of certain elements in the serum offers a very interesting approach in the diagnosis and treatment of various diseases. In this work, trace elements were analyzed in serum of patients with sickle cell anemia (SCA) by Total Reflection X-Ray Fluorescence using Synchrotron Radiation (SRTXRF). Sickle cell Anemia is a blood disorder that affects hemoglobin, the protein found in red blood cells that help carry oxygen throughout the body. SCA occurs when a person inherits two abnormal genes (one from each parent) that cause their red blood cells to change shape. Instead of being flexible and disc-shaped, these cells are more stiff and curved in the shape of the old farm tool known as a sickle (that's where the disease gets its name). There's no cure for most patients. We studied forty-three patients (15 males and 28 females) aged 18 to 50 years, suffering SCA and Sixty healthy volunteers (41 males and 19 females) aged 18 to 60 years. All the serum samples had been collected of people who live in the urban area of Rio de Janeiro City/Brazil. The measurements were performed at the X-Ray Fluorescence beam line at Brazilian National Synchrotron Light Laboratory (LNLS), in Campinas, São Paulo using a polychromatic beam. It was possible to determine the concentrations of the following elements: P, S, Cl, K, Ca, Cu, Zn, Br and Rb. The t-test ($\alpha= 0.05$) was used to verify the variations in the elemental concentrations between patient group (SCA) and control group (CG). The concentrations of P, Cl, K, Fe, Cu, Zn and Br presented significant differences between group of patients with SCA and group of healthy subjects. No significant differences for the concentrations of S, Ca and Rb.

Acknowledgements: This work was developed partially at Brazilian National Synchrotron Light Laboratory (LNLS - Project XRF 6753/07) with financial support of FAPERJ.

TXRF ANALYSIS OF LOW Z ELEMENTS IN SERUM OF PATIENTES WITH IDIOPATHIC THROMBOCYTOPENIC PURPURA BY SYNCHROTRON RADIATION

Pereira, M.O.¹, Canellas, C.G.L.², Leitão, R.G.², de Jesus, E.F.O.², Carvalho, S.M.F.³, Anjos, M. J.⁴, and Lopes, R.T.²

¹ Centro Federal de Educação Tecnológica - Rio de Janeiro RJ Brazil

² Universidade Federal do Rio de Janeiro - Rio de Janeiro RJ Brazil

³ Inst. Estad de hematologia Arthur de Siqueira Cavalcanti - Rio de Janeiro RJ Brazil

⁴ Universidade do Estado do Rio de Janeiro - Rio de Janeiro RJ Brazil

The determination of trace elements levels in human serum can be utilized as indicators for several pathological conditions, the simultaneous detection of certain elements in the serum offers a very interesting approach in the diagnosis and treatment of various diseases. Idiopathic Thrombocytopenic Purpura (ITP) is a blood disorder characterized by an abnormal decrease in the number of platelets in the blood. ITP results from development of an antibody directed against a structural platelet antigen (an autoantibody). The cause of ITP is not known and their diagnosis requires that other disorders be excluded through selective tests. In this work, trace elements were analyzed in serum of patients with Idiopathic Thrombocytopenic Purpura (ITP) by Total Reflection X-Ray Fluorescence using Synchrotron Radiation (SRTXRF). We studied forty patients, suffering from ITP and Sixty healthy volunteers. All the serum samples were collected from people who live in the urban area of Rio de Janeiro City/Brazil. All of them were submitted to medical history. This study was performed with the approval of the ethics committee. It was possible to determine the elemental concentrations of the following six elements: Na, P, S, Cl, K and Ca. By using t-test it could be seen significant differences ($\alpha = 0.05$) between group of healthy subjects and group of ITP. The elements that presented significant differences for the mean of their concentrations between each one of the ITP group and control group were Phosphorous (P), Sulphur (S), Chlorine (Cl), Potassium (K) and Calcium (Ca). The measurements were performed at the X-Ray Fluorescence Beamline at Brazilian National Synchrotron Light Laboratory (LNLS), in Campinas, São Paulo, Brazil.

Acknowledgements: This work was developed partially at Brazilian National Synchrotron Light Laboratory (LNLS - Project XRF 8262) with financial support of FAPERJ.

ELEMENTAL CONCENTRATION ANALYSIS IN PCa, BPH AND NORMAL PROSTATE TISSUES USING SRTXRF

Anjos, M. J.¹, Leitão, R.G.², Canellas, C.G.L², Palumbo, A.J², Souza, P.A.V.R², Nasciutti, L.E², and Lopes, R.T.²

¹ Universidade do Estado do Rio de Janeiro - Rio de Janeiro RJ Brazil

² Universidade Federal do Rio de Janeiro - Rio de Janeiro RJ Brazil

Prostate cancer (PCa) is one of the main causes of illness and death all over the world. In Brazil, prostate cancer currently represents the second most prevalent malignant neoplasia in men, representing 21% of all cancer cases. Benign Prostate Hyperplasia (BPH) is an illness prevailing in men above the age of 50, close to 90% after the age of 80. The prostate presents a high zinc concentration, about 10-fold higher than any other body tissue. In this work, samples of human prostate tissues with cancer (PCa), BPH and normal tissue were analyzed utilizing the Total Reflection X-Ray Fluorescence spectroscopy using synchrotron radiation technique (SRTXRF) to investigate the differences in the elemental concentrations in these tissues. SRTXRF analyses were performed at the X-Ray Fluorescence Beamline at Brazilian National Synchrotron Light Laboratory (LNLS). It was possible to determine the concentrations of the following elements: P, S, K, Ca, Fe, Cu, Zn, Br and Rb. By using Mann-Whitney U test it was observed that almost all elements presented concentrations with significant differences ($\alpha = 0.05$) between the groups studied. The elements and groups were: S, K, Ca, Fe, Zn, Br and Rb (PCa X Normal); S, Fe, Zn and Br (PCa X BPH); K, Ca, Fe, Zn, Br and Rb (BPH X Normal)

Acknowledgements: This work was partially developed at Brazilian National Synchrotron Light Laboratory (projects XRF 5959 and XRF 6736) and had the financial support of CNPq and CAPES.

DETERMINATION OF LOW Z ELEMENTS IN SERUM OF PATIENTS WITH LEUKEMIAS BY SYNCHROTRON RADIATION

Soares, Júlio César de A.C.R.¹, Canellas,C.G.L¹, Leitão,R.G.¹, Carvalho, S.M.F², de Jesus, E.F.O.¹, Anjos, M. J.³, and Lopes, R.T.¹

¹ Universidade Federal do Rio de Janeiro - Rio de Janeiro RJ Brazil

² Inst. Estad de hematologia Arthur de Siqueira Cavalcanti - Rio de Janeiro RJ Brazil

³ Universidade do Estado do Rio de Janeiro - Rio de Janeiro RJ Brazil

Leukemia is a disease that occurs all over the world. Leukemia is a type of cancer. All cancers begin in cells, which make up blood and other tissues. Normally, cells grow and divide to form new cells as the body needs them. When cells grow old, they die, and new cells take their place. Sometimes this orderly process goes wrong. New cells form when the body does not need them, and old cells do not die when they should. Leukemia is a kind of cancer that begins in blood cells. There are four common types of leukemia: Chronic Myelogenous Leukemia (CML), Acute Myelogenous Leukemia (AML), Chronic Lymphocytic Leukemia (CLL) and Acute Lymphocytic Leukemia (ALL). In this work, low Z elements were determined in serum of patients with four groups of leukemia (CML, AML, CLL and ALL) and control group (CG) or healthy subjects using Total Reflection X-Ray Fluorescence induced by Synchrotron Radiation (SRTXRF). We studied thirty patients male gender and feminine gender with ages ranging from 18 to 60 years, suffering from CML, AML, CLL, ALL and thirty healthy volunteers aged 18 to 60 years. All the serum samples were collected from people who live in the urban area of Rio de Janeiro City/Brazil. All of them were submitted to medical history. This study was performed with the approval of the ethics committee. It was possible to determine the elemental concentrations of the following six elements: Na, P, S, Cl, K and Ca. By using t-test it could be seen significant differences ($\alpha=0.05$) between groups of healthy subjects and four groups of leukemia. The t- test showed real differences among the elemental concentrations. Thus, our findings indicate that the elements can be directly related to the biochemical processes in leukemia. The significant differences found between the groups may be indicators of these diseases. This could help biomedical field with regard to early diagnosis and improved medical treatment.

Acknowledgements: This work was developed partially at Brazilian National Synchrotron Light Laboratory (LNLS - Project XRF 7266) with financial support of FAPERJ.

Efeito da aplicação de extratos fitoterápicos para tratamento de úlcera péptica na composição multielementar da mucosa gástrica de roedores

Vieira, L. D.¹, J. Mesa¹, Silva, K. T.¹, Hiruma-Lima, C. A.¹, and Kushima, H.¹

Universidade Estadual Paulista - Botucatu - Botucatu SP Brazil

Úlceras pépticas são doenças que afetam um considerável número de pessoas no mundo inteiro. Estas lesões podem ser desencadeadas e agravadas pelo uso de drogas antiinflamatórias não-esteroidais (DAINES) e pela presença de *Helicobacter pylori* no trato gastrointestinal, entre outros fatores [1].

Para tratamento deste tipo de doença, extratos de plantas têm mostrado grandes resultados, além de serem atrativas fontes de novas drogas [2].

Neste sentido, este trabalho pretende contribuir na compreensão da ação farmacológica dos extratos de *Alchornea glandulosa*, *Davilla elliptica* e *Davilla nitida*, plantas popularmente utilizadas para o tratamento de úlceras gástricas [3-5].

Para o estudo, foi realizada uma análise da composição multielementar dos extratos fitoterápicos e da mucosa gástrica de ratos com úlcera induzida. Esta análise foi feita utilizando fluorescência de raios-X por reflexão total (TXRF) usando radiação síncrotron, no Laboratório Nacional de Luz Síncrotron (LNLS). Após as análises, os dados foram processados no programa AXIL.

A técnica de TXRF mostrou-se bem adequada para determinação das composições multielementares de amostras vegetais.

Foi possível a medida simultânea das concentrações de P, Cl, K, Ca, Ti, V, Cr, Mn, Fe, Co, Ni, Cu, Zn, As, Se, Rb, Sr, Zr, Ba e Br. Ou seja, foram determinados macroelementos, microelementos e até elementos não-essenciais.

Referências Bibliográficas:

[1] J. BELAICHE, J. *et al.* Study group of NSAID-GI complications. Observational survey of NSAID-related upper gastro-intestinal adverse events in Belgium, *Acta Gastroenterology Belgian*, v.65 , pp. 6573, 2002.

[2] BORRELLI, F. and IZZO, A.A. The plant kingdom as a source of anti-ulcer remedies, *Phytotherapy Research*, v.14, pp. 581591, 2000.

[3] CALVO, T. R. *et al.* "Constituents and Antiulcer Effect of *Alchornea glandulosa*: Activation of Cell Proliferation in Gastric Mucosa during the Healing Process", *Biol Pharm. Bull.*, v. 30, n. 3, pp. 451-459, 2007.

[4] AZEVEDO, A. O. *et al.* "Antinociceptive effect from *Davilla elliptica* hydroalcoholic extract", *Journal of Ethnopharmacology*, v. 113, pp. 354-356, 2007.

[5] RODRIGUEZ, C. M. *et al.* "Constituintes das folhas de *Davilla nitida* Vahl (Dilleniaceae)", In: 28 Reunião anual da Sociedade Brasileira de Química, 2005, Poços de Caldas-MG.

Acknowledgements:

Investigation of low-cost bio-adsorbents for heavy metals

W.H. Flores¹, Marques, J. F.¹, Gündel, A.¹, and Jacques, R.A¹

Universidade Federal do Pampa - Bagé RS Brazil

Many inorganic compounds are necessary in animal and plant nutrition while others may be toxic to living matter at concentrations as low as ppm. The presence of metals in aquatic system and soils with quantities above their natural abundances is normally associated with human activities such as industry, agriculture and mining. These contaminants are particularly problematic because they do not undergo degradation. However, redox reactive metals often do have different degrees of toxicity which depend of the specific metal oxidation state. It is therefore essential to determine both the oxidation state of metal and its mechanism of interaction with the adsorbent system. In this context, the abatement of the contaminant to an acceptable level is necessary, and different adsorbent materials has been reported for this purpose. The conventional methods for metal removal involve high capital costs with recurring expenses, which restricts its use on large scale, as an alternative, special attention has been focused on the use of natural adsorbent materials with high metal adsorption capacity and selectivity. On the other hand, it is possible to process the solid residue from the non-profitable part of fruits and convert in to an adsorbent that has a large surface area and thus great potential to adsorb heavy metals from aqueous solutions and industrial waste.

Although many research works have been done recently to find the potential of using various adsorbents, our understanding of metal/adsorbent interaction is lacking. Of special interest is the metal selectivity, the different affinity of specific ligand for different metal ions. The aim of this work is to provide a comparative study of the interactions of selected metal ions with passion fruit peel waste, using X-ray absorption spectroscopy (XAS). This tool is one of the few experimental techniques that can provide structural details on atom-specific sites. In the present work the information content of near edge XAS (XANES) of metals are explored. XANES can be strongly sensitive to formal oxidation state and coordination chemistry of the absorbing atom.

Acknowledgements:

Utilização de fluorescência de raios-X com radiação síncrotron e ferramentas quimiométricas em análises químicas de amostras de solos da Antártica Marítima

GUERRA, M.B.B.¹ and Pereira Filho, E. R.¹

Universidade Federal de São Carlos - São Carlos SP Brazil

Os ecossistemas antárticos são considerados os menos perturbados do planeta, todavia o impacto antrópico vem se intensificando naquela localidade devido às expedições ao continente, atividades das estações de pesquisa e também ao turismo. Desta forma, o objetivo deste trabalho é a análise de amostras de solos coletadas no entorno da Estação Antártica Comandante Ferraz (EACF), única estação brasileira na Antártica e em alguns pontos de coleta não impactados, localizados até 4 km distantes da EACF. Coletou-se 49 amostras de solos em 15 pontos localizados na Península Keller, Ilha Rei George, Antártica Marítima. As amostras foram secas (60 °C), moídas e peneiradas (212 µm). Após a moagem, as amostras foram prensadas para a obtenção de pastilhas delgadas, as quais foram utilizadas na análise por fluorescência de Raios-X com radiação síncrotron (SR-XRF). Os sinais obtidos com a SR-XRF foram tratados com o uso de duas ferramentas quimiométricas: a PCA (Principal Component Analysis) e a PARAFAC (Parallel Factor Analysis). Com o uso da PCA foi possível observar uma nítida distinção entre as amostras de solos com relação ao local de coleta. As amostras de solos coletadas próximas aos tanques de diesel da EACF foram caracterizadas pela presença de Cr, enquanto que as amostras distantes da estação pela presença de Fe, V e Cu. Já com o uso da PARAFAC, verificou-se que a presença de Cr nas amostras próximas aos tanques de diesel da estação é contundente em pontos mais superficiais (0-20 cm). A partir destes resultados, pode-se inferir sobre um padrão de contaminação mais recente destes pontos amostrais e também devido à baixa mobilidade do Cr no ambiente. Esta baixa mobilidade já foi constatada em outros trabalhos, sobretudo relacionada à grande capacidade de retenção dos íons Cr³⁺ por componentes do solo, como matéria orgânica e minerais de argila. Os resultados encontrados neste trabalho permitem concluir que a EACF ao longo dos 25 anos de permanência na Antártica alterou os solos do seu entorno, principalmente próximo aos tanques de diesel. Utilizando-se a SR-XRF juntamente com a PCA e a PARAFAC foi possível constatar a contaminação por Cr nos solos impactados pela estação, sendo possivelmente proveniente da tinta utilizada para pintura dos tanques.

Acknowledgements: XRF-7045; XRF-7046; CAPES; CNPq; FAPESP

TERMINALIA CATAPPA AS BIOINDICATOR OF ENVIRONMENTAL POLLUTION IN CUBATÃO CITY BY SR-TXRF

Moreira, S.¹, Barroso, R.C.², Vives, A. E. S.³, Geraldo, S. M.¹, and Cardoso, S.C.⁴

¹ Universidade Estadual de Campinas - Campinas SP Brazil

² Universidade do Estado do Rio de Janeiro - Rio de Janeiro RJ Brazil

³ Universidade Metodista de Piracicaba - Santa Bárbara DOeste SP Brazil

⁴ Universidade Federal do Rio de Janeiro - Rio de Janeiro RJ Brazil

Fertilizer industries are considered the main environmental polluting of fluoride (F) and the industrial complex of the city of Cubatão, SP, Brazil, is an important fertilizer producer. Thus, this study aimed to evaluate the local pollution for toxic elements and its comparison with fluoride concentration using the urban vegetation as biomarker. For this, leaves of *Terminalia catappa* (popularly known for Hat-of-Sun or Almond tree of the beach) were tested. The leaves were collected in the winter of 2007 in the industrial region around the fertilizer plants and other industries, and, in the urban areas of Cubatão and Santos cities. The samples were dehydrated, powdered and so submitted to an acid digestion for multi-elemental determination by SR-TXRF. The results obtained were compared to fluoride determinations. The variance analysis showed the correlation between F and S concentrations ($p < 0.05$). The concentrations of these elements are concentrated around the fertilizer industries ($p < 0.05$). The average concentration of F founded in the leaves near to the fertilizer industries was 11 times higher than around other industries and 24 times higher than the concentrations determined in trees located in the urban areas of Cubatão and Santos cities. For S the average concentration near to fertilizer industries were 895.2 g.g^{-1} and are not statistically different for other industries (744.5 g.g^{-1}) but for the urban areas of Cubatão and Santos the average concentration is at least 2 times lower than the area near to fertilizer industries. By cluster analysis was possible to assemble the elements in four groups, the first one with major similarities were the group containing F, Sr, Pb, S, Ti and Fe, the second group with high similarity are composed by Si, K and Rb, the third group by Ca, Cr and Ni and, the last one with similarity like the third group are composed by Cu and Zn. Chromium in the area near to fertilizer industries and also in Santos city considered as control present concentrations higher than 18 mg.kg^{-1} value considered as toxicant.

Acknowledgements: The authors are thankful to LNLS for carrying out the measurements and to CNPq by the financial supports (Processes 308432/2007 and 474007/2007).

EVALUATION OF HEAVY METALS IN ATMOSPHERIC EMISSIONS FROM AUTOMOTIVE INDUSTRY BY SR-TXRF

Moreira, S.¹ and Weber Neto, J.¹

Universidade Estadual de Campinas - Campinas SP Brazil

Combustion of fuels in stationary sources was the main emission source for As, Cd, Cr, and Ni (more than a half of the total anthropogenic emissions), while combustion of gasoline was the main source of for lead. There is a continuous reduction of heavy metal emissions during the last 40 years. Better knowledge of heavy metal sources, emissions, pathways, and fate in the environment and progress in developing efficient emission control equipment has resulted in more efficient regulatory efforts to curb heavy metal emissions from anthropogenic sources very substantially. There is a potential for further reduction of these emissions until the year 2010 up to about 40% for As, Cd, Cr, and Ni and about 57% for Pb. This study had as goal to determine heavy metals and other elements (Ba, Br, Ca, Pb, Cl, Cr, Sr, Fe, Mn, Ni, K, Si, Ti and Zn) in atmospheric pollutants generated by an automotive industry located in the city of Engenheiro Coelho, state of São Paulo, Brazil. The sampling and sample preparation procedures were based on methods established by the Company of Sanitation and Technology (CETESB L9.234) and also by the Environmental Protection Agency (EPA - Method 29). The analysis was performed at XRF Beamline (D09B-XRF) using a white beam under total reflection condition. For zinc, iron, barium, calcium and potassium, the values obtained were in the range of 30 mg/Nm³ and, for other elements, the concentrations were approximately 1 mg/Nm³. The sum of As, Be, Co, Cr, Cu, Mn, Ni, Pb, Sb, Se, Sn, Te and Zn concentration was compared with the limits established by CONAMA 264/1999 and SEMA 041/2002 resolutions (7.0 mg/Nm³) and it was observed that, for all samples, sums are higher than the permissive value mainly due to the high concentration of zinc. Detection limits for SR-TXRF technique were 0.10 g/Nm³ for Pb and 0.02 g/Nm³ for Zn. For Pb the emissions are in accordance with the limit established by the Brazilian legislation (0.35 mg/Nm³) practically in all processes except for the furnace exhaustion stage.

Acknowledgements: The authors are thankful to LNLS for carrying out the measurements (Project XRF 5703), to Laboratory Grandis for the assistance in sampling and to CNPq (Processes 308432/2007 and 474007/2007).

Identification of metabolites in the roots of coffee plants by ^1H NMR analyses

Oliveira, D. F.¹, Machado, A.R.T.¹, Campos, V.A.C.¹, Silva, W. J. R.¹, and Zeri, A.C.²

¹ Universidade Federal de Lavras - Lavras MG Brazil

² Laboratório Nacional de Luz Síncrotron - Campinas SP Brazil

Coffee is one of the most important crops in Brazil, which is responsible for about 25% of the world production of such commodity. Thus, great effort has continuously been made to improve the efficiency of the Brazilian coffee production sector, especially by solving phytosanitary problems caused by nematodes like *Meloidogyne exigua* Goeldi. Although environmental friendly methods should be emphasized, synthetic nematicide application is the most used method to control *M. exigua* on coffee farms, which increases production costs and contaminates humans and the environment with toxic substances. Consequently, the present study aimed to contribute to the development of new resistant cultivars to be used in *M. exigua* infested areas, by evaluation of ^1H NMR analyses as a method to identify metabolites produced by coffee plants that can account for the reduction in the population of plant-parasitic nematodes in their roots. A sterile mixture of sand, soil and cow manure was sowed with seeds of coffee plants susceptible and resistant to *M. exigua*. After 120 days in a greenhouse, the nematode was inoculated in each plant. At 24, 48 and 96 h after the inoculation, roots were removed, carefully washed with water, freeze-dried and extracted with a methanol/chloroform/water solution. Liquids from both extractions were combined and added to a mixture of chloroform (30 mL) and water (60 mL). After stirring vigorously, the aqueous phase was separated by decantation and concentrated to dryness. Each sample was dissolved in a phosphate buffer (pH 7.5) prepared with deuterated water (D_2O) containing 2,2-Dimethyl-2-silapentane-5-sulfonate (DSS) as reference, to obtain ^1H NMR spectra on a Varian AS 500 (500 MHz) spectrometer. Analyses of the NMR data by the use of the Chenomx Suit 6.0 software resulted on the identification and quantification of ten substances: L-alanine, 4-aminobutyric acid, chlorogenic acid, choline, formic acid, fumaric acid, D-glucose, quinic acid, D-sucrose and trigonelline. The experiment was successful, since the activities of most of these substances against plant-parasitic nematodes have already been demonstrated.

Acknowledgements: This work has been supported by FAPEMIG, CAPES, CNPq and LNLS (RMN 7861).

MONITORING AND EVALUATION OF DUCT EMISSION AND STATIONARY SOURCES OF CERAMIC INDUSTRIES BY SR-TXRF

Moreira, S.¹ and Fonseca, Roney J.¹

Universidade Estadual de Campinas - Campinas SP Brazil

The aim of this study was to monitor and evaluate metal emissions from ducts and stationary sources in ceramic industries in the region of the ceramic centre of Santa Gertrudes, SP. In Santa Gertrudes city are installed several industries of ceramic pavements, which activities are the potential sources of particulate material into the atmosphere. According to CETESB in Santa Gertrudes (Jardim Luciana) was observed the occurrence of episodes of inadequate and bad air quality in 2008. The maximum daily concentrations exceeded the daily standard of inhaled particles ($150 \mu\text{g}/\text{m}^3$) in Santa Gertrudes (Jardim Luciana) eight times and one day surpassed also the attention level ($250 \mu\text{g}/\text{m}^3$). The annual average of inhaled particles in 2008 was $97 \mu\text{g}/\text{m}^3$, exceeding the annual standard ($50 \mu\text{g}/\text{m}^3$). The emissions of particulate matter by the main three industries of Santa Gertrudes in 2008 were 0.10, 0.13 and 0.08 ton/year. So, from 2005 to 2006, samples of gases emitted by several ceramic companies in that region were collected. Elements as Al, S, Cl, K, Ca, Fe, Cr, Mn, Ni, Cu, Zn and Pb were detected in the samples. The results were compared to the values established by CONAMA 264/1999 legislation, (exclusive for emission patterns of heavy metals for co-processing ovens) because currently in Brazil, there are not norms establishing concentration limits or emission rates of pollutants for atmospheric emissions. For Pb, the maximum emission limits is $0.35 \text{ mg}/\text{Nm}^3$ according CONAMA resolution and this limit was surpassed by two ceramic industries (0.47 ± 0.04 and $1.42 \pm 0.08 \text{ mg}/\text{Nm}^3$). Still in accordance with the same resolution, the sum of element concentrations (As, Be, Co, Cr, Cu, Mn, Ni, Pb, Sb, Se, Sn, Te, Zn) should not exceed $7.0 \text{ mg}/\text{Nm}^3$, as maximum emission limits. It was verified that 60% of the industries investigated in this work presented values for the sum of Cr, Mn, Cu, Zn and Pb concentrations above the values established by CONAMA legislation. Thus, the environmental issue in the region of Santa Gertrudes, where occurrence of problems concerning fluoride emission is seen already, may be related to the presence of these highly toxic elements.

Acknowledgements: The authors thanks to LNLS for carrying out the measurements (Project XRF 5702), to Bioagri Environment Laboratory for assistance with sampling and CNPq (Processes 308432/2007 e 474007/2007) for the financial support.

Quantificação de metais pesados presentes no material particulado na cidade de Limeira (SP) por SR-TXRF

CANTERAS, F. B.¹, Rodrigues, L.V.¹, and Moreira, S.¹

Universidade Estadual de Campinas - Campinas SP Brazil

A preocupação de políticos, cientistas e da comunidade em geral com a qualidade do ar tem crescido nos últimos anos. Isso se deve ao fato da qualidade do ar estar intimamente ligada à qualidade de vida e à saúde da população. Dentre os poluentes ambientais, o material particulado se apresenta como um dos mais significativos e preocupantes, devido a sua emissão por diversas fontes e a não uniformidade na sua composição. O presente trabalho teve como objetivo principal avaliar quantitativamente o material particulado, em suas duas frações, grossa e fina, coletado no município de Limeira, que se apresenta atualmente como um pólo de significativo desenvolvimento e crescimento populacional. Para isso, foi instalado na estação meteorológica do CESET (Centro Superior de Educação Tecnológica- UNICAMP) um sistema de amostragem conhecido como filtração seqüencial, que foi desenvolvido pela FEC (Faculdade de Engenharia Civil, Arquitetura e Urbanismo da UNICAMP), com o apoio do LNLS (Laboratório Nacional de Luz Síncrotron), o amostrador de material particulado fino e grosso (AFG). Com este sistema pode-se obter as frações grossa e fina, que correspondem às frações inaláveis superior e inferior, respectivamente. Para o preparo das amostras, os filtros contendo o material particulado foram submetidos a um processo de remoção ácida e posteriormente analisados por SR-TXRF. As coletas foram realizadas semanalmente em dias alternados, no período de agosto de 2008 a outubro de 2009. Dentre os elementos analisados, destaca-se a presença de cromo, ferro, manganês, níquel, cobre e zinco, os quais podem estar associados as seguintes fontes: ressuspensão do solo, emissões veiculares, emissões industriais e queimadas.

Acknowledgements: Os autores agradecem a FAPESP pela concessão da bolsa de Mestrado (Processo 2008/02443-9), ao CNPq pelo suporte financeiro (Processos 474007/2007-3 e 308432/2007) e ao LNLS (Projeto D09B-XRF 8121 e 8671) pela realização das medidas.

ANALYSIS OF SYNCHROTRON X-RAY DIFFRACTION PATTERNS FROM FLUOROTIC ENAMEL SAMPLES

Barroso, R.C.¹, Porto, IM², Gonçalves, M.V.C¹, Gerlach, R.F.³, Droppa Jr., R.⁴, and Braz, D.⁵

¹ Universidade do Estado do Rio de Janeiro - Rio de Janeiro RJ Brazil

² Universidade Estadual de Campinas - Campinas SP Brazil

³ Universidade de São Paulo - Ribeirão Preto - Ribeirão Preto SP Brazil

⁴ Laboratório Nacional de Luz Síncrotron - Campinas SP Brazil

⁵ Universidade Federal do Rio de Janeiro - Rio de Janeiro RJ Brazil

With the introduction of fluoride as the main anticaries agent used in preventive dentistry, and perhaps an increase in fluoride in our food chain, dental fluorosis has become an increasing world-wide problem. Visible signs of fluorosis begin to become obvious on the enamel surface as opacities, implying some porosity in the tissue. The mechanisms that conduct the formation of fluorotic enamel are unknown, but should involve modifications in the basics physical-chemistry reactions of demineralisation and remineralisation of the enamel of the teeth, which is the same reaction of formation of the enamels hydroxyapatite (HAp) in the maturation phase. The increase of the amount of fluoride inside of the apatita will result in gradual increase of the lattice parameters. The hexagonal symmetry seems to work well with the powder diffraction data, and the crystal structure of HAp is usually described in space group P63/m. X-ray powder profile-fitting structure refinements using the Rietveld method have proved to be a powerful tool in detecting ionic substitution in the HAp structure, even when the extent of substitution is very low. The aim of this work is to characterize the healthy and fluorotic enamel in human tooth using technique Synchrotron X-ray diffraction in order to determine the crystal structure and crystallinity of on fluorapatite (FAp) crystal present in fluoritic enamel. From this preliminary result, it could be observed the agreement between the scattering patterns for fluorotic and health human enamel. The evident similarities of the diffraction patterns point out the analogy between the structures of the hydroxyapatite (HAp) and fluorapatite (FAp). It is expected because of the crystal structure of both hydroxyapatite (HAp) and fluorapatite (FAp) are usually described in space group P63/m, having lattice parameters very close. Further work will include quantitative phase analysis using powder human enamel samples.

Acknowledgements: Research partially supported by National Synchrotron Light Laboratory (LNLS) under Project XRD1-8167. The authors would like to thank the Brazilian agencies CNPq and CAPES for financial support.

Matéria Mole e Flúidos Complexos

SMALL-ANGLE X-RAY SCATTERING STUDIES IN STERIC STABILIZED pH RESPONSIVE POLYSTYRENE COLLOIDAL PARTICLES

Peruzzo, P. J.¹, Anbinder, P. S.¹, Plivelic, T.S.², and Amalvy, J. I.¹

¹ Instituto de Investigaciones Fisicoquimicas Teoricas y Aplic - La Plata BA Argentina

² MAX Laboratory - Lund France

Steric stabilized pH-responsive colloids particles are very useful in several applications like drug delivery. Small-angle X-ray scattering (SAXS) has been reported to be an excellent tool for the study of these composite latexes since the electron densities of the polymers commonly used for the synthesis of such particles differ markedly. Since the excess electron density of polystyrene latex particles in water is very small, the scattering from adsorbed layer of stabilizer, dominates the measured intensity in this particular systems. In this work we report the study of core-shell polystyrene colloidal particles sterically stabilized by a pH-sensitive copolymer formed by methyl methacrylate and N,N-diethyl ethylmethacrylate. Two different molecular weight of the stabilizer copolymer were used changing in that way the thickness of the shell. SAXS measurements on samples were performed at the SAXS2 beam line at the LNLS (Campinas, Brazil) using a monochromatic beam of wavelength 1.488 Å an exposure time of 600 sec, and a sample detector distance of 1909.87 mm. The SAXS data allow determining the thickness of the layer by modeling the core-shell morphology. The thickness of the shell modifies after changing the medium pH by addition of acid. The change in shell thickness is also determined by SAXS data.

Acknowledgements: The authors would like to acknowledge Brazilian Synchrotron Light Laboratory (LNLS), Campinas, Brazil; CICIPBA and ANPCYT are thanked by financial assistance PJP is member of CONICET (Argentina), PSA is a fellow from ANPCyT (Argentina), TSP is a postdoctoral fellow at MAX-lab (Lund University, POB 118, SE-22100 Lund, Sweden) and JIA is a member of CICIPBA (Argentina).

The influence of polyelectrolyte layers on phosphatidylcholine liposomes

Lionzo, M. I. Z.¹, Lorenzini, G. C.¹, and Silveira, N. P.¹

Universidade Federal do Rio Grande do Sul - Porto Alegre RS Brazil

Liposomes prepared with phosphatidylcholine and chitosan (C) give rise to bilayers decorated internally and externally with C [1]. The composite chitosan-phospholipid has been characterized and the results have shown strong interaction between the two components [2,3]. In this study, another layer, composed by chondroitine sulfate (CS) was added. Two C concentrations (1 and 10 mg/mL) were tested and CS was added in different C/CS ratios [1.0/0.5, 1.0/1.0 and 1.0/1.5 (w/w)]. The effects of the additional CS shell were measured. The techniques applied were SAXS [LNLS Campinas, Brazil], dynamic light scattering (DLS) [IQ-UFRGS Porto Alegre, Brazil] and ζ -potential (ZP) analysis [Faculdade de Farmácia-UFRGS Porto Alegre, Brazil]. The SAXS spectra were fitted using the SASfit program. SAXS results pointed out changes over the multilamellar phospholipid structure. The scattering patterns showed two Bragg peaks over the analysed q range. The first one was fitted by the Modified Caillé Theory (MCT) giving the Caillé parameter η . By decreasing the C/CS ratio η was improved. This is related to the influence of the polymer shells on the rigidity of the membrane. To infer about the bilayer bending rigidity, the K_C parameter can be obtained ($\eta = \pi k_B T / 2d^2 (BK_C)^{1/2}$). The bulk modulus of compression B can be assessed through Static Light Scattering experiments, which provides the osmotic modulus. These experiments are in progress. The stability and size of the particles were positively influenced by the CS increase. This effect was noted when higher CS concentrations were used. Particle sizes varied from 190 nm (liposomes) to 235 nm and to 255 nm (C/CS-L vesicles). The ζ -potential is related to the superficial charge of the particles, caused by the different kinds of covering. Free of polymer liposomes presented negative ζ -potential values, whereas chitosan decorated ones had positive values. By adding CS, the superficial charge became negative, indicating a surface interaction. These results give evidences of polyelectrolyte covering and its influence on the particle structure. [1] Mertins, O. Sebben, M. Pohlmann, A. R. Silveira, N. P. *Chem. Phys. Lip.* 138, 29-37, 2005. [2] Mertins, O. Schneider, P.H. Sebben, M. Pohlmann, A.R. Silveira, N.P. *Qui. Nova* 31, 1857-1860, 2008. [3] Mertins, O. Lionzo, M. Micheletto, Y. S. M. M. Pohlmann, A. R. Silveira *Mat. Sci. Eng. C* 29(2), 463-469, 2009.

Acknowledgements: Rede Nanocosméticos, MCT/CNPq and LNLS for financial support of the project 2360.

SAXS characterization of thermoresponsive soft matter-based systems

Azzaroni, O.¹, Picco, A.¹, Bruvera, I.J.², and Ceolin M.¹

¹ Instituto de Investigaciones Fisicoquímicas Teóricas y Aplicadas - La Plata BA Argentina

² Universidad Nacional de La Plata - La Plata Bs.As Argentina

Soft matter materials are attractive because of their great versatility as building blocks in multi-functional systems as well as the possibility of the fine tuning in their mechanical, structural and chemical properties. Among them, stimuli (pH, temperature, pressure, external fields, etc.) responsive molecules and supramolecules have attracted wide interest because of the possibility of tight control of their properties and possible specific uses as mechanical actuators at nano(meso)metric scale. In this report we present Small Angle X-ray Scattering experiments on the thermally induced structural changes observed in hyperbranched polyethileneimine(core)-palmitic (shell) (HPEI-C16) colloidal suspensions and hyperbranched polyvinylpyrrolidone (hbPNIPAM). The experiments were performed using 0.1488 nm wavelength and 410 mm sample-to-detector distance.

HPEI-C16 room temperature SAXS displays a clear Bragg peak indicating the existence of long range ordered structure with an interplanar distance of 5.65 nm. From the line width of the Bragg peak a crystallite size of 113 nm (at room temperature) was deduced. The thermal evolution of the line area indicates that the ordered phase vanishes around 30 C giving rise to a SAXS diagram typical for a colloidal suspension. Also the thermal evolution of the peak position indicates that the interplanar distance slightly decreases from 5.65 nm at 22 C down to 5.60 nm just before line vanishing. The reduction of the interplanar distance coincides with a reduction of the crystallite size (reflected in the line width) as expected from the reduction of the interplanar distance. Taken together, the SAXS results for HPEI-C16 indicates the occurrence of an ordered low temperature phase in close resemblance to those observed in liquid crystals. The thermoresponsive polymer hbPNIPAM was also characterized using SAXS. A clear transition from a globular low temperature structure (as indicated for a typical bell-shaped Kratky plot) to an extended and aggregation prone structure was determined to occur around 30 C. Both, the transitions observed in HPEI-C16 and hbPNIPAM were verified to be fully reversible.

Acknowledgements: This work was partially supported by CONICET, ANPCyT and Centro Interdisciplinario de Nanociencia y Nanotecnología-ANPCyT (Argentina), Max Planck Society (Germany) and Laboratorio Nacional de Luz Síncrotron (Brazil).

Evidences of hydrotropic organization in aqueous solution by SAXS

MACHADO, D. S.¹, Schmitt, C.C. ou Cavalheiro, C.C.S¹, Neumann, M. G.¹, Oliveira Neto M.¹, Craievich AF², and Polikarpov, I.¹

¹ Universidade de São Paulo - São Carlos - São Carlos SP Brazil

² Universidade de São Paulo - São Paulo - São Paulo SP Brazil

Hydrotropes are molecules that can increase the solubility of poorly soluble organic molecules in water when added above a specific concentration, the minimal hydrotropic concentration (MHC) [1]. There are several applications for these phenomena, including processes of cleaning and laundry, pharmaceutical, feeding, science of the cosmetics, and solubilizing medium for chemical synthesis. Although, the origin of the hydrotropic effect is still not completely understood. Previous results of various techniques had showed that above de MHC the hydrotropes form aggregates [2], leading to believe that the aggregation is the drive force of the hydrotropic effect. In this work we studied the hydrotropes Sodium Styrene Sulfonate (SSS) and Sodium n-Butylbenzene Sulfonate (SBS) at concentrations below and above the MHC using the small angle x-ray scattering technique. The data was collected at the SAXS beamline at the Brazilian Synchrotron Light Laboratory (LNLS, Brazil), using wavelength $\lambda = 0.1488$ nm, a bidimensional detector MARCCD and sample detector distance equal 1480 mm (momentum transfer (q) ranging from 0.11 nm^{-1} to 2.50 nm^{-1}). In concentrations higher than the MHC these hydrotropes shows scattering profiles related to some form of aggregation, where by the Guinier approximation is possible to determine a radius of gyration of 20 nm for the SSS. The SBS above the MHC shows a correlation peak that is position dependant of the concentration, indicating a phase transition in the concentration range studied. Because of the small hydrophobic part, a non-spherical shape is expected with a low curvature due to the repulsion of the sulfonate groups [3].

[1] BALASUBRAMANIAN, D.; SRINIVAS, V.; GAIKAR, V. G.; SHARMA, M. M.; Aggregation Behaviour of Hydrotropic Compounds in Aqueous Solution, J. Phys. Chem., 93, p 3865-3870, 1989

[2] SRINIVAS, V.; RODLEY, G. A.; RAVIKUMAR, K.; ROBINSON, W. T.; TURNBULL, M. M.; BALASUBRAMANIAN, D.; Molecular Organization in Hydrotrope Assemblies, Langmuir, 13, p. 3235-3239, 1997.

[3] ISRAELACHVILI, J. N. Intermolecular and surface forces. 2nd edition. London: Academic Press, 1991. 450 p.

Acknowledgements: FAPESP, CNPq, LNLS

DEVELOPMENT AND IN VITRO EVALUATION OF SURFACTANT SYSTEMS FOR CONTROLLED RELEASE OF ZIDOVUDINE

Carvalho, F. C.¹, Sarmiento, V.H.V², Chiavacci, L.A.¹, Barbi, M. S.¹, and Gremião, M. P. D.¹

¹ Universidade Estadual Paulista - Araraquara - Araraquara SP Brazil

² Universidade Federal de Sergipe - São Cristóvão SE Brazil

The development of a controlled-release dosage form of zidovudine (AZT) is of crucial importance, in view of the pharmacokinetics of its toxic activity. A suitable drug delivery system could increase AZT bioavailability, reducing its dose-dependent side effects. In this study, systems composed of polyoxypropylene (5) polyoxyethylene (20) cetyl alcohol as surfactant (S), oleic acid as oil phase (O) and water (W) were developed, as possible AZT control release systems. They were characterized by polarized light microscopy (PLM), SAXS and rheological analysis, followed by in vitro release assay. PLM and SAXS results indicated that the mixtures of S/O/W in the proportions 55/35/10 and 55/25/20 formed microemulsion (ME) systems, while 55/20/25 formed lamellar phase. The incorporation of AZT in these systems was greater than in water or oil; moreover, AZT incorporation did not significantly change the phase behavior of the mixtures. MEs behave as Newtonian fluids in flow rheological analysis and the lamellar phase as a pseudoplastic fluid. The release profile indicated that AZT could be released in a controlled manner, since an exponential pattern governs AZT diffusion, as demonstrated by the Weibull mathematical model. These systems are potential carriers for AZT and could have advantages over conventional pharmaceutical forms.

Acknowledgements: The authors wish to thank CAPES and CNPq for the financial support and LNLS for the SAXS measurements.

SURFACTANT SYSTEMS FOR NASAL AZT DELIVERY: STRUCTURAL, RHEOLOGICAL AND MUCOADHESIVE PROPERTIES

Carvalho, F. C.¹, Barbi, M. S.¹, Sarmiento, V.H.V², Chiavacci, L.A.¹, Netto, F.M.³, and Gremião, M. P. D.¹

¹ Universidade Estadual Paulista - Araraquara - Araraquara SP Brazil

² Universidade Federal de Sergipe - São Cristóvão SE Brazil

³ Universidade Estadual de Campinas - Campinas SP Brazil

Zidovudine (AZT) is the antiretroviral most frequently used for treatment of AIDS. Although its effectiveness is recognized, it undergoes extensive first-pass metabolism and exhibits poor oral bioavailability. The nasal route is an option for enhanced therapeutic efficacy and to reduce the extent of the first-pass effect. There are some mechanisms that limit intranasal absorption, such as mucociliary clearance, which rapidly removes the formulation from the nasal cavity. To improve the nasal residence time of AZT on the nasal mucosa, it was proposed to develop a mucoadhesive surfactant system for AZT nasal administration. Systems composed of PPG-5- CETETH-20 as surfactant, oleic acid and water were characterized by polarized light microscopy, SAXS and rheological measurements. Mucoadhesion was investigated by phase behavior studies, rheological synergism and mucoadhesive strength determination. Results indicate that the original formulations are microemulsions, which display phase transition to a lamellar phase when brought into contact with aqueous nasal simulated mucus (SM). The phase transition is accompanied by an increase in system elasticity and, irrespective of phase behavior, all the systems showed a good mucoadhesive force. Thus, a viscous and mucoadhesive liquid crystalline matrix can be formed when the formulations are in contact with SM, which may prolong the residence time of AZT in the nasal cavity. These findings indicate a potentially useful system for nasal administration of AZT.

Acknowledgements: The authors wish to thank CAPES and CNPq for the financial support and LNLS for the SAXS measurements.

SAXS measurement and modeling of *in situ* formation of mesoporous silica

Oliveira, C. L. P¹, Sundblom, A.², Palmqvist, A.², and Pedersen, J.S.¹

¹ Aarhus University - Aarhus Denmark

² Chalmers University of Technology - Göteborg Sweden

Mesoporous silica is a material with walls made of silica and pores in the size range of 2-50 nm. Since the silica is amorphous, the material lacks crystalline order but the pores may be arranged in different structures generating a long-range order. This field has attracted a lot of attention due to the multitude of possible applications. The main characteristics of mesoporous silica, such as high surface area, ordered structure and tuneable pore size, are often desirable properties. Despite extensive studies of different syntheses the molecular mechanisms involved in the formation of these materials are not yet fully understood. Here we present an *in situ* SAXS study [1] of a synthesis of mesoporous silica using non-ionic surfactants as the template. The data obtained from the *in situ* time-resolved SAXS measurements was fitted using an advanced least squares model based on a methods proposed by Förster et al [2] and Freiburger et al [3]. Approximations in the model enable a factorization of the scattering intensity into contributions from the form factor and the structure factor which means that these two contributions can be modelled separately. The limited order is included using a modified Caillé theory-based structure factor, whereas the constituting cylinders are described as core-shell cylinders with a graded outer surface in the form factor. Also, for a proper description of the diffraction peaks, corrections for the instrumental smearing of the peaks were included in the program routine by the use of resolution functions. As it will be shown, the data analysis indicates that in the beginning of the synthesis there were only small changes with time and no meso order was observed. After a reasonable lag time (200 min for the presente data) the first indications of meso order appeared, where large aggregates of silica and surfactant with the ordered phase are formed in the solution. The continues improvements of the meso order was then followed and after about 1000 min a stable result was obtained showing four diffraction peaks indicating an hexagonal structure. The advanced modelling procedure of the SAXS data enabled a detailed description of the mesoporous formation. The time evolution of the several parameters used for the modelling enabled a better understanding of synthesis process.

References

- [1] A. Sundblom et al. 2009 J. Phys. Chem. C, 113(18), 7706-7713
- [2] S. Förster et al. 2005 J. Phys. Chem B, 109, 1347.
- [3] N. Freiburger and O. Glatter. 2006 J. Phys. Chem B, 110, 14719.

Acknowledgements:

Determinação de propriedades estruturais de coacervados de xantana e poli(etilenoimina) por espalhamento de raios-x a baixos ângulos

Guerra, J. P. T. A.¹, Bellettini, I. C.¹, and Minatti, E.¹

Universidade Federal de Santa Catarina - Florianópolis SC Brazil

Coacervação é a separação em duas fases líquidas em sistemas coloidais. Em muitos casos, entretanto, os complexos possuem natureza sólida. Separação de fases associativa de dois polímeros em água ocorre caso exista atração eletrostática. Espalhamento de raios-x a baixos ângulos (SAXS) é uma técnica útil para estudar a estrutura de materiais na escala de 0,5 a 200 nm. Nesta técnica, é possível estudar a estrutura superficial externa de materiais poliméricos por medidas da intensidade de espalhamento $I(q)$ e do vetor de espalhamento q . O objetivo deste trabalho foi investigar por SAXS a estrutura e o tamanho de agregados macromoleculares formados na coacervação de xantana (XT, um poliânion) e poli(etilenoimina) (PEI, um polication) com e sem dodecil sulfato de sódio (SDS, um surfactante aniônico). A análise por SAXS de misturas aquosas de XT e PEI mostrou que o módulo do coeficiente angular no gráfico de $\ln I(q)$ vs. $\ln q$ para valores altos de q são inferiores a 1, significando que os agregados macromoleculares não apresentam estrutura fractal. Foi verificado que o SDS exerce um ordenamento no espalhamento de misturas aquosas de XT e PEI. A ordenação em baixos valores de q deve-se à formação de estruturas micelares. Também foi determinado pelo gráfico de Guinier que os raios de giração dos agregados estão em torno de 30 nm.

Acknowledgements: Ao CNPQ pelo suporte financeiro e ao LNLS.

Materiais Estruturais e Aplicações na Indústria

Optical proprieties of calcogenic alloys under VUV irradiation

Almeida, D. P.¹, Moura, P. R.¹, C.R. Ponciano², Campos, C. E. M.¹, and De Lima, J.C.¹

¹ Universidade Federal de Santa Catarina - Florianópolis SC Brazil

² PUC - Rio de Janeiro - Rio de Janeiro RJ Brazil

Studies on photoinduced changes occurring in SbTe and Te₂₄In₃₈Sb₃₈ alloys prepared as thin films are presented. Both systems have been investigated under several irradiation regimes. The experimental techniques employed are also presented. The studied alloys were prepared by a mechanical alloying using a right energy balls mill. Subsequently, the milled alloys were deposited as thin films on glass substrates and then exposed to synchrotron radiation with photons energies ranging from the visible to vacuum ultraviolet (VUV).

Acknowledgements: Agradecemos aos funcionários do LNLS pela inestimável cooperação.

MORPHOLOGICAL STUDY OF PP/EPDM/ORGANOCLAY NANOCOMPOSITE DEFORMED BY UNIAXIAL COMPRESSION

Machado, G.¹, Thompson, A.², Dal Acqua, N.², Teixeira, S.R.³, Bianchi, O.³, and Crespo, S.J.²

¹ Centro de Tecnologias Estratégicas do Nordeste - RECIFE PE Brazil

² Universidade de Caxias do Sul - Caxias do Sul RS Brazil

³ Universidade Federal do Rio Grande do Sul - Porto Alegre RS Brazil

Morphological and structural properties of a polypropylene (PP)/ethylene propylene diene teropolymer rubber (EPDM)/organoclay nanocomposite, submitted to uniaxial plain strain deformation, at room temperature and under compression rates of 5, 10 and 20 MPa, have been investigated using wide angle X-ray diffraction (WAXD), small angle X-ray scattering (SAXS), transmission electron microscopy (TEM) and scanning electron microscopy (SEM). In relation to PP and EPDM blend, three different compositions was analyzed (blend with 90, 75 and 65

Acknowledgements: This work was supported by CNPq, CAPES, FAPERGS

Desenvolvimento de um Protótipo de Micro-Sensor de Pressão Piezoresistivo de SiC

Fraga, M. A.¹, Massi, M.¹, Oliveira, I.C.¹, and Maciel, H. S.¹

Instituto Tecnológico de Aeronáutica - São José dos Campos SP Brazil

Neste trabalho é apresentada uma metodologia para desenvolvimento de um protótipo de micro-sensor de pressão piezoresistivo baseado em filme de carbeto de silício (SiC). O sensor desenvolvido é constituído por seis piezoresistores de SiC, configurados em ponte de Wheatstone, sobre um diafragma quadrado de Si e os contatos elétricos são de Ti/Au. Para fabricar piezoresistores isolados, o filme de SiC foi depositado por PECVD (plasma enhanced chemical vapor deposition) sobre a camada de SiO₂ obtida por oxidação térmica do substrato de Si. Os piezoresistores foram fabricados por corrosão RIE do filme de SiC e o diafragma por corrosão anisotrópica do Si em solução de KOH. Para realizar a caracterização do funcionamento do sensor foi necessário encapsulá-lo. Um adesivo RTV (room temperature vulcanizing silicone rubber) foi utilizado para colar o sensor sobre uma placa de alumina com trilhas de alumínio, fios de ouro foram utilizados para realizar a conexão elétrica entre os pads do sensor e as trilhas de alumínio da placa e uma tampa de alumínio foi colada sobre a placa para isolar o sensor das interferências ambientais. A etapa final deste trabalho foi caracterizar os sensores encapsulados em função da pressão aplicada. Os testes realizados determinaram a tensão de offset e a sensibilidade do sensor para pressões de até 12 psi. As medidas não foram realizadas em seqüência, havendo um intervalo de 10 dias entre a 1^a e a 2^a medida e de 45 dias entre a 2^a e a 3^a. Os sensores apresentaram uma sensibilidade média de 2,7 mV/psi próxima a de sensores comerciais. Isto mostra que a metodologia desenvolvida é eficiente uma vez que possibilitou a fabricação de um protótipo de micro-sensor de pressão piezoresistivo de SiC com bom desempenho.

Acknowledgements: Ao CNPq pelo suporte financeiro

SAXS evaluation of Renex-based self-assembly for mullite preparation

Garcia, R. B. R.¹, QUEIROZ, HIURE A. A. S¹, Pascoli, A.S.¹, and Kawachi, E. Y.¹

Instituto Tecnológico de Aeronáutica - São José dos Campos SP Brazil

Nanostructured materials may be prepared by the surfactant self-assembly approach, in which a liquid crystalline phase acts as a template for the synthesis of inorganic materials. The thermodynamic tendency of surfactant molecules to self-assemble is strongly affected by either the composition or temperature of the system.

In this work, nanostructured mullite ($3\text{Al}_2\text{O}_3 \cdot 2\text{SiO}_2$) was prepared by a sol-gel process associated to a surfactant self-assembly approach. The liquid crystal was formed by the mixture of a nonylphenol ethoxylated surfactant (Renex 100, from Oxiteno) and water. A systematic study of the influence of the sol-gel precursors and the reaction by products in the liquid crystal structure was conducted by SAXS on the D11A-SAXS1 beamline, using a radiation wavelength of $\lambda = 1,488$ Å. Samples were injected in a 1-mm thick sample holder between two mica sheets and the transmitted signal was collected in a marCCD detector positioned at 1000 mm far from the sample. Temperature influence was evaluated from 20 to 60 °C.

The results showed that Renex 100/water binary systems formed a hexagonal mesophase, which was preserved after the addition of nitric acid (a sol-gel catalyst), TEOS (a silicium alcoxide precursor) or ethanol (a by-product) at 20 °C. From 30 °C up, the systems containing nitric acid and ethanol showed a decrease in the hexagonal organization with a flattening of the SAXS peaks. For the system containing TEOS, above 30 °C, it was observed the presence of only one peak in the SAXS profile, at approximately 1 nm^{-1} , indicating that the hexagonal organization faded. The addition of aluminum nitrate nonahydrate as aluminum precursor destabilized the structure at all temperatures studied, indicating that the presence of Al^{3+} ions and/or water of hydration may have a negative influence on the liquid crystal structure. Even though a specific structural organization was not observed, a structured mixed oxide could be obtained by this simple method after calcination.

References: These results were partially presented in AutoOrg 2008 and submitted to the LNLS Activity Report 2008.

Acknowledgements: This work was supported by the Brazilian Synchrotron Light Laboratory (LNLS) under proposals D11A-SAXS1-7788 and 8078, and by the National Council for Scientific and Technological Development (CNPq) under process 475971/2007-8.

Estudo do Processo de Redução dos Íons Eu Durante a Síntese via Sol-Gel Protéico de Aluminatos de Sr e Ca

Montes, PJR¹ and Valerio, M.E.G.¹

Universidade Federal de Sergipe - São Cristóvão SE Brazil

Os aluminatos de estrôncio (SrAl_2O_4) e cálcio ($\text{Ca}_{12}\text{Al}_{14}\text{O}_{33}$) dopados com terras raras (RE) têm atraído muita atenção devido ao seu grande potencial em aplicações práticas como materiais que apresentam fosforescência com longo tempo de vida. Este trabalho tem como objetivo estudar a cinética de produção dos sistemas $\text{SrO-Al}_2\text{O}_3$ e $\text{CaO-Al}_2\text{O}_3$ dopados com íons terras raras utilizando a técnica DXAS, medindo amostras pré-calcinadas produzidas através do método sol-gel protéico [1]. Neste trabalho foram preparadas amostras pré-calcinadas com estequiometrias $\text{Sr:Al} = 1:2$ e $\text{Ca:Al} = 6:7$ dopadas com 4 mol% de Eu, ou combinação Eu/Dy^{3+} , ou combinação Eu/Nd^{3+} e amostras puras. Os espectros DXAS, obtidos em torno da borda L3 do Eu, foram coletados em função da temperatura das amostras. Os materiais preparados apresentaram estrutura amorfa bem como a presença dos reagentes de partida (sais de cálcio, estrôncio e alumínio) na forma desidratada, confirmada por medidas de difração de raios X de pó. As curvas de DTA-TG indicam a formação dos sistemas SrAl_2O_4 e $\text{Ca}_{12}\text{Al}_{14}\text{O}_{33}$ em 1100 °C e 900 °C, respectivamente. Espectros DXAS das amostras calcinadas sob fluxo de ar sintético não exibem variação na posição da borda de absorção dos íons Eu. Já as amostras submetidas ao tratamento térmico sob fluxo da mistura gasosa $\text{N}_2+5\%\text{H}_2$ exibem mudanças na borda de absorção, mostrando a evolução do processo da redução dos íons Eu durante a síntese dos materiais. A valência dos íons de Eu nos sistemas $\text{SrO-Al}_2\text{O}_3$ e $\text{CaO-Al}_2\text{O}_3$: RE depende da atmosfera usada durante a síntese. O estudo da dinâmica de interação gás/amostra pré-calcinada, durante a síntese, nos permite obter as melhores condições de tempo de síntese e fluxo do gás redutor, que levem a produzir estruturas dopadas com uma ótima razão $\text{RE}^{2+}/\text{RE}^{3+}$ [2]. Essas informações podem ser bastante úteis para o setor industrial, no caso de aplicação em indústria cerâmica como material de fosforescência longa em avisos luminosos sem gasto de energia, decoração em fachadas, etc. [1] M. A. Macedo, J. M. Sasaki, Processo de Fabricação de Pós Nanoparticulados, INPI 0203876-5. [2] F. Clabau, X. Rocquefelte, T. Le Mercier, P. Deniard, S. Jobic, and M.-H. Whangbo. Chem. Mater., 2006, 18 (14), 3212-3220.

Acknowledgements: Apoio: CAPES, CNEN, Renami/CNPq e INCT-INAMI/CNPq. Pesquisa realizada com apoio do Laboratório Nacional de Luz Síncrotron/MCT Projeto n 8825/09.

INVESTIGATION OF NANOSTRUCTURE AND PROPERTIES OF SOL-GEL DERIVED ZIRCONIUM OXIDE-SPEEK MEMBRANES FOR DIRECT ETHANOL FUEL CELLS

Kawaguti C.A.¹, DAHMOUCHE, K¹, and Gomes, A.S.²

¹ Centro Universitário da Zona Oeste - Rio de Janeiro RJ Brazil

² Universidade Federal do Rio de Janeiro - Rio de Janeiro RJ Brazil

New hybrid zirconia-sulfonated poly(ether ether ketone) (SPEEK) proton conducting membranes for direct ethanol fuel cells have been prepared. For ZrO₂ containing membranes without phosphotungstic acid (HPW), water sorption is similar to pure SPEEK ones, while incorporation of HPW drastically increases water sorption. For all membranes containing zirconia, ethanol permeability is reduced resulting on an increase of barriers properties. Membranes performance is related to nanostructural features investigated by SAXS. The SAXS results show that water sorption and protonic conductivity are related to the presence or absence of SO₃H-rich primary nanodomains, the domains size, the connectivity between domains and the inter-domain distance. On the contrary ethanol permeability seems not to be correlated to nanostructure. In this sense, this investigation performed by SAXS is of fundamental importance to understand the effect of nanoscopic structure on membranes properties, aiming the optimization of the membranes performance.

Acknowledgements: This work has been sponsored by Fundação de Amparo à Pesquisa do Estado do Rio de Janeiro (FAPERJ). The authors would also like to thank the Brazilian Synchrotron Light Laboratory (LNLS) for the help in SAXS measurements.

Proton conducting membrane based on SPEEK and modified silica for direct ethanol fuel cell

de Ramos Filho, F. G.¹, DAHMOUCHE, K², and Gomes, A.S.¹

¹ Universidade Federal do Rio de Janeiro - Rio de Janeiro RJ Brazil

² Centro Universitário da Zona Oeste - Rio de Janeiro RJ Brazil

The aim of this study is to develop membranes for direct ethanol fuel cell (DEFC), which should have much lower cost than commercial perfluorinated membranes and some requirements as good stability, low alcohol crossover and high proton conductivity. To overcome drawbacks such as instability to ethanol and high alcohol permeability, due to the affinity of alcohol to the sulfonic groups, composite membranes compounded by sulfonated polymers and modified silica have been proposed for direct methanol fuel cell. Membranes based on sulfonated poly(1,4phenyleneoxy-1,4phenylenecarbonyl-1,4phenylene) (SPEEK) (SD= 43%) were mixed with 4% (mass weight) modified silica. The influence of phosphotungstic acid (HPW) immobilized in the silica matrix (8.3% and 16.0% of HPW, determined by X-ray fluorescence analysis) and the influence of sulfonic group attached in silica matrix through reaction of (3-mercaptopropyl)trimethoxysilane and tetraethoxysilane by sol-gel method (4.2% and 9.0% total sulfur by elemental analysis) were evaluated on proton conductivity, water and alcohol uptake of membranes. The water and ethanol solution (20% mass weight) uptake going through 40 up to 90°C during 24h for each temperature decreased with loading of modified silica in the composites. The conductivity of composite membranes was half of the plain membrane (SPEEK). However, the membranes with modified silica had conductivity higher than the membranes with unmodified silica. SAXS measurement showed composite membranes are constituted by nanometric morphology.

Acknowledgements: CNPq, LNLS

Expansão térmica negativa e transição de fase do $\text{In}_2\text{Mo}_3\text{O}_{12}$

Ari M.¹, Marinkovic, B. A.¹, Jardim, P. M.¹, de Avillez, R. R.¹, Rizzo, F.¹, and Ferreira, F. F.²

¹ PUC - Rio de Janeiro - Rio de Janeiro RJ Brazil

² Universidade de São Paulo - São Paulo - São Paulo SP Brazil

Óxidos cerâmicos da família $\text{A}_2\text{M}_3\text{O}_{12}$, onde A = metal de transição trivalente e M = Mo^{+6} ou W^{+6} , apresentam expansão térmica baixa ou negativa após a transição de fase da estrutura monoclinica ($\text{P}2_1/\text{a}$) à ortorrômbica (Pbcn). Ambas as estruturas consistem de octaedros AO_6 e tetraedros MO_4 interconectados pelos vértices através do átomo de oxigênio e a transição de fase acontece sem quebra de ligações. O fenômeno de expansão térmica negativa é atribuído ao movimento térmico transversal do oxigênio na ligação A-O-M na estrutura ortorrômbica. Este tipo de materiais com expansão térmica baixa, zero e negativa são requeridos para diversas aplicações tecnológicas. No presente trabalho, o $\text{In}_2\text{Mo}_3\text{O}_{12}$ foi produzido pela técnica de reação no estado sólido. As análises térmicas mostraram que este composto não é higroscópico (TG) e que a transição de fase da estrutura monoclinica ($\text{P}2_1/\text{a}$) a ortorrômbica (Pbcn) ocorre a 340°C (DSC). As amostras foram analisadas por difração de raios-X de alta resolução utilizando luz síncrotron (LNLS), linha D10B-XPB. Obtiveram-se difratogramas na estrutura monoclinica (100 , 200 e 320°C) e após a transição de fase, na estrutura ortorrômbica (370 , 500 , 630 e 760°C). Os padrões de difração foram refinados utilizando o método de LeBail e Rietveld, dando como resultado que: - Na estrutura **monoclinica**, todos os eixos aumentam em função da temperatura, logo, o coeficiente de expansão térmica linear, $\alpha_l = 12,4 \times 10^{-6}/^\circ\text{C}$, - Na estrutura **ortorrômbica**, os eixos *b* e *c* diminuem em função da temperatura ($\alpha_b = -4,5 \times 10^{-6}/^\circ\text{C}$ e $\alpha_c = -6,5 \times 10^{-6}/^\circ\text{C}$), enquanto que, o eixo *a* aumenta ($\alpha_a = 5,4 \times 10^{-6}/^\circ\text{C}$), resultando que o coeficiente de expansão térmica linear é negativo, $\alpha_l = -1,85 \times 10^{-6}/^\circ\text{C}$.

Acknowledgements: Ao Laboratório Nacional de Luz Síncrotron (LNLS) pelo projeto D10B-XPB 7756. Ao Departamento de Engenharia de Materiais, DEMa, da PUC-Rio. M. S. Ari agradece à FAPERJ pela bolsa de pós-doutorado concedida.

X-ray Study of Carbide Evolution of Cr-Mo Steels during Aging

Lemus, L.F.¹, J. H. Rodrigues², dos Santos, D. S.¹, and L. H. Almeida¹

¹ Universidade Federal do Rio de Janeiro - Rio de Janeiro RJ Brazil

² Petrobrás - Cenpes - Rio de Janeiro RJ Brazil

The microstructural evolution of two Cr-Mo steels widely used in petrochemical industry as base material for hydrotreating/hydrocracking reactors was studied. Samples of the steels 2.25Cr–1Mo and 2.25Cr–1Mo vanadium modified were examined using X–ray diffraction in as-received condition and after artificial aging at 600C performed between 100h to 2000h under both inert and hydrogen rich atmospheres. The precipitates present in each sample have been identified and the influence of hydrogen on their evolution during the aging treatment was analyzed.

Initially, both steels had a bainitic microstructure with a finely disperse carbides. With the progression of the heat treatments, the precipitates suffer coarsening and evolve toward more stable forms enhancing their molybdenum content. For 2.25Cr–1Mo steel, even after 100h of treatment, the presence of the molybdenum rich carbide $M_{23}C_6$ was observed. The M_6C carbide could be also detected after 500h of aging, but a decrease on its peaks for the hydrogen aged sample was observed. Under inert atmosphere, the carbides present on the 2.25Cr–1Mo Vanadium modified steel exhibited more stability during ageing.

Acknowledgements: The authors acknowledge the financial support of LNLS, CNPq, and PETROBRAS for this work.

Effect of addition of acrylic acid and thioglycolic acid on nanostructure and thermal stability of PMMA/montmorillonite nanocomposites

Soares, B.G.¹, DAHMOUCHE, K², and Silva, A.A.¹

¹ Universidade Federal do Rio de Janeiro - Rio de Janeiro RJ Brazil

² Centro Universitário da Zona Oeste - Rio de Janeiro RJ Brazil

Poly(methyl methacrylate) (PMMA)/ organophilic montmorillonite (OMMT) nanocomposites were synthesized by the in situ free radical bulk polymerization of methyl methacrylate. The effect of small amount of acrylic acid as the co-monomer and thioglycolic acid as the chain transfer agent on the nanostructure of these nanocomposites was investigated by X-ray diffraction (XRD) and small angle X-ray scattering (SAXS) analyses. No diffraction peak was discernible in the XRD patterns of all samples. From SAXS experiments, it was possible to determine the presence of great amount of small clay aggregates (less than 40). This result is significant when acrylic acid was used as co-monomer, indicating a greater affinity between the clay and the polymer, resulting in better dispersion of the clay. The glass transition temperature of the nanocomposites was evaluated by differential scanning calorimetry (DSC) and the thermal stability was investigated by thermogravimetric studies (TGA). As expected, the presence of the clay increased the glass transition temperature in all studied systems. The thermal stability of nanocomposites was substantially higher than pure PMMA and the presence of small amount of acrylic acid as the co-monomer, exerts additional increase in this property.

Acknowledgements: This work has been sponsored by Conselho Nacional de Desenvolvimento Científico e Tecnológico (CNPq) and Fundação de Amparo à Pesquisa do Estado do Rio de Janeiro (FAPERJ). The authors would like to thank the Brazilian Synchrotron Light Laboratory (LNLS, Campinas - Brazil) for the financial and technical support in the SAXS measurements.

Estudo dos catalisadores compósitos à base de Pd e nanoóxidos à base de Nb e de Zr

Lagreca, E. R.¹, dos Santos, D. S.¹, and Conceição, M. O. T.¹

Universidade Federal do Rio de Janeiro - Rio de Janeiro RJ Brazil

Atualmente, o cenário mundial enfatiza como grande importância as questões ambientais ligadas a emissão de gases intensificadores do efeito estufa, dentre eles destaca-se o dióxido de carbono, que é produzido principalmente pela queima de combustíveis fósseis. Somando-se a isso há um constante aumento na demanda de energia por parte dos países emergentes, chega-se à conclusão de que o desenvolvimento de tecnologias limpas, sustentáveis e renováveis de geração de energia é urgente. Dentre as soluções propostas, a utilização do hidrogênio como fonte principal de energia, chamada economia do hidrogênio, é apontada por muitos como a que tem a melhor relação energia limpa e capacidade energética. Porém, um dos grandes problemas, se não o maior, no que diz respeito à viabilidade desta economia está no fato de não haver uma forma segura e econômica de armazenar o hidrogênio. Sob este aspecto, os hidretos metálicos se tornam muito atrativos do ponto de vista tecnológico, pois são uma opção promissora para o armazenamento de forma compacta e segura. O magnésio e ligas a base de magnésio apresentam boas propriedades: alta capacidade de armazenar hidrogênio (~7.5% wt.) e baixa densidade volumétrica. Entretanto, a cinética de absorção e dessorção de hidrogênio são lentas. Para promover esta cinética, a adição de diferentes catalisadores vem sendo estudadas. O paládio possui uma alta difusibilidade e solubilidade do hidrogênio por esta razão uma liga a base de Pd foi escolhida como o catalisador desta pesquisa. Com base nesse contexto, o objetivo desta pesquisa foi caracterizar ligas à base de Pd ($\text{Pd-Nb}_x\text{O}_x$ e $\text{Pd-Zr}_x\text{O}_x$) com nanoóxidos dispersos na matriz que serão usadas como catalisadores em ligas à base de magnésio. A análise por SAXS teve o objetivo de estudar a distribuição de tamanhos e a morfologia dos precipitados nanométricos dos óxidos de Nb e Zr dispersos na matriz. As ligas foram produzidas a partir dos elementos metálicos puros e em seguida submetidas a tratamentos térmicos de oxidação interna. Variando o tempo e a temperatura de tratamento, os óxidos crescem e se distribuem em locais de maior energia potencial tal como os contornos de grãos e de maclas. As amostras analisadas foram submetidas a tratamentos térmicos de oxidação interna em tempo fixo de 24h para as temperaturas iguais a 800°C, 1000°C e 1200°C.

Acknowledgements: Os autores agradecem o suporte financeiro dado pela CAPES e LNLS ao trabalho.

Fabricação de Strain Gauges para Aplicações em Altas Temperaturas

Fraga, M. A.¹, Massi, M.¹, Oliveira, I.C.¹, Furlan, H.², Wakavaiachi, S. M.¹, and Maciel, H. S.¹

¹ Instituto Tecnológico de Aeronáutica - São José dos Campos SP Brazil

² Faculdade de Tecnologia de São Paulo - São Paulo SP Brazil

A principal limitação dos strain gauges baseados em silício ou em metais é a influência da temperatura sobre o GF (Gauge Factor) desses materiais. Isto despertou o interesse pelo estudo das propriedades piezoresistivas de materiais semicondutores com estabilidade térmica e química, como o carbeto de silício (SiC) e o SOI (Silicon-On-Insulator), visando o desenvolvimento de strain gauges para aplicação em altas temperaturas. Neste trabalho foram fabricados strain gauges baseados em substratos SOI e em filmes amorfos de SiC. A estrutura desses dispositivos consiste de um resistor com contatos elétricos de Ti/Au. Um arranjo experimental foi montado para determinar a variação da resistência elétrica do resistor em função da tensão mecânica aplicada. Um resistor foi colado próximo à extremidade engastada de uma viga de aço em balanço e sobre a extremidade livre foram aplicadas diferentes forças. A resistência elétrica do resistor foi medida para cada força aplicada sobre a viga. Através desse experimento foi determinado o gauge factor de cada material. Para avaliar a influência da temperatura sobre o desempenho dos strain gauges foi determinado o coeficiente térmico de resistividade (TCR) para temperaturas de até 250C. A resistência elétrica foi medida a temperatura ambiente (25C) e a cada 10 minutos a temperatura foi aumentada em 25C. Para cada temperatura mediu-se a resistência elétrica. Observou-se que os strain gauges de SiC apresentaram um GF= 48 e TCR= 31 ppm/C enquanto que os SOI apresentaram GF= 22 e TCR= 140 ppm/C.

Acknowledgements: Ao CNPq pelo suporte financeiro

Non-destructive Analyses of Internal Stresses, Texture and Damage in Engineering Materials Using High-Energy Synchrotron X-Ray Diffraction

H. (C.) Pinto¹, Ch. Genzel², A. Pyzalla², and T. Wroblewski³

¹ Universidade de São Paulo - São Carlos - São Carlos SP Brazil

² Helmholtz-Zentrum Berlin für Materialien und Energie - Berlin Germany

³ Hamburger Synchrotronstrahlungslabor - Hamburg nc Germany

Material deterioration is caused by microstructure changes and formation of internal stresses, which occur as a result of the service conditions. Both can be determined non-destructively in the surface and the bulk of materials using synchrotron radiation. In this work, the use of diffraction methods with monochromatic and white hard synchrotron X-rays in the in- and ex-situ characterization of engineering materials will be illustrated using three case studies. The investigations were carried out at the Materials Science Beamlines located at the ESRF (ID15 and ID31), HASYLAB (MAXIM G3) and BESSY (EDDI). First, the influence of environmental conditions on the deterioration of austenitic CrNi steels during cryogenic wear will be presented. At extremely low temperatures these steels still exhibit good mechanical properties combined with sufficient ductility. However, high mechanical loads at low temperatures favor martensitic transformation and material embrittlement. The effect of stacking fault energy and a hydrogen atmosphere on phase transformation and deformation mechanisms are discussed. The second case study deals with the interaction between microstructure changes and internal stress formation in Li₂O-2SiO₂ glass-ceramics. Glass-ceramics are polycrystalline solids with very low coefficient of thermal expansion (CTE). This is achieved by controlling the growth of crystals, which have a lower CTE if compared to the amorphous matrix. The thermal mismatch between crystal and glass generates internal stresses, which may cause micro cracks and, thus, compromise the functionality of glass-ceramics. Synchrotron X-ray diffraction reveals for the first time the anisotropy of the residual stresses in embedded crystals directly in the interior of a glass-ceramic without the need to eliminate the crystallized surface layer. The third example concerns the formation of oxide scales on metallic substrates at high temperatures. The growth incompatibilities give rise to internal stresses capable of deteriorating the shielding efficiency of oxide scales. In addition, the crystallographic orientation of the substrate also influences the oxidation kinetics. Thus, the distinct oxidation behavior of single crystals might be associated with particular internal stress states resulting from textured oxides. Energy-dispersive diffraction using a white synchrotron X-ray beam is applied to study in-situ the influence of substrate orientation and texture of the oxides on the growth stress state of multi-phase iron oxide scales.

Acknowledgements:

Characterization of the activation process of LTS industrial catalysts by *in situ* X ray diffraction

Rodella, C. B.¹ and Zanchet, D.¹

Laboratório Nacional de Luz Síncrotron - Campinas SP Brazil

Cu/ZnO/Al₂O₃ catalysts are widely used in industry in water gas shift reaction at low temperatures (LTS Low Temperature Shift). In this reaction, CO reacts with steam forming CO₂ and H₂. The active phase of these catalysts is metallic Cu, obtained by the reduction with H₂. In present study the activation process of two industrial LTS catalysts was evaluated by *in situ* X ray Diffraction (XRD), to identify the structural differences between samples during the reduction process. Industrial LTS catalysts (LTS1 and LTS2) were provided by OXITENO Ind. e Com. *In situ* XRD experiments were performed at XRD2 beamline at LNLS, using a furnace installed at the beamline diffractometer and connected to a mass spectrometer. The samples were heated up to 230⁰C (5 ⁰C/min up to 190⁰C and 2⁰C/min up to 230⁰C) under a flow of 40ml/min of 0.5XRD data showed that the LTS1 sample is initially formed by a crystalline CuO phase but a disordered ZnO/Al₂O₃ phase, whereas in LTS2 sample all phases are highly disordered. Both samples showed a partial reduction of the Cu²⁺ to Cu¹⁺ before transforming to Cu⁰. In general, the thermal treatment led to the reduction of Cu and formation of a crystalline phase, and increase of ZnO crystallinity. According to mass spectrometry analysis of the hydrogen consumption during the activation process, LTS1 sample spent 140 min to complete the Cu reduction, whereas LTS2 spent 175 min in the same conditions. The mean crystalline size of the Cu obtained for LTS1 was 16 nm and 10 nm for LTS2. It is likely that the initial amorphous structure of LTS2 reflects smaller domains of CuO and ZnO particles and a better grain interconnectivity between the oxides, compared with the sample LTS1. These characteristics could be responsible for decreasing the activation rate, as well as to difficulty the sinterization of the Cu⁰ in LTS2 sample.

Acknowledgements: We are grateful for the use of XRD2 beamline at LNLS and staff support and to Oxiteno, for the samples and fruitful discussions.

Development of catalytic materials for glycerol hydrogenolysis

R.J.Chimentão¹, Rodella, C. B.¹, Ferreira, R. A. A.¹, Queiroz, C. M. S.², VICENTINI, Valéria Perfeito², and Zanchet, D.¹

¹ Laboratório Nacional de Luz Síncrotron - Campinas SP Brazil

² Oxiteno S/A Indústria e Comércio - Mauá SP Brazil

Glycerol is the major byproduct of biodiesel production by transesterification of vegetable oil. One industrially relevant route to process glycerol into more valuable commodity chemical involves its hydrogenolysis to ethylene glycol (EG) and propylene glycol (PG). Heterogeneous catalysts based on precious metals have demonstrated effectiveness in the hydrogenolysis. Transition-metal carbides such as W and Mo have attracted much attention due to the similar performance to precious metals in reactions involving hydrogen. The objective of this work is the development of catalysts for the hydrogenolysis of glycerol to the production of EG as part of the industrial collaboration of the LNLS. Propane hydrogenolysis was used as probe reaction. Hydrogenolysis of glycerol was carried out in an autoclave. By impregnation 5wt.%Ru/C (Ru/C) and 5wt.%Ni/C (Ni/C) samples were prepared. A reference sample of 5%Ru/C (Ru/C-REF) supplied by OXITENO was evaluated. The XRD of Ru/C sample does not exhibit peaks of Ru species indicating good dispersion. The Ni/C sample shows diffraction peaks of Ni metallic, with average crystallite size estimated by the peak (200) of about 5 nm. The probe reaction shows that the activity ($\text{mol}_{C_3H_8} \cdot \text{g}_{\text{metal}}^{-1} \text{s}^{-1}$) of Ru catalysts was higher than the Ni/C. The hydrogenolysis of glycerol studies depicted conversions of about 20-30% for Ru catalysts and 50% for Ni. The Ru/C-REF sample lead mainly to the formation of 2-propanol, while Ru/C and Ni/C lead to 1,2-PG. Hydrogenolysis experiments are being implemented to the metal carbide materials. From the literature the metastable W_2C and Mo_2C phases are considered to have intrinsically higher activity than the thermally stable WC and MoC phases. Carbon supported W and Mo carbide samples were prepared by carbothermal hydrogen reduction (CHR) at 1073 K. The gas composition in the CHR can modulate the carbide phase. Based on the XRD W_2C and Mo_2C were obtained when pure hydrogen was employed.

Acknowledgements: LME and XRD1 facilities and LSQ, Labcat-UFSCar and OXITENO teams for help. Funding: FAPESP-OXITENO-LNLS.

Estudo dos efeitos do bombardeamento atômico com gás nobre sobre a microestrutura de aços

Droppa Jr., R.¹, Ochoa, E.A.², H. (C.) Pinto³, F. Alvarez², and Garcia, J.⁴

¹ Universidade Federal do ABC - Santo André SP Brazil

² Universidade Estadual de Campinas - Campinas SP Brazil

³ Universidade de São Paulo - São Carlos - São Carlos SP Brazil

⁴ Hahn Meitner Institute - Berlin Germany

Em um artigo de 2006 [1] ficou demonstrado que o bombardeamento atômico de substratos de aço com Xe melhora a difusão do nitrogênio nas camadas próximas à superfície, graças à diminuição do tamanho de grão nessas regiões. Este processo, além de facilitar a nitretação do substrato, pode ser usado também para modificar a superfície em nível atômico, tornando-a mais rugosa e aumentando, assim, a capacidade de aderência de revestimentos duros sobre a mesma, por exemplo. Atualmente, o desenvolvimento de processos que levem à melhoria da qualidade dos revestimentos duros em ferramentas tem um papel de extrema importância para a indústria e esse desenvolvimento passa necessariamente pela compreensão dos processos de pré-tratamento dos substratos. Nesse sentido, foram caracterizados substratos de aço 100Cr6, que receberam um pré-tratamento por bombardeamento atômico com Xe em diferentes energias, com relação a suas estruturas cristalinas, estrutura de grãos e quanto ao estado de tensão residual induzida pelo tratamento, para correlacionar com os efeitos sobre a aderência e microestrutura dos recobrimentos duros de TiN depositados em substratos submetidos a este tratamento. As amostras foram analisadas tanto quanto à sua microestrutura como quanto ao seu estado de tensão residual por difração de raios X em incidência rasante. A morfologia da superfície dos substratos, bem como a distribuição de tamanho de grãos e de microtrincas das amostras foram obtidas por microscopia eletrônica de varredura. Os resultados obtidos deverão fazer parte de um conjunto mais amplo de dados que deverá servir para se obter o quadro mais completo possível dos mecanismos e mudanças envolvidas nos processos de pré-tratamento das amostras, os quais servirão de base para o desenvolvimento de recobrimentos duros com propriedades melhoradas.

Referência: [1] E. A. Ochoa, C. A. Figueroa, T. Czerwiec and F. Alvarez, Applied Physics Letters, 88, 254109 (2006).

Acknowledgements: LNLS

XRD STUDIES OF ENGINEERING MATERIALS USING THERMOMECHANICAL SIMULATOR

Wu, L.¹, Isaac, A.¹, and Ramirez, A.J.¹

Laboratório Nacional de Luz Síncrotron - Campinas SP Brazil

This project will combine a thermomechanical simulator (Gleeble system) with synchrotron x-ray diffraction. The Gleeble system allows for producing microstructural changes representative of those experienced during solid-state phase transformation, high-temperature corrosion, materials processing (e.g. welding, heat treatment and metal forming), and thermomechanical loads (e.g. uniaxial tensile and compressive deformation, fatigue and creep). This physical simulator comprises a 44kN hydraulic uniaxial testing machine for tension and compression. Heating and cooling rates up to 1,000°C/s may be readily achieved, with mechanical loads superimposed, if required. It is also capable of cyclic deformation and/or cyclic temperature. The materials science activities will focus on three intersecting topics which are industrial, applied, and fundamental research. The beamline shall combine two main features. First, the high flux associated to fast detector systems allowing complex and dynamic *in situ* experiments. Second, a high flexibility in beam shaping will be available, fully exploiting the high brilliance of the source. This novel set-up will enable us to follow *in situ* phase transformations and residual stresses development under service and/or manufacturing conditions.

Acknowledgements: This work is funded by PETROBRAS

Friction Stir Welding of ISO 3183 X80M Steel

Santos, T. F. A.¹, Ramirez, A.J.¹, Hermenegildo.T.F¹, Benati, D. M.¹, and Afonso, C R M¹

Laboratório Nacional de Luz Síncrotron - Campinas SP Brazil

Friction Stir Welding (FSW) is a solid-state joining process with numerous advantages as good dimensional stability and repeatability. 12 mm thick ISO 3183 X80M (API-5L-X80) steel plates were friction stir welded in two passes using ceramic tools. Different heat inputs were obtained using a fix travel (welding) speed in combination with several spindle speeds aiming the achievement of better mechanical properties. The microstructure of base material (BM) was formed by ferrite (F), degenerated perlite (DP) and Martensite-Austenite constituent (M-A). The heat affected zone (HAZ) microstructure was composed by F, some carbides (Fe₃C), and M-A. The microstructure of the stir zone (SZ) presented F, M-A constituent, and degenerated upper bainite (DUB). Tensile tests were performed in joints according API 1104. The samples failed at the BM indicating higher tensile strength within the SZ and HAZ. The HAZ showed minor increment of hardness whereas the SZ showed considerable increment. The fracture toughness of the two-pass joint BM, HAZ and SZ was evaluated at 25C using single edge bend specimen CTOD. The joint showed CTOD-values above the offshore standard requirements (DNV-OS-F101), turning FSW a technically viable technology for high strength structural steel welding, without compromising the material fracture toughness. Therefore, FSW should be considered and developed as a key technology in the energy generation industry, especially for advanced construction and critical repair applications.

Acknowledgements: The authors are indebt to Petrobras and Finep for financial support.

Numerical Modelling and Experimental Analysis during Solidification of Arc Weld in Ni-Cr-Fe Alloys with Hf Additions

Unfried S., J.¹, Fonseca, E. B.², Afonso, C R M¹, and Ramirez, A.J.¹

¹ Laboratório Nacional de Luz Síncrotron - Campinas SP Brazil

² Universidade Estadual de Campinas - Campinas SP Brazil

In this work were studied the effects of small additions of Hafnium (Hf) in Ni-Cr-Fe based solid solution hardened superalloys. The effects are related to precipitation of primary carbides, partitioning of elements and grain boundary format. A numerical modelling based on the Calphad methodology was used to simulate eutectic transformation and distribution of elements in experimental alloys with different levels of Hf content. Characterization based on optical, electron microscopy and, XEDS techniques were used to obtain experimental evidence of grain boundary format, carbides precipitation and partitioning of elements, respectively. It has been observed that increasing Hafnium additions increase the fraction of carbides, grain boundaries serrated and probability of welding solidification cracking.

Acknowledgements:

Métodos e Instrumentação

Pressure cell for XPD, XAS and SAXS experiments using Synchrotron Light

Orlando, M. T. D.¹, J.L.Passamai Jr¹, Martinez, L. G.², Rossi, J. L.², Corrêa, H. P. S.³, Garcia, F.⁴, Ferreira, F. F.⁴, Melo, F. C. L.⁵, and Souza Jr, F. G.⁶

¹ Universidade Federal do Espírito Santo - Vitória ES Brazil

² Instituto de Pesquisas Energéticas e Nucleares - São Paulo SP Brazil

³ Universidade Federal do Mato Grosso do Sul - Campo Grande MS Brazil

⁴ Laboratório Nacional de Luz Síncrotron - Campinas SP Brazil

⁵ Centro Técnico Aeroespacial - São José dos Campos SP Brazil

⁶ Universidade Federal do Rio de Janeiro - Rio de Janeiro RJ Brazil

A high pressure CuBe cell with B4C anvil has been developed since 2004 for small- and wide-angle synchrotron x-ray scattering experiments under hydrostatic pressure up to 2GPa, at room temperatures. Recently, an optimized version of this cell was used to measure the pressure effect on structure of Cardanol-Furfural-PAni Green Blend in SAXS beam line at Laboratório Nacional de Luz Síncrotron - LNLS - Campinas . This cell has also been applied to investigate solid samples behaviour under external hydrostatic pressure since 2007 at LNLS. Moreover, it might also be used to investigate biological system as lipid-water dispersions without changes in its design. Magnetic field up to 1.6 kGauss can be applied together the hydrostatic pressure in this cell, taken into account there is no magnetic signal from de CuBe, B4C anvil, and CuBe gasket used. Investigations about ReO₂ behavior under hydrostatic pressure up to 1.6 GPa were performed at LNLS-XPD and XAFS Synchrotron beam line, and the results revealed to be the ReO₂ a good inner gauge pressure for 8keV-13keV energy range. This project has been developed by LNLS, UFES, IPEN/CNEN and IEA/CTA collaboration.

Acknowledgements: We would like to thank CNPq Grant 471536-2004-0, CT-Energ 504578-2004-9, and CAPES for financial supports. Thanks also to Cia. Vale do Rio Doce (CVRD), Cia Siderurgica de Tubarao (AcelorMittal), and National Laboratory of Synchrotron Light - LNLS, Brazil (XPD 2950-04, XPD 4742-05, XPD 5720-06, DXAS 2950-04, DXAS 2952-04, DXAS 5741-06, D02A - SAXS2 8519/09).

Current Status of the High Energy Resolution System of the XRF Beamline

Pérez, C. A.¹ and H. J. Sánchez²

¹ Laboratório Nacional de Luz Síncrotron - Campinas SP Brazil

² Universidad Nacional de Cordoba - Córdoba Cba Argentina

This work presents the status of the high energy resolution system that is being currently commissioned in the XRF beamline of the LNLS.

A high energy resolution system for detecting characteristic radiation, based in a wavelength dispersive system, is currently mounted and in the final stages of commissioning in the XRF beamline of the LNLS. The module was tested many times with a conventional x-ray tube and then mounted in the beamline in order to be used as a routine experiment of the line. The system has been mounted on a special device placed in the beamline. This device allows fine movements in order to align the module very precisely. This is a critical point to get the best available resolution. The radius of the Rowland Circle of the spectrometer is 140 mm, the detector is a proportional counter one with a 300 microns windows. Currently a Si(111) crystal is being used and the resolution of the angular stage is 0.017° . The energy resolution strongly depends on the dimensions of the incident beam. A final configuration of 0.1 mm (horizontal) and 0.5 mm (vertical) was adopted.

Pure foils samples of Fe, V and Ti were used to characterize the system. Measurements of $K\alpha$ and $K\beta$ lines were obtained using the high resolution module and a conventional solid state detector. Measured spectra were analyzed with typical programs for spectrum analysis and the Full Width Half Maximums (FWHM) were calculated for all the samples and lines. In addition, theoretical calculations of the expected resolution were carried out. The results and their comparison with the theoretical values are summarized in the following table.

Line	Measured Resolution (eV)	Calculated Resolution (eV)
Fe $K\alpha$	28 ± 3	35
Fe $K\beta$	47 ± 5	46
V $K\alpha$	13 ± 3	15
V $K\beta$	27 ± 3	21
Ti $K\alpha$	13 ± 1	12
Ti $K\beta$	21 ± 2	15

The results indicate an obvious significant improvement in the energy resolution of the high resolution system as compared with a conventional energy dispersive system. The calculated values of resolution agree very well with the measured ones.

The future implementation of other crystals will allow getting even higher resolutions. We expect to open the use of the system to users very soon.

Acknowledgements: This work has been partially supported by the LNLS

Synchrotron and Neutron Diffraction of Standard Reference Samples for Powder Diffraction Developed at IPEN-CNEN/SP

Martinez, L. G.¹, Galvão, A. S. A.¹, Mazzocchi, V. L.¹, Parente, C.B.R.¹, Corrêa, H. P. S.², and Orlando, M. T. D.³

¹ Instituto de Pesquisas Energéticas e Nucleares - São Paulo SP Brazil

² Universidade Federal do Mato Grosso do Sul - Campo Grande MS Brazil

³ Universidade Federal do Espírito Santo - Vitória ES Brazil

The verification of alignment and calibration of powder diffractometers is generally performed by the measurement of standard samples. For neutron and synchrotron diffraction it is also necessary the precise determination of the energy or wavelength of the radiation, which is done by using reference samples. For powder diffraction line profile analysis, used for instance in determination of crystallite sizes and microstrains, it is imperative the determination of the instrumental breadth and this is also done by means of standard reference samples. These standard reference samples, besides other properties like crystal structure and cell parameters very well defined, must present high crystallite size and no microstrains in order to present diffraction peaks broadening due exclusively to the instrumental factors. For this purpose are generally used the NIST Standard Reference Materials for Powder Diffraction like Al_2O_3 , Si, LaB_6 etc. In order to have an alternative source of standard reference materials for powder diffraction we are studying and developing some standard samples and comparing their diffraction properties to the NIST standards. In this work are presented some results of our $\alpha-Al_2O_3$, Y_2O_3 and Si standard samples measured by synchrotron powder diffraction (D10B-XPD and D12A-XRD1 - LNLS) and neutron powder diffraction (Neutron Powder Diffractometer - IPEN/CNEN). The measurements of our standard samples are compared to measurements of LaB_6 , Al_2O_3 and Si NIST standards, measured at the same conditions. The results show that our standard samples fulfill the requirements to be used as powder diffraction standards and can be used in substitution to the NIST standards.

Acknowledgements: The authors acknowledge to Nuclear and Energy Research Institute - IPEN/CNEN and Brazilian Synchrotron Light Laboratory LNLS. Work supported by the Brazilian Agency CNPq (proj. 480337/2007-1).

THE ZINC DISTRIBUTION IN PROSTATE TISSUES BY μ SRXRF

Leitão, R.G.¹, Anjos, M. J.², Canellas, C.G.L¹, Pereira, M.O.³, Pereira, G.R.¹,
Correia, R. C.², Palumbo, A.J¹, Souza, P.A.V.R¹, Ferreira, L. C.⁴, Nasciutti,
L.E¹, and Lopes, R.T.¹

¹ Universidade Federal do Rio de Janeiro - Rio de Janeiro RJ Brazil

² Universidade do Estado do Rio de Janeiro - Rio de Janeiro RJ Brazil

³ Centro Federal de Educação Tecnológica - Rio de Janeiro RJ Brazil

⁴ Fundação Instituto Osvaldo Cruz - Rio de Janeiro RJ Brazil

Many elements play an essential role in a number of biological processes as activators or inhibitors of cellular and enzymatic activity. The topographic and quantitative elemental analysis of pathologically changed tissues may shed some new light on processes leading to the degeneration of cells in case of selected diseases. Zinc concentration in a prostate gland is much higher than that in other human tissues. The high concentration of zinc in the prostate suggests that zinc may play a role in prostate health. The aim of this work was to study the elemental distribution for Zinc in prostate tissues from patterns of relative fluorescence intensities. The measurements were performed in standard geometry of 45° incidence, exciting with a white beam and using a conventional system collimation (orthogonal slits) in the XRF beam line at the Synchrotron Light National Laboratory (Campinas, Brazil). The prostate glands were cut into pieces (slice) with thickness of 0.5 mm. The results showed the zinc distribution was not uniform for different zones of the prostate analyzed.

Acknowledgements: This work was partially developed at Brazilian National Synchrotron Light Laboratory (projects XRF 8266) and had the financial support of CNPq and CAPES.

Scanning of citrus leaves to evaluate stages of citrus greening disease using micro synchrotron radiation X-ray fluorescence in association with chemometric tools

Pereira, F. M. V.¹ and Milori, D. M. B. P.¹

Empresa Brasileira de Pesquisas Agropecuárias - São Carlos SP Brazil

Citrus greening has been considered the worst citrus pest since 2004 both in Brazil and in the United States. This disease has had serious consequences in agricultural production and highlights the urgent need for early diagnostic methods. This analytical study investigated the mineral constituents of healthy leaves and leaves infected with citrus greening (or Huanglongbing) using micro synchrotron radiation X-ray fluorescence (μ SR-XRF) scanning combined with chemometric tools. Plants infected by citrus greening have two different stages: asymptomatic and symptomatic. The asymptomatic stage is very dangerous because the plant is contaminated. Depending on the incubation period, this condition is not perceptible by visual inspection. The main symptoms of citrus greening are yellowing of the leaves and the production of small and deformed fruits. The information obtained using the μ SR-XRF spectra profiles and the chemometric tools allowed the construction of predictive models to identify healthy and infected trees with and without symptoms. The signals for K, Ca, Fe, Cu and Zn and the region of coherent and incoherent scatterings were relevant to the differentiation of the healthy and infected samples. The calibration model correctly classified up to 95 - 98% of samples, and the validation data correctly assigned 90% of samples with a 95% significance level.

Acknowledgements: We are grateful to Fundação de Amparo à Pesquisa do Estado de São Paulo (FAPESP) for the fellowship awarded to F. M. V. Pereira (Process 2007/08618-2), to Conselho Nacional de Desenvolvimento Científico e Tecnológico (CNPq) (Process 578576/2008-2), to Grupo Fischer - Divisão Citrosuco for providing the plant material and to the D09B X-ray fluorescence beam line at the Brazilian Synchrotron Light Source - LNLS (Process D09B - XRF-8491/09) for the μ SR-XRF measurements.

Microchips de PDMS/SiO₂/Vidro contendo Detecção Condutométrica Sem Contato: Estudo de Configurações e Geometrias dos Eletrodos

Lima, R. S.¹, Piazzetta, O.M.H.², Gobbi, A. L.², Carrilho, E.¹, Coltro, W. K. T.³, Rodrigues Filho, U.P.¹, and Nascente, P. A. P.⁴

¹ Universidade de São Paulo - São Carlos - São Carlos SP Brazil

² Laboratório Nacional de Luz Síncrotron - Campinas SP Brazil

³ Universidade Federal de Goiás - Goiânia GO Brazil

⁴ Universidade Federal de São Carlos - São Carlos SP Brazil

Este trabalho vem a descrever um estudo sistemático sobre diferentes configurações e geometrias de celas condutométricas sem contato (C4D) em microchips de vidro/SiO₂/PDMS visando um aumento na sensibilidade do método. Foram avaliados três detectores, a saber: (i) C4D com cela de detecção convencional, contendo eletrodos em formato retangular e orientação antiparalela; (ii) C4D com eletrodos segundo geometria e dimensões propostas recentemente por Kuban e Hauser (C4Dalt) e (iii) detecção condutométrica híbrida (HCD), em que o eletrodo de excitação (eexc) é mantido em contato com o eletrólito. Para estudo comparativo entre os microdispositivos, foram feitas sete medidas para cada um dos seguintes níveis de concentração de NH₄Cl: 50; 75; 100; 125 e 150 micromol.L⁻¹. Como uma estimativa da sensibilidade dos detectores, foram calculados os limites de detecção (LOD) e quantificação (LOQ) segundo parâmetros das curvas analíticas obtidas. A um nível de confiança de 95 por cento, os valores de LOD foram: 18,33 (C4D); 14,05 (C4Dalt) e 16,02 micromol.L⁻¹ (HCD). Observa-se que as alterações na configuração e geometria da cela condutométrica sem contato não acarretaram em aumento significativo da sensibilidade. Conclui-se, logo, que a geometria da cela de detecção adotada em C4Dalt não reduziu de forma efetiva o acoplamento capacitivo direto entre os eletrodos, ao passo que para a detecção híbrida, é proposta uma base teórica fundamentada em leis da física elétrica com vista a explicar os resultados ocorrentes. Em linhas gerais, em HCD a capacitância equivalente relacionada aos sistemas eletrodo/solução é uma função somente da capacitância intrínseca ao eletrodo receptor (Cr). Logo, uma vez que as celas de detecção seletivas a C4D e HCD utilizadas neste estudo não diferiram entre si com relação aos parâmetros intervenientes em Cr, conclui-se que para tais detectores são esperados níveis de detectabilidade similares.

Acknowledgements: FAPESP, CNPq e CAPES.

Detecção direta de raios x com APD de 10 mm x 10 mm

Kakuno, E. M.¹, Scorzato, C. R.², and Giacomolli, B.A.¹

¹ Universidade Federal do Pampa - Bagé RS Brazil

² Laboratório Nacional de Luz Síncrotron - Campinas SP Brazil

Medidas que envolvem caracterização estrutural de filmes finos e pontos quânticos crescidos sobre substratos monocristalinos, requerem detectores com faixa dinâmica de contagens da ordem de 10^7 contagens por segundo (CPS), pois o pico do substrato é utilizado como referência para a análise dos picos das superestruturas e dos picos satélites destes. Como o volume difratante do substrato é infinitamente maior que o volume das superestruturas, a intensidade do pico do substrato facilmente chega a ser 6 ordens de grandeza maior que os picos das superestruturas e os picos satélites deste chegam a ser 3 ordens de grandeza menor que os picos da superestrutura. Portanto são necessários detectores que suportem taxas de contagens da ordem de 10^7 CPS a 10^{-2} CPS. Neste trabalho reportamos os primeiros resultados de testes de detectores para raios x, de conversão direta, do tipo silicon avalanche photo-diode (Si-APD). Este tipo de detector é uma alternativa atraente aos detectores convencionais (cintiladores) de raios x, pois oferecem as seguintes vantagens: uma maior faixa dinâmica de operação, da ordem de 10^9 e resolução em energias de 30% a 50%. Adicionado a isto, o know-how de construir detectores nos permitirá oferecer apoio técnico a qualquer instante. Atualmente dispomos de um aplicador de RF (home-made) de 3 estágios com um APD da Hamamatsu, operando satisfatoriamente no infra-vermelho. Obtemos pulsos com largura da ordem de $1 \mu\text{s}$ e amplitude da ordem de 1 Vp. Para detectarmos raios x, recentemente adquirimos APDs adequados, produzidos pela Perkin Elmer: C30703F-200 de $10 \times 10 \text{ mm}^2$, com recursos provenientes do CNPq. Concomitantemente aos testes, estaremos realizando o desenvolvimento de hardware (amplificador de RF, fonte de alta tensão (HV), shaper amplifier, discriminador e contadores rápidos). Além da cooperação técnica com o grupo de detectores do LNLS, contamos com um aluno da graduação na condição de iniciação científica e bolsa concedida pela FAPERGS

Acknowledgements: Este trabalho está sendo suportado pelo CNPq (Edital MCT/CNPq 14/2008, processo 479557/2008-0) e pela FAPERGS (BIC-0950-1.05/09).

The new XAFS beamline at LNLS

Azevedo, G. de M.¹, Fabbris, G. F. L.², Sotero, A.P.S.¹, Oliveira, J.J.², Gasperini, A. A.³, Rodrigues, F.¹, and Neueschwander, R.¹

¹ Laboratório Nacional de Luz Síncrotron - Campinas SP Brazil

² Laboratório Nacional de Luz Síncrotron - SP Brazil

³ Universidade Estadual de Campinas - Campinas SP Brazil

Before 2007, only the XAFS1 beam line was available at LNLS for conventional (i.e sequential) XAFS measurements in the hard X-ray domain. XAFS1 yields a modest photon flux, in the intermediate 108 photons/mms/second range. With an increasing demand for more complex and sophisticated experiments by the LNLS XAFS community , there was an urgent need for a better beam line performance.

To suit such demands, a new beam line was commissioned and made available to the LNLS XAFS community in 2007. XAFS2 has been planned aiming at a maximization of the photon flux impinging at the sample position. To this purpose, the optics is comprised of a vertically collimating and a toroidal focusing mirror before and after, respectively, the Si 111 double crystal monochromator. The new beam line covers the 4-18 keV energy range, with better energy resolution and a 60-fold increase in photon flux, as compared to XAFS1. With the higher flux, the detection limit in fluorescence detection mode was lowered down to a few tens of ppm, enabling a number of experiments which are either impossible or extremely difficult in XAFS-1. The higher signal to noise ratio permits EXAFS scans up to higher wave numbers, improving in the spatial resolution of the technique.

In this contribution, we describe the new beam line optics in detail, some of its operational parameters and the instrumentation available for users (sample environments, detectors, etc). Some commissioning results and examples of recent scientific results will be utilized to demonstrate the beam line capabilities.

Acknowledgements: The authors wish to acknowledge the Brazilian agency FINEP and ABTLuS for financial support

Metal mesh resonant filters for terahertz frequencies

Melo A. M.¹, Kornberg, M. A.², Kaufmann, P.¹, Piazzetta, O.M.H.³, Gobbi, A. L.³, Bortolucci, E. C.⁴, Zakia, M.B.P.⁴, Bauer, O. H.⁵, Poglitsch, A.⁵, and da Silva, A. M. P. A.⁴

¹ Universidade Presbiteriana Mackenzie - São Paulo SP Brazil

² European Space Agency - Noordwijk Netherlands

³ Laboratório Nacional de Luz Síncrotron - Campinas SP Brazil

⁴ Universidade Estadual de Campinas - Campinas SP Brazil

⁵ Max-Planck-Institut für extraterrestrische Physik - Germany Germany

The interest in terahertz photometric and imaging measurements has motivated the development of bandpass resonant filters to be coupled to multiple-pixel devices such as bolometer arrays. Resonant grids are relatively simple to fabricate, exhibiting high transmission at the central frequency, a narrow bandpass, and good rejection of the side frequencies of the spectrum. We have fabricated filters centered at different frequencies between 0.4 and 10 THz, using photolithography and electroforming techniques. Transmission measurements have shown center frequencies and bandwidths close to the design predictions. The performance of the filters was found not to be critically dependent on small physical deformations in the mesh, becoming more noticeable at higher frequencies (i.e., for smaller physical sizes). Wider bandwidths, needed to attain higher sensitivities in the continuum, were obtained by changing the design parameters for filters at 2 and 3 THz.

Acknowledgements: This work was supported by FAPESP and LNLS laboratories.

Design, fabrication and tests of metal microstructures applied to studies of DNA damage

Melo A. M.¹, Krawczyk, P.², Bortolucci, E. C.³, Gobbi, A. L.⁴, and Piazzetta, O.M.H⁴

¹ Universidade Presbiteriana Mackenzie - São Paulo SP Brazil

² University of Amsterdam - Amsterdam Netherlands

³ Universidade Estadual de Campinas - Campinas SP Brazil

⁴ Laboratório Nacional de Luz Síncrotron - Campinas SP Brazil

Here we describe the design and fabrication process of thin metal perforated surfaces. These structures could be defined by the diameter and periodicity of the circular apertures and by the thickness of the metal film. The fabrication process was performed at Microfabrication Laboratory of National Synchrotron Light Laboratory, using lithography techniques followed for metal deposition. The first structures fabricated presented diameter from 2 to 5 micrometers with periodicity between 5 to 10 micrometers. These structures have been used as a mask to induce DNA damage in restricted nuclear areas of living mammalian cells. Such microbeam irradiation of living cells is a powerful method for studying the induction and processing of DNA lesions.

Acknowledgements:

Fabricação de plataformas microfluídicas a partir do uso de toner

Coltro, W. K. T.¹

Universidade Federal de Goiás - Goiânia GO Brazil

A apresentação abordará os avanços no desenvolvimento de sistemas analíticos miniaturizados a partir do uso de toner, direta ou indiretamente. No processo direto, o toner é depositado sobre um filme de poliéster através de uma impressora laser. Neste caso, a espessura da camada de toner (7 microns) define a profundidade do microcanal que será formado após uma etapa de laminação térmica. No processo indireto, uma camada de toner é depositada sobre uma folha de papel vegetal e pode ser transferida para superfícies planares, como vidro e poli(carbonato) ou mesmo superfícies condutoras, como placas de circuito impresso ou discos compactos não regraváveis (CD-R) revestidos com uma camada de ouro. Devido a esta versatilidade, o toner pode servir como máscara para corrosão química do vidro (usando ácido fluorídrico), para deposição metálica via sputtering ou ainda para a definição de eletrodos em superfícies condutoras (como cobre e Au). Além destes exemplos, o uso de toner pigmentado também será abordado como plataforma analítica de alta eficiência de separação, bem como novas perspectivas de aplicações analíticas.

Acknowledgements: LNLS, FAPESP and CNPq.

In situ SEM High Temperature Deformation Experiments to Quantification of Susceptibility and Grain Boundary Sliding in Ductility Dip Cracking of Ni-Base Alloys

Torres, E. A.¹ and Ramirez, A.J.¹

Laboratório Nacional de Luz Síncrotron - Campinas SP Brazil

The phase transformation and cracking study has been growing due to a better understanding and identification of different specific characteristic of phenomenon. One important cause of this growing is the development of new tests and the evolution of characterization techniques, especially the evolution in electron microscopy. Nowadays the advent of in situ test gives new impulse allowing direct observation of phenomena live, at submicron and even atomic scale. Develop and implement of these kinds of experiments to entail overcoming many changes related whit the characteristics of instruments and intrinsic of phenomenon. A novel in situ high temperature-strain test into a Scanning Electron Microscopy (SEM) was developed to observations of phenomena with submicron resolution. This setup has been used to study the cracking phenomenon knowing as Ductility-Dip Cracking (DDC), and the Grain Boundary Sliding as possible mechanism of lost of ductility at high temperature. The materials used for this evaluation was the nickel base alloys AWS A5.14 ERNiCrFe-7 and ERNiCr-3 which were evaluated between 700 and 1000 C. The DDC susceptibility (threshold strain - ϵ_{min}) for both alloys was quantified and compare with another referenced results to verify the fact that the observe phenomena correspond to DDC. The ϵ_{min} of ERNiCrFe-7 and ERNiCr-3 alloys was 7.5 % and 16.5 % respectively, confirming the better resistance of ERNiCr-3 to DDC. Furthermore, two separated components of grain boundary sliding: pure sliding (Sp) and deformation sliding (Sd), were identified and quantified. A direct and quantitative link between GB tortuosity, GBS, and DDC resistance has been established for the ERNiCrFe-7 and ERNiCr-3 alloys.

Acknowledgements:

Paper based microfluidic devices for low-cost diagnostics. Bioassays and fundamental issues

Carrilho, E.¹

Universidade de São Paulo - São Carlos - São Carlos SP Brazil

Paper based assays has the potential for being the platform of choice for applications on the field, point of care, and emergency responses because of simplicity, low cost, and flexibility of assays. Hydrophilic paper patterned with hydrophobic polymers, such as photoresists and wax, allow conduction of fluids within channels towards reaction and detection zones. The portability of such systems is compatible with detection schemes such as electrochemistry and reflectance.

Acknowledgements: This work has been funded by FAPESP

**Propriedades Estruturais, Eletrônicas e
Magnéticas de Sólidos**

Fabrication and Testing of RF-MEMS Switches Using PCB Techniques

Silva, M. W. B.¹ and Kretly, L. C.¹

Universidade Estadual de Campinas - Campinas SP Brazil

In this paper some design considerations and process development for fabricating RF MEMS switches on microwave laminate printed circuit boards (PCBs) are presented. PCB MEMS is a new technology, in which RF MEMS devices can be fabricated on any PCB substrate, and they can be monolithically integrated with other elements on the same substrate offering adaptability and reconfigurability features to the communication systems. This work describes an important technique to improve manufacturing for fabrication of RF-MEMS switches on PCB. The integrated process uses metal as part of the sacrificial layer and the isotropic profile (undercut) of the wet etching to help on the bridge release. The mechanical characteristic and theory of operation of capacitive membrane switches is detailed. Pull-in voltage is in the range of 30-40 V. In the OFF state (up-position), the insertion loss is less than 0.3-0.4 dB up to 6 GHz. In ON state (down-position), the isolation value is about 16 dB at 6 GHz and increases to 34 dB at 18 GHz.

Acknowledgements: This work was partially sponsored by CNPq and Brazilian Synchrotron Light Laboratory - LNLS (Microfabrication Laboratory - LMF).

EXAFS and XANES of Ca₂MnReO₆ under pressure up to 1.2 GPa

Orlando, M. T. D.¹, J.L.Passamai Jr¹, Depianti, J. B.¹, Souza, D. O.¹, Rodrigues, V. A.¹, Corrêa, H. P. S.², Rossi, J. L.³, Martinez, L. G.³, and Melo, F. C. L.⁴

¹ Universidade Federal do Espírito Santo - Vitória ES Brazil

² Universidade Federal do Mato Grosso do Sul - Campo Grande MS Brazil

³ Instituto de Pesquisas Energéticas e Nucleares - São Paulo SP Brazil

⁴ Centro Técnico Aeroespacial - São José dos Campos SP Brazil

EXAFS measurements at ambient pressure were investigated in order to determine the ReO₆ and MnO₆ octahedral coordination in the Ca₂MnReO₆ double perovskite. The valence of Mn and Re was determined taken into account the MnO, MnO₂, ReO₂ and ReO₃ calibrators. EXAFS pattern behavior of ReO₆ and MnO₆ octahedral was also investigated under hydrostatic pressure up to 1.2 GPa. A CuBe pressure cell with B₄C anvils was used to applied pressure in situ. Our conclusions are that the both octahedral present a tilt under pressure without change its Re-O and Mn-O coordination distances.

Acknowledgements: We thanks to LNLS - Campinas - Barsil, CNPq, CAPES, Cia Vale do Rio Doce, CST- AcerlorMittal.

Properties of nanostructured Pd/gadolinia-doped ceria nanotubes: XPD, XANES and HRTEM investigation

Muñoz, F.F.¹, Acuña, L. M.¹, Cabezas, M.D.¹, Baker, R.T.², and Fuentes, R. O.¹

¹ Consejo Nacional de Investigaciones Científicas y Técnicas - Buenos Aires Argentina

² University of St Andrews - St Andrews UK United Kingdom

Ceria (CeO₂) and rare earth-doped ceria powders have a number of important applications especially in catalysts and solid oxide fuel cells (SOFC). In the case of gadolinia-doped ceria (GDC) compounds, the ionic conductivity of this solid solution is one of the highest among this class of solid electrolytes. For this reason, it is one of the ceria-based materials proposed for intermediate temperature application of SOFCs. However, the creation of both ionic and electronic charge carriers at low O₂ partial pressures gives rise to mixed conducting behaviour. In the last years, several studies on the use of GDC as anode material and as a catalyst support have been reported. For the latter application, it is necessary to obtain materials with large specific surface area (SSA) and high porosity. Previously, we reported on the synthesis of ceria-based nanotubes with large specific surface areas (100 m².g⁻¹) as potential candidates for catalytic applications, particularly as catalysts metal support. The addition of low levels of noble metals alters the redox properties and hydrocarbon oxidation activity of ceria-based materials. Pd-based catalysts are active for NO reduction and CO and hydrocarbon oxidation reactions.

In this work, 1 wt.% Pd/Gd_{0.1}Ce_{0.9}O_{1.95} (GDC) nanotubes were synthesized, using a commercial polycarbonate membrane (pore size 800 nm) as a template. The resulting Pd/GDC nanotubes were characterized by employing synchrotron X-ray diffraction (SR-XRD), X-ray absorption near-edge spectroscopy (XANES) and scanning and high resolution transmission electron microscopy (SEM and HRTEM). A qualitative analysis of the XRD data indicated that all samples exhibited a cubic phase (fluorite type crystal structure with space group Fm3m). SEM observations confirmed the tubular shape and high nanotube yield. The nanotube walls were composed of nanoparticles, with a homogeneous distribution of Pd nanoparticles. XANES results indicate that the extent of reduction of these materials is small and that the Ce⁴⁺ state is highly predominant.

Acknowledgements: This work has been supported by the Brazilian Synchrotron Light Laboratory (LNLS) under proposals D10B-XPD-8572 and D04B-XAFS1-8175; Agencia Nacional de Promoción Científica y Tecnológica (Argentina, PICT No. 38309); PIDDEF No. 0022/08/CITEDEF and the Latin-american Centre of Physics (CLAF). The TEM and SEM were performed at the Electron Microscopy Facility, University of St Andrews and at the CHIPS Facility, University of Dundee, respectively.

Pressure Effect on Structure of Cardanol/Furfural/PAni Blends A Synchrotron XRD Study

Souza Jr, F. G.¹, Orlando, M. T. D.², Michel, R. C.¹, Pinto, J.C.¹, Cosme, T. A.¹, and Oliveira, G. E.²

¹ Universidade Federal do Rio de Janeiro - Rio de Janeiro RJ Brazil

² Universidade Federal do Espírito Santo - Vitória ES Brazil

Pressure sensitive green polymers able to present reasonable electrical conducting allied with thermosetting behavior and softness are, usually, hard to develop. Aiming that, a cardanol phenolic resin, which possesses C15 dangling chains along polymeric backbone, was prepared and, before completely cured, blended with polyaniline. Samples were characterized through X-ray scattering (XRD) under hydrostatic pressure using the XPD beamline of the Brazilian Synchrotron Light Laboratory [1] (wavelength equal to 1.24252(3)). The samples were loaded into a CuBe pressure cell, which was kept at an incident θ -angle of 8° , and data were recorded at room temperature for 40 s at each step of 0.007° from 5° to 30° (2θ). Among tested materials, samples containing 25 wt% of PAni were selected for a more detailed analytical study. In these samples, the crystalline distance between (0 1 0) planes, showed no changes with pressure increments, possibly due to the compact assembly of the intermolecular rings that are occupying the same unit cell face. The distance of ~ 5.3 between adjacent (0 1 0) faces is very similar to the size of these rings, 5 to 6 . Calculated data indicate that the distance between adjacent (0 0 1) planes increases and that the distance between (1 0 0) planes decreases when samples containing 25 wt% of PAni are exposed to pressure increments. The decrease of the crystalline distance between (1 0 0) planes with pressure increment can be related to the increase of the crystalline distance between (0 0 1) planes, as both effects are probably caused by the reduction of entropy of the polymer chains. Therefore, it was shown for the first time through DRX analyses under pressure that PAni chains are considerably disturbed by compressive stresses.

Reference 1. Giles, C. et al, J. Synchrotron Rad. 2003 10, 430-434.

Acknowledgements: The authors thank CNPq - Conselho Nacional de Desenvolvimento Científico e Tecnológico and FAPERJ - Fundação Carlos Chagas Filho de Amparo à Pesquisa do Estado do Rio de Janeiro - for financial support and scholarships. The authors also thank LNLS for technical and financial support on XRD (LNLS, Brazil - D10B-XPD 6651/07 and 7085/07) experiments.

The local structure of TM-doped (TM= Fe, Co and Mn) magnetic semiconductor studied by XAS

Meneses, C. T.¹, Lima, R. J. S.¹, and Duque J.G.S.¹

Universidade Federal de Sergipe - São Cristóvão SE Brazil

In the last years, studies involving in situ X-ray using synchrotron radiations have increased tremendously and proved to be milestone to study time resolved crystallization and structural changes in several materials [1]. Certainly, the interest in these studies is important in order to control exactly over the particle size and the various synthesis conditions. The good control of these parameters is one of the main reasons for that these materials can be used for futures applications. In this work we concentrate to study the kinetic formation of CuO and ZnO nanoparticles both doped with metal transitions for different concentrations using the techniques X-ray absorption near edge spectroscopy (XANES). For such studies were used precursor materials of the nanoparticles obtained by co-precipitation method. In this sense the samples were submitted to a thermal treatment from room temperature up to $500^{\circ}C$, in atmosphere air at $5^{\circ}C.min^{-1}$ rates. Results XANES for Zn and Cu K-edge no difference significant is observed in the spectra indicating TM ions substitute for Cu, Zn-sites in the semiconductor host without changing. Therefore, the results in the doping K-edge the spectra are changed continuing with increasing temperature remaining unchanged for temperature higher than $400^{\circ}C$. The results also for Fe-doped samples is visible a change continuous of oxidation state of the Fe following structures to final stage one of mixed valence (LNLS-CNPq).

Referências

1. Danzig, A., Mattern, N. and Doyle, S. Nucl. Instrum. Methods Phys. Res. B, 97 (1995) 465.

Acknowledgements: This work was supported by CNPq and LNLS.

Morphology of PANi / γ -Fe₂O₃ hybrids - A SAXS study

Marins, J. A.¹, Souza Jr, F. G.¹, Pinto, J.C.¹, Oliveira, G. E.², Manzini R., C. H.³, and Lima, L. M. T. R.¹

¹ Universidade Federal do Rio de Janeiro - Rio de Janeiro RJ Brazil

² Universidade Federal do Espírito Santo - Vitória ES Brazil

³ Universidade Estadual Norte Fluminense - Campos dos Goytacazes RJ Brazil

Hybrids material of maghemite (γ -Fe₂O₃) and polyaniline doped with dodecylbenzenesulfonic acid (DBSA) were prepared by in situ polymerization in aqueous media. These hybrid materials, such as pure maghemite, possess nanometric dimensions having also good electrical and magnetic properties. Trying to improve the size characterization of the nanoparticles, SAXS measurements were performed at the beam line of the Brazilian Synchrotron Light Laboratory. These measurements allowed the calculation of the radius of gyration (R_g), evaluated in real space using the pair distribution function, P(r). Each one of the computed models presented correlation higher than 0.9993. The radius of gyration of the pure maghemite is equal to 9.6(3) nm. On the other hand, R_g of the hybrids containing 8wt% and 25wt% of maghemite are equal to 25.5(5) nm and 26.8(1) nm, respectively. Therefore, these hybrid materials still present nanometric dimensions, associated with a reasonable electric conductivity, which is around 260 times larger than pure maghemite, keeping 60% of the original magnetic force.

Reference: Fernando Gomes de Souza Jr., Jéssica Alves Marins, José Carlos Pinto, Geiza Esperandio de Oliveira, Cezar Manzini Rodrigues, and Luis Mauricio T. R. Lima; Magnetic field sensor based on a maghemite / polyaniline hybrid material; *Macromol. Mater. Eng.*, Submetido

Acknowledgements: Authors tank CAPES, CNPq and FAPERJ for financial support and scholarships. Authors also thank LNLS for support on D02A -SAXS2 7086/08 and 8507/09 experiments.

High Pressure Local Probe of Structural Phase Transitions in $R\text{NiO}_3$ ($R = \text{Nd}, \text{Pr}$)

Nestor E. Massa¹, Garcia, F.², and Alonso, J.A.³

¹ Universidad Nacional de La Plata - La Plata B.A. Argentina

² Laboratório Nacional de Luz Síncrotron - Campinas SP Brazil

³ Consejo Superior de Investigaciones Científicas - Madrid Spain

Most perovskites at ambient pressure have lattice distortions departing from the ideal cubic structure that implies an octahedral orientation proclivity, by tilting and rotation, toward lower symmetry space groups. In this report we comment on our very preliminary results on reverting this trend by applying high enough quasi-hydrostatic pressure to orthorhombic NdNiO_3 and PrNiO_3 perovskites. These compounds undergo a metal-insulator transition with decreasing temperature at $T_{MI} \sim 200$ K and $T_{MI} \sim 140$ K, respectively. It is known that applied pressure induces a downshift of the T_{MI} temperature.[1] In our studies, at the DXAS beamline, we monitored the Ni K-edge aiming to observe changes in the pre-edge structure and Ni oxygen nearest neighbors that might denote changes in the electronic or lattice configurations in the room temperature metallic phase. Our preliminary results on applying quasi-hydrostatic pressure up to about 10 GPa using a conventional diamond anvil cell at room temperature yield a remarkable enhancement and increase in the pre-edge structure in the Ni K-edge as both compounds change toward a rhombohedral phase.[2] We attribute this to the likelihood of having pressure altered Ni pre-edge features associated with transitions from the Ni 1s to 3d states mixed with the oxygen 2p orbital in an increased hybridization pattern. Simultaneously, EXAFS for nearest neighbors show much weaker modifications attributed to small changes in oxygen positions around the nickel ion in the octahedra.

¹X. Obradors, L. M. Paulius, M. B. Maple, J. B. Torrance, A. I. Nazzari, J. Fontcuberta and X. Granados, Phys. Rev. B **47**, R12353 (1993).

²M. Amboage 2003 PhD Thesis, University of the Basque Country (UPV/EHU), Bilbao, Spain.

Acknowledgements: This work was supported by LNLS

Lattice distortions produced in the X-ray Multiple Diffraction peak under electric field.

Almeida, J. M. A.¹, dos Santos, A. O.², de Menezes, A. S.³, Cardoso, L.P.³, and Sasaki, J.M.⁴

¹ Universidade Federal de Sergipe - São Cristóvão SE Brazil

² Universidade Federal do Maranhão - Imperatriz MA Brazil

³ Universidade Estadual de Campinas - Campinas SP Brazil

⁴ Universidade Federal do Ceará - Fortaleza CE Brazil

L-arginine hydrochloride monohydrate is one of those nonlinear optical materials that have been extensively discussed in terms of its physical properties, for instance, piezoelectric. The crystal of L-AHCl.H₂O belongs to semi-organic crystals group with non-linear optical properties [1, 2] in which the L-arginine molecule is arranged in the form of a dipolar ion (zwitterion). L-AHCl H₂O crystallizes in a monoclinic structure with P2₁ space group. In its structure ($a = 11.044$, $b = 8.481$, $c = 11.214$ and $\beta = 91.31^\circ$) [3] has two molecules per unit cell and the crystal polar axis is oriented along the crystallographic b-axis. The L-arginine.HCl was prepared to carry out the crystalline perfection on the sample surface as a function of electric field using the X-ray Multiple Diffraction (XRMD). A special 3-beams case, where the secondary beam propagation along to sample surface called Bragg surface diffraction (BSD), has been investigated in the L-arginine.HCl samples with electric field of 4000V/cm. The BSD peak profile is very sensitive to the diffraction regime (dynamical or kinematical) and provides information regarding crystalline perfection to the sample surface. Results from reciprocal space mapping [4] are also reported.

[1] Mukerji S and Kar T 1998 Materials Chemistry and Physics 57 72 [2] Petrosyan A M, Sukiasyan R P, Karapetyan H A, Terzyan S S and Feigelson R S 2000 J. Crystal Growth 213 103-111 [3] Dow, J. and Jesen, L. H., Acta Cryst. 1970, B26, 1662 [4] L. H. Avanci and S. L. Morelhão, Acta Cryst. (2000). A56, 507-508

Acknowledgements: This work was supported by LNLS, CNPq and FAPESP

Structural Properties of Pd/Ce-Zr Mixed Oxide Nanotubes

Acuña, L. M.¹, Muñoz, F.F.¹, Cabezas, M.D.¹, Fantini, M. C. A.², Lamas, D. G.¹, Baker, R.T.³, and Fuentes, R. O.¹

¹ Consejo Nacional de Investigaciones Científicas y Técnicas - Buenos Aires Argentina

² Universidade de São Paulo - São Paulo - São Paulo SP Brazil

³ University of St Andrews - St Andrews UK United Kingdom

ZrO₂-CeO₂ substitutional solid solutions are extensively used as redox or oxygen storage promoters in three-way catalysts, which are applied in controlling the emissions of NO_x, CO and hydrocarbons from automotive exhausts. The properties of zirconia-ceria mixed oxides are strongly related to their crystal structure and local order. Several investigators have reported the noble metal-ceria interaction and its effects on catalytic activities. Particularly, Pd-based catalysts are active for NO reduction and CO and hydrocarbon oxidation reactions. The presence of Pd in the lattice of ceria-based catalysts for methane combustion has shown the beneficial catalytic effect.

In this work, 1 wt % Pd/ZrO₂-CeO₂ mixed oxide nanotubes with 90%mol CeO₂ were synthesized following a very simple, high yield procedure and their properties were characterized by synchrotron radiation XPD, X-ray absorption (XANES and EXAFS) and by high resolution electron microscopy (HRTEM). The Pd/Ce-based nanotubes exhibited the cubic phase (Fm3m space group). The nanotube walls were composed of nanoparticles with an average crystallite size about 7 nm and the nanotubes exhibited large specific surface area (100 m²g⁻¹). The SEM and TEM results showed that individual nanotubes were composed of a curved sheet of these nanoparticles. Elemental analysis showed that Ce:Zr:Pd ratios appeared to be constant across space, suggesting compositional homogeneity in the samples. XANES results indicate that the extent of reduction of these materials is small and that the Ce⁴⁺ state is in the majority.

Acknowledgements: This work has been supported by the Brazilian Synchrotron Light Laboratory (LNLS) under proposals D10B-XPD-8572 and D04B-XAFS1-8175; Agencia Nacional de Promoción Científica y Tecnológica (Argentina, PICT No. 38309); PIDDEF No. 0022/08/CITEDEF and the Latin-american Centre of Physics (CLAF). The TEM and SEM were performed at the Electron Microscopy Facility, University of St Andrews and at the CHIPS Facility, University of Dundee, respectively.

EXAFS and XRD study of $\text{Pb}_{1-x}\text{R}_x\text{Zr}_{0.40}\text{Ti}_{0.60}\text{O}_3$ ($\text{R} = \text{La}, \text{Ba}$) ferroelectric ceramic materials

Mesquita, A.¹, Michalowicz, A.², and Mastelaro, V.R.¹

¹ Universidade de São Paulo - São Carlos - São Carlos SP Brazil

² Université Paris XII - Val de Marne - Creteil cedex France

Solid solutions of lead zirconate and lead titanate ($\text{PbZr}_{1-y}\text{Ti}_y\text{O}_3$ or PZT) represent an important technological family of ferroelectrics and antiferroelectrics whose properties and phase transitions have been extensively studied. These materials have been used as capacitors, actuators, transducers and electro-optic devices. At high temperature, these materials present a cubic perovskite (ABO_3) structure and on cooling below the maximum of the dielectric permittivity curve, they undergo a phase transition to a lower symmetry phase. It is well known that the substitution of Pb^{2+} by La^{3+} or Ba^{2+} atoms lead to a significant variation on electrical and structural properties of the $\text{PbZr}_{0.40}\text{Ti}_{0.60}\text{O}_3$ ceramic system. For samples containing a large amount of La^{3+} or Ba^{2+} , a transition from a normal to a relaxor ferroelectric behavior has been observed. From the structural point of view, a transition from a low to a high symmetric phase has been observed. In order to better understand the effect of substitution of Pb^{2+} by La^{3+} or Ba^{2+} atoms at the short and long-range order structure of $\text{Pb}_{1-x}\text{La}_x\text{Zr}_{0.40}\text{Ti}_{0.60}\text{O}_3$ (PLZT) and ($\text{Pb}_{1-x}\text{Ba}_x\text{Zr}_{0.40}\text{Ti}_{0.60}\text{O}_3$) PBZT ceramic systems, X-ray absorption spectra at the Ti K-edge and Pb L_{III}-edge and X-ray diffraction patterns were respectively measured. PLZT compositions with x varying from 0.0 to 0.21 and PBZT compositions with x varying from 0.10 to 0.50 were prepared by using a solid state reaction route. Ti K-edge and Pb L_{III}-edge X-ray absorption spectra were collected at the LNLS (National Synchrotron Light Laboratory) facility using the D04B-XAS2 beam line. X-ray powder diffraction measurements were carried out at different temperatures at the D10B-XPD LNLS beam line. The analysis of the EXAFS spectra collected at the Pb L_{III}-edge indicates that the local structure around Pb atoms is affected by the introduction of La or Ba atoms in the structure. Our X-ray powder diffraction results collected at different temperatures clearly indicate that, although the samples with relatively large lanthanum or barium content presented a relaxor behavior and frequency dispersion below T_{max} , a spontaneous phase transition from relaxor to normal behavior was identified by a structural phase transition. A relationship between the structural results and the dielectric properties will be discussed.

Acknowledgements: This work was supported by FAPESP and Capes.

EXAFS characterization of the local disorder in Y₂O₃ nanoparticles produced via a coconut water-assisted sol-gel method

Macedo, Z.S.¹, Valerio, M.E.G.¹, and Gomes, M.A.¹

Universidade Federal de Sergipe - São Cristóvão SE Brazil

The aim of the present work is the production of rare-earth doped Y₂O₃ nanoparticles and the study of the correlation between synthesis procedures, structural characteristics and optical properties of this material. When associated with polymers and functional molecules, fluorescent nanoparticles can be used as probes in biological imaging systems. Yttria was prepared using a coconut water-based sol-gel method. During the production process, the pH of the start solution was adjusted by adding ammonia hydroxide. This adjustment controls the agglomeration degree and, consequently, the size of the particles. The crystallization of the material was investigated by powder X-ray diffraction technique performed in situ during the calcinations. It was observed a strong dependence between the pH of the sample and the temperature of crystallization of the cubic equilibrium phase Ia-3. For samples prepared at pH 9 the crystallization temperature was 350 C, which is much lower than the temperature 850 C necessary to crystallize the samples without pH control. The particle size of the samples produced at different pH values ranged from 50nm to 7nm. From the EXAFS measurements of these samples it was possible to determine that particles of 15 nm present the same local order than bulk Y₂O₃. For the samples with particles size smaller than 10 nm, a more disordered crystal structure, accompanied by a blue shift in the optical absorption spectra, was observed. XEOL (X-ray Excited Optical Luminescence) spectra of Nd and Eu doped samples were also measured, with incident X-ray energy at the absorption edges of dopants. These results are being analyzed at the current stage of the work.

Acknowledgements: This work was supported by CAPES, CNPq and FAPITEC/SE.

Pressure study of Ca₂CrReO₆ by EXAFS and XANES up to 1.2 GPa

Souza, D. O.¹ and Orlando, M. T. D.¹

Universidade Federal do Espírito Santo - Vitória ES Brazil

EXAFS measurements at ambient pressure were investigated in order to determine the ReO₆ octahedral coordination in the Ca₂CrReO₆ double perovskite. The valence of Re was determined taken into account the ReO₂ and ReO₃ calibrators. EXAFS pattern behavior of ReO₆ octahedral was also investigated under hydrostatic pressure up to 1.2 GPa. A CuBe pressure cell with B₄C anvils was used to applied pressure in situ. Our conclusions are that the octahedral present a tilt under pressure without change its Re-O and coordination distances.

Acknowledgements:

Structural study of $\text{Ca}_2\text{CrReO}_6$

Corrêa, H. P. S.¹, Cavalcante, I. P.¹, Bozano, D. F.¹, Orlando, M. T. D.², Souza, D.O.², Martinez, L. G.³, and Rossi, J. L.³

¹ Universidade Federal do Mato Grosso do Sul - Campo Grande MS Brazil

² Universidade Federal do Espírito Santo - Vitória ES Brazil

³ Instituto de Pesquisas Energéticas e Nucleares - São Paulo SP Brazil

A sample of $\text{Ca}_2\text{CrReO}_6$ double perovskite was prepared in a polycrystalline form by using the encapsulated quartz tube method. The morphology and chemical composition of the sample was investigated by scanning electron microscopy (SEM) and EDS. The crystal structure parameters were determined by analysis of synchrotron high-resolution X-ray powder diffraction pattern and the crystal parameters were compared with results from Bond-Valence Method, predicted by the SPuDS program. The analysis indicates that the sample presents an ideal single-phase compound and a monoclinic crystal structure (space group $P2_1/n$) with $a = 5.44445(2)$; $b = 5.63957(3)$; $c = 7.77524(3)$; and $\beta = 90.18(1)^\circ$.

Acknowledgements: We thank to LNLS - Campinas - Brasil, CNPq, CAPES and Functect/MS for financial support.

Development of Conducting Polyaniline/Poly(lactic acid) Nanofibers by Electrospinning

Picciani, P.H.S¹, Soares, B.G.¹, Souza Jr, F. G.¹, MEDEIROS, E. S.², and MATTOSO, Luiz Henrique Capparelli³

¹ Universidade Federal do Rio de Janeiro - Rio de Janeiro RJ Brazil

² Universidade Federal da Paraíba - João Pessoa PB Brazil

³ Empresa Brasileira de Pesquisas Agropecuárias - São Carlos SP Brazil

Nanofibers of conducting polymers and their blends with conventional insulating polymers have received great attention over the last decade because of their unique and useful properties, which are important for several potential applications such as electronic devices in optics and electronic and biomedical materials, protective clothing, filtration media, charge storage devices, and sensors and actuators. The electrostatic spinning process has emerged as an efficient and promising technique for the preparation of fibers with diameters in the submicrometer to micrometer range because of its simplicity and its ability to scale up into a continuous process. In this work ultrafine blended fibers of polyaniline doped with p-toluene sulfonic acid and poly(L-lactic acid) were prepared by electrospinning. The presence of polyaniline resulted in fibers with diameters as thin as 100 nm and a significant reduction of bead formation. These fibers were visually homogeneous, indicating a good interaction between the components of the polyaniline/poly(L-lactic acid) blend. The high interaction between the components and the rapid evaporation of the solvent during electrospinning resulted in nanofibers with a lower degree of crystallinity in comparison with cast films. It was not possible to evaluate the nanostructure of the electrospun polymer mats only with scanning electron microscopy (SEM) and wide angle x-ray scattering (WAXS). In this way small angle x-ray scattering of the electrospun polymer fiber of PLA/PAni can be used to characterize the nanometric organization of the fibers. From SAXS experiments it was possible to observe the presence of hierarchical structures and phase segregation on PLA/PAni in cast films. The same was not observed in PLA/PAni electrospun fibers. A Porods scattering regime was found in all fiber mats indicating that these fibers have smooth surface and the absence of others scattering patterns showed that there are no nanostructures inside electrospun fibers. This indicates that the electrospinning process is a efficient method in obtaining homogeneously polymeric blended fibers down to the nanometer scale.

Acknowledgements: This work has been sponsored by CNPq, CAPES and FAPERJ. The authors would like to thank the LNLS for the technical support on the SAXS measurements.

Structural and dielectric characterization of $Ba_{0,9}Sr_{0,1}Zr_xTi_{1-x}O_3$ system

Favarim, H.R.¹, Mastelaro, V.R.¹, Michalowicz, A.², Doriguetto, A.C.³, and Neves P.P.³

¹ Universidade de São Paulo - São Carlos - São Carlos SP Brazil

² Université Paris XII - Val de Marne - Creteil cedex France

³ Universidade Federal de Alfenas - Alfenas MG Brazil

Ferroelectric materials have been applied to a large field of applications due its excellent dielectric, piezoelectric and ferroelectric properties. Lead-free ferroelectric materials have attracted the attention of different researches due to the protection environment restriction and thus, many investigations were focused on BaTiO₃-based materials. The substitution of barium by strontium and zirconium atoms in the BaTiO₃ structure ($Ba_{0,9}Sr_{0,1}Ti_{1-0,9x}Zr_{0,9x}O_3$, BSZT) lead to significant changes in the electrical and structural properties which can varies from a normal to a relaxor ferroelectric behavior depending of the Zr/Ti ratio as well as the amount of strontium. In this work, the effect of composition variation on the long-range order structural properties of the $Ba_{0,9}Sr_{0,1}Ti_{1-0,9x}Zr_{0,9x}O_3$ ($0 \leq x \leq 30$) system was studied at the D10B- XPD LNLS beam line. The ceramics were prepared by a sol-gel method and the dielectric permittivity and long range order structures were characterized. Dielectric measurements show a typical relaxor behavior for samples with higher incorporation of zirconium and that the degree of diffuseness became more pronounced as the amount of Zr increases. HRXRD results showed changes in the structural symmetry of samples with a lower amount of zirconium and no phase transition with the temperature was observed for the relaxor samples.

Acknowledgements: This work was supported by CNPq and FAPESP. This research was partially carried out at the Brazilian Synchrotron Light Laboratory (LNLS). Project D10B-XPD 8101

X-ray absorption spectroscopy characterization of nanocrystalline $\text{SrTi}_{1-x}\text{Fe}_x\text{O}_3$

da Silva, L. F.¹, M.I.B.Bernardi¹, and Mastelaro, V.R.¹

Universidade de São Paulo - São Carlos - São Carlos SP Brazil

Perovskite based compounds are promising materials in current science and technology because its structure are very versatile having different and useful technological applications. Among the several perovskite based compounds, more recently, the $\text{SrTi}_{1-x}\text{Fe}_x\text{O}_3$ (STF) solid solution has attracted the attention of many researches due to its potential application as oxygen gas sensor for automotive emission control. The addition of Fe_2O_3 in SrTiO_3 network implies in the substitution of some Ti^{4+} by Fe^{3+} ions which may create different types of defects due the difference in the oxidation state. When Fe^{3+} ion occupies the Ti^{4+} octahedral site, mobile oxygen vacancies are formed in order to balance the electric charge and thus, the introduction of a large amount of iron creates a relatively large concentration of defects. Recently, our group synthesized the STF compound from a soft chemical process. This chemical synthesis based on the polymeric precursor method allows a low temperature (about 700°C) crystallization and provides a high degree of control on the composition and on the particle size from some nanometers to micrometric size [1]. In this work, we will present the results concerning the short-range order study of nanostructured STF particles ($x= 0.0$ up to 1.0) obtained by using the polymeric precursors method. The Ti and Fe K-edge X-ray absorption spectra were collected at the XAFS1 and XAFS2 LNLS beam lines in order to investigate the effect of the substitution of Ti by Fe atoms on the short range order as well as on the chemical state of titanium and iron. A significative variation was observed on the chemical state of iron atoms.

[1] L. F. da Silva, M. I. B. Bernardi, V. R. Mastelaro, et al. Thin Solid Films. (2009) submitted.

Acknowledgements: This work was supported by Brazilian financing agencies FAPESP and CNPq

Probing vacancies in CeO₂ thin films through Ce valence states: a XANES and XPS investigation

I. L. Graff¹, V. Fernandes¹, J. Varalda¹, P. F. P. Fichtner², AMARAL L.², and Mosca, D. H.¹

¹ Universidade Federal do Paraná - Curitiba PR Brazil

² Universidade Federal do Rio Grande do Sul - Porto Alegre RS Brazil

This work reports on the effects of ion irradiation on electrodeposited CeO₂ thin films. CeO₂ films constitute a new class of ferromagnetic materials that present room-temperature ferromagnetism even without ferromagnetic ion dopants. Such films can be grown on semiconductor substrates and therefore rise as an alternative for ferromagnetic-semiconductor devices. It has been shown by our group that the origin of the ferromagnetic behavior is related to the oxygen as well as cerium vacancies present in the films [1, 2].

In order to investigate the relationship between vacancies and the magnetic behavior the films were submitted to ion irradiation with Ne ions. Ion irradiation is one of the most effective tools to generate a great quantity of defects in solid materials, being the quantity of defects controllable through the variation of the ion fluence. Two energies were used, 30 and 350 keV, with fluences varying from 1×10^{14} to 1×10^{16} ions/cm². The irradiation experiments were performed at room-temperature and 77 K under high-vacuum conditions.

The quantity of defects (O vacancies mainly) was obtained through the relative concentration of Ce³⁺ replacing Ce⁴⁺ ions by two complementary techniques; X-ray absorption near-edge structure spectroscopy (XANES) and X-ray photoelectron spectroscopy (XPS). The Ce³⁺ concentration determined by XPS corresponds to the surface of the films (1.0–3.0 nm) whereas XANES probes the whole film volume. The results from both techniques are in good agreement with previous works, corroborating theoretical calculations. The irradiation enhances O vacancies resulting in an increase of Ce³⁺ concentration, which in turn reflects on the increase of saturation magnetization.

[1] V. Fernandes, J. J. Klein, E. Silveira, E. Ribeiro, A. J. A. de Oliveira, J. Varalda, N. Mattoso, W. H. Schreiner, D. H. Mosca, Phys. Rev. B **75**, 121304(R) (2007).

[2] V. Fernandes, R. J. O. Mossaneck, P. Schio, J. J. Klein, A. J. A. de Oliveira, W. A. Ortiz, N. Mattoso, J. Varalda, W. H. Schreiner, M. Abbate, D. H. Mosca, Phys. Rev. B **80**(3), 035202 (2009).

Acknowledgements:

Transições martensíticas em ligas de Heusler do Tipo $Ni_2Mn_{1.44}Sn_{0.56}$

Alves, A.L¹, Nascimento, V. P.², Passamani, E. C.¹, Proveti, J. R.², and A. Y. Takeuchi¹

¹ Universidade Federal do Espírito Santo - Vitória ES Brazil

² Universidade Federal do Espírito Santo - São Mateus ES Brazil

O efeito magnetocalórico (EMC) é a variação de temperatura de um material magnético sujeito a uma variação de um campo magnético aplicado, num processo adiabático. Este é um processo mais econômico e limpo de transformação de energia elétrica em térmica, para uso em refrigeração doméstica e industrial, apresentando ganhos para o meio ambiente. O EMC é substancialmente amplificado quando combinamos transições de fases magnéticas com estruturais, como no caso dos intermetálicos de Heusler $Ni_2Mn_{1.44}Sn_{0.56}$ que apresentam um EMC inverso gigante em temperaturas próximas da ambiente. A aplicação da moagem de altas energias sobre esses compostos aniquilou a transição de fase martensítica. Uma análise do espectro de EXAFS da liga moída foi feita para verificar se a mecanossíntese gerou uma desordem na coordenação química da vizinhança dos átomos de Ni e de Mn, com uma possível inclusão de defeitos.

Acknowledgements: Agradecemos ao LNLS e ao CNPq pelo apoio financeiro.

X-ray powder diffraction study of fine-grained $\text{ZrO}_2\text{-Sc}_2\text{O}_3$ dense ceramics

Abdala, P. M.¹, Craievich AF², Fantini, M. C. A.², and Lamas, D. G.¹

¹ Consejo Nacional de Investigaciones Científicas y Técnicas - Buenos Aires Argentina

² Universidade de São Paulo - São Paulo - São Paulo SP Brazil

$\text{ZrO}_2\text{-Sc}_2\text{O}_3$ exhibits the highest ionic conductivity among ZrO_2 -based material, thus it is considered as a candidate for the electrolyte in intermediate temperature solid oxide fuel cells. The dependence of the ionic conductivity with the crystal structure in addition to its complex phase diagram make fundamental the phase study of this system. The polymorphs observed in these materials have monoclinic, tetragonal, cubic or rhombohedral symmetries. The tetragonal phase in ZrO_2 -based solid solutions is classified into three forms: t, t' and t'', its features are explained elsewhere [1]. The existence of rhombohedral phases, such as β , γ and δ , is a unique feature of $\text{ZrO}_2\text{-Sc}_2\text{O}_3$ and many efforts are focused on avoiding this phases. In previous works performed in $\text{ZrO}_2\text{-Sc}_2\text{O}_3$ nanopowders, carried out at LNLS, we concluded that the cubic or tetragonal structure (t-form) can be retained below a critical crystallite size of about 25nm, avoiding β and γ phases. However, in technological applications of dense ceramics, significant grain growth occurs during sintering at high-temperature (above 1500C). Recently, we achieved submicrometric grain sizes ceramics by low-temperature sintering of nanopowders synthesized by gel-combustion routes. Moreover, the phases of dense ceramics may differ from the powder treated at the same temperature, mainly due to the presence of strains. In this work, we have investigated the crystalline phases in $\text{ZrO}_2\text{-X}$ mol% Sc_2O_3 (X = 8, 9, 10) dense ceramics (above 95% of the theoretical), sintered at different temperatures from 1050 to 1350C. Samples co-doped with Y_2O_3 or CeO_2 have also been analyzed. By studying qualitatively and quantitatively (Rietveld refinements) the whole synchrotron-XPD patterns, we were able to precisely discriminate the phases and their contents in these ceramics. The results indicate that the β phase can be avoided in 9 and 10 mol% Sc_2O_3 ceramics at an optimal sintering temperature, instead a mixture of cubic and tetragonal phases appears. For lower sintering temperatures, the cubic and β phases were observed.

1. M. Yashima et al., Solid State Ionics 86-88 (1996) 1131

Acknowledgements: This work has been supported by the Brazilian Synchrotron Light Laboratory (LNLS, Brazil, proposal D10B-D10B - XPD-8674), scientific collaboration agreement CAPES-MinCyT (Brazil-Argentina), CNPq (Brazil, PROSUL Program), AN-PCyT (Argentina) and CLAF.

EXAFS AND XEOL SIMULTANEOUS MEASUREMENTS OF CdWO₄

Novais, S. M. V.¹, Valerio, M.E.G.¹, and Macedo, Z.S.¹

Universidade Federal de Sergipe - São Cristóvão SE Brazil

Cadmium tungstate (CdWO₄ CWO) is a useful scintillator with wolframite structure that presents high detection efficiency for UV, X- and gamma-rays. In its matrix, there are two different energetically inequivalent oxygen ion sites: type 1 is bound to one W ion and two Cd ions, while type 2 is connected to two W ions and one Cd ion. In this work, EXAFS and XEOL simultaneous measurements of CdWO₄ were performed at L₁ Cd edge (4018 eV) and L₃ W edge (10207 eV). Samples produced from precursors with different purities (3N or 4N) were calcined in open atmosphere furnace and annealed in oxygen or nitrogen atmospheres. The radioluminescent spectra presented a small shoulder at around 450 nm in addition to the intrinsic luminescence in 500 nm that arises due to annihilation of self-trapped exciton (STE) which forms the excited WO₆⁶⁻ complex in CWO. For the XEOL measurements at the W edge, the integrated emission as a function of the excitation energy presented the same oscillations observed in the EXAFS spectra, indicating a strong dependence between the scintillation process and the absorption by W ions in the CdWO₄ matrix.

Acknowledgements: CAPES, CNPq and FAPITEC/SE.

XEOL and EXAFS investigations of the long-lasting phosphor CdSiO₃

Abreu, C. M.¹, Novais, S. M. V.¹, Silva, R.S.¹, Valerio, M.E.G.¹, and Macedo, Z.S.¹

Universidade Federal de Sergipe - São Cristóvão SE Brazil

Cadmium silicate CdSiO₃ is a long lasting luminescent material with potential applications in phosphorescent paints and opto-electronic devices. This material may present crystalline structure monoclinic or triclinic, or a mixture of these two phases. It presents an intrinsic luminescence with long lasting emission (light persistence of about 3 h) in the visible region. In this work, we have studied the properties of CdSiO₃ pure, doped with Mn²⁺, Ni²⁺ and Cr³⁺ and co-doped with (Mn²⁺, Cr³⁺) and (Mn²⁺, Ni³⁺). The powders were synthesized by a conventional solid-state method, using low-purity industrial reagents. The inspection of the crystalline phases during the synthesis was performed by X-ray diffraction measurements (XRD). The optical and structural properties of the synthesized powders were studied via photoluminescence (PL), radioluminescence (RL), thermoluminescence (TL), X-ray Emission Optical Luminescence (XEOL) and X-ray absorption fine structure (EXAFS) techniques. The emission spectra of the pure, doped and co-doped samples presented broad emission bands near 496 nm and 593 nm. Pure samples presented TL glow curves with peaks around 330 K and 390 K and additional peaks arise from the presence of the dopands in the samples. XEOL (X-ray Excited Optical Luminescence) and EXAFS (Extended X-ray Absorption Fine Structure) at the L1 Cd absorption edge, as well as at the K absorption edge of the transition metals (Mn, Ni and Cr). XEOL and EXAFS spectra were measured simultaneously for all the samples and the results are being analyzed at the current stage of the work.

Acknowledgements: CAPES, CNPq and FAPITEC/SE.

In-situ structural characterization of nano-sized scandia-doped zirconia.

Fernández Werner, L.¹, Suescun, L.¹, Abdala, P. M.², Lamas, D. G.², Chen, H.³, and Craievich AF⁴

¹ Universidad de la República - Montevideo Uruguay

² Consejo Nacional de Investigaciones Científicas y Técnicas - Buenos Aires Argentina

³ Brookhaven National Laboratory - Upton NY United States of America

⁴ Universidade de São Paulo - São Paulo - São Paulo SP Brazil

Oxides with fluorite structure doped with trivalent cations such as $Zr_{1-x}M_x^{III}O_{2-x/2}$ and $Ce_{1-x}M_x^{III}O_{2-x/2}$ are currently the most adequate materials for high and intermediate temperature Solid Oxide Fuel Cells (SOFC) electrolytes respectively. Particularly, $ZrO_2 - Sc_2O_3$ electrolytes are widely investigated because they exhibit the highest ionic conductivity among all ZrO_2 -based materials. The main problem of the use of these ceramics is to avoid the presence of the low-conductivity monoclinic and rhombohedral phases. This is generally achieved by adding a second dopant that stabilizes the cubic phase being Y_2O_3 or CeO_2 the most used, but reducing ionic conductivity. $ZrO_2 - Sc_2O_3$ ceramics exhibit different polymorphs depending on the composition and temperature, with monoclinic, tetragonal, cubic or rhombohedral symmetries (for low Sc doping the most important is the β phase). Yashima and coworkers constructed a metastable phase diagram for compositionally homogeneous materials $ZrO_2 - Sc_2O_3$ synthesized at high-temperatures. In ZrO_2 -based systems, the tetragonal phase can exhibit three metastable forms: t, t' and t'' forms. The stable tetragonal form is called the t-form. The t'-form has a wider solubility, but is unstable in comparison with the mixture of the t-form and cubic phase. The t-form has an axial ratio, c/a, of unity with the oxygen atoms displaced along the c axis from their ideal sites of the cubic phase. In recent studies, Abdala et al. showed that the t-form can be retained in nanopowders for Sc_2O_3 contents close to 10 mol% if the crystallite size is smaller than 25-30 nm and proposed a metastable phase diagram for these nanomaterials. In this way, the β -phase can be avoided without the incorporation of additional dopants. In this presentation we will show the latest results obtained from an in-situ characterization of nanosized powders of $ZrO_2 - Sc_2O_3$ (10%) performed at Brookhaven National Laboratory's NSLS (X7B station) to precisely determine phases present at different temperatures and grain sizes in order to avoid the formation of undesired phases upon processing of the material for applications.

Acknowledgements: The authors are indebted with Dr. Jonathan Hanson from X7B station at NSLS-BNL for providing beam time.

Caracterização estrutural da hidroxiapatita usando radiação síncrotron

Lima, T.A.R.M.¹, Valerio, M.E.G.¹, and Sarmento, V.H.V¹

Universidade Federal de Sergipe - São Cristóvão SE Brazil

Dentre os biomateriais, os fosfatos de cálcio são os que apresentam uma crescente utilização no campo da saúde, particularmente a hidroxiapatita (HAP), $\text{Ca}_{10}(\text{PO}_4)_6(\text{OH})_2$. No presente estudo foi investigado a estrutura local dos átomos de Ca, Zn e Cr na matriz cristalina da hidroxiapatita. Os pós de hidroxiapatita com razão Ca/P 1,67 foram produzidos através da reação do $\text{Ca}(\text{NO}_3)_2 \cdot 4\text{H}_2\text{O}$ com $(\text{NH}_4)_2\text{HPO}_4$, utilizando NH_4OH para controle do pH. Para as amostras dopadas com Cr^{3+} e Zn^{2+} adicionou-se à solução de $\text{Ca}(\text{NO}_3)_2 \cdot 4\text{H}_2\text{O}$ uma solução de $\text{Cr}(\text{NO}_3)_3 \cdot 9\text{H}_2\text{O}$ e $\text{Zn}(\text{NO}_3)_2 \cdot 6\text{H}_2\text{O}$ nas concentrações de 0,01 M, 0,05 M e 0,1 M. A caracterização dos pós foi feita através da difratometria de raios-X (XRD), microscopia de transmissão eletrônica (TEM) e técnicas de espectroscopia de absorção de raios-X (XAS). Os resultados de XRD mostram uma diminuição na cristalinidade com o aumento da concentração de íons dopantes Cr^{3+} e Zn^{2+} . As imagens de TEM revelaram mudança no formato e tamanho dos grãos nas amostras dopadas. Dados de XANES, EXAFS e SAXS confirmaram que o tipo e a concentração dos dopantes influencia a valência, grau de desordem estrutural, preferência entre os sítios Ca1 e Ca2 da matriz cristalina e distribuição do tamanho das partículas. Logo, a incorporação de íons influencia tanto aspectos estruturais como a morfologia dos grãos de fosfatos de cálcio.

Acknowledgements: RENAMI/CNPQ, INCT-INAMI/CNPQ, FAPITEC/SE, FINEP

ESTUDO DO EFEITO DA DOPAGEM NAS PROPRIEDADES MAGNÉTICAS E ESTRUTURAIS DO SISTEMA $\text{Cu}_{1-x}\text{TM}_x\text{O}$ (TM=Fe,Ni,Mn e La) e Al

SANTOS,C.L¹, Duque J.G.S.¹, and Meneses, C. T.¹

Universidade Federal de Sergipe - São Cristóvão SE Brazil

Este trabalho consiste em estudar as mudanças estruturais causadas pela substituição de Cu por metais de transição (MT = Ni, Fe, Mn, La) e Al, para diferentes concentrações de dopantes (1% a 10%). Partindo do material precursor, obtido pelo método químico denominado de co-precipitação, o material foi sintetizado por um período de 5 horas a uma temperatura de 800C. Resultados de difração de raio X e análise de refinamento Rietveld das amostras calcinadas foram realizadas para verificação de mudanças na estrutura cristalina causadas pela inserção de átomos dopantes. Apenas foi verificada a formação de fases isomorfas não desejadas em estruturas dopadas com Ni com alta concentração de dopante. Além disso, foi também observado um deslocamento nos picos para baixos ângulos em todas as amostras, sugerindo um provável aumento na célula unitária. Para estudar a estrutura local utilizamos a absorção de raios-X, para obter informações sobre a vizinhança dos metais de transição, com a finalidade de elucidar a estrutura local das fases formadas. Medidas de EXAFS nas bordas K do Cu, Fe e Ni. É importante ressaltar que foram realizadas medidas EXAFS em dois desses sistemas (CuO dopado com Fe e Ni) em temperatura ambiente e baixa temperatura. No entanto, esses resultados ainda não foram satisfatórios para verificação do efeito de supressão do ordenamento magnético, visto que para todas as amostras, o efeito acontece abaixo de 230K. Medidas de magnetização foram realizadas com o intuito de estudar as mudanças nas propriedades magnéticas após a inserção do dopante, nos quais foi verificada uma supressão da TN (Temperatura de Néel) para baixas temperaturas em todas as amostras de Fe e Ni, sendo a supressão mais acentuada nas amostras com o dopante Fe

Acknowledgements: CNPQ,FAPESSE,UFS

NANOSTRUCTURAL CHARACTERIZATION OF POLYBUTADIENE-MODIFIED EPOXY RESIN: EFFECT OF THE CURING AGENT

Lima, V.D.¹, Soares, B.G.¹, and DAHMOUCHE, K²

¹ Universidade Federal do Rio de Janeiro - Rio de Janeiro RJ Brazil

² Centro Universitário da Zona Oeste - Rio de Janeiro RJ Brazil

The interest on the development of nanostructured epoxy networks has been increased significantly due to the possibility in designing new material structures for desired properties, by controlling the morphology of the dispersed phase in nanoscale dimension. Recently we have functionalized hydroxyl terminated polybutadiene with isocyanate groups and used this new telechelic polymer as a rubber modifier for epoxy matrix. The isocyanate groups reacted with the OH groups of the epoxy resin, resulting in a triblock copolymer constituted by epoxy resin and PBD segments (ER-b-PBD-b-ER). The presence of the rubber resulted in a visually transparent and homogeneous material indicating no discernible phase separation and a complete adhesion between the components. The goal of the present study is to confirm the nano-scale rubber domain size in this system by using small angle X-ray scattering (SAXS) combined with atomic force microscopy and to investigate the effect of the different curing system, based on amine (which promotes the cure at room temperature) and tetrahydrophthalic anhydride (which requires higher curing temperature).

Acknowledgements: This work has been supported by the Brazilian Synchrotron Light Laboratory (LNLS), Conselho Nacional de Desenvolvimento Científico e Tecnológico - CNPq, and Fundação de amparo a Pesquisa do Esta Rio de Janeiro - FAPERJ.

IRON-STABILIZED NANOCRYSTALLINE ZrO_2 SOLID SOLUTIONS: A PRELIMINARY STUDY BY X-RAY DIFFRACTION AND VIBRATIONAL SPECTROSCOPIES

Alconchel, S. A.¹, Pierini, B. T.², Abdala, P. M.³, and Lamas, D. G.³

¹ Universidad Nacional del Litoral - Santa Fe Argentina

² Universidad Nacional del Litoral - Santa Fe Santa Argentina

³ Consejo Nacional de Investigaciones Científicas y Técnicas - Buenos Aires Argentina

Iron-stabilized nanocrystalline ZrO_2 solid solutions have found important applications as catalysts, gas sensors, pigments and adsorbents. Recently, Fe-doped ZrO_2 has been predicted as potential spintronic material and its magnetic properties have been studied. It is well known that metal cations (notably Ca^{2+} , Mg^{2+} , Y^{3+} , and some rare earth cations) form solid solutions with zirconia, thus stabilizing either the tetragonal or cubic form, at increasing contents. However, the influence of iron as stabilizer was comparatively less studied and the obtained results have varied significantly according to the preparation conditions [1, 2]. In the present work, we first reported a study on the formation of the $Zr_{0.70}Fe_{0.30}O_{1.85}$ solid solution and its thermal stability in air by classical X-Ray diffraction and vibrational spectroscopies (Fourier transform infrared, laser Raman). Two synthetic routes are compared: coprecipitation and PVA-Sucrose combustion. Then, we presented an advance of the synchrotron powder X-ray diffraction results corresponding to $Zr_{1-x}Fe_xO_{2-x/2}$ samples ($x=0.10, 0.30, 0.40$ and 0.50) prepared by coprecipitation. Nanocrystalline powders of $Zr_{0.70}Fe_{0.30}O_{1.85}$ with tetragonal/cubic- ZrO_2 structure were obtained at 873-973 K. Higher calcination temperatures (1073-1273 K) caused the partial segregation of hematite and the conversion to the monoclinic form. Samples derived from the PVA-Sucrose combustion route had a lower thermal stability. FTIR and Raman spectra always showed the typical bands of Fe_2O_3 , indicating that at 873-973 K it would be either amorphous or in the form of small clusters. The use of synchrotron powder X-Ray diffraction allowed as the preliminary detection of very weak reflections of the tetragonal phase in coprecipitated samples. The solubility limit of iron in zirconia was about $x=0.40$ after calcination at 973 K. Further experiments will be carried out in order to complete others compositions and their detailed structural characterization.

References: [1] Yu, L. Duan, Y. Wang, G. Rao, Physica B 403 (2008) 4264-4268.
[2] F. García, V. de Resende, E. De Grave, A. Peigney, A. Barnabé, C. Laurent, Mater. Res. Bull. 44 (2009) 1301-1311.

Acknowledgements: This work supported by UNL and LNLS.

ELETRONIC PROPERTIES OF COORDINATION COMPOUNDS OF INDIUM, BISMUTH AND ANTIMONY WITH MALEONITRILE DITHIOLATE (MNT) LIGAND IN THE C1s AND N1s REGIONS

Almeida, G. C.¹, Lopes, L. J. S.¹, A. L. F. de Barros², Guerra, A. C. O.², Ferreira, G. B.¹, and Turci, C. C.¹

¹ Universidade Federal do Rio de Janeiro - Rio de Janeiro RJ Brazil

² Centro Federal de Educação Tecnológica - Rio de Janeiro RJ Brazil

Polysulphurated ligands represent a very important class of coordination compounds, due to their several applications as charge transfer salts on the development of high technology electronic materials. The π delocalization among the entire molecule has been appointed as the main factor for the properties of these compounds [1], although the effect of such delocalization has not been yet evaluated for the core levels. XPS Photoabsorption spectra in the C1s and N1s regions have been acquired at Spherical Grating Monochromator (SGM) beamline at LCLS-Campinas for $[\text{NEt}_4][\text{In}(\text{MNT})_2]$, $[\text{NEt}_4][\text{Sb}(\text{MNT})_2]$ and $[\text{NEt}_4]_2[\text{Bi}_2(\text{MNT})_3]\text{Br}_2$ complexes. All of them have been synthesized following the literature [2-4]. The compounds were introduced into the main chamber as solid samples using a carbon sticky tape. The work pressure was kept at 1.5×10^{-7} mBar. The spectral analysis of these compounds allowed us to identify the different chemical environments in both, C1s and N1s regions. Ab initio calculations associated with improved virtual orbital (IVO) method, carried out with the GSCF3 program, were used to help us to establish the assignments.

Referências

1. Stiefel, E.I. Prog. Inorg. Chem. 52, 2004.
2. Davidson, A.; Holm R.H. Inorg. Syn. 10, 8-17, 1967.
3. Tuck, D.G.; Yang, M.K. J.Chem.Soc. (A), 1971.
4. Hunter G. J.Chem. Soc. Dalton Trans. 1972.

Acknowledgements: Agradecimentos: This work was supported by D08A-SGM-8775, CAPES, FAPERJ, CNPq, FUNEMAC.

ELECTRONIC PROPERTIES OF THE NEUTRAL COORDINATION COMPOUNDS OF THE DMIT LIGAND IN THE S 1s REGION.

Turci, C. C.¹, Ferreira, G. B.¹, Guerra, A. C. O.², Lopes, L. J. S.¹, and Comerlato, N.M.¹

¹ Universidade Federal do Rio de Janeiro - Rio de Janeiro RJ Brazil

² Centro Federal de Educação Tecnológica - Rio de Janeiro RJ Brazil

Complexes of the 1,3-dithiole-2-thione-4,5-dithiolato (dmit) ligand have been extensively studied both because for their properties and structural features and also due to their potentially useful conductive properties[1-3]. Furthermore, complexes of the poly sulfur-containing dmit ligand have structures of considerable interest and different from those with other 1,2-dithiolato ligands [1]. This is exemplified by the antimony complexes [4, 5]. Similarly our group has been working on the synthesis of neutral complexes of dmit with a strong intermolecular interaction among the units of dmit. Photoabsorption and Photoelectron spectra in the S 1s region have been acquired for BrBi(dmit), BrSb(dmit) and ISb(dmit) compounds. All complexes were synthesized following the literature [6]. TEY and XPS spectra have been acquired at the Soft X-ray Spectroscopy (SXS) beamline, LNLS-Campinas. The samples were introduced into the main chamber as a solid using a carbon sticky tape. The work pressure was kept at 2×10^{-8} mBar. The spectra analysis of these compounds allowed to identify the different chemical environment in the S 1s region. Ab initio calculations associated with improved virtual orbital (IVO) method, carried out with the GSCF3 program, were used to help us to establish the assignments. The geometric parameters were optimized using the GAMESS program.

Referências

1. Pullen, A.E., Olk, R.M., Coord. Chem. Rev., 188, 211, 1999.
2. Cassoux, P., Coord. Chem. Rev., 185, 213, 1999.
3. Matsubayashi, G., Nakano, M., Tamura, H., Coord. Chem. Rev., 226, 143, 2002.
4. Spencer, G.M., Wardell, J.L., Aupers, J.H., Polyhedron, 2701, 15, 1996.
5. Avarvari, N., Faulques, E., Fourmigue, M., Inorg. Chem. 40, 2570, 2001.
6. Abrantes, L.T. et al., Inorg. Chem. Comm., 9, 522, 2006.

Acknowledgements: Agradecimentos: This work was supported by D04A-SXS-5725/06, FAPERJ, CNPq, FUNEMAC.

Estructura atómica, dinámica local, anarmonicidad y expansión térmica en nanoaleaciones $\text{Fe}_x\text{Au}_{100-x}$: Determinación del potencial interatómico mediante EXAFS empleando teoría de perturbaciones estadístico-cuántica.

Lede, E. J.¹ and Socolovsky, L. M.²

¹ Universidad Nacional de La Plata - La Plata Bs.As Argentina

² Universidad de Buenos Aires - Buenos Aires CapFe Argentina

Las técnicas de aleamiento mecánico han mostrado ser eficaces en la síntesis de aleaciones binarias nanoestructuradas metaestables. Presenta gran interés el estudio de sistemas binarios en los cuales la solubilidad mutua de sus componente básicos es baja en el equilibrio termodinámico debido a su calor de formación positivo. En el presente trabajo se investigaron mediante XAFS, nanoaleaciones ($\text{Fe}_x\text{Au}_{100-x}$). Los datos EXAFS obtenidos sobre un conjunto de 3 muestras con diferentes tenores de Fe, fueron tratados simultáneamente en ambos bordes de absorción (Fe-K, Au-K) y diferentes temperaturas (11, 50, 100, 130, 160, 190, 220, 250, 280, 310K). Un tratamiento convencional previo de los datos, sugirió una estructura FCC con una gran distribución de sitios ligeramente diferentes tanto para el Fe como para el Cu, variando con la concentración local (CL) de Fe. Para contemplar este hecho, se realizó un tratamiento de datos más potente y ambicioso, mostrando ser muy promisorio y aplicable a estos sistemas [2, 3]. En la ecuación de ajuste se empleó un potencial cuántico (Teoría de perturbaciones estadístico-cuántica de 4to orden [3]) en función de CL, convolucionado con una función densidad de probabilidad. La determinación precisa del potencial permitió conocer las propiedades termodinámicas locales y las características estructurales de Fe-Au, para correlacionarlas con su comportamiento magnético.

[1] A.N. Kravtsova, G.E. Yalovega, A.V. Soldatov, W.S. Yan, S.Q. Wei. Journal of Alloys and Compounds (2008)

[2] Newville, PhD thesis, (1995)

[3] Haug et al. Phys. Rev. B 77, 184115 (2008)

Acknowledgements: Los autores agradecen al LNLS

Study of the Morphology Evolution of Vanadium Pentoxide Nanostructures by TEM and SAXS

Avansi, W.¹, Oliveira, C. L. P², Leite, E.R.³, Ribeiro, C.⁴, and Mastelaro, V.R.¹

¹ Universidade de São Paulo - São Carlos - São Carlos SP Brazil

² Aarhus University - Aarhus Denmark

³ Universidade Federal de São Carlos - São Carlos SP Brazil

⁴ Empresa Brasileira de Pesquisas Agropecuárias - São Carlos SP Brazil

In the last decade, nanostructured vanadium oxide compounds have attracted the interest due to their chemical and physical properties and their large potential for applications in catalysis, as sensors, in electrochromic devices and photocatalytic activities. The wide range of application of this compound is strongly related to its crystalline phase and morphology. Recently our group showed that it is possible through easy and clean methodology to obtain $V_2O_5 \cdot nH_2O$ nanocrystals with controlled morphology and crystal structure only through the control of the hydrothermal treatment variables [1]. The main objective of this work was to study by Transmission Electron Microscopy (TEM) and Small Angle X-Ray Scattering (SAXS) technique the morphology evolution of the $V_2O_5 \cdot nH_2O$ nanostructures under different temperatures and treatment times in hydrothermal conditions. The synthesis of different $V_2O_5 \cdot nH_2O$ nanostructures was made using the H_2O_2 - V_2O_5 route described in greater detail elsewhere by Avansi et al. The as-synthesized sample consisted of stable colloidal suspensions of $V_2O_5 \cdot nH_2O$ nanostructures in water, with 0.06M. The TEM images confirm an evolution of the morphology of $V_2O_5 \cdot nH_2O$ nanostructures from nanoribbon to nanorod forms with increasing of temperature or treatment time. HRTEM images show that the growth of these nanostructures occurs preferentially on the [010] direction. The structural models used for the SAXS data for the as-obtained colloidal suspensions can be described satisfactorily in good agreement of the dimensions and morphology observed by TEM images.

[1] W. Avansi, C. Ribeiro, E.R. Leite and V.R. Mastelaro, *Crystal Growth and Design*, Vol. 9, No. 8, 2009.

Acknowledgements: The authors gratefully acknowledge the financial support of the Brazilian research funding agencies FAPESP and CNPq. SAXS measurements and TEM microscopy facilities were provided by LNLS-Campinas, SP, Brazil.

Transition Metal Cations Doping in Ammonium Dihydrogen Phosphate As Examined by Synchrotron Radiation Renninger Scanning

C. M. R. Remedios¹, Lai, X², Roberts, K. J.³, GOMES, E.J.L.¹, de Menezes, A. S.⁴, and Cardoso, L.P.⁴

¹ Universidade Federal do Pará - Belém PA Brazil

² University of Leeds - West Yorkshire United Kingdom

³ University of Leeds - Leeds United Kingdom

⁴ Universidade Estadual de Campinas - Campinas SP Brazil

X-ray multiple diffraction through Renninger scanning (RS) using synchrotron radiation has been applied to study transition metal cations Mn^{3+} and Ni^{2+} incorporated into Ammonium Dihydrogen Phosphate (ADP) crystal lattice. ADP crystal has been studied over the last 70 years for its well-known properties such as ferroelectricity, ferroelasticity and nonlinear optical properties. Single crystals of Mn^{3+} and Ni^{2+} doped ADP were grown by slow evaporation from supersaturated aqueous solutions. $NiCl_2$ was added to the ADP solution to prepare Ni^{2+} doped samples, $KMnO_4$ and $MnCl_2$ at a 1:1 molar were added to the ADP solution in the preparation of Mn^{3+} doped samples. High-resolution RS of KDP crystals were carried out at XRD1 station of the Brazilian Synchrotron radiation facility (LNLS). Wavelengths either side of the impurity species K-absorption edges: $\lambda = 1.5149(5)$, $1.4664(5)$ and $1.9133(5)$ for ADP: Ni^{2+} and $\lambda = 1.9133(5)$ and $1.8900(5)$ for ADP: Mn^{3+} . The (400) primary reflection was chosen for these experiments. Accurate calculation of the unit-cell parameters by using RS secondary peaks reveals that there is not significant contraction of the lattice parameters following Ni^{2+} and Mn^{3+} dopant incorporation and the crystal symmetry are practically the same regardless of the incorporation of Mn^{3+} and Ni^{2+} cations. In the measurements for the two wavelengths ADP:Mn crystal exhibit asymmetric peak profiles and no extra peak appears in the whole Mn doped RS. On the other hand, in the ADP:Ni measurements one can clearly observe: i) suppression of the intensity profile asymmetry in secondary peaks for the Ni doped RS (below λ Ni Kedge) and also, ii) marked asymmetry inversion (above λ Ni Kedge), for example the peak (031)(431) which represents a four beam case. These results indicate that synchrotron radiation RS is a high resolution probe to be used in the impurity incorporation in the ADP lattice.

Acknowledgements: The authors gratefully acknowledge the LNLS staff for valuable help during the experiments and the financial support from Brazilian Agencies CNPq, FAPESP and CAPES

Influence of microstructure on the corrosion behavior of nitrocarburized AISI H13 **Influence of microstructure on the corrosion behavior of nitrocarburized AISI H13 tool steel obtained by pulsed DC plasma**

Basso, R. L. O.¹, Candal, R.J.², C. A. Figueroa¹, Wisnivesky, D.³, and F. Alvarez³

¹ Universidade de Caxias do Sul - Caxias do Sul RS Brazil

² Universidad de Buenos Aires - Buenos Aires DF Argentina

³ Universidade Estadual de Campinas - Campinas SP Brazil

The influence of microstructure on the corrosion behavior of pulsed plasma nitrocarburized AISI H13 tool steel in NaCl 0.9 wt/V % solution is reported. The samples were prepared with different nitrocarburizing treatment times using a constant [CH₄/H₂+N₂] gaseous mixture by a DC pulsed plasma system. The microstructure of the nitrocarburized layers was analyzed by scanning electron microscopy (SEM), X-ray photoelectron spectroscopy (XPS) and X-ray diffraction. The corrosion behavior was evaluated by potentiodynamic polarization experiments. The nitrocarburizing process considerably improves the corrosion resistance of the material in a NaCl environment as compared to the untreated H13 steel. The modified surface layer mainly consisting of ϵ -Fe₂₋₃(C,N) and γ -Fe₄N phases confers this outstanding behavior. The corrosion resistance dependence on specific nitrocarburizing processes is reported and the role of the surface porosity is discussed.

Acknowledgements: The authors are indebted to the Laboratório Nacional de Luz Síncrotron (LNLS). This work was partially supported by FAPESP (grant 05/53926-1). FA is Fapesp and CNPq fellow. RJC is a member of CONICET and CAPES-SPU supported his sojourn at the IFGW. At the present, RLOB and CAF is at the CCET, UCS, CEP 95070-560, Caxias do Sul, Rio Grande do Sul, Brazil.

Acoplamento magnético entre os íons de Gd e Pr e efeito magnetocalórico no composto $Gd_{0,5}Pr_{0,5}Al_2$

A. Magnus G. Carvalho¹, Garcia, F.², de Sousa, V. S. R.³, von Ranke, P. J.³, Rocco, D. L.⁴, Loula, G. D.⁵, E. J. Carvalho², Coelho, A. A.⁵, da Silva, L. M.⁶, and Gandra F. G⁵

¹ Instituto Nacional de Metrologia, Normal e Qualidade Industr - Xerém RJ Brazil

² Laboratório Nacional de Luz Síncrotron - Campinas SP Brazil

³ Universidade do Estado do Rio de Janeiro - Rio de Janeiro RJ Brazil

⁴ Universidade Federal de Ouro Preto - Ouro Preto MG Brazil

⁵ Universidade Estadual de Campinas - Campinas SP Brazil

⁶ Universidade Estadual do Maranhão - São Luis MA Brazil

Neste trabalho, reportamos estudos teóricos e experimentais de propriedades magnéticas e magnetocalóricas do composto $Gd_{0,5}Pr_{0,5}Al_2$ em diferentes campos magnéticos aplicados. Os perfis das curvas de magnetização indicam que esse composto é ferrimagnético em baixas temperaturas. Também apresentamos dados de experimentos de dicroísmo circular magnético de raios-X (XMCD) para esse composto, com os quais confirmamos que os momentos magnéticos dos íons de Pr são antiparalelos aos momentos magnéticos dos íons de Gd. Os parâmetros magnetocalóricos, ΔT_S and ΔS_T , foram obtidos de dados calorimétricos e ambas as curvas apresentam efeito magnetocalórico normal e inverso. Um modelo teórico para o acoplamento ferrimagnético, incluindo a anisotropia de campo elétrico cristalino, foi usado para descrever ΔT_S and ΔS_T experimentais.

Acknowledgements: Os autores agradecem o financiamento das agências CAPES, FAPESP, FAPERJ e CNPq. Os autores também são gratos ao Laboratório Nacional de Luz Síncrotron (LNLS).

Structural and optical properties of CaTiO_3 perovskite-based materials obtained by microwave-assisted hydrothermal synthesis: An experimental and theoretical insight

Moreira M. L.¹, Mastelaro, V.R.², Longo, V. M.¹, E. C. Paris¹, Longo, E.³, Varela, J.A.³, and Andrés, J.⁴

¹ Universidade Federal de São Carlos - São Carlos SP Brazil

² Universidade de São Paulo - São Carlos - São Carlos SP Brazil

³ Universidade Estadual Paulista - Araraquara - Araraquara SP Brazil

⁴ Universitat Jaume I - Castelló de la Plana Spain

CaTiO_3 powders were synthesized using both a polymeric precursor method (CT_{ref}) and a microwave-assisted hydrothermal (CT_{HTMW}) method in order to compare the chemical and physical properties of the perovskite-based material as a function of the synthesis method. To this end, X-ray diffraction, Raman spectroscopy, inductively coupled plasma atomic emission spectroscopy and experimental Ti and Ca K-edge X-ray absorption near-edge structure spectroscopy, as well as measurements of photoluminescence (PL) emission, were used to characterize the typical bottom-up process of the CaTiO_3 perovskite phase at different times. Detailed Rietveld refinements show a random polycrystalline distortion in the powder structure, which can be associated with the tilting (a angle O - Ti - O) between adjacent TiO_6 octahedra (intermediate range) for CT_{HTMW} samples and an intrinsic TiO_6 distortion (short range) in relation to the polymeric precursor CT_{ref} sample. These properties were further investigated by first-principles calculations based on the density functional theory at the B3LYP level. The relationship between this tilting on the PL profile is highlighted and discussed. Thus, a structural model derived from both experimental results and theoretical simulations reveals a close relationship between this tilting and the presence of intermediate energy states within the band gap which are mainly responsible for PL emissions.

Acknowledgements: The authors acknowledge the support agencies CAPES, CNPq and FAPESP/CEPID 98/14324-8. to Ministerio de Educacion y Cultura of the Spanish Government to provide research mobility. Thanks for XANES facilities provided by LNLS, Campinas, SP, Brazil.

Study Of Copper Hardened Composites With Nanoparticles Of Alumina

Bagnato, O. R.¹, Francisco, F. R.¹, and Barros, R. M.²

¹ Laboratório Nacional de Luz Síncrotron - Campinas SP Brazil

² Universidade Estadual de Campinas - Campinas SP Brazil

The copper, despite having excellent properties of thermal and electrical conduction, has low mechanical strength when compared to other materials. The enrichment of copper for incorporation of fine particles causes hardening of its structure without significant loss of its thermal and electrical properties [1].

The mixture of 0,3 - 1,1%wt of nanoparticles of alumina with copper causes these effects, because of the alumina proprieties that are hard and thermally stable at high temperatures [1 - 2].

The specimens were prepared as follows: the copper and alumina powders were mixed, after that they were uniaxial pressed at 500 MPa and sinterized at temperatures of 600°C, 700°C and 800°C in a vacuum furnace. This process had to be made in controlled atmosphere to avoid oxidation. The maximum internal pressure used to sinterize was 5×10^{-5} mbar. These specimens were submitted to hardness and microstructural analysis. The composite structure was determined by SEM and EDS analysis.

The composite samples obtained were porous, and the nanoparticles of alumina were agglomerated. The hardness test showed that the composite hardness were still low when compared to pure copper, all specimens were between 50 and 70HV. These results demonstrate that there was probably a mistake in the mixing of powders and, because of that, the nanoparticles agglomerated and consequently the hardness did not increase.

References

- 1- Upadhyaya A.; Upadhyaya G.S., Materials and Design, Volum 16, Number 1, 1995 , pp. 41-45(5).
- 2- Smith, F. W., Princípios de Ciência e Engenharia de dos Materiais. 3 ed. Alfragide, Portugal, 1996.

Acknowledgements: Materials Group, Laboratory of Electron Microscopy

Gênese e propriedades estruturais e fotocatalíticas de partículas micro e nanoestruturadas de ZnO.

Feltrin, C.W¹, Rodrigues, A¹, Bernardi, F.¹, Moraes, J.¹, and Alves, M.C.M.¹

Universidade Federal do Rio Grande do Sul - Porto Alegre RS Brazil

O óxido de zinco tem sido estudado por décadas e podemos observar que nos últimos anos este semicondutor teve seu interesse renovado pelas perspectivas de sua aplicação em optoeletrônica, devido ao seu band gap direto de 3,37 eV [1]. Grande parte das pesquisas hoje realizadas em ZnO é dedicada ao uso do mesmo em reações fotocatalíticas [2-3]. Esta área tem grande apelo ambiental, pois tem aplicação direta na degradação da matéria orgânica presente em efluentes de processos industriais. No presente trabalho será apresentada a caracterização das propriedades eletrônicas, estruturais e fotocatalíticas de ZnO sintetizado por via química. Foram realizados experimentos de espectroscopia de UV-VIS, infravermelho e de absorção de raios-X na borda K do Zn. A morfologia do produto final foi estudada por microscopia eletrônica. As condições experimentais permitiram o controle da morfologia e tamanho micro e nano estruturado. Estes resultados serão correlacionados com resultados de atividade fotocatalítica. 1 - U. Ozgur, Ya I. Alivov; C. Liu; A. Teke; M. A. Reshchikov; S. Dogan; V. Avrutin; S. J. Cho; H. Morkoç.; J. of Appl. Phys. 98, 41301, (2005). 2 - A. Akyol; H. C. Yatmaz; M. Bayramoglu; Appl. Cat. B Environm. 54, 19 (2004). 3 - C. Lizama; J. Freer; J. Baeza; H.D. Mansilla; Cat. Today 76, 235 (2002).

Acknowledgements: Agradecemos ao apoio do LNLS e CNPq.

Propriedades Estruturais de Vidros Aluminato de Cálcio Dopados com Praseodímio

Sampaio, J. A.¹, Peixoto, S. M. B.¹, Filadelpho, M. C.¹, dos Santos, D. R.¹, and Baesso, M.L.²

¹ Universidade Estadual Norte Fluminense - Campos dos Goytacazes RJ Brazil

² Universidade Estadual de Maringá - Maringá PR Brazil

A área de fotônica que compreende os lasers, as telecomunicações que utilizam fibras ópticas, amplificadores, bem como sensores óticos ou químicos, desfrutam das propriedades luminescentes dos íons terras raras, que por terem a camada 4f incompleta permite que várias transições óticas ocorram. O íon Pr^{3+} vem sendo estudado nos últimos anos como dopante em diversas matrizes vítreas e cristalinas, pois possui a habilidade de emitir radiação desde o visível até o infravermelho próximo, porém apresentam propriedades espectroscópicas distintas dependentes da matriz hospedeira. Isto se deve ao fato dos vidros se apresentarem como um meio desordenado onde o ambiente dos íons dopantes não é uniforme como em um material cristalino. O praseodímio trivalente quando dopado em uma matriz vítrea que apresenta baixa energia de fônons, emite radiação no comprimento de onda, $\sim 1,3 \mu\text{m}$, para o qual as fibras óticas disponíveis comercialmente são otimizadas, e também é capaz de converter radiação infravermelha monocromática em radiação visível policromática através do processo de ganho ascendente de energia (*upconversion*).

Os vidros aluminato de cálcio são vidros que possuem boas propriedades óticas, térmicas e mecânicas, que quando dopados com íons terras raras são ideais para serem utilizados como meio ativo de laser de estado sólido. No presente trabalho são apresentados os resultados da investigação do ambiente químico desses vidros dopados com Pr. Foi utilizada nesse estudo a Espectroscopia da Estrutura Fina da Absorção de Raios X (EXAFS), onde determinou-se o número de coordenação em torno do Pr, as distâncias interatômicas bem como a dispersão da rede, dada pelo fator de Debye-Waller. Esses dados são comparados com aqueles obtidos pela Espectroscopia de Lente Térmica e luminescência, onde determinados a difusividade térmica, eficiência quântica e outras propriedades óticas.

Acknowledgements: Este trabalho teve apoio financeiro do CNPq e FAPERJ. Os autores agradecem o apoio da equipe técnica da linha D08B-XAFS2 do LNLS.

Caracterização do ambiente químico do neodímio em vidro aluminato de cálcio com baixa concentração de sílica

Peixoto, S. M. B.¹, Filadelpho, M. C.¹, dos Santos, D. R.¹, and Sampaio, J. A.¹

Universidade Estadual Norte Fluminense - Campos dos Goytacazes RJ Brazil

Os vidros aluminato de cálcio dopados com íons terras raras, por possuir boas propriedades térmicas, mecânicas e óticas são bons candidatos a meio ativo de laser do estado sólido, que podem ser empregados na medicina, odontologia ou em outras aplicações que necessitem de lasers compactos. A vantagem de usar vidros em relação aos cristais dopados, usados comercialmente, está no fato da facilidade de produzi-los e no custo mais baixo. Os íons das terras raras por possuir a camada 4f incompleta apresenta uma série de transições óticas, e o Nd sendo um deles apresenta um sistema laser de quatro níveis, nos quais são possíveis observar três linhas de emissão laser, a saber em $0.93 \mu\text{m}$, $1.06 \mu\text{m}$ e $1.34 \mu\text{m}$. Sendo a emissão mais intensa aquela em $1.06 \mu\text{m}$. Para se otimizar essa emissão laser é necessário investigar a concentração de Nd a ser usado na composição da matriz vítrea. Todavia a eficiência quântica da fluorescência depende também da proximidade entre os íons terras raras no material, que leva a vários efeitos óticos que minimizam tal propriedade, o que não é desejável. Para isso é salutar investigar o ambiente químico desses íons a fim de se obter um valor otimizado da eficiência quântica, bem como servir de base para corroborar os resultados obtidos por outras técnicas de caracterização.

O objetivo da presente investigação foi de verificar o ambiente químico do Nd em função da concentração desse terra, através da Espectroscopia da Estrutura Fina de Absorção de Raios X (EXAFS). Através dessa técnica, utilizando as oscilações de EXAFS extraídas do espectro de absorção de raio X obtido em torno da sua borda L_{III} , foi possível determinar o número de coordenação, o seja, o número de vizinhos mais próximos do Nd, as distâncias interatômicas, bem como a desordem da rede dada pelo fator Debye-Waller. Esses dados foram corroborados com os dados da eficiência quântica, bem como difusividade térmica obtidos pela Espectroscopia de Lente Térmica.

Acknowledgements: Este trabalho teve ajuda financeira da FAPERJ e do CNPQ.

Controle morfológico de nanopartículas de óxido de gadolínio dopadas com íon európio(III)

Gaspar, R. D. L.¹, Sigoli, F.A.¹, and MAZALI, I. O.¹

Universidade Estadual de Campinas - Campinas SP Brazil

Materiais luminescentes tem atraído atenção para o uso em dispositivos de alta tecnologia, por exemplo, displays, guias de onda e cintiladores. Nanopartículas dopadas com íons terras raras possuem interessantes propriedades luminescentes, sendo que a morfologia e a composição dessas nanopartículas tem grande influência nestas propriedades. Uma morfologia esférica é desejável, pois resulta em propriedades ópticas isotrópicas e reduzem o efeito de supressão de superfície na luminescência dessas partículas. Alguns métodos de síntese tem sido utilizados na obtenção de nanopartículas de óxidos dopados com íons terras raras visando o controle do tamanho e da forma, como os métodos Pechini, combustão e poliol. Um método utilizado com sucesso no controle da forma do tamanho de partículas é a precipitação homogênea combinada com a variação da constante dielétrica do meio de reação através da mistura água/álcool. Neste trabalho, controlou-se o tamanho das nanopartículas esféricas de óxido de gadolínio dopadas com európio(III) através da precipitação homogênea com o uso de diferentes ânions e misturas água/álcool (etanol, etilenoglicol e terc-butanol), e estudou-se o efeito da natureza dos alcoóis utilizados e dos ânions na precipitação dos precursores. O tamanho médio das partículas de óxido de gadolínio obtidas variou-se de 92 a 31 nm, e verificou-se uma diminuição do tamanho de partículas das amostras obtidas na mistura água/etanol e água/etilenoglicol em função da constante dielétrica do meio, porém isto não é observado nas amostras precipitadas em água e terc-butanol, mostrando um efeito da natureza dos alcoóis na precipitação dos precursores, e conseqüentemente dos óxidos de gadolínio. As propriedades luminescentes dos óxidos são devidas às transições intraconfiguracionais $f \rightarrow f$ do íon európio(III), sendo a transição ${}^5D_0 \rightarrow {}^7F_2$ a de maior intensidade.

Acknowledgements: Os autores agradecem a FAPESP, CAPES, CNPq pelo suporte financeiro e ao Laboratório de Microscopia Eletrônica do LNLS, proposta SEM-FEG - 8510.

CARACTERIZAÇÃO DE ROCHAS CARBONÁTICAS

Bagnato, O. R.¹, Francisco, F. R.¹, and Brandão, E.M.²

¹ Laboratório Nacional de Luz Síncrotron - Campinas SP Brazil

² Faculdade de Engenharia Civil (FEC) - Unicamp

As rochas carbonáticas ocupam um expressivo volume da crosta terrestre. De maneira geral, pode-se dizer que essas rochas estão presentes nas diversas unidades litoestratigráficas que compõem a história geológica da Terra, registrando episódios de sedimentação química e bioquímica acontecidos desde os tempos mais antigos (Arqueano) até os mais novos (Quaternário). Tais rochas apresentam como componentes mineralógicos essenciais a calcita ($CaCO_3$) e a dolomita [$CaMg(CO_3)_2$], ocorrendo em diferentes proporções. Este tipo de rocha também podem conter outros tipos de minerais, em menores proporções, como a siderita ($FeCO_3$), ankerita [$Ca(Mg, Fe, Mn)(CO_3)_2$]; ankerita normal [$Ca_2MgFe(CO_3)_4$] e magnesita ($MgCO_3$) [1].

Com a finalidade de analisar as rochas tipo carbonáticas química e morfológicamente, um total de cinco amostras de rochas foram submetidas a análises de Microscopia Eletrônica de Varredura, Espectroscopia por Dispersão de Elétrons, análise por fluorescência e difração de raios-X convencionais e o aprimoramento da análise utilizando técnicas de síncrotron.

Através do método convencional de difração, as principais fases encontradas foram calcita, ankerita, quartzo e dolomita. Pela técnica de difração utilizando síncrotron, com o ajuste de Rietveld, foi possível identificar frações de fase de CaF_2 . Além da técnica de DFX, as amostras foram submetidas a fluorescência de raios-X, utilizando a técnica convencional e síncrotron. Através da técnica por síncrotron foi possível identificar um maior número de elementos, além de obter a distribuição qualitativa dos elementos. Para a caracterização da morfologia das rochas carbonáticas foram utilizadas as técnicas de MEV e EDS.

Os métodos convencionais de difração e fluorescência por raios-X e de MEV permitem resolver as amostras em seus aspectos composicionais, distribuição de fases e de relevo, já os métodos envolvendo as técnicas de síncrotron apresentam maior acuidade no mapeamento por fluorescência e difração. Na técnica de fluorescência por síncrotron foi possível a identificação de um maior número de elementos, como: titânio e vanádio. Na difração de raios-X por síncrotron foi possível identificar uma fase não detectada por raios-X convencional, CaF_2 . Os resultados também indicaram que as amostras apresentam uma variação tanto de composição quanto na estrutura das fases em função da posição dentro de uma mesma amostra tanto quanto na variação de uma amostra para outra. Estas técnicas são complementares e bastante adequadas para trabalhos futuros envolvendo ataque químico nas rochas carbonáticas.

Referências

[1] Souza, J. F., Vidal, F. W. H., Rochas Carbonáticas, Centro de Tecnologia Mineral, Ministério da Ciência e Tecnologia, Coordenação de Apoio Tecnológico a Micro e Pequena Empresa CATE. Rio de Janeiro RJ 2005.

Acknowledgements: Ao Laboratório Nacional de Luz Síncrotron (LNLS)
Ao Centro de Pesquisa Petrobrás (Cenpes)

In-plane strain anisotropy due to induced re-crystallization process (IBIEC) by means of X-ray multiple diffraction

dos Santos, A. O.¹, Lang R², de Menezes, A. S.³, Meneses, E. A.³, AMARAL L.², and Cardoso, L.P.³

¹ Universidade Federal do Maranhão - Imperatriz MA Brazil

² Universidade Federal do Rio Grande do Sul - Porto Alegre RS Brazil

³ Universidade Estadual de Campinas - Campinas SP Brazil

Metastable silicides are important because they can possess special properties and find application in rapidly developing nanoelectronics and spintronics. A considerable attention has been devoted to $\beta - FeSi_2$, semiconductor phase because of its energy gap value around 0.8 eV at room temperature [1], which gives rise to a photoresponse in the near-infrared region at about 1.5 μm . Many earlier works using molecular beam epitaxy (MBE) or liquid phase epitaxy methods have shown that a metastable metallic $\gamma - FeSi_2$ phase with a CaF_2 structure appeared prior to the formation of $\beta - FeSi_2$ [2]. The X-ray multiple diffraction (XRMD), which is a very special technique for providing enough sensitivity for detecting subtle distortions in the lattice as those caused by an external stimulus. XRMD has been applied in the study of ion-implanted semiconductors for the first time in 1997 [3] in the study of Se implanted in GaAs(001). Recently [4], the use of XRMD in the shallow junction of B in Si was crucial for the understanding of the shallow junction formation. In this work, it was clearly observed in-plane strain anisotropy due to the induced re-crystallization process (IBIEC) in Fe^+ ion implantation in Si(001). Electron Microscopy images have shown the occurrence of nanocrystals of $\gamma - FeSi_2$ phase in the implanted region with different orientations responsible for the strain anisotropy. The mappings of the (111) Bragg-Surface Diffraction (BSD) reflections show a clearly anisotropy between $\phi=0$ and 90° maps and also a marked broadening between Si (matrix) and implanted sample profiles. Reciprocal space mappings obtained for both directions confirm the BSD results.

[1] Bost, M.C. and Mahan, J.E. (1985). J. Appl. Phys. 58, p. 2696.

[2] Le, T.V. , Chevrier, J. and Derrien, J. (1992). Phys. Rev. B 46, 15946.

[3] Hayashi, M.A., Avanci, L.H., Cardoso, L.P., Sasaki, J.M., Kretly, L.C., Chang, S.L.(1997). Appl. Phys. Lett. 71(18), 2614.

[4] Orloski. R.V., Pudenzi, M.A.A., Hayashi, M.A., Swart, J.W., Cardoso, L.P. (2005). J. Mol. Catal. A - Chemical 228(1/2), 177.

Acknowledgements: This work has been supported by the Brazilian Synchrotron Light Laboratory (LNLS), CNPq and FAPESP.

Small-angle X-ray scattering (SAXS) of ordered magnetic systems

Beron, F.¹, Vargas, J. M.¹, Sharma, S.K.¹, Pirota, K. R.², and Knobel, M.¹

¹ Universidade Estadual de Campinas - Campinas SP Brazil

² Consejo Superior de Investigaciones Científicas - Madrid Spain

Nowadays, the improvement in the fabrication techniques allows to create magnetic nanostructures smaller, more dense and of increasing complex shape. The novel properties of these nanostructures can be used in areas such as information storage, sensors, high frequency devices, biomedical applications, etc. In the case of systems exhibiting a spatial ordering (nanoparticles, nanodot array, nanowire array, antidot array, etc.), this can influence both their global and local magnetic behavior. Therefore, an adequate design of the nanostructures, in function of the specific characteristics required for the wanted application, can only be achieved through the knowledge of the geometric parameters. Small-angle X-ray scattering (SAXS) method can help resolve this question, by giving both the local and global structure geometry. It was successfully applied to crystalline Fe_3O_4 nanoparticles system and antidot arrays (thin film with holes). SAXS was performed in transmission mode for nanoparticles in colloidal solution (to obtain the nanoparticles size distribution) and dispersed in different concentrations in polymer. Results show that the nanoparticles tend to agglomerate and form clusters into the polymer, instead of remaining separate as in the colloidal solution. Changing the solvent could overcome this problem. The antidot arrays were studied in grazing incidence, because transmission mode was impossible due to the substrate presence. Two series were investigated: permalloy antidot arrays with different anodization time of the alumina substrate and FePd ones with different antidot diameters (35 and 70 nm). From the GISAXS measurements, we concluded that increasing the anodization time increases both the local and global antidot order, while increasing the pore diameter by chemical etching decreases the structure order, the etch being thought not to be completely isotropic. All results will be related to those obtained by magnetostatic measurements, both global (major hysteresis curves) and local (first-order reversal curves), in order to completely understand the magnetic behavior of these nanostructures.

Acknowledgements: This work was supported by FAPESP (Brazil) and Fonds Québécois de la Recherche sur la Nature et les Technologies (FQRNT, Canada).

Microfluídica em PDMS e papel com detecção eletroquímica

Carvalho, R. F.¹, Kubota, L.T.¹, and Martins, L. F.¹

Universidade Estadual de Campinas - Campinas SP Brazil

Um dos projetos do grupo visa à obtenção de microdispositivos em PDMS/vidro para detecção amperométrica. Os canais são criados em PDMS, enquanto os eletrodos de ouro são fabricados em uma placa de vidro. Estes necessitam ser alinhados ao canal, de forma que fiquem apenas encostados em um dos lados do mesmo, de forma que ocorra apenas a detecção de espécies deste lado do canal. Isto possibilita a realização de processos de separação no canal, seguidos de detecção eletroquímica. No grupo de pesquisa também trabalhamos em diferentes dispositivos microfluídicos construídos sobre papel com detecção eletroquímica. Um dispositivo de separação em papel com detecção amperométrica foi desenvolvido para a determinação de ácido úrico e ascórbico em misturas. Novas configurações para o mesmo dispositivo estão sendo desenvolvidas no intuito de tornar a análise mais versátil e de baixo custo. Um segundo projeto está em desenvolvimento e consiste em modificar a superfície de eletrodos descartáveis construídos sobre poliéster com papel previamente modificado com a enzima lactato oxidase e um mediador específico. Este projeto tem como objetivo o desenvolvimento de biossensores descartáveis e robustos para emprego comercial.

Acknowledgements: CNPq

Construção de Dispositivos Microfluídicos Contendo Multi-Canais e Eletrodos Integrados para Detecção Amperométrica Simultânea

Silva, J. A. F.¹

Universidade Estadual de Campinas - Campinas SP Brazil

Microsistemas de análise, ou microTAS, têm proporcionado novas perspectivas para as técnicas de análise. Nestes microTAS, podem ser incorporadas a um ou mais substratos várias etapas de processamento de amostras, como por exemplo, diluição, pré-concentração, separação e detecção, para citar algumas. Um aspecto interessante dos microTAS capacidade de processamento paralelo de amostras, o que aumenta de maneira considerável a frequência analítica e o volume de dados gerados. Convencionalmente, utiliza-se um detector para cada canal (ou amostra) ou ainda um único detector que faz a varredura por todos os canais do dispositivo. Recentemente, nosso grupo de pesquisa propôs a utilização de um único detector amperométrico compartilhado por cinco canais microfluídicos e foi demonstrado que pode ser obtida resposta aditiva. Aspectos da implementação, utilização, vantagens e limitações destes dispositivos serão abordados nesta apresentação.

Acknowledgements: Laboratório Nacional de Luz Síncrotron (LNLS/LMF) Fundação de Amparo à Pesquisa do Estado de São Paulo (FAPESP) Conselho Nacional de Desenvolvimento Científico e Tecnológico (CNPq)

Superfícies, Interfaces e Nanossistemas

Characterization of ultra-thin films of Au deposited on Pd(111)

Pancotti A.¹, Carazzolle M.F.¹, Tallarico, D.A.², de Siervo A.¹, Nascente, P. A. P.², Landers R¹, and Kleiman, G.G.¹

¹ Universidade Estadual de Campinas - Campinas SP Brazil

² Universidade Federal de São Carlos - São Carlos SP Brazil

Ultra-thin films of transition metals deposited on single crystal metal substrates have attracted considerable scientific interest due to their catalytic, electronic and magnetic properties. Lately, there has been an increasing interest on the Au/Pd(111) system, mainly regarding its catalytic behavior [1-3]. In this work, we present preliminary results on the surface composition and structure of gold ultra-thin films deposited on Pd(111). The films were evaporated in ultra-high vacuum; the surface composition and structure were characterized by X-ray photoelectron spectroscopy (XPS), low-energy electron diffraction (LEED), and X-ray photoelectron diffraction (XPD).

The experiments were performed at LNLS using the soft X-ray spectroscopy (SXS) beam line. It was used a InSb(111) monochromator and the photon energy was 1840 eV. The measurements were done with a surface analysis system equipped with LEED optics, a high-resolution electron analyzer (Omicron HA 125HR) mounted in the plane of the storage ring, a differentially pumped argon ion sputter gun and a two axis sample manipulator. The Pd(111) surface was cleaned by cycles of argon ion sputtering and annealing, and the cleanliness was verified by XPS and the surface ordering, by LEED. The XPD patterns were simulated by using the multiple scattering calculation of diffraction (MSCD) code with a genetic algorithm (GA) for structure optimization [4, 5]. A full analysis is under development.

Acknowledgements: This work received financial support from FAPESP, CAPES, CNPq, and LNLS.

Estudo da morfologia de híbridos de maghemita e polianilina usando AFM

Lopes, M. C.¹, Souza Jr, F. G.¹, Marins, J. A.¹, Pinto, J.C.¹, Oliveira, G. E.², Manzini R., C. H.³, and Lima, L. M. T. R.¹

¹ Universidade Federal do Rio de Janeiro - Rio de Janeiro RJ Brazil

² Universidade Federal do Espírito Santo - Vitória ES Brazil

³ Universidade Estadual Norte Fluminense - Campos dos Goytacazes RJ Brazil

Híbridos de maghemita e polianilina dopada com ácido dodecilbenzenosulfônico foram preparados via polimerização in situ, capaz de gerar materiais nanométricos e não aglomerados. A morfologia destes materiais foi estudada por Microscopia de Força Atômica, AFM, (microscópio DI IIIa Nanoscope do LNLS, modo não-contato). Os resultados de AFM indicam que a maghemita apresenta uma estrutura nanométrica de morfologia esférica, caracterizada por um tamanho médio de partícula igual a 28 (16) nm. Os materiais híbridos mostraram morfologia similar. Embora tenham apresentado um considerável aumento do tamanho de partícula (~ 16 nm), estes materiais ainda possuem tamanho nanométrico, importante para a manutenção das suas características super-paramagnéticas. Além disso, estes materiais apresentaram um considerável aumento da condutividade elétrica, cerca de 256 vezes maior que a maghemita pura, possibilitando seu uso em aplicações diversas, como a blindagem eletromagnética e a construção de nano-relés.

Referência: Fernando Gomes de Souza Jr., Jéssica Alves Marins, José Carlos Pinto, Geiza Esperandio de Oliveira, Cezar Manzini Rodrigues, and Luis Mauricio T. R. Lima; Magnetic field sensor based on a maghemite / polyaniline hybrid material; Macromol. Mater. Eng., Submetido

Acknowledgements: Os autores agradecem ao CNPq, a CAPES e a FAPERJ pela ajuda financeira e pelas bolsas. Os autores também agradecem ao Laboratório Nacional de Luz Síncrotron pelo apoio no experimento AFM 8421/08.

Estudio de superficies de películas de O-DMS utilizando TXRF-XANES

A.M. Mudarra Navarro¹, F. Golmar², and Rodríguez Torres, C. E.¹

¹ Universidad Nacional de La Plata - La Plata Bs.As Argentina

² Universidad de Buenos Aires - Buenos Aires CapFe Argentina

Los óxidos semiconductores dopados con impurezas magnéticas (O-DMS) han suscitado gran interés desde el descubrimiento de ferromagnetismo a temperatura ambiente en semiconductores basados en óxidos tales como TiO_2 , SnO_2 y ZnO dopados con diversos metales de transición tales como Co, Fe, Cr, etc. No obstante el auge de la investigación en este tema, el origen del ferromagnetismo es aún incierto y hay serias controversias. En particular, se observa magnetismo en materiales con niveles de dopaje tan bajos que hacen imposible un acoplamiento de corto alcance y principalmente en películas delgadas (10-150 nm). Además, los momentos magnéticos no parecen depender del espesor de las películas (este resultado es usado como evidencia de la influencia de la interfase o superficie en el orden magnético). Una posible explicación de la presencia de ferromagnetismo en óxidos dopados con tan baja dilución de iones magnéticos es suponer que la distribución de dopantes no es aleatoria, sino que existan zonas más ricas en dopante. Por esto estudiar el perfil de concentración de dopante y la relación de este con las condiciones de deposición de las películas (por ejemplo el sustrato) es fundamental para la comprensión del mecanismo de acoplamiento magnético en estos materiales. Es posible que la presencia de interfase (sustrato/film) y de superficie (film/aire) derive en regiones más ricas (o pobres) en dopantes en estas zonas. En este trabajo se utiliza la combinación de las técnicas GIXRF y XANES para estudiar los perfiles de composición y las estructuras formadas como función de la profundidad en películas de TiO_2 y SnO_2 dopadas con Co. Las películas a estudiar fueron depositadas por el método de ablación láser, con composiciones $\text{Ti}_{0.9}\text{Co}_{0.1}\text{O}_2$ y $\text{Sn}_{0.9}\text{Co}_{0.1}\text{O}_2$ sobre tres sustratos diferentes: AlLaO_3 , SrTiO_3 monocristalinos y silicio. Los resultados así obtenidos se combinan con los resultantes de DRX, magnetometría y microscopía de fuerza atómica para elaborar un modelo sobre la relación entre parámetros extrínsecos y el comportamiento magnético de las muestras.

Acknowledgements: Los autores desean agradecer A Carlos Pérez de la línea XRF por la valiosa colaboración para llevar a cabo estas medidas.

SMALL-ANGLE X-RAY SCATTERING STUDIES IN COLLOIDAL SILICA/PMMA NANOCOMPOSITES

Peruzzo, P. J.¹, Anbinder, P. S.¹, Plivelic, T.S.², and Amalvy, J. I.¹

¹ Instituto de Investigaciones Fisicoquimicas Teoricas y Aplic - La Plata BA Argentina

² MAX Laboratory - Lund France

In a previous work (1) we have studied the morphology of silica/polymethylmethacrylate nanocomposites in solid form. SAXS results indicated the existence of different morphology according to silica particles characteristics. However agglomeration of particles in the solid state could modify the scattering pattern. To avoid solid state effects we have performed new SAXS determinations using the colloidal form of particles. SAXS measurements on samples were performed at the SAXS2 beam line at the LNLS (Campinas, Brazil) using a monochromatic beam of wavelength 1.608 Å and exposure time of 300 sec, and a sample detector distance of 1805.6 mm. As expected the curves obtained in the dispersion state exhibit more signals allowing a more detailed analysis of the morphology which include information about the particle size and their PSD. Porod's plots have an asymptotic linear regime for all the samples indicating the presence of abrupt and well-defined interfaces. The modeling of the latex particles is performed assuming that the particles are randomly oriented in the sample using the morphology suggested by transmission electron microscopy.

(1) Morphology of silica/polymethylmethacrylate nanocomposites, Peruzzo, P. J. and Amalvy, J. I. 2006 Activity Report (2007).

Acknowledgements: The authors would like to acknowledge Brazilian Synchrotron Light Laboratory (LNLS), Campinas, Brazil; CICIPBA and ANPCYT are thanked by financial assistance and Peter Greenwood from Eka Chemicals AB, Sweden for donating the colloidal silica samples. PJP is member of CONICET, PSA is a fellow from ANPCyT (Argentina) and JIA is member of CIC. TSP is a postdoctoral Fellow at MAX-lab (Lund University, POB 118, SE-22100 Lund, Sweden).

Fotofragmentação do politiofeno induzida por luz síncrotron na borda 1s do enxofre

Rita, J.R.S.¹, Rocco, M.L.M.¹, Roman, L. S.², and Arantes, C.¹

¹ Universidade Federal do Rio de Janeiro - Rio de Janeiro RJ Brazil

² Universidade Federal do Paraná - Curitiba PR Brazil

A fragmentação molecular e a dessorção de espécies ionizadas pode ser induzidas com irradiação da amostra com fótons de energia específica como decorrência de processos intramoleculares de decaimento a partir de sua ionização ou excitação, sendo este um importante processo não térmico de dessorção, podendo-se, inclusive, obter-se uma dessorção sítio-seletiva ou elemento-seletiva. Foi feito um estudo sistemático de caracterização espectroscópica, morfológica e de fragmentação envolvendo polímeros condutores (politiofenos), tendo sido obtidos espectros de NEXAFS e de dessorção iônica na linha de luz SXS do laboratório Nacional de Luz Síncrotron (LNLS). Duas estruturas foram observadas no espectros de fotoabsorção em 2472 eV e em 2480 eV, atribuídas a transições $1s \rightarrow \pi^*(4b_1)$ e $1s \rightarrow \sigma^*(8b_2)$ (C-S) e a transição $1s \rightarrow \sigma^*(8b_2)$ (C-C), respectivamente. Espectros de massas foram obtidos com um espectrômetro de massas do tipo TOF para amostras irradiadas nas energias indicadas pelo espectro de NEXAFS. Observou-se ainda o surgimento dos íons S^+ e S^{2+} , na energia de 2472 eV demonstrando a importância do processo Auger na formação destes íons. Diferentemente, as demais espécies podem ser observadas antes e depois da borda de absorção e seus rendimentos acompanham o rendimento de elétrons (NEXAFS). O estudo de rendimento de íons de enxofre em função da energia dos fótons nos leva a concluir que a dessorção destes íons é favorecida na energia de ressonância (2472 eV), pela quebra da ligação C-S, através do processo de decaimento ressonante Auger. Para as demais espécies, o processo XESD predomina.

Acknowledgements: Ao LNLS pelo uso de suas instalações, suporte logístico e de infraestrutura. Ao CNPq pelo suporte financeiro

EFFECTS OF ULTRAVIOLET LIGHT ON AlQ_3 THIN FILMS STUDIED BY PHOTOABSORPTION AND PHOTOEMISSION

Ricardo, W.¹, Rocco, M.L.M.¹, M. Cremona², Araujo, G.S.¹, and Quirino, W.³

¹ Universidade Federal do Rio de Janeiro - Rio de Janeiro RJ Brazil

² PUC - Rio de Janeiro - Rio de Janeiro RJ Brazil

³ Instituto Nacional de Metrologia, Normal e Qualidade Industr - Xerém RJ Brazil

Due to their applications in many different areas and manufacturing simplicity, organic light emitting diodes (OLEDs) represent a promising research line in the development of new optoelectronic devices. However, the degradation of the organic materials which are commonly used in the OLED fabrication is still the principal weakness of these devices. Many efforts were made in order to understand the factors that influenced the different degradation mechanisms of the OLEDs and their organic materials, being tris-(8-hydroxyquinoline)-aluminum (AlQ_3) one of the most attractive electroluminescent materials. In order to gain insight into the degradation mechanisms and evaluate the electronic structure of this organic material used as electroluminescence and electron transport layer in the elaboration of OLEDs, synchrotron radiation-based photoabsorption and photoemission techniques at carbon, nitrogen and oxygen 1s edges were employed using the SGM beam line from the Brazilian Synchrotron Light Source (LNLS). The unoccupied molecular orbitals (LUMOs) of AlQ_3 unexposed and exposed to ultraviolet light were probe using near-edge x-ray absorption fine structure (NEXAFS) in the total electron yield (TEY) mode while the occupied states (HOMO) were investigated by x-ray photoelectron spectroscopy (XPS). The results showed remarkable differences between exposed and non exposed AlQ_3 . Attenuation of peak intensities at C and N 1s transitions and shift in energy of the O1s transitions were observed for the exposed film. This suggests changes in the chemical environment with damage of the π -system of the molecule that might cause lost of electroluminescence and electron transport properties, and formation of dark emissive zone. We hope that theses studies contribute to the understanding of the irradiation damage mechanisms in AlQ_3 .

Acknowledgements: The authors would like to thank LNLS, CAPES and CNPq for financial support.

Nitrate hydrogenation on Pt,In/Al₂O₃. EXAFS and XANES characterization of fresh and used catalysts

Ramallo-López, J. M.¹, Requejo, F. G.¹, E.E.Miro², and Marchesini, F. A.²

¹ Universidad Nacional de La Plata - La Plata Bs.As Argentina

² Instituto de Investigaciones en Catalisis y Petroquimica - Santa Fé Argentina

In this work, bimetallic Pt,In supported on Al₂O₃ catalysts active for the reduction of nitrate to N₂ in water using H₂ as reducing agent were characterized by EXAFS and XANES. Among the catalysts studied, the one that contained 1 wt. % of Pt and 0.25 wt. % of In had a remarkable high initial activity which decreased with reaction time. For this catalyst, EXAFS characterization showed that the fresh solid consisted of a mixture of bimetallic Pt-In nanoparticles and monometallic Pt ones. Both EXAFS and XANES results show that after the nitrate hydrogenation reaction in aqueous media at room temperature was carried out, the amount of bimetallic nanoparticles decreased and that of unalloyed Pt considerably increased. This phase segregation could explain the partial deactivation of the catalyst.

Acknowledgements: This work was partially supported by ANPCyT (PICT 2008-00038 and 25515), UNLP, UNL and CONICET (PIP 12-200801-03079, CIAM Collaborative Program) from Argentina and by the LNLS, Brazil.

***In-situ* XANES study of Pt_xPd_{1-x} (x = 1, 0.7 or 0.5) nanoparticles subjected to H₂ reduction**

Bernardi, F.¹, Alves, M.C.M.¹, KILIAN, A. S.¹, BOITA, Jocenir.¹, Rodrigues, A.¹, and Morais, J.¹

Universidade Federal do Rio Grande do Sul - Porto Alegre RS Brazil

The nanoscience provides numerous and interesting applications of metallic nanoparticles in areas such as catalysis, information storage and optoelectronic. In catalysis, numerous efforts have been directed towards the search of new and more efficient catalysts for their use in the petroleum refinement processes. However, the present catalysts are very susceptible to sulfur poisoning and their use is limited, unless sulfur tolerance can be greatly improved. The XANES measurement of the L₃ and L₂ edges is an important tool used to obtain information about the electronic structure of the catalysts. In special for Pt containing materials, it is possible to quantitatively extract the fractional change in the number of *d*-band holes relative to a reference material. In a previous work (F. Bernardi et al., J. Phys. Chem. C, 113, 3909, 2009), non-supported Pt_xPd_{1-x} (x = 1, 0.7 or 0.5) nanoparticles were studied during H₂ reduction and sulfidation under H₂S atmosphere, both at 300 °C. The study revealed that the presence of sulfur atoms increases with the amount of palladium. In this work, we have studied Pt_xPd_{1-x} (x = 1, 0.7 or 0.5) nanoparticles subjected to H₂ reduction at 300 °C. The system was studied by *in-situ* x-ray absorption near edge spectroscopy (*in-situ* XANES) technique before and after the thermal annealing. The results show that the degree of sulfidation is proportional to the decrease of the fractional change in the number of *d*-band holes relative to the as-prepared sample after the reduction process.

Acknowledgements: We gratefully acknowledge the support given by the CNPq, CAPES, LNLS (proposals XAFS1 - 6574, XAFS1 - 6575, XAFS1 - 8179) and the LNLS staff. F. B. thanks the CNPq for his PhD fellowship and A. S. K. for his master PhD. J. B. and A. R. thank CAPES for the master fellowship.

Characterization of titanium dioxide films obtained with a vacuum arc

A. Kleiman¹, Lamas, D. G.², and A. Márquez¹

¹ Universidad de Buenos Aires - Buenos Aires DF Argentina

² Consejo Nacional de Investigaciones Científicas y Técnicas - Buenos Aires Argentina

The performance of TiO₂ films applied in heterogeneous catalysis for the removal of contaminant or as sensor of oxidant gasses depend mainly on the crystallographic phases present in the film and on the surface morphology. Films obtained by vacuum arc deposition (VAD) are attractive due to the high energy of the ions involved in this process and the high deposition rate. The films deposited with this method grow nano-structured and often show a structure with a preferential plane orientation. In this work a study of the crystalline structure and of the homogeneity, density and thickness of TiO₂ films grown with VAD at different conditions (substrate temperature, deposition time and number of discharges) on glass and silicon substrates is presented. The measurements were carried out at the XRD1 beam line of the LNLS using x-ray reflectometry (XRR) and x-ray diffraction (XRD) with grazing incidence. The measured XRR patterns were fitted employing the Parrat formalism. In all XRR registers, independently of the sample deposition conditions, the interference fringes were clearly observed, this result indicates a high homogeneity of the films and a low roughness (lower than 10 nm). The film density values obtained from XRR agreed with the tabulated values for anatase and rutile TiO₂ phases in accord with the structure determined from XRD. From XRR interference fringes film thickness from 70 to 300 nm were determined, by showing a good agreement with the thickness values estimated through transmittance measurements in the UV-visible range. These results were complemented by the analysis of the surfaces with an atomic force microscope.

Acknowledgements: This work was supported by grants from Buenos Aires University (PID X131), ANPCyT (PICT05 38251) and PROSUL (490580/2008-4)

Observation of Pd magnetism in carbon nanotube catalyst nanoparticles by X-ray circular dichroism

Roa, D. B.¹, Lacerda, R. G.¹, Magalhaes-Paniago, R.¹, and de Siervo A.²

¹ Universidade Federal de Minas Gerais - Belo Horizonte MG Brazil

² Universidade Estadual de Campinas - Campinas SP Brazil

Fe, Co and Ni nanoparticles are extensively used as catalysts to induce the formation of carbon nanotubes in general. The diameter of these nanoparticles range from 1-100nm, and should exhibit superparamagnetism. Recently, it has been observed that the introduction of Pd into these particles can stabilize its ferromagnetism [1].

We have here performed an extensive work of X-ray Magnetic Circular Dichroism (XMCD) at beamlines SGM and SXS of LNLS. XMCD was measured on Pd(Fe, Co,Ni) nanoparticles (with diameters ranging from 30-100nm) formed by plasma-enhanced chemical vapor deposition [2]. By accessing the L3 and L2 edges of Fe (707-720eV), Co (778-793eV), Ni(855-872eV) and Pd (3173-3330eV) we have clearly observed a dichroic signal in all atoms. Their magnetic moments in these materials was experimentally determined using the sum rules for XMCD [3]. The origin of magnetism in the formed alloys will be briefly discussed based on their electronic and nanostructural properties.

[1] T. Fujita, Y. Hayashi and T. Tokunaga, Appl. Phys. Lett. 90, 133116 (2007).

[2] Z.F. Ren et al., Science 282, 1105 (1998).

[3] C. T. Chen, Y. U. Idzerda, H. J. Lin, N. V. Smith, G. Meigs, E. Chaban, G. H. Ho, E. Pellegrin, and F. Sette, Phys. Rev. Lett. 75, 152 (1995).

Acknowledgements: This work was supported by LNLS, RedeNano Nanotubos and INCT Nanocarbono (CNPq).

Structural analyses of Laponite RD particles by SAXS

Batista, T.¹, MACHADO, D. S.¹, Oliveira Neto M.¹, Schmitt, C.C. ou Cavalheiro, C.C.S¹, Polikarpov, I.¹, A.F. Craievich², and Neumann, M. G.¹

¹ Universidade de São Paulo - São Carlos - São Carlos SP Brazil

² Universidade de São Paulo - São Paulo - São Paulo SP Brazil

Small Angle X-ray Scattering (SAXS) has become a powerful technique in colloidal science for determining size, shape and internal structure. Laponite RD suspension represents a colloidal system, which shows unique disk shape in aqueous solution, with radius of about 25 nm and thickness of 1 nm. Interaction between inorganic layered mineral and organic substances has attracted interest from both scientific and industrial perspectives. Understanding the structure of the clays in aqueous suspension is important for characterizing nanocomposites formed by clays and polymers [1]. It is known that periodic order in clay particles may induce changes in polymerization behavior that could influence final nanocomposite properties [2]. The present work consists in a SAXS study of Laponite RD aqueous suspension aiming to determinate structure parameter. Small angle X ray scattering (SAXS) was collected for different concentration of Laponite RD (0.25 to 2 g.L⁻¹) at the SAXS beamline at the Brazilian Synchrotron Light Laboratory (LNLS, Brazil), using wavelength $\lambda = 0.148$ nm, a bidimensional detector MARCCD and sample/detector distance equal to 1193.4 mm (momentum transfer (q) ranging from 0.18 nm⁻¹ to 2.24 nm⁻¹). The radius of gyration for Laponite RD was obtained by Guinier approximation ($\ln(I(q))$ as function of q^2) at smallest q range, $R_g \cdot q$ smaller or equal to 1.3 (q ranging from 0.12 nm⁻¹ to 0.16 nm⁻¹). The R_g value obtained was 10.8 nm. The intermediate q range from 0.6 nm⁻¹ to 1.15 nm⁻¹ give information about particle thickness. Laponite RD scattering curves show a decay of q^{-2} , indicating a flat particles shape.

1. Ho, D, L., Briber, R. M., Glinka, C. J., Chem. Matter., 2001, 13, 1923 - 1931.
2. Adom, K., Guymon, C. A., Polymer, 2008, 49, 2636 - 2643

Acknowledgements: LNLS, Fapesp, Capes

PROPRIEDADES ESTRUTURAIS E MAGNÉTICAS EM NANOPARTÍCULAS DE $\alpha - Fe_2O_3$

Lima, R. J. S.¹, Jesus, J. R.¹, Cunha, T. R.², Moura, K. O.¹, Duque J.G.S.¹, and Meneses, C. T.¹

¹ Universidade Federal de Sergipe - São Cristóvão SE Brazil

² Universidade Federal de Sergipe - São Cristóvão SE Brazil

O estudo do desenvolvimento, produção e caracterização de nanomateriais tem sido um dos temas mais atraentes da pesquisa nos últimos anos. O grande interesse nesses materiais está relacionado às diversas aplicações que estes podem ser destinados. Dentro da classe dos nanomateriais, os nanomagnéticos têm atraído interesse devido às mudanças em suas propriedades magnéticas quando comparadas com as do material em forma massiva. Independente do composto estudado, em geral, uma das principais características apresentada por materiais nanomagnéticos é o superparamagnetismo. Esta característica é apresentada em nanopartículas (NPs) abaixo de um tamanho crítico, pois apresentam somente um monodomínio magnético (que difere dos materiais massivos que se dividem em múltiplos domínios magnéticos). Neste sentido, as propriedades físicas desses sistemas podem ser controladas de acordo com o interesse científico ou tecnológico específico. Sendo assim, a preparação e obtenção desses sistemas de modo controlado são de extrema relevância. Por isso, o interesse em métodos de síntese de NPs tem crescido nos últimos anos com o intuito de aprimorar o controle no crescimento e as características física e químicas desses materiais. Neste trabalho nós temos usado o método de co-precipitação para sintetizar nanopartículas de óxidos de ferro III (Fe_2O_3) e estudar as propriedades estruturais e magnéticas controlando os tamanhos e efeitos após a adição de um precursor orgânico (PO). Resultados de difração de raios-x (DRX) juntamente com refinamento Rietveld mostram a formação de NPs de 15nm. Adicionalmente, foi verificada uma forte dependência do decréscimo no tamanho com a adição do precursor orgânico, assim como, com a redução da temperatura de síntese. Resultados de magnetização em função do campo confirmam a formação de NPs com propriedades superparamagnética para amostras preparadas com a adição de PO indicando um decréscimo no tamanho da partícula. Resultados de MEV (FEG) mostram uma mudança de habito cristalográfico, assim como uniformidade nos tamanhos quando preparadas com a adição do PO.

Acknowledgements: Pelo suporte financeiro FAPITEC/SE, CAPES e CNPq.

Electronics, local structure and morphology of heterogeneous nanoparticles investigated by SAXS and XAFS techniques

Giovanetti, L. J.¹, Ramallo-López, J. M.¹, Requejo, F. G.¹, E. V. Shevchenko², and Craievich AF³

¹ Universidad Nacional de La Plata - La Plata Bs.As Argentina

² Lawrence Berkeley National Laboratory - Berkeley CA United States of America

³ Universidade de São Paulo - São Paulo - São Paulo SP Brazil

Nanoparticles (NP) with heterogeneous structures like core@shell, that comprise a core of one material and a coating shell of another material, or dumbbell-shaped NP (where one NP is linked to another) are of great interest because of their different possibilities to control their physicochemical properties. Since the size and material properties in dumbbell NP can be manipulated at will, a vast range of particles can be made with myriad properties, useful in areas like catalysis, nano-sensors for cellular imaging, gap controlled semiconductor, etc[1, 2]. In this work we present a combined study using Transmission Electron Microscopy (TEM), Small Angle X-ray Scattering (SAXS) and X-Ray absorption spectroscopy (XAS) of Pt_3Co and Pt_3Co /Au dumbbell-shaped NP. The synthesis of dumbbell-shaped NP containing Pt_3Co and Au NP involves two steps: (i) synthesis of Pt_3Co NPs and (ii) deposition of gold onto one of facets of Pt_3Co NP[3]. TEM and SAXS experiments were done on the dumbbell system and the isolated NP. By modeling of the obtained experimental SAXS curves it was possible to elucidate the morphology of the isolated NP and the structural modification introduced during the formation of the dumbbell structure. By the analysis of XAFS spectra obtained in $Co - K$, $Au - L_3$ and $Pt - L_3$ edges, changes in the electronic structure introduced by the stinking of the NP were analyzed.

Referências

- [1] Daniel, M.-C. , Astruc, D. Chem. Rev. 104, (1), 2004, 293-346.
- [2] Burda, C., Chen, X., Narayanan, R., El-Sayed, M.A. Chem. Rev. 105, (4), 2005, 1025-1102.
- [3] Pellegrino, T., A. Fiore, et al. J. of the Am. Chem. Soc. 128(20), 2006, 6690-6698.

Acknowledgements: This work was partially supported by projects PIP 03079 (CONICET, Argentina), CIAM Argentine-Brazil-Canada collaborative project (CONICET-CNPq-NSERC), PICT 00038 and PICT 25515 (ANPCyT, Argentina) and D04B - XAS 6609/07 (LNLS, Brazil).

Aplicação de AFM/EFM na caracterização de eletrodos carbono cerâmicos

Arguello, J.¹, ARENAS, Leliz Ticona², Pimentel, V. L.³, and Gushikem, Y.²

¹ Centro Universitário Franciscano - Santa Maria RS Brazil

² Universidade Estadual de Campinas - Campinas SP Brazil

³ Laboratório Nacional de Luz Síncrotron - Campinas SP Brazil

Eletrodos carbono cerâmicos (ECCs) têm encontrado importantes aplicações como materiais na construção de sensores eletroquímicos desde o pioneiro trabalho de Lev [1]. ECCs à base de matrizes inorgânicas de óxido de silício com partículas de grafite dispersas foram caracterizados morfológica e eletricamente por Microscopia de Força Atômica (AFM) e de Força Elétrica (EFM). As propriedades elétricas são fortemente influenciadas pela estrutura, e o EFM permite monitorar os gradientes verticais de força elétrica entre a ponta do cantilever e a amostra [2]. Visto que as reações eletroquímicas acontecem na interface eletrodo- dissolução, as técnicas de AFM/EFM auxiliam na caracterização superficial de estes eletrodos, oferecendo informações elétricas e morfológicas que acrescentam ao conhecimento sobre o sistema e explicam alguns efeitos eletrocatalíticos observados. ECCs em forma de discos prensados (5 mm de diâmetro) foram analisados com um microscópio de força atômica modelo Nanoscope IIIa (Digital Instruments) à temperatura ambiente. A análise dos perfis topográficos e as imagens de EFM sugerem uma distribuição de carga homogênea, o que estaria em concordância com os dados que indicam uma boa reprodutibilidade nas medidas após o processo de renovação de superfície.

Referencias 1) M. Tsionsky, G. Gun, V. Giezer, O. Lev, Analytical Chemistry 66 (1994) 1747 2) P. Girard, Nanotechnology 12 (2001) 485

Acknowledgements: Ao MTA, Laboratório Nacional de Luz Síncrotron (LNLS), a Rede Nacional de Pesquisa em Nanotubos-CNPq e a FAPESP.

Structure of PbTe(SiO₂)/SiO₂ multilayers deposited on Si (111)

Kellermann, G.¹, Rodriguez, E.², Cesar, C. L.³, E. Jimenez⁴, Barbosa, L. C.³, and Craievich AF⁵

¹ Laboratório Nacional de Luz Síncrotron - Campinas SP Brazil

² Centro de Investigación en Ciencia Aplicada y Tecnología Ava - Altamira Tamau Mexico

³ Universidade Estadual de Campinas - Campinas SP Brazil

⁴ Universidad de la Havana - Habana Cuba

⁵ Universidade de São Paulo - São Paulo - São Paulo SP Brazil

The structure of multilayers composed of layers of PbTe nanocrystals embedded in SiO₂, named as PbTe(SiO₂), between homogeneous layers of amorphous SiO₂ deposited on a single crystal Si (111) substrate, was studied by grazing-incidence small-angle x-ray scattering (GISAXS) as a function of PbTe content. PbTe(SiO₂)/SiO₂ multilayers were produced by alternatively applying plasma enhanced chemical vapor deposition and pulsed laser deposition techniques. From the analysis of the experimental GISAXS patterns, the average radius and radius dispersion of PbTe nanocrystals were determined. For increasing deposition dose the size of PbTe nanocrystals progressively increases while their number density decreases. The analysis of the GISAXS intensity profiles along the normal to the sample surface allowed us to determine the period parameter of the layers and a structure parameter that characterizes the disorder in the distances between PbTe layers.

Acknowledgements: This work was supported by Brazilian Synchrotron Light Laboratory (LNLS) and Brazilian founding agencies: PRONEX, CNPq and FAPESP.

Caracterização de Processos de Silanização em Superfície de SiO₂ por MEV, XPS e AFM para Construção de Biossensores

Lima, R. S.¹, Rodrigues Filho, U.P.¹, Nascente, P. A. P.², Piazzetta, O.M.H.³, Gobbi, A. L.³, Pimentel, V. L.³, Coltro, W. K. T.⁴, and Carrilho, E.¹

¹ Universidade de São Paulo - São Carlos - São Carlos SP Brazil

² Universidade Federal de São Carlos - São Carlos SP Brazil

³ Laboratório Nacional de Luz Síncrotron - Campinas SP Brazil

⁴ Universidade Federal de Goiás - Goiânia GO Brazil

O reagente 3-(aminopropil)trietoxissilano (APTS) é um dos intermediários de imobilização mais empregados na construção de biossensores. Porém, o uso dessa substância pode acarretar em suspensões coloidais ou polimerizar-se na superfície do substrato gerando depósitos irregulares [2]. O objetivo deste trabalho é otimizar as condições de silanização em superfície de SiO₂ utilizando-se o composto 4-(trietoxissilil)butironitrila (ButCN) com vista à não formação de aglomerados coloidais. Serão empregadas as técnicas: MEV, XPS e AFM. Foram investigados diferentes tempos de reação, a saber: 15, 30, 60, 150 e 300 min. As micrografias indicaram que não houve formação de depósitos irregulares sobre as superfícies de SiO₂. Em relação aos espectros de XPS, os picos do N(1s) apresentaram forma de linha assimétrica, com identificação do grupo nitrila em 400,6 eV apenas após 30 min de imersão das placas de SiO₂ em solução de ButCN. Isso nos mostra que não houve silanização decorridos 15 min de imersão. Para os demais tempos, as relações percentuais N/Si foram: 2,8 (30 min); 5,2 (60 min); 4,8 (150 min) e 5,1 (300 min). Observa-se que a relação N/Si se manteve aproximadamente constante após 60 min de adsorção do ButCN, o que pode ser atribuído à saturação dos grupos silanóis da superfície de SiO₂ disponíveis para silanização. A partir das análises de AFM, foi verificada uma elevação razoável na rugosidade média quadrática da amostra modificada por tempo de 1 h em relação ao substrato não modificado (aumento de 0,5 para 1,2 nm), o que evidencia a ocorrência de silanização. Adicionalmente, gráficos fractais mostraram uma distribuição de matéria uniforme sobre o dióxido de silício. Por fim, conclui-se que a metodologia proposta resultou em uma modificação efetiva da superfície de SiO₂ pelo ButCN, sendo verificado o tempo de adsorção de 1 h como satisfatório para os objetivos desejados.

Acknowledgements: FAPESP, CNPq e CAPES

Efficient Microwave-Assisted Hydrothermal Synthesis of CuO Sea Urchin-Like Architectures via a Mesoscale Self-Assembly

Volanti, D.P.¹, Orlandi, M.O.¹, Longo, E.¹, and Andrés, J.²

¹ Universidade Estadual Paulista - Araraquara - Araraquara SP Brazil

² Universitat Jaume I - Castelló de la Plana Spain

For the first time, we provide evidence for both nucleation at the mesoscale and the progression of the crystallization process during microwave-assisted hydrothermal environment of cupric oxide (CuO) with sea urchin-like morphology. In the study presented here, CuO microcrystals were growth via applied microwave electrical radiation obtained by reaction of Cu(II) ions with aqueous ammonia at 20°C without the use organic additives. The entire sequence of the crystallization procedure of CuO intermediates was monitored by field emission scanning electron microscopy in combination with transmission electron microscopy carried out on the precipitates collected after 30 seconds and final stage after 15 minutes. By carefully analyzing the nanoparticles, intermediates and the final CuO architectures, we found that the nature of the mechanism follows a nonclassical growth process involving mesoscale self-assemblies and oriented attachment of CuO nanoparticles.

Acknowledgements: Brazilian agencies FAPESP and CNPq for their financial support. The TEM facilities were supplied by LME-LNLS (National Laboratory of Synchrotron Light-Brazil). Professor Juan Andrés acknowledges research funds provided by the Ministerio de Educación y Cultura of the Spanish Government.

Alterações composicionais induzidas por luz ultravioleta de vácuo em filmes finos calcogênicos

Moura, P. R.¹ and Almeida, D. P.¹

Universidade Federal de Santa Catarina - Florianópolis SC Brazil

Apresentamos aqui os resultados das caracterizações composicionais das ligas calcogênicas Sb₅₀Te₅₀ e Te₂₄In₃₈Sb₃₈ na forma de filmes finos. Para tal foi usada a técnica de espectroscopia de fluorescência de raios - X por dispersão de energia (EDS). As ligas calcogênicas Sb₅₀Te₅₀ e Te₂₄In₃₈Sb₃₈ foram sintetizadas por moagem mecânica em um moinho de bolas de alta energia e posteriormente depositadas em vácuo sobre substratos de mylar por evaporação térmica resistiva na forma de filmes finos. Posteriormente os filmes finos foram expostos à luz ultravioleta de vácuo, proveniente da linha de luz TGM. Através dos resultados de fluorescência de raios - X por dispersão de energia observou-se que as composições químicas dos filmes finos ficaram levemente alteradas no interior das regiões irradiadas em comparação com as regiões como depositadas, indicando uma migração dos elementos constituintes, demonstrando que os filmes finos calcogênicos estudados têm potencial como material de mudança de fase para gravação óptica na região do ultravioleta.

Acknowledgements: Os autores agradecem ao LNLS e ao Laboratório Central de Microscopia Eletrônica (LCME) da UFSC.

Caracterização estrutural e química da superfície de $Cu_{84}Al_{16}(100)$ e $Cu_{90}Au_{10}(100)$ usando XPD

Martins, M. D.¹, Cotta, A. C.¹, Soares, E.A.², and W. A. A. Macedo¹

¹ Centro de Desenvolvimento Tecnologia Nuclear - Belo Horizonte MG Brazil

² Universidade Federal de Minas Gerais - Belo Horizonte MG Brazil

O estudo da correlação entre estrutura e magnetismo em sistemas magnéticos epitaxiais tem atraído grande interesse tanto do ponto de vista experimental quanto teórico. Um sistema típico é a fase ccc (cúbico de corpo centrado) do Fe estabilizada à temperatura ambiente via crescimento epitaxial sobre substratos ccc, intensamente estudado nos últimos 20 anos e que ainda hoje desperta grande interesse. Este sistema apresenta uma complexa correlação entre estrutura e magnetismo, conhecida como instabilidade magneto-volumétrica, caracterizada pela forte dependência do estado magnético com o volume atômico (parâmetro de rede), que pode variar de não-magnético, antiferromagnético e ferromagnético. Neste contexto, temos estudado o efeito da variação do parâmetro de rede no magnetismo de sistemas contendo Fe-ccc via crescimento epitaxial sobre diferentes substratos monocristalinos, em especial o $Cu(100)$, e ligas de cobre como, por exemplo, $Cu_3Au(100)$, $Cu_{90}Au_{10}(100)$ e $Cu_{84}Al_{16}(100)$. A liga $Cu_{84}Al_{16}(100)$, utilizada de modo inédito pelo nosso grupo de pesquisa, apresenta uma expansão da rede cristalina de 1% em relação ao $Cu(100)$. Investigamos em detalhes o crescimento epitaxial de filmes ultrafinos de Fe sobre estes substratos e correlacionamos as propriedades estruturais e magnéticas. No entanto, percebemos que não existe na literatura um estudo detalhado do ordenamento estrutural e da composição química da superfície das ligas $Cu_{84}Al_{16}(100)$ e $Cu_{90}Au_{10}(100)$ (todas as informações obtidas se referem ao volume). Neste projeto, investigamos a estrutura cristalina e a composição química da superfície de $Cu_{84}Al_{16}(100)$ e $Cu_{90}Au_{10}(100)$ utilizando espectroscopia (PES) e difração de fotoelétrons, nos modos de varredura angular (XPD X-ray photoelectron diffraction) e varredura em energia (PhD Photoelectron Diffraction), técnicas sensíveis à superfície e ao elemento químico e que permitem um estudo individualizado da superfície, relativo ao volume da amostra, e de cada um dos elementos que compõem as ligas. O experimento foi realizado na linha de luz SGM equipada com a estação de trabalho de análise de superfícies (câmara ultra alto vácuo equipada com manipulação de amostras com capacidade de aquecimento e movimentação angular (theta,phi), canhão de sputtering, analisador de elétrons de baixa energia) utilizando radiação síncrotron com energia dos fótons na faixa de 300 a 900 eV.

Acknowledgements: Este trabalho tem apoio do CNPq, FAPEMIG e CNEN.

Síntese e caracterização de nanopartículas de Pt suportadas em γ -alumina.

Meira, D. M.¹, Ribeiro, R.U.¹, Zanchet, D.², and Bueno, J.M.C.¹

¹ Universidade Federal de São Carlos - São Carlos SP Brazil

² Laboratório Nacional de Luz Síncrotron - Campinas SP Brazil

Nanopartículas (NPs) de Pt coloidais protegidas por PVP (polivinilpirrolidona) foram preparadas por meio da redução química do H_2PtCl_6 por etilenoglicol ou metanol de acordo com a literatura [1,2] e incorporadas durante a preparação de boehmita pelo método sol-gel. O objetivo é a preparação de catalisadores com estreita distribuição de tamanhos e estáveis em diversas reações. Variando-se parâmetros de síntese das NPs como álcool redutor e/ou quantidade de PVP foram preparadas NPs com tamanho médio de 2, 4 e 10 nm e a estreita distribuição de tamanho foi confirmada por microscopia eletrônica de transmissão (TEM). A boehmita contendo as NPs foi submetida a tratamentos térmicos para conferir estabilidade em condições severas de reação. Diversos tratamentos *ex-situ* em He, ar e H_2 foram realizados. Medidas de infravermelho por refletância difusa (DRIFTS) *in-situ* indicaram que a remoção do PVP ocorre em atmosferas ricas em O_2 em temperaturas ~ 400 °C. Já a transição de fase de boehmita para γ -alumina ocorre tanto em atmosfera de He como ar. Medidas de difração de raios X (DRX) e TEM dos catalisadores após os tratamentos indicaram que o tratamento em atmosfera de He seguido de ar é menos agressivo as partículas menores, porém um tratamento subsequente em H_2 provoca aglomeração severa da Pt. Por outro lado, uma maior quantidade de PVP adicionado durante a síntese das NPs com menor tamanho promove maior estabilidade e evita a aglomeração da Pt. Este efeito também foi observado para as NPs com tamanho médio. Estudos de redução à temperatura programada (500 °C a 10 °C /min) e reação de reforma a vapor do metano (760 °C) foram acompanhados de medidas de espectroscopia de raios X (XAS) *in-situ*. A região próxima a borda (XANES) permitiu o monitoramento do perfil de redução das partículas de Pt por meio da variação de intensidade da linha branca. Medidas da estrutura fina após a borda (EXAFS) possibilitaram a determinação do tamanho das partículas através do número de coordenação e verificar que em altas temperaturas ocorre variação de morfologia das mesmas. Além disso, não ocorreu aglomeração significativa das partículas após reação o que indica que estes materiais podem ser utilizados como catalisadores promissores em reações sensíveis a estrutura. [1] H. Song, et al. JACS 2006, 128, 3027. [2] Teranishi et al. J. Phys. Chem. B, 103, 19, 1999.

Acknowledgements: Agradecimentos ao LSQ, LME, XRD2 e XAFS2.

Characterization of TiO₂ films made by anodic oxidation on Ti-6Al-4V

Vera, M. L.¹, Ares, A.E.¹, Rosenberger, M. R.¹, Lamas, D. G.², and Schvezov, C. E.¹

¹ CONICET - Universidad Nacional de Misiones - Posadas-Misiones Argen Argentina

² Consejo Nacional de Investigaciones Científicas y Técnicas - Buenos Aires Argentina

The Ti-6Al-4V alloy is widely used as a structural material due to its excellent mechanical and corrosion resistant properties. At present they are also used in mechanical prosthetic devices for human implants due to the excellent biocompatibility. The bio and chemical properties of titanium alloys are known to be associated to the formation of TiO₂ on the surface which occurs naturally. Oxide films in metals can also be produced by anodic oxidation, resulting in films which may be thicker and denser than the natural oxides [1-3]. In this work TiO₂ films on Ti-6Al-4V substrates were produced by anodic oxidation, using a H₂SO₄ 1 M solution as electrolyte at different voltages (from 10V to 70V). Thickness and phase composition of the films were determined by X-ray reflectometry and X-ray diffraction, respectively. These experiments were carried out at the D12A-XRD1 beamline of the LNLS. The results of the influence of voltage on color, thickness, morphology and crystalline structure of the oxides are presented which are necessary to analyze for the production of coatings for biomedical applications. TiO₂ films of different colors were obtained, with thickness ranging from 20 to 200 nm depending on the applied voltage. Relationships among voltage, color and thickness were confirmed. The film roughness is of the order of the substrate roughness and it increases with the applied voltage. The oxide layers produced at low voltages up to 50V are smooth and amorphous. A spark discharge occurs, at voltages larger than 60V, producing porous and crystalline (anatase and rutile) coatings. Each of these morphologies and structures of the coatings are suitable to different biomedical applications and devices.

[1] D. Velten, V. Biehl, F. Aubertin, B. Valeske, W. Possart, and J. Breime, *Journal of Biomedical Material Research*, 59 (2002), 18-28. [2] A.K. Sharma, *Thin Solid Films*, 208 (1992), 48-54. [3] M.V. Diamanti, and M.P. Pedefferri, *Corrosion Science*, 49 (2007), 939-948.

Acknowledgements: The authors acknowledge various funding supports provided by 1) Laboratório Nacional de Luz Síncrotron (LNLS), Campinas, Sao Paulo-Brasil, 2) National Agency for Science and Technology Promotion (ANPCyT), Buenos Aires-Argentina and 3) National Council of Scientific and Technical Research (CONICET), Buenos Aires-Argentina.

Mechanical Deformation of Gold Atomic-size Nanowires

Lagos, M.J.¹, Sato F.², D. S. Galvao¹, and Ugarte, D.¹

¹ Universidade Estadual de Campinas - Campinas SP Brazil

² Universidade Federal de Minas Gerais - Belo Horizonte MG Brazil

The mechanical properties of a strained nanoscale volume of matter represent a fundamental issue for understanding phenomena such as friction, fracture, adhesion, etc. Miniaturization levels are raising the need of accurately characterizing nanodevices and nanomaterials, to develop models and predictions of their mechanical performance and reliability. But, we must also consider that the deformation of macroscopic matter continues to be a very interesting and dynamic research field displaying open questions and polemical issues. In this work, we have analyzed the atomistic aspects of the elongation of one-nm-wide metal rods as function of temperature using in-situ high resolution electron microscopy. For gold nanorods (NR) no extended defect could be observed at room temperature, while at 150 K stacking faults (SF) and twins (TW) are generated frequently. In fact, we have observed that as their size is reduced, the energy barriers became very small that thermal ambient energy is sufficient to overcome them. Then, NRs display an extended elastic regime until a mechanism with high enough blocking barrier can be nucleated. We have also determined experimentally the barrier energy associated to SF recombination process, which is about 40 meV. We have also developed ab initio calculations to derive the total energy changes associated with SF formation in NRs. Ab-initio calculations revealed that contribution from surface steps overrule stacking fault energetics in NRs, in such a way that system size and shape determines preferred faults gliding directions. The relation between morphology and surface steps can produce anisotropic behavior and, even large differences in elastic or plastic response for elongation or compression.

Acknowledgements: We acknowledge P.C.Silva for support during sample preparation. We also thank LNLS, FAPESP and CNPq for financial support.

Study under pressure of XANES spectra in K-edge of zirconium in ZrO₂-CeO₂ nanopowders at different concentrations of ceria

Caravaca, M.A.¹, Casali, R.A.², Ponce, C.A.², Garcia, F.³, Lamas, D. G.⁴, and Fuentes, R. O.⁴

¹ Universidad Nacional del Nordeste - Resistencia CHACO Argentina

² Universidad Nacional del Nordeste - Corrientes Argentina

³ Laboratório Nacional de Luz Síncrotron - Campinas SP Brazil

⁴ Consejo Nacional de Investigaciones Científicas y Técnicas - Buenos Aires Argentina

ZrO₂-x%CeO₂ is useful in oxygen storage, gas sensors and presently studied as electrolyte in fuel cell batteries. These solid solutions show phase transformation with Ce concentrations: the tetragonal phase is stable at 10% < x < 70% while the cubic is fully stabilized at $x > 80\%$ CeO₂. The influence of Ce on structure was studied by XRD and analyzed by the X-ray absorption technique EXAFS [1]. However possible phase transformation under extreme conditions as hydrostatic pressures is not well known. The aim of the present work is to study possible local changes of 18 KeV Zr K-edge of XANES spectra due to the applied pressure. The experimental setup consist of a Diamond Anvil Cell Device where the sample, fluid and pressure gauge were mounted in the Dispersive X-ray Absorption Spectroscopy (DXAS) line of LNLS. Samples of nanostructured ZrO₂- CeO₂ solid solutions at different concentration of ceria in tetragonal phase are studied under pressures in the range 0-12 GPa and compared with XANES spectra at normal conditions, in order to clarify if there is change in the structural domain asociated with zirconia oxide in the whole matrix. This changes are analized in terms of the nanoparticle size and applied pressure. Due that the oxygen storage capacity (OSC) performance is asociated with the presence of ZrO₂ in the cubic form, this work can reveal if OSC is improved in an hydrostatic stressed enviroment.

[1] D. G. Lamas, R. O. Fuentes, I. O. Fábregas, M. E. Fernández de Rapp, G. E. Lascalea, J. R. Casanova, N. E. Walsöe de Reça and A. F. Craievich, J. Appl. Cryst. (2005). 38, 867-873

Acknowledgements: This work was supported by Universidad Nacional del Nordeste, LNLS, ANPCyT and CONICET. We acknowledge the support of Edson J. de Carvalho during the development of the work at LNLS

Estudo de catalisadores industriais LTS por absorção de raios X *in situ* no processo de ativação e na reação de deslocamento água - gás

Oliveira, D. C.¹, Oliveira, M. P.¹, and Zanchet, D.¹

Laboratório Nacional de Luz Síncrotron - Campinas SP Brazil

A obtenção de hidrogênio (H₂) pode ser realizada por diversas vias industriais conhecidas, dentre elas a reação de deslocamento água-gás (também chamada de *shift*). Nesta reação, o hidrogênio (e também o dióxido de carbono, CO₂) é produzido pela reação de CO e vapor de água utilizando-se catalisadores conhecidos como LTS (ou *low shift reaction*), que são formados essencialmente por Al₂O₃, ZnO e CuO, sendo o último composto considerado o responsável pela atividade catalítica. Este trabalho avaliou o processo de ativação de dois catalisadores industriais LTS fornecidos pela Oxiten S. A. Ind e Com., no processo de ativação *in situ* e na reação de deslocamento água-gás, utilizando-se a técnica de espectroscopia de absorção de raios X (XAFS). Estes experimentos foram realizados na linha de luz XAFS1 do LNLS, com um forno acoplado a um sistema de alimentação de gases (H₂ para a ativação e CO, He e vapor d'água para *shift*). Industrialmente a ativação ocorre até 230°C, temperatura na qual se inicia a reação de *shift*, pois os catalisadores podem se tornar ineficientes devido às alterações que sofrem na sua estrutura em temperaturas superiores. Nestes experimentos, a ativação de cada catalisador foi acompanhada por medidas de absorção de raios X na borda K do Cu (8979 eV). Após a confirmação da redução, o mesmo catalisador foi submetido às condições da reação de *shift*, e a reação foi acompanhada por absorção de raios X na borda K do Cu e por espectrometria de massas através dos sinais dos produtos da reação (CO₂ e H₂). Os resultados mostraram que a redução da fase CuO à Cu metálico ocorre em diferentes temperaturas para as duas amostras, e que estas temperaturas dependem fortemente das condições utilizadas. As diferenças entre as amostras são maiores antes do processo de ativação; após este processo e também após a reação de *shift* não foram notadas diferenças significativas.

Acknowledgements: Marco A. Logli e Valéria P. Vicentin Oxiten e linha XAFS1.

Estudo da ativação de catalisadores comerciais LTS por XPS

Oliveira, D. C.¹, Zambello, F. R.¹, and Zanchet, D.¹

Laboratório Nacional de Luz Síncrotron - Campinas SP Brazil

Os catalisadores LTS (do inglês *low shift reaction*) são utilizados na obtenção de hidrogênio (H_2), que é um gás extremamente importante como combustível e também em diversos processos industriais, como por exemplo, a obtenção de amônia (NH_3). Estes catalisadores são utilizados na reação de CO com H_2O (vapor) para obtenção de H_2 e CO_2 sob condições brandas de temperatura. A composição dos catalisadores estudados aqui, fornecidos pela Oxiteno S. A. Ind e Com., é de Al_2O_3 , ZnO e CuO, sendo o último composto considerado o responsável pela atividade catalítica. Para isso, é necessária a redução do CuO a Cu metálico, durante o processo de ativação do catalisador. Neste trabalho foram estudados os processos de ativação de 2 catalisadores industriais, de composições similares, através da técnica de espectroscopia de fotoelétrons excitados por raios X (XPS), para o estudo da redução do cobre e da estrutura inicial e final da superfície dos mesmos em relação aos outros componentes. Os catalisadores foram submetidos individualmente a diferentes tratamentos térmicos, sob diferentes fluxos de H_2 , em um forno acoplado ao equipamento de XPS. Após o tratamento, os catalisadores foram transferidos para o equipamento sem haver exposição ao ar. As análises foram realizadas em temperatura ambiente e sob vácuo (10^{-8} mbar), no intervalo de 1200 a 0 eV, e análises mais detalhadas foram realizadas na região do Cu 2p, Zn 2p, O 1s e Al 2s e 2p. Os resultados na região do Cu mostraram que ocorre a redução do CuO a Cu metálico e que, por XPS, os outros componentes não são significativamente alterados pelo processo de redução. Foi observado ainda que a eficiência da redução é fortemente influenciada pela geometria do forno, pelo fluxo de gases e pela maneira de preparação das amostras.

Acknowledgements: Ao prof. Dr. Richard Landers pelo auxílio na interpretação de dados.

Monitoring the formation of Cu-based nanoparticles by in-situ DXAS

BOITA, Jocenir.¹, Bernardi, F.¹, KILIAN, A. S.¹, Rodrigues, A¹, Alves, M.C.M.¹, and Morais, J.¹

Universidade Federal do Rio Grande do Sul - Porto Alegre RS Brazil

Metal nanoparticles have attracted a great deal of attention and have been extensively exploited for their unique optical, electric, magnetic and catalytic properties, which are different from those of bulk materials. The basic properties of metal nanoparticles are mainly determined by size, shape, composition, crystallinity, and structure. The importance of producing copper based nanoparticles is exemplified by their applications such as high surface area catalysts, e. g., butanol dehydrogenation reaction, carbon monoxide oxidation and photocatalysis [3-6]. We have synthesized copper-based nanoparticles under mild conditions and followed the formation of the solid clusters during the reduction process using in-situ x-ray absorption spectroscopy (XAS). The in-situ XAS measurements were performed at the DXAS beamline of the LNLS. The samples were also characterized by x-ray photoelectron spectroscopy (XPS), x-ray diffraction, (XRD) and electron microscopy. The results show the formation of crystalline systems with particle size in the sub-micrometer scale, and a correlation between the data obtained by the different techniques used will be presented.

Acknowledgements: We gratefully acknowledge the support given by the CNPq, CAPES, LNLS (proposals DXAS 8150, DXAS 8768 and SXS - 7648) and the LNLS staff.

Structural Properties Control of InP Semiconductor NWs

Th. Chiaramonte¹, Tizei, L. H. G.¹, Ugarte, D.¹, and Cotta, M.A.¹

Universidade Estadual de Campinas - Campinas SP Brazil

An important signature of InP NWs is the presence of an inversion structure (stacking faults SFs) along their axial length. The InP inversion is a phenomena known as polytypism whereby crystalline planes can be stacked as zincblend (ZB) and wurtzite (WZ) alternating segments, even if a ZB substrate is used as a mechanical support for the Au nanoparticles (NPs). The presence of WZ and ZB InP NW structures has been attributed to different supersaturation levels in the NP during growth. Furthermore, another important crystallographic property which depends on the supersaturation levels in the NP during growth is the NW sidewall roughness. However, neither vapor-liquid-solid (VLS) or vapor-solid-solid (VSS) mechanisms could yet provide rough NW sidewalls and analyze their formation. In this work we investigate the effects of growth kinetics on the overall structure of InP NWs grown at 420°C, showing that, by carefully choosing growth parameters, both morphology and crystallography can be controlled to obtain from almost perfect WZ InP NWs to rough NWs with large SFs density. Using scanning and high resolution transmission electron microscopy and energy dispersive X-Ray spectrometry (SEM, HRTEM and EDS, respectively), we analyzed NW diameter dependence, SFs density and supersaturation level in NP as a function of the In precursor flow used for growth. Our results show that for low In flows the NWs are tapered. For high In flows increasing diameter variation along the NW length and the SFs density were observed. EDS measurements in the NP volume exhibited only the presence of In and Au elements and the In concentration is around 25 at %, particularly for those grown with larger TMI flows. A closer examination of the NW sidewalls grown under high In flow, by HRTEM, suggests facet formation along the NW. However, we observed different NWs structures under constant supersaturation level at the NP. Then, we believe that a competition for nucleation sites at the three phases (the vapor-liquid-solid or the triple phase line, TPL) occurs, from material diffusing either through or around the NP, according to the interpretation of our data based on mass transport models. We believe that SF formation is intrinsically related to this competition which might lead to ZB nucleation at sites away from TPL. In other words, our results point to the different routes of In incorporation at TPL as the origin of the different NW properties reported. Moreover, our work opens up new possibilities to control the polytypism in InP NWs, from pure WZ to band-engineered WZ-ZB nanowires.

Acknowledgements: This work is supported by FAPESP.

Obtenção e crescimento de nanopartículas de prata em N,N-dimetilformamida

LUIZ P. DA COSTA¹, Silva, JMDE¹, Souza, E. R.¹, Sigoli, F.A.¹, and MAZALI, I. O.¹

Universidade Estadual de Campinas - Campinas SP Brazil

A preparação de nanopartículas metálicas tem atraído grande interesse em grupos de pesquisa nas últimas décadas devido às suas propriedades óticas, elétricas e catalíticas. As propriedades óticas de nanopartículas de metais nobres (Au, Ag, Cu) são dominadas pela oscilação coletiva dos elétrons de condução resultando em uma interação com a radiação eletromagnética e, tais propriedades, dependem do tamanho e da forma das partículas. Neste trabalho, foram preparadas nanopartículas de prata a fim de estudar, pela espectroscopia de UV-Vis, a influência do tempo de reação no tamanho, na forma das partículas e, conseqüentemente, nas bandas atribuídas a diferentes modos de plásmon (multipólos). As nanopartículas foram preparadas pela reação de redução do íon prata (I) a partir de nitrato de prata (3,8 mmol/L) em N,N-dimetilformamida, nas condições ambiente. A suspensão coloidal de prata metálica foi caracterizada por espectroscopia UV-Vis e por microscopia eletrônica de transmissão. A N,N-dimetilformamida atua como agente redutor dos íons prata e, também, como passivante das nanopartículas obtidas, uma vez que tais partículas encontram-se distribuídas sem aglomeração. No estudo por espectroscopia UV-Vis, observa-se que até 8 horas de reação a banda atribuída ao plásmon da prata apresenta um máximo em torno de 438 nm. A partir de 9 horas há um deslocamento desta banda para região de maior energia (416 nm) e, a partir de 12 horas ocorre uma diminuição de sua intensidade devido ao crescimento das nanopartículas e/ou a formação de outros modos vibracionais de plásmon (multipólos), que podem ser atribuídos a mudanças de forma e tamanho de partículas. A imagem de microscopia eletrônica de transmissão obtida após 12 horas de reação mostra a presença de populações de nanopartículas de prata de diversos tamanhos, com média de 28 nm e formação de algumas nanopartículas de face quadrada. Nesse trabalho foi possível preparar, de forma versátil, nanopartículas de prata de tamanho controlado e observar como a variação da banda de plásmon pode contribuir na interpretação do crescimento e/ou forma das nanopartículas.

Acknowledgements: IQ-UNICAMP, CNPq, FAPESP e LNLS.

Characterization by High Resolution Transmission Electron Microscopy of Nanometric TiO₂/MoO₃ Synthesized in Porous Vycor Glass.

Santos, E. B.¹ and MAZALI, I. O.¹

Universidade Estadual de Campinas - Campinas SP Brazil

Recently, there has been growing technological interest in the synthesis of nanoparticles with controlled composition and size. Efforts to understand the physics and chemistry of the structures in nanometric regime are combined with attempts to explore their properties and uses. The TiO₂/MoO₃ nanoparticles dispersed in porous Vycor glass was prepared by metalorganic decomposition process (MOD). The precursors used were titanium (IV) di-(propoxy)-di-(2-ethylhexanoate), Ti(Prop)₂(Hex)₂, or molybdenum (VI) 2-ethylhexanoate, Mo(Hex)₆. The impregnation was done in PVG pieces during 8 h. For the decomposition of the precursors, the impregnated PVG was submitted to thermal treatments under air at 750 C during 8 h and 550 C during 8 h, for Ti(Prop)₂(Hex)₂ and Mo(Hex)₆, respectively. This procedure is denominated impregnation-decomposition cycle (IDC). The sample masses were determined by weight PVG pieces at 100 C after each IDC. The HRTEM images were obtained from the JEOL JEM3010 microscope (300 kV, 1,7 point resolution). The obtained solids were designed PVG/5TiO₂/7MoO₃ and PVG/5MoO₃/7TiO₂ depending on the starting precursor and the number of IDC. The IDC methodology promoted a linear mass increase resulting in a controlled size of the sphere-like nanoparticles. HRTEM images of the samples PVG/5TiO₂/7MoO₃ and PVG/5MoO₃/7TiO₂ show that the nanoparticles grow in a dispersed way inside the PVG pores. Particles average size distribution for PVG/5TiO₂/7MoO₃ is 5.0 nm. This sample is formed for nanoparticles with sphere-like shape, as observed in the HRTEM images. In detail, a single crystal nanoparticle with (141) lattice planes, characteristic of the orthorhombic phase α -MoO₃, is shown. The sample PVG/5MoO₃/7TiO₂ presents nanoparticles with sphere-like shape and average size distribution of 4.9 nm. It is possible to observe in its HRTEM image crystalline nanoparticles with different interplanar distances, which are referred to (101) and (141) lattice planes, attributed to the TiO₂ anatase phase and to α -MoO₃ orthorhombic phase. Besides, is possible to observe in the HRTEM images that some crystalline nanoparticles of the molybdenum and titanium oxides are in contact. That is an evidence of the formation of heterostructured nanoparticles among the two oxides.

Acknowledgements: FAPESP, Institute of Chemistry/UNICAMP and LNLs for the access of LME (HRTEM).

Utilização da espectroscopia de alta resolução da borda de absorção (XANES) na investigação das propriedades oxi-redutoras de catalisadores a base de cério

Mortola, V. B.¹, Duarte, R. B.¹, and Bueno, J.M.C.¹

Universidade Federal de São Carlos - São Carlos SP Brazil

As reações de reforma do metano para a obtenção de produtos de maior valor comercial têm sido alvo de uma série de estudos nos últimos anos. Catalisadores de Pt suportados em óxidos mistos de cério e alumina apresentam-se como promissores para estas reações, demonstrando-se bastante ativos e estáveis. No entanto, para o desenvolvimento de novos catalisadores, é necessário um maior entendimento do comportamento destes materiais nas condições de reação. Desta maneira, neste trabalho a aplicação de catalisadores de Pt suportados em óxidos mistos de CeO_2 - Al_2O_3 , na oxidação parcial do metano foi investigada. As amostras obtidas por meio da técnica sol-gel foram preparadas com um valor de 0 e 12 m/m de CeO_2 sob a alumina. Os catalisadores foram caracterizados por difração de raios-X (DRX), adsorção de N_2 , redução a temperatura programada (TPR) e espectroscopia de alta resolução da borda de absorção (XANES). Os precursores obtidos apresentaram estrutura do tipo pseudo-boemita e, após calcinação obteve-se uma mistura dos óxidos γ - Al_2O_3 e CeO_2 com estrutura fluorita. Os dados de BET apresentaram uma perda na área superficial específica com a adição de CeO_2 . No entanto, foi verificada uma maior atividade na reação de oxidação parcial do metano para esta amostra. Pelos dados de espectroscopia de alta resolução da borda de absorção observa-se a tendência de recobrimento das partículas de Pt pela céria quando submetidas à aquecimento sob uma atmosfera redutora, o que pode explicar a leve tendência à desativação destes catalisadores durante os testes catalíticos.

Acknowledgements: Ao CNPq pelo suporte financeiro e ao LNLS pelas medidas de XANES.

Análise de difração de raios-x em nanoestruturas cristalinas via método de elementos finitos

Calseverino, C.¹ and Malachias, A.¹

Laboratório Nacional de Luz Síncrotron - Campinas SP Brazil

Neste projeto de iniciação científica estudamos a relaxação do parâmetro de rede, a deformação elástica e a interdifusão em ilhas de InAs crescidas em um substrato de GaAs (100). Os dados experimentais foram obtidos através de medidas de difração de raios-X sob incidência rasante (GID), difração anômala e microscopia de força atômica (AFM), utilizando-se para os dois primeiros a fonte de radiação síncrotron do LNLS. O primeiro tratamento de dados e simulação das nanoestruturas foi feito por análise direta. Dois tipos de amostra foram estudadas: uma com ilhas de InAs descobertas e outra com ilhas de InAs enterradas em GaAs, sendo esta última a de maior motivação para o projeto, dado o seu potencial para aplicação tecnológica e a ausência de um método padronizado para o estudo de deformações elásticas neste sistema. A análise direta, aplicada até o presente momento, não se mostrou eficiente para o estudo das ilhas enterradas e o tratamento futuro de dados visa suprir esta dificuldade. Resultados da análise direta serão explicados detalhadamente para as duas amostras estudadas, explicitando a possibilidade de quantificar o gradiente de deformação elástica e composição química nas ilhas descobertas. Para compreender o caso das ilhas enterradas estamos utilizando o método de elementos finitos. As primeiras simulações já estão em andamento, com uso do software COMSOL. . Na presente fase do projeto estamos extraindo e ordenando uma matriz de saída do software de elementos finitos, em que as posições atômicas e deslocamentos em x, y e z são utilizados como dados de entrada para simular perfis de difração de raios-x. A consolidação deste projeto proverá um método pioneiro no LNLS para análise de medidas de difração de raios-X em nanoestruturas encapsuladas com gradientes de deformação não monotônicos.

Acknowledgements: Este trabalho foi financiado pelo CNPq e realizado nas instalações do LNLS.

Síntese e estudo da remoção de ligante de um nanocatalisador de Ni para aplicações em reações de reforma

Braga, A. H.¹, Parizotto, N. V.², Borin, A.¹, and Zanchet, D.³

¹ Universidade Estadual de Campinas - Campinas SP Brazil

² Universidade Federal de São Carlos - São Carlos SP Brazil

³ Laboratório Nacional de Luz Síncrotron - Campinas SP Brazil

Em busca de novas fontes de energia, limpas e alternativas ao petróleo, o hidrogênio tem recebido bastante destaque. Como combustível, tem atraído muita atenção por gerar como resíduo a água. O processo mais utilizado para produção deste gás é a reforma a vapor do metano, devido à abundância deste na forma de gás natural. Tal reação exige catalisadores; o Ni é um potencial catalisador, já que apresenta boa atividade e tem baixo custo. Recentemente, nanopartículas metálicas coloidais tem sido exploradas, já que as características desses nanomateriais, tais como controle de tamanho e estreita distribuição, fazem desses materiais sistemas modelo para a catálise. Assim, buscou-se sintetizar nanopartículas de Ni via rota coloidal. Para tanto, partiu-se de 200 mg do precursor $\text{NiCl}_2 \cdot 6\text{H}_2\text{O}$, e de 466 mg de polivinilpirrolidona (PVP - ligante), dissolvidos em 100 mL de metanol; em seguida 10 mL de solução 300 mM (116 mg) de NaBH_4 (reduzidor) foi adicionada. As nanopartículas sintetizadas foram impregnadas em sílica aerossil, em um teor nominal de 15% em massa. A perda de ligante é um passo importante na ativação destes catalisadores; tal etapa foi investigada por análise termogravimétrica e por lavagens das nanopartículas com solventes, neste caso a perda do PVP foi medida por espectroscopia no infravermelho próximo (NIR). Os resultados indicam até o momento que o melhor método de ativação é o térmico, em atmosfera inerte, que mostra uma perda parcial de ligante em 300°C.

Acknowledgements: Agradecimentos à toda a equipe do LSQ, onde foram realizadas as sínteses, e ao LAQQA da UNICAMP, onde foram feitas as medidas de NIR.

Determination of the thickness and crystalline structure of TiO₂ coatings made by sol-gel dip coating

Alterach, M.A.¹, Rosenberger, M. R.¹, Ares, A.E.¹, Lamas, D. G.², and Schvezov, C. E.¹

¹ CONICET - Universidad Nacional de Misiones - Posadas-Misiones Argen Argentina

² Consejo Nacional de Investigaciones Científicas y Técnicas - Buenos Aires Argentina

TiO₂ coatings are fabricated by the sol-gel dip coating route using a Ti-6Al-4V alloy as substrate, relating the parameters of process with the thickness and crystalline structure [1,2]. In this research, the process involves: a) immersing the substrate (Ti-6Al-4V) in a colloidal dispersion (sol), b) extraction of the substrate at low and constant speed, c) drying of the coating and d) heat treatment. For the preparation of dispersions were used titanium butoxide, isopropanol, ethyl acetoacetate HCl and distilled H₂O. The speed of dip-coating and the number of deposited layers were varied from 1 to 3 cm / min and from 1 to 3, respectively. Dispersions were used with molar ratios of titanium butoxide / isopropanol 1 / 20 and 1 / 10, respectively. The coatings were realized using dispersions of different times of aging (1 to 10 days). The samples received a heat treatment of one hour at fixed temperature of 500 C to each layer of coating and heated to 10 C / min and cooling inside the furnace. The morphology of the coatings was observed by optical microscopy, the crystalline structure was determined by X-ray diffraction with a grazing incidence angle of 1 and the thickness was determined by X-ray reflectometry technique. These experiments were carried out at the D12A-XRD1 beamline of the LNLS. By microscopy it was determined that the coatings were homogeneous, compact and smooth and all of different colors depending on their thickness. With increasing speed of dip-coating, the number of deposited layers, the ratio of titanium butoxide / isopropanol and the aging time of the dispersions, greater thicknesses of the coatings in a range that varied from 25 nm to 200 nm were obtained. By X-ray diffraction of the monolayer and multilayer coatings was determined the presence of anatase and rutile.

1. J. Liu, D. Yang, F. Shi and Y. Cai, *Thin Solid Films*, 429 (2003)225-230.
2. N. Huang, P. Yang, Y.X. Leng, J.Y. Chen, H. Sun, J. Wang, G.J. Wang, P.D. Ding, T.F. Xi, Y. Leng, *Biomaterials*,24 (2003)2177-2187.

Acknowledgements: The authors acknowledge various funding supports provided by 1) Laboratorio Nacional de Luz Sincrotron (LNLS), Campinas, Sao Paulo-Brasil, 2) National Agency for Science and Technology Promotion (ANPCyT), Buenos Aires-Argentina and 3) National Council of Scientific and Technical Research (CONICET), Buenos Aires-Argentina.

Characterization of magnetic nanourchins and nanoflowers

Socolovsky, L. M.¹, Lloret, P.E.², Ybarra, G.², and Moina, C²

¹ Universidad de Buenos Aires - Buenos Aires CapFe Argentina

² Instituto Nacional de Tecnología Industrial - San Martín Argentina

Chemical synthesis of nanoparticles allows producing functionalized structures that join features coming from the core and those coming from the shells. These features are useful for applications in several fields, among them, clinical therapies or sensing. A magnetic core of a nanoparticle capped with an organic substance can be used as a marker, or for carrying drugs to a specific site guided by an external magnetic field. Conversely, a convenient capping would attach to a specific substance or microorganism, and its magnetic core will help us to collect that, to later be analyzed in a sensing device; or modify their electrical transport properties. Fe_3O_4 nanoparticles of about 10 nm in diameter produced by a new precipitation method where chemically covered by several layers of gold, creating in this way nanourchin-like structures of about 200 nm in size. Gold surfaces are easily functionalized with organic groups like thiols. Because of the used method, we were interested in assessing structure of resultant nanourchin. We characterized these structures by High Resolution Transmission Electron Microscopy (HR-TEM), Energy-Dispersive Spectroscopy (EDS) and magnetic measurements. We found that magnetite nanoparticles are well covered by deposited gold. Resultant nanostructure keeps original superparamagnetism, needed for practical applications.

Acknowledgements: LMS acknowledges CONICET; P.LI., G.Y. and C. M. acknowledge INTI; for financial support. LME-LNLS is also acknowledged for the use of HR-TEM.

A novel approach for high resolution strain mapping and elastic properties assessments of alloyed strained nanostructures

Montoro, L. A.¹, Medeiros-Ribeiro, G.¹, and Ramirez, A.J.¹

Laboratório Nacional de Luz Síncrotron - Campinas SP Brazil

In recent years the advent of nanotechnology has awaked a great interest on the nanostructures elastic properties. This fact arise from that almost all physical properties of materials can be affected by elastic strain or stress state, such as band-gaps, vibrational properties, spectroscopic properties, mass transport by diffusion (which affects the components intermixing or dopant distribution), thermal and electrical transport, and several other. Thus, the knowledge of the strain and stress state at the nanoscale is of great importance for applications ranging from semiconductor nanostructures and devices to structural engineering components. Hence, these requirements further call for advanced experimental techniques that allow accurate measurement and mapping of elastic/chemical properties with high spatial resolution. In a recent work we demonstrate the development of a new method to obtain projected 2D quantitative chemical maps of self-assembled $Si_{1-x}Ge_x : Si(001)$ strained alloyed epitaxial islands [1]. This self-consistent methodology allows the evaluation of strained alloyed nanostructures, where the combination of projected 2D chemical information obtained from two different zone axis, [100] and [110], with iterative simulation made possible the reconstruction of the three-dimensional (3D) chemical arrangement inside the islands. Here, we go one step further using the $Si_{1-x}Ge_x : Si(001)$ strain state information to a deep evaluation of the elastic properties at the nanoscale. Our findings show that this methodology can be highlighted as a powerful technique for an accurate chemical and elastic properties assessment of specific strained alloyed nanostructures. Indeed, this technique arises as a remarkable tool to provide useful clues for shed light to the nanocrystals growth, evolution and chemical/electronic/optical properties.

[1] L.A. Montoro, M.S. Leite, D. Biggemann, F.G. Peternella, K.J. Batenburg, G. Medeiros-Ribeiro, A.J. Ramirez, J. Phys. Chem. C, 113, 9018 (2009).

Acknowledgements: This work was supported by FAPESP 2007/05165-7

Analysis of Sb dopant influence on SnO_2 nanoparticles morphology and growth mechanism

Stroppa, D. G.¹, Montoro, L. A.¹, Leite, E.R.², and Ramirez, A.J.¹

¹ Laboratório Nacional de Luz Síncrotron - Campinas SP Brazil

² Universidade Federal de São Carlos - São Carlos SP Brazil

The development of novel and reliable nanostructured devices requires the ability to synthesize and characterize materials on the atomic scale. Among the most significant challenges in nanostructural characterization is the evaluation of crystal growth mechanisms and their dependence on the distribution of doping elements. This work provides an evaluation of Sb dopant influence on SnO_2 nanoparticles morphology and growth mechanism by the combined use of HRTEM characterization and ab initio calculations for surface energy. SnO_2 and $Sb : SnO_2$ (18%_{atom}) nanocrystals were obtained by a nonaqueous synthesis route. HRTEM characterization was performed using a JEM-3010 URP at 300 kV with a LaB_6 electron gun. Wulff construction using the ab initio calculated surface energies was applied to model the nanocrystals. Oriented attachment was identified as the growth mechanism for both systems and the preferential growth directions, [110] for the SnO_2 nanocrystals and [100] and [101] for $Sb : SnO_2$ nanocrystals, could be successfully described by the ab initio calculated surface energy distribution [1].

[1] Stroppa, D. G., Montoro, L. A., Beltran, A., Conti, T. G., da Silva, R. O., Andres, J., Longo, E., Leite, E. R., Ramirez, A. J.; Unveiling the Chemical and Morphological Features of $Sb : SnO_2$ Nanocrystals by the Combined Use of High-Resolution Transmission Electron Microscopy and ab Initio Surface Energy Calculations. *Journal of the American Chemical Society*, v.131, p.14544 - 14548, 2009.

Acknowledgements: This work was supported by FAPESP

Índice Remissivo

- (dos) Santos, J. I., 19
Álvares, A.C.M., 29, 30
- A. Kleiman, 207
A. Márquez, 207
A. Magnus G. Carvalho, 185
A. Pyzalla, 127
A. Y. Takeuchi, 170
A.F. Craievich, 209
A.L.F. de Barros, 64, 66, 179
A.M. Mudarra Navarro, 201
Abdala, P. M., 171, 174, 178
Abreu, C. M., 173
ACF Santos, 69
Acuña, L. M., 155, 161
Afonso, C R M, 132, 133
Akao, P.K., 37
Alborghetti, MR, 23, 24
Alconchel, S. A., 178
Almeida, D. P., 69, 115, 216
Almeida, J. M. A., 160
Almeida,A.P., 84
Almeida,G.C., 66, 179
Alonso, J.A., 159
Alterach, M.A., 231
Alves, A.L, 170
Alves, D.L.H., 87
Alves, M.C.M., 188, 206, 224
Amalvy, J. I., 105, 202
AMARAL L., 169, 193
Anbinder, P. S., 105, 202
Andersen, E. S., 25
Andersen, F. F., 25
Andrés, J., 186, 215
Andrade, D. P. P., 68
Anjos, M. J., 89, 91–93, 140
Aparicio, R., 57
Arantes, C., 203
Araujo,G.S, 204
- ARENAS, Leliz Ticona, 212
Ares, A.E., 219, 231
Arguello, J., 212
Ari M., 122
Arni, R.K., 36, 38
Arruda, M. A. Z., 48, 58
Avansi, W., 182
Azevedo, G. de M., 144
Azzaroni, O., 107
- B Paulsen, 82
Baesso, M.L., 189
Bagnato, O. R., 187, 192
Baker, R.T., 155, 161
Balan, A., 43
Barbi, M. S., 109, 110
Barbosa, J.A.R.G., 21, 29, 30, 34, 43, 88
Barbosa, L. C., 213
Barros, R. M., 187
Barroso, R.C., 84, 97, 102
Basso, R. L. O., 184
Batista, T., 209
Bauer, O. H., 145
Behrens, M. A., 26
Bellettini, I. C., 112
Belloni, M, 35
Benati, D. M., 132
Benedetti C.E., 21, 44, 47, 51–53
Bernardes, A., 11
Bernardi, F., 188, 206, 224
Bernini, R.B., 63
Beron, F., 194
Bezerra, E.H.S., 16
Bezerra,M. J. B., 16
Bianchi, O., 116
Bjerre AB, 7
Boechat-Roberty , H.M., 68
BOITA, Jocenir., 206, 224
Bongiovanni, G.A., 83

- Borba, F.H, 79, 81
 Borges, J.C., 28, 31, 46
 Borges, R. J., 19
 Borin, A., 230
 Bortolucci, E. C., 145, 146
 Bozano, D. F., 165
 Braga, A. H., 230
 Brandão, E.M., 192
 Braz, D., 84, 102
 Bressan, G.C., 27, 28, 45, 49
 Bruvera, I.J., 107
 Bueno, J.M.C., 218, 228
- C. A. Figueroa, 184
 C. Lage, 42, 88
 C. M. R. Remedios, 183
 C.R. Ponciano, 75, 115
 Câmara, P.R.S, 35
 Cabezas, M.D., 155, 161
 Calasans-Maia, 85
 Calseverino, C., 229
 Camargo, R., 32
 Camera, A.S., 80
 Campos, B.M., 21
 Campos, C. E. M., 115
 Campos, J. L. O., 20
 Campos, V.A.C., 99
 Candal, R.J., 184
 Canellas,C.G.L, 89, 91–93, 140
 CANTERAS, F. B., 101
 Caravaca, M.A., 221
 Carazzolle M.F., 199
 Cardoso, L.P., 160, 183, 193
 Cardoso, S.C., 82, 84, 97
 Carrilho, E., 142, 149, 214
 Carvalhal, R. F., 195
 CARVALHO, A.C.B., 73
 Carvalho, F. C., 109, 110
 Carvalho, S.M.F, 89, 91, 93
 Casali, R.A., 221
 Cassago, A., 12
 Cavada, B.S., 16, 17
 Cavalcante, I. P., 165
 Cavasso Filho, R. L., 70, 71, 74
 Ceolin M., 107
 Cernadas, R. A., 44, 47, 53
 Cesar, C. L., 213
 Ch. Genzel, 127
 Chen, H., 174
 Chiavacci, L.A., 109, 110
 Coelho, A. A., 185
 Coltro, W. K. T., 142, 147, 214
 Colussi,F., 18
 Comerlato, N.M., 180
- Conceição, M. O. T., 125
 Corrêa, H. P. S., 137, 139, 154, 165
 Correia, R. C., 140
 Cosme, T. A., 156
 Cotta, A. C., 217
 Cotta, M.A., 225
 Coutinho, L. H., 63
 Craievich AF, 15, 108, 171, 174, 211, 213
 Crespo, S.J, 116
 Cunha, T. R., 210
 Cury, J. A., 56
 Cyr, D.M., 46
- D. S. Galvao, 220
 da Silva, A. M. P. A., 145
 da Silva, L. F., 168
 da Silva, L. M., 185
 da Silva,M. A. O., 48
 DAHMOUCHE, K, 120, 121, 124, 177
 Dal Acqua, N, 116
 Dalmaso, G. Z. L., 88
 de Avillez, R. R., 122
 de Jesus, E.F.O., 89, 91, 93
 De Lima, J.C., 115
 de Menezes, A. S., 160, 183, 193
 de Oliveira, A.H.C., 38
 de Paula-Pereira Jr., M. V., 42
 de Ramos Filho, F. G., 121
 de Siervo A., 199, 208
 de Sousa, V. S. R., 185
 de Souza Guerra, C, 84
 de Souza, G.G.B., 63, 65
 Delatorre, P., 16, 17
 Della Védova, Carlos O., 70, 71
 Denadai, A M L, 41
 Depianti, J. B., 154
 Docena, C., 44
 Domingues, M. N., 44, 47
 Doriguetto, A.C., 167
 dos Santos, A. O., 160, 193
 dos Santos, D. R., 189, 190
 dos Santos, D. S., 123, 125
 Droppa Jr., R., 102, 130
 Duarte, R. B., 228
 Duque J.G.S., 157, 176, 210
- E. C. Paris, 186
 E. F. da Silveira, 68, 75
 E. J. Carvalho, 185
 E. Jimenez, 213
 E. V. Shevchenko, 211
 E.E.Miro, 205
 Erben, Mauricio F., 70, 71
 Erlacher, K, 26

Espinoza Quiñones, F.R., 79–81

F. Alvarez, 130, 184
 F. Golmar, 201
 Fábregas, I. O., 14
 Fabbris, G. F. L., 144
 Fantini, M. C. A., 161, 171
 Farah, C.S., 44
 Fattori, J., 57
 Favarin, H.R., 167
 Feltrin, C.W, 188
 Fernández de Rapp, M. E., 14
 Fernández Werner, L., 174
 Fernandes, D.H.L., 64
 Ferreira, F. F., 122, 137
 Ferreira, G. B., 66, 179, 180
 Ferreira, L. C., 140
 Ferreira, R. A. A., 129
 Ferreira-Rodrigues, A. M., 75
 Filadelpho, M. C., 189, 190
 Fischer, H., 15
 Fonseca, E. B., 133
 Fonseca, Roney J., 100
 Fontes, M. R. M., 19
 Fraga, M. A., 117, 126
 Francisco, F. R., 187, 192
 Freitas, S. M., 29, 30, 32, 34
 Fuentes, R. O., 155, 161, 221
 Furlan AS, 23, 24
 Furlan, H., 126

G. Evans, 4
 G. Ferreira, 64
 G. Panaccione, 3
 Gündel, A., 95
 Galante, D., 88
 Galvão, A. S. A., 139
 Gandra F. G, 185
 Garcia, F., 137, 159, 185, 221
 Garcia, J., 130
 Garcia, R. B. R., 118
 Gaspar, R. D. L., 191
 Gasperini, A. A., 144
 Gasperini, F. M., 85
 Geraldo, S. M., 97
 Gerlach, R.F., 84, 102
 Geronés, Mariana, 70, 71
 Giacomolli, B.A., 143
 Giovanetti, L. J., 211
 Gobbi, A. L., 142, 145, 146, 214
 GOMES MD, 45
 Gomes, A.S., 120, 121
 Gomes, M.A., 163
 GOMES,E.J.L., 183

Gonçalves, K.A., 31
 Gonçalves, M.V.C, 102
 Grangeiro,L.B., 63, 65
 Granjeiro, J. M., 73, 85
 Gremião, M. P. D., 109, 110
 Guerra, A. C. O., 64, 66, 179, 180
 Guerra, J. P. T. A., 112
 GUERRA, M.B.B., 96
 Gushikem, Y., 212
 GUZMAN-SILVA, M.A., 73

H. (C.) Pinto, 127, 130
 H. J. Sánchez, 67, 72, 138
 Hermenegildo.T,F, 132
 Hiruma-Lima, C. A., 94
 Homem, M. G. P., 69, 75
 Horjales,E., 12

I. L. Graff, 169
 Irish, E., 25
 Isaac, A., 131

J. H. Rodrigues, 123
 J. Mesa, 94
 J. Susini, 5
 J. Varalda, 169
 J.L.Passamai Jr, 137, 154
 Jacques, R.A, 95
 Jardim, P. M., 122
 Jesus, J. R., 210
 Joanitti, G. A., 32

Kakuno, E. M., 143
 Kaufmann, P., 145
 Kawachi, E. Y., 118
 Kawaguti C.A., 120
 Kellermann, G., 213
 KILIAN, A. S., 206, 224
 Kjemis, J., 25
 Kleiman, G.G., 199
 Knobel, M., 194
 Knudsen, B. R., 25
 Kobarg, J., 22–24, 27, 28, 31, 45, 49, 50
 Kornberg, M. A., 145
 Krawczyk, P., 146
 Kretly, L. C., 153
 kubota, L.T., 195
 Kuniyoshi, T.M., 45
 Kushima, H., 94

L. H. Almeida, 123
 Labean, T., 25
 Lacerda, R. G., 208
 Lago, A. F., 74
 Lagos, M.J., 220

- Lagreca, E. R., 125
 Lai, X, 183
 Lamas, D. G., 161, 171, 174, 178, 207, 219, 221, 231
 Landers R, 199
 Lang R, 193
 Lanza, D.C.F, 22, 27
 Leani, J.J., 67
 Lede, E. J., 181
 Leitão, A.C., 42, 88
 Leitão,R.G., 89, 91–93, 140
 Leite,E.R., 182, 234
 Lemus, L.F., 123
 LIMA, I., 73, 85–87
 LIMA, I. G. P., 88
 Lima, L. M. T. R., 158, 200
 Lima, P. M., 48
 Lima, R. J. S., 157, 210
 Lima, R. S., 142, 214
 Lima, T.A.R.M., 175
 Lima, V.D., 177
 Lionzo, M. I. Z., 106
 Lloret, P.E., 232
 Longo, E., 186, 215
 Longo, V. M., 186
 Lopes, L. J. S., 66, 179, 180
 Lopes, M. C., 200
 Lopes, R.T., 73, 85–87, 89, 91–93, 140
 Lorenzini, G. C., 106
 Lottermann, M. T., 32
 Loula, G. D., 185
 LUIZ P. DA COSTA, 226
 Lula, I., 41

 M. Cremona, 204
 M.I.B.Bernardi, 168
 Módenes, A.N., 79–81
 Macedo, Z.S., 163, 172, 173
 Machado, A.R.T., 99
 MACHADO, D. S., 108, 209
 Machado, G, 116
 Maciel, H. S., 117, 126
 Magalhaes-Paniago, R., 208
 Malachias, A., 229
 Manenti, D. R., 79, 81
 Manfiolli A, 45
 Manzine, LR, 12
 Manzini R., C. H., 158, 200
 Marchesini, F. A., 205
 Marinkovic, B. A., 122
 Marins, J. A., 158, 200
 Marques, J. F., 95
 Martinez, L. G., 137, 139, 154, 165
 Martins de Sá, C, 32
 Martins, A. M., 58
 Martins, L. F., 195
 Martins, M. D., 217
 Massi, M., 117, 126
 Mastelaro, V.R., 162, 167, 168, 182, 186
 MATTOSO, Luiz Henrique Capparelli, 166
 MAZALI, I. O., 191, 226, 227
 Mazzocchi, V. L., 139
 MEDEIROS, E. S., 166
 Medeiros-Ribeiro, G., 233
 Meira, D. M., 218
 Meirelles, G. V., 22
 Melo A. M., 145, 146
 Melo, F. C. L., 137, 154
 Meneses, C. T., 157, 176, 210
 Meneses, E. A., 193
 Mesquita, A., 162
 Michalowicz, A., 162, 167
 Michel, R. C., 156
 Milori, D. M. B. P., 141
 Minatti, E., 112
 Mocellin,A., 74
 Moi, G.P., 56
 Moina, C, 232
 Montes, PJR, 119
 Montoro, L. A., 233, 234
 Moraes, E.C., 45
 Morais, J., 188, 206, 224
 Moreira M. L., 186
 Moreira, S., 84, 97, 98, 100, 101
 Mortola, V. B., 228
 Mosca, D. H., 169
 Moura TR, 16
 Moura, K. O., 210
 Moura, P. R., 115, 216
 Muñoz, F.F., 155, 161
 Mundim, M. S. P., 74
 Murakami, M. T., 36–38, 55

 Naganao, C.S., 16
 Napolitano, H. B., 15
 Nascente, P. A. P., 142, 199, 214
 Nascimento, V. P., 170
 Nasciutti, L.E, 92, 140
 Naves de Brito, A., 74, 75, 88
 Nestor E. Massa, 159
 Netto, F.M., 110
 Netto, L.E.S., 59
 Neuschwander, R., 144
 Neumann, M. G., 108, 209
 Neves P.P, 167
 Neves, J.L., 33
 Neves, R.C.F., 48

- Novais, S. M. V., 172, 173
- Ochoa, E.A., 130
- Oliveira Neto M., 11, 15, 18, 108, 209
- Oliveira, C. L. P., 25, 26, 111, 182
- Oliveira, D. C., 222, 223
- Oliveira, D. F., 99
- Oliveira, G. E., 156, 158, 200
- Oliveira, I.C., 117, 126
- Oliveira, J.J., 144
- Oliveira, L. F., 84
- Oliveira, M. L. P., 44, 52, 53
- Oliveira, M. P., 222
- Oliveira, M.A., 59
- Orlandi, M.O., 215
- Orlando, M. T. D., 137, 139, 154, 156, 164, 165
- Otzen, D. E., 26
- P. F. P. Fichtner, 169
- Pérez, C. A., 48, 67, 83, 86, 138
- Padilha, P. M., 48
- Paes Leme, A.F., 22, 24, 35, 54, 56
- Palacio, S.M., 79–81
- Palmqvist, A., 111
- Palumbo, A.J., 92, 140
- Pancotti A., 199
- Papa, PF, 31
- Parente, C.B.R., 139
- Parizotto, N. V., 230
- Pascoli, A.S., 118
- Passamani, E. C., 170
- Passos, D. O., 45
- Pedersen, J. S., 26
- Pedersen, J.S., 25, 26, 111
- Peixoto, S. M. B., 189, 190
- Pereira Filho, E. R., 96
- Pereira, A. L. A., 53
- Pereira, F. M. V., 141
- Pereira, G.R., 140
- Pereira, H.M, 12
- Pereira, M.O., 91, 140
- Peruzzo, P. J., 105, 202
- Piazzetta, O.M.H, 142, 145, 146, 214
- Picciani, P.H.S, 166
- Picco, A., 107
- Pierini, B. T., 178
- Pilling, S., 68
- Pimentel, V. L., 212, 214
- Pinto, J.C., 156, 158, 200
- Pinto, N.G.V, 84
- Pirota, K. R., 194
- Plivelic, T.S., 105, 202
- Poglitsch, A., 145
- Polikarpov, I., 11, 13, 15, 18, 20, 108, 209
- Ponce, C.A., 221
- Porto, IM, 102
- Proveti, J. R., 170
- Puhl, A. C., 20
- Quaresma, A. J. C., 28, 47
- Queiroz, C. M. S., 129
- QUEIROZ, HIURE A. A. S, 118
- Quirino, W., 204
- R.D. Pérez, 83
- R.J.Chimentão, 129
- Ramallo-López, J. M., 205, 211
- Ramirez, A.J., 131–133, 148, 233, 234
- Ramos, C.H.I., 28, 46
- Rehen, S, 82
- REIS, C.V., 13
- Requejo, F. G., 205, 211
- Ribeiro, C., 182
- Ribeiro, D. A., 55
- Ribeiro, R.U., 218
- Ricardo, W., 204
- Rita, J.R.S., 203
- Rizzo, F., 122
- Roa, D. B, 208
- Roberts, K. J., 183
- Rocco, D. L., 185
- Rocco, M.L.M., 68, 203, 204
- Rocha, B.A.M., 16, 17
- Rodella, C. B., 128, 129
- Rodríguez Torres, C. E., 201
- Rodrigues Filho, U.P., 142, 214
- Rodrigues, A, 188, 206, 224
- Rodrigues, F, 144
- Rodrigues, F. N., 63
- Rodrigues, V. A., 154
- Rodrigues, L.V., 101
- Rodriguez Pirani, Lucas, 70, 71
- Rodriguez, E., 213
- Roman, L. S., 203
- Romano, Rosana M., 70, 71
- Rosenberger, M. R., 219, 231
- Rosseto, Flávio R., 18
- Rossi A. M., 85
- Rossi, J. L., 137, 154, 165
- Rubio, M., 83
- Ruller, R., 55
- Ruller, R., 37
- Sales, E., 73, 85–87
- Sampaio, J. A., 189, 190
- Santana JB, 22
- Santana, J. M., 29
- Santos, C. R., 34, 36

- Santos, E. B., 227
 Santos, F.A., 48
 Santos, R.A.S., 41
 Santos, T. F. A., 132
 Santos, V.F., 59
 SANTOS,C.L, 176
 Sarmiento, V.H.V, 109, 110, 175
 Sasaki, J.M., 160
 Sato F., 220
 Schmitt, C.C. ou Cavalheiro, C.C.S, 108, 209
 Schvezov, C. E., 219, 231
 Scorzato. C. R., 143
 Serpa, V.I., 18
 Sforça, ML, 24, 33, 47
 Sharma, S.K., 194
 Sigoli, F.A., 191, 226
 Silva, A. J., 29, 30, 32, 34
 Silva, A.A., 124
 Silva, C. L., 84
 Silva, J. A. F., 196
 Silva, J.C., 22-24, 27, 28, 31
 Silva, JMDE, 226
 Silva, K. T., 94
 Silva, M. W. B., 153
 Silva, R.S., 173
 Silva, W. J. R., 99
 Silveira, N. P., 106
 Simões, G., 65
 Simabuco, F. M., 54
 Sinisterra R. D., 41
 Smetana, J. H. C., 49
 Soares, A. M., 19
 Soares, B.G., 124, 166, 177
 Soares, E.A., 217
 Soares, Júlio César de A.C.R., 93
 Soares, M., 42
 Socolovsky, L. M., 181, 232
 Soprano, A. S, 51
 Sotero, A.P.S., 144
 Souza Jr, F. G., 137, 156, 158, 166, 200
 Souza, D. O., 154, 164
 Souza, D.O., 165
 Souza, E. R., 226
 Souza, L. C., 32
 Souza, P.A.V.R, 92, 140
 Souza, T. A., 44, 47, 51
 Souza, T.A.C.B., 21
 Squina, F. M., 55
 Stelling, M.P., 82
 Stroppa, D. G., 234
 Stutz, G., 80
 Suescun, L., 174
 Sundblom, A., 111
 Szymanski, N., 79, 81
 T. Wroblewski, 127
 Taam, P. ; Taam, Pedro, 87
 Tallarico, D.A., 199
 Tasic, L., 57, 58
 Teixeira, S.R., 116
 Th. Chiaramonte, 225
 Thiemann, O. H., 12
 Thompson, A., 116
 Tirao G., 80
 Tizei, L. H. G., 225
 Tonoli, C. C. C., 36, 38
 Torres, E. A., 148
 Torriani, I., 22-24, 31
 Torriani, I.L., 27, 28
 Toyama MH, 17
 Trindade, D.M., 38
 Trivella, D.B.B., 13
 Turci, C. C., 64, 66, 179, 180
 Ugarte, D., 220, 225
 Unfried S., J., 133
 V. Fernandes, 169
 Valentinuzzi, M. C., 67, 72
 Valerio, M.E.G., 119, 163, 172, 173, 175
 Varela, J.A., 186
 Vargas, J. M., 194
 Vaz, T. H., 54
 Venturino,A., 83
 Vera, M. L., 219
 VICENTINI, Valéria Perfeito, 129
 Vieira, L. D., 94
 Vives, A. E. S., 97
 Volanti, D.P., 215
 von Ranke, P. J., 185
 W. A. A. Macedo, 217
 W.H. Flores, 95
 Wakavaiaichi, S. M., 126
 Weber Neto, J., 98
 Wisnivesky, D., 184
 Wu, L., 131
 Ybarra, G., 232
 Yokoo, S, 35
 Yunes, J. A., 50
 Zakia, M.B.P., 145
 Zambello, F. R., 223
 Zanchet, D., 128, 129, 218, 222, 223, 230
 Zanchin, N. I. T, 49, 54
 Zenati PP, 50
 Zeri, A. C., 47

Zeri, A.C., 33, 99

Zeri, A.C.; Zeri, A; Zeri, A.C.M., 24

